WestVirginiaUniversity
THE RESEARCH REPOSITORY @ WVU

Graduate Theses, Dissertations, and Problem Reports

2003

Genetic, metabolic, and histopathological studies of particle -associated respiratory alterations

Mohamed Mohamedy Ghanem
West Virginia University

Follow this and additional works at: https://researchrepository.wvu.edu/etd

Recommended Citation

Ghanem, Mohamed Mohamedy, "Genetic, metabolic, and histopathological studies of particle -associated respiratory alterations" (2003). *Graduate Theses, Dissertations, and Problem Reports*. 1868.
https://researchrepository.wvu.edu/etd/1868

This Dissertation is protected by copyright and/or related rights. It has been brought to you by the The Research Repository @ WVU with permission from the rights-holder(s). You are free to use this Dissertation in any way that is permitted by the copyright and related rights legislation that applies to your use. For other uses you must obtain permission from the rights-holder(s) directly, unless additional rights are indicated by a Creative Commons license in the record and/ or on the work itself. This Dissertation has been accepted for inclusion in WVU Graduate Theses, Dissertations, and Problem Reports collection by an authorized administrator of The Research Repository @ WVU. For more information, please contact researchrepository@mail.wvu.edu.

GENETIC, METABOLIC, AND HISTOPATHOLOGICAL STUDIES OF PARTICLE-ASSOCIATED RESPIRATORY ALTERATIONS

Mohamed Mohamedy Ghanem

Dissertation submitted to
Davis College of Agriculture, Forestry, and Consumer Sciences
at West Virginia University in partial fulfillment
for the degree of

Doctor of Philosophy
in
Genetics and Developmental Biology

Joginder Nath, Ph.D., Chair
Ann Hubbs, DVM, Ph.D., Co-Chair
Vincent Castranova, Ph.D.
Sharon Wenger, Ph.D.
Jed Doelling, Ph.D.

Department of Plant and Soil Sciences

Morgantown, West Virginia
2003

Keywords: Cytochrome P4501A1, polycyclic aromatic hydrocarbons, particle exposures

ABSTRACT

GENETIC, METABOLIC, AND HISTOPATHOLOGICAL STUDIES OF PARTICLE-ASSOCIATED RESPIRATORY ALTERATIONS

Mohamed Mohamedy Ghanem

Cytochrome P450s (CYPs) form a superfamily of enzymes crucial for the oxidative metabolism of a wide variety of endogenous and exogenous (xenobiotic) compounds. Cytochrome P4501A1 (CYP1A1) is a member of the CYP1A subfamily that is involved in pulmonary carcinogenesis. CYP1A1 metabolizes polycyclic aromatic hydrocarbons (PAH), such as benzo[a]pyrene in cigarette smoke into DNA-binding reactive metabolites resulting in gene mutation and carcinogenesis. Silicosis and coal workers' pneumoconiosis (CWP) are two pulmonary diseases associated with occupational exposure to silica and coal dust (CD), respectively. Most coal miners are smokers or ex-smokers and epidemiologic studies of coal dust carcinogenesis are confounded by the presence of both cigarette smoke and respirable particles. To clarify the nature of this interaction, we investigated the hypotheses that (1) CYP1A1 induction and activity (EROD) are inhibited by CD and silica. (2) CYP1A1 inhibition by particle exposure is associated with changes in the cellular populations in the exposed lung. Western blot analysis, immunofluorescent-labeling, bronchoalveolar lavage fluid analysis, biochemical assays, and histopathology were used to evaluate our hypotheses. Because of a current debate about using the rat to extrapolate particle-induced pulmonary alterations to humans, the rabbit silicosis and sheep CWP model, were also used. The results indicate that (1) CYP1A1 induction and its metabolic activity (EROD) were suppressed by CD exposure in rats and sheep; and by silica in rabbits (2) CYP1A1 expression was reduced in alveolar epithelial cells by CD or silica exposure (3) silica and CD increased the size (hypertrophy) and number (hyperplasia) of alveolar type II cell with reduction of CYP1A1 expression in these cells (4) CD particles induced dose-dependent pulmonary inflammation, manifested by recruitment of alveolar macrophages and polymorphonuclear leucocytes (5) CD particles induced the preapoptotic Bax protein expression in alveolar epithelial cells and triggered apoptosis (6) inhibition of apoptosis and Bax by the caspase inhibitor, Q-VD-OPH, did not alter CYP1A1 induction (7) suppression of CYP1A1 induction was associated with pulmonary inflammation. These findings are consistent with the hypothesis that CYP1A1 induction and its metabolic activity are inhibited by particle exposure and associated with pulmonary inflammation.

Dedicated to
My parents
and to my
Family

ACKNOWLEDGEMENTS

I am proud to express my deepest gratitude to Dr. Joginder Nath and Dr. Ann Hubbs, my major advisors for their continuous valuable guidance, moral support, and helpful suggestions that maximize the execution of this study.

I am also deeply grateful to Dr. Vincent Castranova for his unlimited support and constructive criticism, which paved the way to accomplish this work. I also extend my gratitude to my committee members including Dr. Sharon Wenger and Dr. Jed Doelling for their continuous moral support and valuable discussions.

I am also indebted to Dr. David Weissman for his help in bronchoscopy of sheep. I am also thankful to Dr. Robert Pitts at the Department of Veterinary Sciences for his help and support in sheep experiment.

I am also grateful to Dr. Robert Mercer and Jim Scabilloni for their help and valuable suggestions in doing the TUNEL assay. I extend my thanks to Dr. Dale Porter for the help in BAL analysis and Dr. Val Vallyathan for providing the coal dust particles and useful scientific discussions. I am totally indebted to Michael Kashon for helping me in statistical analyses and his fruitful discussions.

I gratefully acknowledge all people at PPRB branch at NIOSH particularly, Lori Battelli for her help in sacrificing animals, Lyndell Millecchia for her expert help in photomicroscopy and Diane Schwegler-Berry and Patsy Willard for tissue sectioning and histopathology. I extend my thanks to Mark Barger for his help in biochemical assays and western blotting, and Mike Whitmer for doing the endotoxin analysis.

I also express my sincere thanks to all my friends at NIOSH and WVU who helped me by valuable suggestions and continuous encouragement that support my completion of this study.

I am unlimitedly indebted to my parents and my family including my wife, Eman, and my kids, Mirna, Walaa, and Reham for their spiritual support that make completion of this work possible.

Finally, I am totally indebted to my country, Egypt for the continuous support particularly the Vice Dean of Zagazig University, Prof. Dr. Hussam El-Attar for his moral support throughout the dissertation work.

Mohamed Ghanem

TABLE of CONTENTS

LIST of TABLES

LIST of FIGURES

LIST of IMPORTANT SYMBOLS and ABBREVIATION

Abbreviation	Definition
AAALAC	Assessment and accreditation of laboratory animal Care
AhR	Aryl hydrocarbon receptor
AhRR	Aryl hydrocarbon receptor repressor
AIF	Apoptosis inducing factor
AIP	Aryl hydrocarbon receptor interacting protein
AM	Alveolar macrophage
Arnt	Aryl hydrocarbon receptor nuclear translocator
AS	Acute silicosis
AT-II	Alveolar type II
CS	Chronic silicosis
BALF	Bronchoalveolar lavage fluid
BNF	Beta-naphthoflavone
BCA	Bicinchoninic acid
bHlH	Base Helix-loop-Helix
BSA	Bovine serum albumin
BW	Body weight
CD	Coal dust
CL	Chemiluminescence
CWP	Coal worker pneumoconiosis
CYP	Cytochrome P450
CYP1A1	Cytochrome P4501A1
CYP2B1	Cytochrome P4502B1
CYP2B4	Cytochrome P4502B4
DMSO	Dimethyl sulphoxide
dUTP	Deoxy uridine triphosphate
EDTA	Ethyenediamine tetraacetate
ECL	Enhanced chemiluminescence
EROD	7-ethoxyresorufin-*O*-deethylase
FADD	Fas-associated death domain
FITC	Fluorescein isothiocyanate
HAT	Histone acetyle transferase
H&E	Hematoxylin and Eosin
HRP	Hose radish peroxidase
IF	immunofluorescence
IGF	Insulin-like growth factor
IgG	Immunoglobulin G
IARC	International Agency for Research on Cancer
ICAM-1	Intercellular adhesion molecule-1
IL-1β	Interleukin-1β
IL-6	Interleukin-6
IL-8	Inteleukin-8
iNOS	Inducible NO synthase
IP	Intraperitoneal

IT	Intratracheal
L-NAME	N^G-nitro-L-argenine methyl ester
LPS	Lipopolysaccharide
LSD	Least square difference
MCP	Macrophage chemotactic protein
MIP	Macrophage inflammatory protein
NADPH	Nicotinamide adenine dinucleotide phosphate
NBF	Neutral buffer formalin
NF-κB	Nuclear factor Kappa B
NO	Nitric oxide
NT-II	Non-type II
PA	Proximal alveolar
PAF	Platelet-activating factor
PAH	Polycyclic aromatic hydrocarbon
PAS	Per.Arnt.Sim
PBS	Phosphate buffer saline
PCNA	Proliferating cell nuclear antigen
PDGF	Platelet derived growth factor
PMF	Progressive massive fibrosis
PMN	Polymorphonuclear leucocyt
Q-VD-OPH	Quinoline-Val-Asp (ome)-VH2-OPH
RA	Random alveolar
ROI	Reactive oxygen intermediate
PROD	7-pentoxyresorufin-*O*-deethylase
SDS	Sodium dodecyl sulphate
TBS	Tris buffer saline
TdT	Terminal deoxynucleotidyl transferase
TGF	Transforming growth factor
TNF-α	Tumor necrosis factor alpha
TNFR	Tumor necrosis factor receptor
TUNEL	TdT-mediayed dUTP Nick-End Labeling
VCAM-1	Vascular cell adhesion molecule
XRE	Xenobiotic responsive element

CHAPTER 1
GENETIC, METABOLIC, AND HISTOPATHOLOGICAL STUDIES OF PARTICLE-ASSOCIATED RESPIRATORY ALTERATIONS

INTRODUCTION

One of the most biologically important enzymatic systems involved in the metabolism of xenobiotics in the lung is cytochrome P450. Cytochrome P450s (CYPs) are monooxygenases that activate molecular oxygen necessary for oxidative metabolism of different internal or external lipophilic xenobiotics (Barker *et al*, 1992; Hasler *et al*, 1999) producing less lipophilic substances, thus facilitating their excretion (Mucci *et al*, 2001). Some CYP members, such as CYP1A1 are induced by substrates, such as polycyclic aromatic hydrocarbons (PAHs). Unfortunately the induced CYP1A1 may metabolize the PAH into highly reactive intermediates. For example, a CYP1A1-dependent enzymatic process can metabolize the PAH benzo(a)pyrene in cigarette smoke into the highly carcinogenic metabolite, benzo(a)pyrene diol epoxide (BPDE) (Bjelogrlic *et al*, 1993). This reactive intermediate covalently interacts with DNA nucleotide bases, particularly guanine and adenine, producing DNA adducts with potential ensuing mutations of important genes. Cells with damaged DNA may be removed by apoptosis (programmed cell death) (Venkatachalam *et al*, 1993). Alternatively, if a permanent mutation occurs in a critical region, an oncogene may be activated, or a tumor suppressor gene, such as p53 may be inactivated (Wang *et al*, 1995). The excessive presence of such mutational events leads to aberrant cells with loss of normal growth control and, ultimately, to cancer (Liang *et al*, 2003).

Pulmonary xenobiotic metabolism is currently a subject of extensive research from the standpoints of genetic and metabolic aspects because of our increasing exposures to foreign respirable compounds that may alter and modify the metabolic activity and expression of pulmonary enzymatic systems. The lung, being exposed to air is a target organ frequently exposed to xenobiotics via inhalation (Pairon *et al*, 1994). Examples of lung diseases associated with respirable foreign particulate inhalation are coal workers' pneumoconiosis (CWP), bronchitis, emphysema, and silicosis (Green and Vallyathan, 1998; Kleinerman *et al*, 1979). CWP is an occupational lung disease associated with inhalation of poorly soluble respirable dust (Schins and Borm, 1999). It

may occur as a simple form or a complicated form known as progressive massive fibrosis (PMF) (Yeoh and Yang, 2002). In the simple form, only macules (<0.5 cm in diameter) appear in the lung and these consist mainly of dust-laden macrophages (Castranova, 2000). In the complicated form, PMF, the lesion is irregular coal dust-laden, fibrotic masses with haphazardly arranged collagen fibers associated with compromised lung functions (Castranova and Vallyathan, 2000).

At least one epidemiological study stated that lung cancer risk in smoking miners is not statistically different from, or even less than, other smoking populations (Costello *et al*, 1974). Although silica has been classified as carcinogenic by the International Agency for Research in Cancer (IARC, 1997), lung cancer was almost absent in lungs concomitantly exposed to silica and chemical carcinogens, such as PAH (Cocco *et al*, 2001). Attempts to determine the carcinogenic effect of coal dust and silica exposure in miners may be invalid because smoking miners are exposed to a mixture of the carcinogenic PAHs in cigarette smoke and the respirable insoluble particles that may modify chemical carcinogenesis. If respirable particles modify chemical carcinogen metabolism in the lung, epidemiologic studies of respirable particles in smoking miners may need to control respirable particles and smoking as modifiers rather than covariables.

Extrapolating from a rat model to determine the human response to inhaled particles is controversial (Mauderly, 1997), particularly when Nikula *et al* (1997) showed a difference in particle retention and pulmonary response to inhaled respirable particulates between rats and primates.

In this study, we investigated the hypothesis that pulmonary CYP1A1 induction by the model PAH, beta-naphthoflavone, is inhibited by respirable coal dust and silica. To overcome limitations of any specific animal model, we have investigated this hypothesis in rats, rabbits, and lambs. In addition, we have investigated changes in lung cell populations and their changing CYP1A1 expression after particle exposure. Finally, we investigated the association between altered CYP1A1 expression and particle associated apoptosis, caspase inhibition, Bax expression and inflammation.

OBJECTIVES

The objectives of this study were to:

1- Establish a relationship between coal dust or silica inhalation and deposition in the lung and CYP1A1 induction.

2- Establish a relationship between particle exposure and histopathological changes associated with deposition of these particles in lung alveoli, such as alveolar type II cell hyperplasia and hypertrophy and pulmonary inflammation.

3- Establish a relationship between particle-associated pulmonary changes and the pattern of CYP1A1 expression in lung alveolar cells.

4- Investigate these relationships in different animal models including rats, rabbits, and lambs.

5- Investigate the association of apoptosis, caspase inhibition, Bax expression, and inflammation with regulation of CYP1A1 expression by pulmonary exposure to respirable particles.

CHAPTER 2
REVIEW OF LITERATURE

1-Cytochrome P450s (CYPs)

1.A. Introduction

CYPs are membrane-bound heme-containing proteins (hemeproteins) resulting from expression of a gene superfamily containing about 1000 members that is found in all species ranging from prokaryotes to plants and animals (Hasler *et al*, 1999, Mckinnon, 2000). The letter P means a pigment that produces a broad absorption band with a peak of 450 nm (Omura and Sato, 1964; Remmer and Merker, 1965). Although the name cytochrome is a misnomer, because these are enzymes and not pigments, it has been established as a nomenclature for these proteins (Mckinnon, 2000). These proteins comprise a class of monooxygenases or mixed function oxidases, which activate molecular oxygen necessary for oxidative metabolism of a diversity of lipophilic organic materials (Barker *et al*, 1992; Hasler *et al*, 1999).

CYPs play vital roles in catalyzing biological reactions involved in drug and xenobiotic metabolism, steroid hormone biosynthesis, oxidation and metabolism of unsaturated fatty acids (Kawajiri and Fujii-Kriyama, 1991; Hasler *et al*, 1999, Petersen *et al*, 1991). The human CYP1A subfamily, which is the most extensively studied of these enzyme systems, consists of 2 functional genes: CYP1A1, which is involved in the metabolism of PAHs, and CYP1A2, which is involved in the metabolism of arylamine (Peterson *et al*, 1991).

1.B. History and Background

The first experimental evidence relating to CYP was documented in 1955 by Axelrod and Brodie *et al*, who identified an enzyme system in the endoplasmic reticulum of the liver that was able to oxidize xenobiotic compounds. In 1958, Garfinkel detected a carbon monoxide binding pigment in liver microsomes which had an absorption maximum at 450nm (Figure 1) during their spectrophotometric studies. This characteristic absorbance peak has been used since then as the signature of P450 proteins; i.e. the name P450 was derived from this property of the pigment. Because this absorbance was unique to CYPs among all hemeproteins (except nitric oxide synthase), it was used for specrtophotometric identification and quantification of CYPs activity. CYPs

remained a spectrophotometric puzzle until they were unveiled by Omura and Sato (1962, 1964) who identified the pigment as a hemeprotein. Soon after that, Estabrook *et al* (1963) demonstrated the role of adrenal cortex P450 hydroxylation of progesterone using the classic photochemical action spectrum technique developed by Otto Warburg (1949). By using the same methods, Cooper *et al* (1965) confirmed that P450s occurring in liver microsomes metabolize drugs and other xenobiotics.

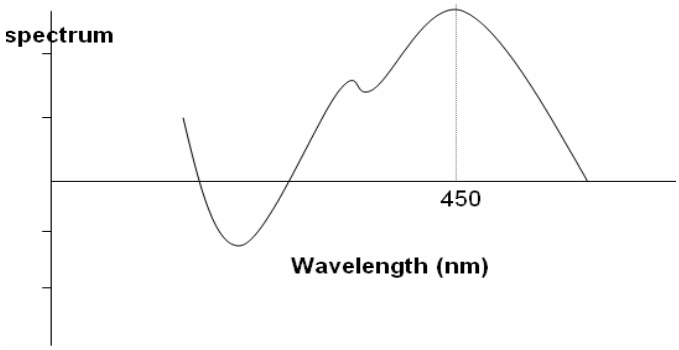

Figure 1. Absorbance spectrum of reduced form of CYP showing the maximum peak at 450 nm (Adapted from Thomas and Gillham, 1989).

CYPs enzymes have a wide tissue distribution as they have been isolated from many different mammalian tissues, including liver, kidney, lung, intestine, and adrenal cortex (Hasler *et al*, 1999). The amount of microsomal CYP in a human liver is comparatively high (e.g., ~7500 nmoles in a 1.5-kg liver). CYPs have also been isolated from insects, plants, yeast, and bacteria (Mckinnon, 2000). While CYPs are distributed in almost every organ, the types of CYPs in a tissue appear to be specific (Hasler *et al*, 1999). Ten families and 16 subfamilies of human CYPs have been identified, and their structure, function and regulation have been investigated. The contribution of each individual isoform of human CYPs to the metabolism and bioactivation of different carcinogens has been extensively studied by using gene- or cDNA-directed expression of CYPs and human liver microsomes in conjunction with specific antibodies (Kawajiri and Fujii-Kriyama, 1991).

1.C. Structure of CYPs

CYPs are hemeproteins that consist of a protein (the apoprotein or apoenzyme) and a heme moiety, called iron-protoporphyrin IX (Testa, 1995). This porphyrin is not only present in all CYP enzymes, but also in other hemeproteins -and enzymes such as

hemoglobin, myoglobin, catalase and most peroxidases. The protein component of the enzyme varies greatly from one enzyme/isozyme to the other. Therefore, differences in isozyme properties, such as molecular weight (approximate range 45 to 60 kDa), substrate and product specificities, and sensitivity to inhibitors could be attributable to this variation in protein.

The structure of the prosthetic heme of CYP is portrayed in Figure 2 (Testa *et al*, 1995). An iron cation is bound to the four pyrrole nitrogens. Two additional non-porphyrin ligands in axial positions, the fifth ligand X and the sixth ligand Y, are also shown. The X is the thiolate ligand, the chiral orientation of the heme shown in the Figure 1 is that found in CYP. The detailed structure of protoporphyrin IX has been revealed by X-ray crystallographic studies (Caughey and Ibers, 1977). Cytochrome P450cam, a soluble bacterial enzyme, showed comparable results by crystallographic examination (Poulos, 1988 and 1991; Poulos and Raag, 1992, Poulus *et al* 1986).

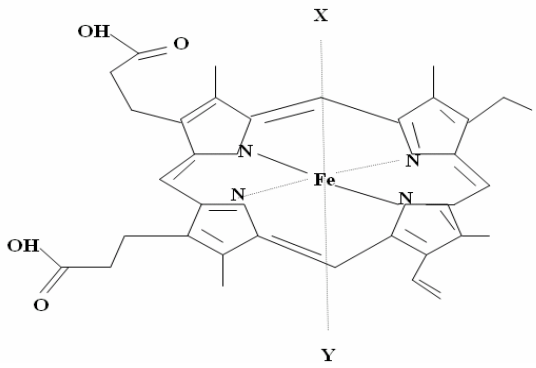

Figure 2. The structure of iron-protoporphyrin IX, the prosthetic heme of CYPs (Adapted from Pasta, 1995).

The fifth ligand to the iron cation (X) is a thiolate group that occurs near the carboxyl end of the protein from an essential cysteine. This ligand binds to the central heme by an extraordinary strong iron-sulfur bond, which is indispensible for the catalytic activity of CYPs (Black and Coon, 1985; Collman *et al*, 1976; Poulos and Raag, 1992; Silver and Lukas, 1982; Ruf *et al*, 1979.

The composition of the sixth ligand (Y) is controversial. Some years ago, a number of investigators demonstrated that this ligand was not a strong nitrogen-containing ligand, but a weaker, oxygen-containing one (Dawson *et al*, 1982; White and

Coon, 1982). This decision was based on the observation of a hydroxyl group, either from an adjacent amino acid residue or a water molecule (Kumaki and Nebert, 1978). Recently, the sixth ligand has been described as a hydroxyl group related to a tyrosinyl residue located near the heme, while in cytochrome P450cam (bacterial enzyme) it appears to be a water molecule (Janig *et al*, 1984; Poulos and Raag, 1992; Poulos *et al*, 1986).

The significance of the liganded heme in CYPs structure is extremely important. It can exist in different electronic states (either ferric or ferrous oxidation state) which are responsible for many of the properties of CYP, most significantly for the binding of ligands and the activation of molecular oxygen (Testa, 1995).

1.D. Nomenclature of CYP Genes and Proteins

It has been recommended that CYP genes be named according to the following rules (McKinnon, 2000; Nelson *et al*, 1996):

-The root symbol *CYP* for cytochrome P450

-An Arabic number for the cytochrome P450 family

-A capital letter for the subfamily; and

-An Arabic number for the individual gene

-When describing a CYP gene, all letters and numbers should be written in italics

-When describing a CYP protein, all letters and numbers should be in non-italicized form.

For example, *CYP1A1* is the gene encoding CYP1A1 where:

CYP: is the cytochrome P450

1: is the CYP family,

A: is the subfamily (expression of this particular subfamily is induced by aromatic hydrocarbons)

1: is the individual gene.

It is estimated that the various CYP families diverged from one another more than 1.2 billion years ago (McKinnon, 2000); consequently, any enzyme in a particular CYP family is less than 40% similar to any enzyme from another CYP family at the amino acid level (Nebert *et al*, 1987). In addition, the subfamilies diverged from one

another about 400 million years ago. Any 2 enzymes within the same subfamily generally share more than 55% amino acid similarity (Nebert *et al*, 1987). It is noteworthy that the nomenclature system was based upon the evolutionary relationships among CYP enzymes and not on substrate profiles because some CYPs from the same family have different substrate profiles or physiological functions (McKinnon, 2000).

1.E. Functions and Mechanism of Actions of CYPs

CYPs are known to catalyze reactions such as epoxidations, hydroxylations, *N-, S-, and O-* dealkylation, sulfoxidations, dehalogenations, *N*-oxidations, and many other reactions (Groves, 1985). The iron protoporphyrin IX center is the primary reactive site for these reactions. Seven sequential catalytic steps have been associated with CYPs-catalyzed reactions, which can be summarized as follows: (1) Substrate binding, (2) Reduction of the CYP from resting (ferric) to the ferrous state, (3) Formation of a ferrous CYP-dioxygen complex by binding of molecular oxygen, (4) Transfer of a second electron to the complex producing a peroxoiron (III) complex, (5) Protonation and cleavage of the O-O bond with the formation of reactive iron-oxo species, (6) Oxygen atom transfer from this oxo complex to the bound substrate, (7) Dissociation of the product. Therefore, CYPs function as monooxygenases (Hayaishi, 1962) or mixed function oxidases (Mason, 1957) by incorporating one of the two oxygen atoms of an O_2 molecule into a wide variety of lipophilic substrates with concomitant reduction of the other oxygen atom by two electrons to H_2O (Hasler *et al* 1999) as shown in the following CYP-dependent oxygenation reaction:

$$NADPH + O_2 + AH_2 + H^+ \longrightarrow NADP^+ + AHOH + H_2O$$

Ortiz de Montellano (1995) reported that some extrahepatic human CYPs have key roles in maintaining homeostasis and signal transduction as well as drug metabolism. For example, lungs and nasal tissues contain a considerable amount of CYP, and these sites may be important in the oxidation of xenobiotics entering the respiratory system. Renal CYPs may have a significant role in processing compounds generated in the kidneys or transported there from the liver. Moreover, one of the extrahepatic tissues with an important CYP activity is the small intestine (Orton and Parker, 1982) where CYP3A4 is abundant (Tamburini *et al*, 1984). It plays a major role in the metabolism of many orally administered drugs (Hardwick *et al*, 1987; Reddy *et al*, 1986). As a consequence, it

may considerably inactivate these drugs and reduce their bioavailability. The functions of CYPs in different human subfamilies are shown in Table 1 (Hasler et al, 1999).

CYP isoform	Metabolic functions
CYP1A and B	Polycyclic hydrocarbons. Nitrosamines
CYP2A	Drugs. Alcohols. Steroids
CYP3A	Drugs. Antibiotics. Flavenoids
CYP4	ω-oxidation fatty acids
CYP5	Thromboxane synthase
CYP7A	7α-Hydroxylase. Bile Acids
CYP8A and B	Prostacyclin Synthase. Bile Acids
*CYP11A and B	Cholesterol side-chain cleavage. Aldosterone synthesis
CYP51	Cholesterol Biosynthesis. 14-demthylase
*CYP40	Vitamin D3- 1α Hydroxylase
*CYP27	Bile Acid Synthesis
CYP26	Retinoic Acid Hydroxylase
*CYP24	Vitamin D degradation
CYP21	Progesterone 21-Hydroxylase
CYP19	Estrogen Biosyhthesis. Aromatase
CYP17	Steroid 17 α-Hydroxylase. Steroid C17/21 Lyase

Table 1: The human CYP subfamilies and their metabolic functions. An asterisk next to an isoform indicates mitochondrial enzymes. (Adapted from Hasler *et al*, 1999).

1.F. Biological Importance of CYPs and Their Role in Carcinogenesis

CYPs are important in the metabolism of xenobiotics and in the critical steps of steroid hormone biosynthesis. Because of these important roles, the regulation and mechanism of these enzymes have occupied a central place in the interests of pharmacologists and toxicologists. Accordingly, it was not surprising that when recombinant DNA technology emerged, CYPs were one of the first classes of enzymes to be cloned. The CYP1A1 cDNA (Kawajiri *et al*, 1986) and gene (Jaiswal *et al*, 1985a, 1985b; Kawajiri *et al*, 1986) have been cloned, sequenced, and localized on chromosome 15 near the *MPI* locus (Hildebrand *et al*, 1985).

Carcinogens that enter the body by different routes are metabolized by two major enzymatic systems: phase I and phase II enzymes (Mucci *et al*, 2001). Generally, phase I enzymes function by attaching specific groups to the compound thereby producing intermediate metabolites that are usually more reactive and carcinogenic than the original compound. Phase II enzymes also act to attach additional groups. These modifications detoxify or inactivate the reactive intermediate and prepare them for breakdown or excretion in a less lipophilic form (Mucci *et al*, 2001).

Human lung cancer often involves exposure to procarcinogens mainly contained in cigarette smoke, although the association of cigarette smoking with lung cancer differs by histological types. Most chemical procarcinogens require activation by Phase I enzymes, CYPs, to become reactive electrophilic forms that exert toxic or carcinogenic effects. Thus, CYPs are the key enzymes responsible for the initial metabolism of various procarcinogens present in our environment. Although several species of CYPs have been linked to lung carcinogenesis, CYP1A1 is one of the most important. It is expressed in human lung tissue and can metabolize PAHs in cigarette smoke such as benzo[a]pyrene (Hasler *et al*, 1999). In addition to its role in the production of electrophilic intermediate metabolites, CYP1A1 is also involved in the formation of highly reactive oxygen free radical species, such as hydroxyl radicals or superoxides as byproducts. These alterations may result in toxic responses or cellular damage and eventual carcinogenesis (Hasler *et al*, 1995).

1.G. The Inducibility of CYPs

Some of the CYP enzymes can be induced by substrate binding, thereby allowing the cells to adapt to changes in their chemical environment and maintain homeostasis (Denison and Whitlock, 1995). Drug and xenobiotic metabolism can be altered by induction of CYPs and other metabolizing enzymes. For example, the tolerance to barbiturates is a common body reaction associated with induction of drug metabolizing enzymes (James and Whitlock, 1999). Similarly, chemical carcinogenesis may be attenuated or inhibited by enzyme induction that increases the rate of detoxification (James and Whitlock, 1999). Consequently, enzyme induction can be a protective mechanism by which the cells metabolize the lipophilic compounds; otherwise they will accumulate to deleterious levels that overcome the defense mechanisms. By contrast,

induction can be disadvantageous in some instances. The enzyme induced by one substrate may increase the metabolism of a drug leading to attenuation of drug effects (Guengerich, 1997). Moreover, CYPs induction may lead to toxicity or neoplasia as a result of the oxygenation of PAHs (PAHs), present in cigarette smoke and other combustion products, producing highly reactive electrophiles called arene oxides that bind covalently to the cellular macromolecules resulting in carcinogenesis (Conney, 1982; Miller and Miller; 1981; Phillips, 1983)

2-Cytochrome P450 1A1 (CYP1A1)

(Family 1, subfamily A, polypeptide 1)

2.A. Introduction

CYP1A1, an inducible CYP (Hasler *et al*, 1995), is a member of the human P4501A subfamily which includes only 2 members, CYP1A1 and CYP1A2 (Ortiz de Montellano, 1995). These 2 isoforms have 70% similarity in their amino acid sequence (Ortiz de Montellano, 1995). In addition to liver (Whitlock, 1986; Issemann and Green, 1990; Gottlicher *et al*. 1992), CYP1A1 has also been detected in lungs (Antilla *et al*, 1991), placenta (Song *et al*, 1985), brain (Yun *et al*, 1998), and lymphocytes (Jaiswal *et al*, 1985b). CYP1A1 enzyme is involved in the metabolism of PAHs, whereas CYP1A2 is involved in the metabolism of arylamines (Peterson *et al*, 1991). It has been demonstrated that high inducibility of CYP1A1 is considered a risk factor for lung cancer in tobacco smokers (Anttila *et al*, 2001; Ishibe *et al*, 2001). Because smokers are exposed to carcinogenic PAHs, their CYP1A1 expression is induced (Willey *et al*, 1997).

2.B. Genetic Polymorphisms of *CYP1A1*

Since CYP1A1 participates in the biochemical activation of PAHs to produce mutagenic and carcinogenic derivatives, genetic polymorphism in CYP1A1 activity may alter susceptibility to PAH-associated diseases, such as lung cancer in smokers (James and Whitlock, 1999). Phenotypic polymorphism in the inducibility of CYP1A1 was originally described by Kellermann *et al* (1973) when he found that 10 % of Caucasians showed much higher lymphocytic CYP1A1 activity after exposure to an inducer than the rest of the group. In genotyping studies, two closely linked polymorphisms of the *CYP1Al* gene have been demonstrated in Caucasian and Oriental populations (Hasler *et al*, 1995). These include a 3'-flanking region Msp1 site (also called m2 allele) and the

exon 7 Ile-Val substitution (Val allele). The m2 allele has been associated with increased CYP1A1 inducibility in some studies whereas the Val allele is associated with enhanced enzyme activity *in vitro* (Hayashi *et al*., 1991, 1992). A new CYP1A1 polymorphism has been observed among black populations called Msp I AA (Kawajiri, 1999) and has a striking association with breast cancer risk (Taioli *et al*, 1995; Taioli *et al*, 1999).

2.C. Induction of *CYP1A1*

CYP1A1 induction was first discovered because it was observed that PAHs mediate their own metabolism. The studying of its induction mechanism was facilitated by several important observations (James and Whitlock, 1999). First, its induction is strong and evident compared to the background level. Second, the induction is affected by genetic polymorphisms, which made the genetic analysis possible. Third, *CYP1A1* induction has been demonstrated in cell cultures, which facilitates the gene transfer experiments. Experiments involving induction-defective mouse hepatoma cells demonstrated various groups of genes that synergistically contributed to the induction mechanism (Hankinson, 1995; Whitlock *et al*, 1996). It has been demonstrated that inducer binding was reduced in one mutant associated with low levels of aromatic (aryl) hydrocarbon receptor (AhR), which is an intracellular protein essential for the initiation of the induction process (Gonzalez *et al*, 1996; Okey, 1994). Another mutant defective in a protein called Ah receptor nuclear translocator (Arnt) showed disturbance of nuclear localization of liganded AhR (Whitlock *et al*, 1996). The studying of these mutants highlighted the possible role of different proteins in the mechanism of CYP1A1 induction (Hankinson, 1995; Whitlock *et al*, 1996).

2.D. Mechanism of *CYP1A1* Induction

It is well known that genomic DNA is associated with histones and other DNA-binding proteins to form chromatin, whose basic units are called nucleosomes. Chromatin configuration plays a key role in gene expression in that the presence of nucleosomes represses transcription (Grunstein, 1997; Wu, 1997; Kadonaga, 1998; Struhl, 1998; Gregory and Horz, 1998). It is important that transcription factors such as AhR and Arnt gain access to their cognate recognition sites on the chromatin to overcome the repressive effect of nucleosomes on gene expression (James and Whitlock, 1999). In uninduced cells, the *CYP1A1* enhancer/promoter region been suggested to be bound by nucleosome

according to indirect end-labeling analysis in mouse hepatoma cells (Morgan and Whitlock, 1992). The apparent cause of the low levels of CYP1A1 in uninduced cells is that the enhancer/promoter region is not accessible to transcription factors, particularly when the DNA binding sites are facing inward toward the histone (James and Whitlock, 1999). The induction process is initiated by binding of the inducer, such as PAHs to the AhR, which is usually located in the cytoplasm complexed with hsp90 and the AhR-interacting protein (AIP) (Ma and Whitlock, 1997). This binding results in the dissociation of the hsp90 and AIP followed by translocation of the AhR to the nucleus where it is conjugated with Arnt forming a heterodimer complex. The process of heterodimerization may be enhanced by phosphorylation at particular sites most probably on AhR (Career *et al*, 1992). The AhR/Arnt heterodimer binds to the xenobiotic responsive element (XRE) on the *CYP1A1* enhancer region resulting in gene transcription (Figure 3)

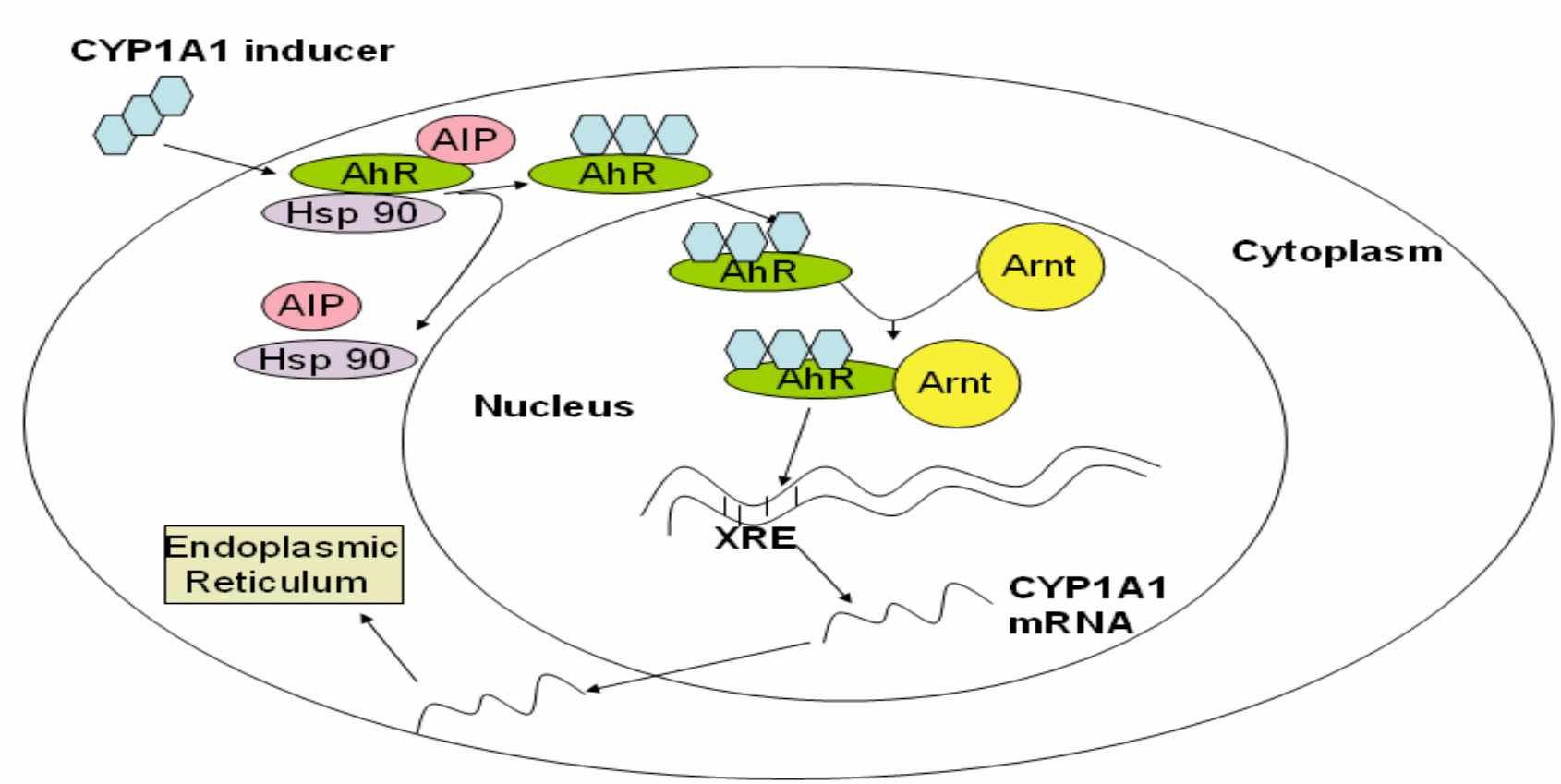

Figure 3. *CYP1A1* induction mechanism (Adapted from James and Whitlock, 1999). The binding of ligand to the AhR results in dissociation of the AhR-associated cytoplasmic proteins (Hsp90 and AIP) followed by translocation of AhR to the nucleus where it dimerizes with Arnt. AhR/Arnt heterodimer binds to the xenobiotic responsive element (XRE) at the enhancer region of *CYP1A1* gene stimulating chromatin changes, binding of initiating complex and *CYP1A1* induction.

2.E. The *CYP1A1* Inducers

Constitutive (background) expression of *CYP1A1* is very low in contrast to the inducible expression which is extremely robust. Most CYP1A1 inducers are also substrates metabolized by that enzyme which suggest that the induction process is an adaptive reaction of the body to enhance the detoxification process, particularly with the low concentrations of the inducers (James and Whitlock, 1999). Inducers for CYP1A1 are also ligands for the AhR, since most of the inducers, such as 2,3,7,8-tetrachlorodibenzo-*p*-dioxin (TCDD) have an extraordinary affinity for the AhR (Poland *et al*, 1986). Based on studies of structure-activity relationships, it was suggested that the AhR ligands are planar and interact with a hydrophobic pocket in AhR (Poland and Knotson, 1982). However, it was found that CYP1A1 expression can be mediated by the binding of compounds of different structure and lipophility to the AhR (Denison *et al*, 1998). Ligands for AhR may include specific indoles and other compounds from ingested food which suggests a relationship between diet and cancer prevention because ingestion of inducer-containing food may enhance the detoxification or activation of other potential chemical carcinogens (Bjeldanes *et al*, 1991; Fahey *et al*, 1997). Ligands for AhR also include PAHs, such as 3-methylcholanthrene, benzo(a)pyrene, polyhalogenated aromatic hydrocarbons, such as the 2,3,7,8-tetrachlorodibenzo p-dioxin (TCDD), and certain congeners of polyhalogenated biphenyls (Ke *et al*, 2001).

2.F. The role of CYP1A1 in carcinogenesis

The most commonly described mechanism of CYP1A1-mediated carcinogenesis involves the oxidation of benzo(a)pyrene (in cigarette smoke) into the intermediate reactive metabolite, benzo[a]pyrene diol epoxide (BPDE) (Bjelogrlic *et al*, 1993; Liang *et al*, 2003). This unstable epoxide is able bind to the DNA nucleotide bases, mainly adenine and guanine, producing stable adducts (Figure 4) that result in DNA mutations (Szeliga and Dipple, 1998). When such a mutation involves a critical gene, such as p53, it can lead to lung cancer (Vogelstein and Kinzler, 1992; Denissenko *et al*, 1996; Wang *et al*, 1995). A positive correlation has been established between DNA adducts and human lung cancer (Denissenko *et al*, 1996). Denissenko and his co-workers demonstrated that the DNA adducts caused by BPDE are distributed along exons of the P53 gene in Hela cells and bronchial epithelial cells, particularly at guanine positions in codons 157, 248,

ad 273. These positions are the same main mutational hotspots observed in human lung cancer (Denissenko *et al*, 1996).

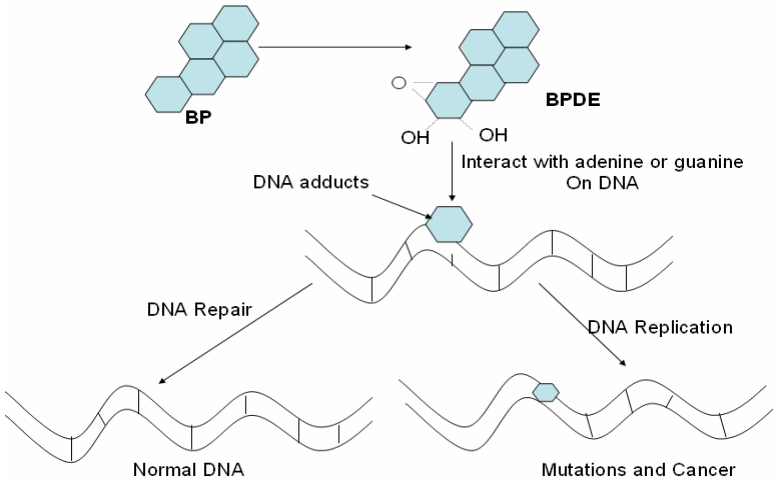

Figure 4: Mechanism of carcinogenesis induced by CYP1A1-catalyzed reaction (Adapted from: Geacintov, NE: http://www.nyu.edu/projects/geacintov/images/WEB_Figures/WEB_PAH3.htm).

2.G. Modification of CYP1A1 induction

2.G.1. Effect of Nuclear Factor Kappa B (NF- κB) and Tumor Necrosis Factor- α (TNF- α)

NF-κB is a pleiotropic transcription factor that plays important roles in the regulation of diverse physiological processes, such as inflammatory reactions, immune responses, cell proliferation, apoptosis, and developmental processes (Ke *et al*, 2001; Baldwin, 1996). NF-κB is a heterodimer which basically consists of a p65 (RelA) and a p50 (NF-κB -1) subunit, with RelA being the subunit conferring robust transcription activity. Some recent studies indicate a reciprocal inhibitory interaction between the AhR and NF-κB signaling pathways (Tian *et al*, 1999) which suggests that the NF-κB plays a key role in suppression of CYP1A1 expression by inflammatory responses associated with exposure to different agents.

Four different mechanisms have used to describe the regulation of CYP1A1 induction by NF-κB and TNF-α: (A) the interaction between NF-κB and the AhR repressor (AhRR), (B) the interaction between NF-κB and AhR itself, (C) the inhibition of histone acetylation of *CYP1A1* promoter by NF-κB, and (D) the suppression of CYP1A1 transcriptional elongation by NF-κB.

2.G.1.a. Effect of NF-κB on aryl hydrocarbon receptor repressor (AhRR)

AhRR is a member of the bHLH/PAS superfamily of transcription factors that is associated with the repression of AhR function (Baba *et al*, 2001, Mimura *et al*, 1999). This polypeptide (AhRR) represses AhR's function as a transcription factor by competing with it in forming a heterodimer complex with Arnt capable of binding to the XRE sequence. In addition, the expression of AhRR is induced by the AhR/Arnt heterodimer binding to an upstream XRE enhancer sequence; consequently regulation of AhR function is mediated by feedback inhibition of AhRR (Mimura *et al*, 1999). The *AhRR* gene has been localized to mouse chromosome 13C2, rat chromosome 1p11.2, and human chromosome 5p15.3 by fluorescence in situ hybridization analysis (Baba *et al*, 2001). Screening of the promoter sequence of the *AhRR* revealed multiple enhancer DNA elements: three XRE sequences (at the -45, -388, and -1296 position), three GC box sequences (at -36, -53, and -58), and one NF-κB binding site (at -28) (Baba *et al*, 2001). Since the binding of NF-κB to its cognate enhancer sequence of the AhRR gene upregulates AhRR expression, it was suggested that NF-κB downregulates CYP1A1 induction via repression of the AhR functional activity (Baba *et al*, 2001). This suggestion was supported by the suppressive effect of different cytokines, such as TNF-α, interleukin-1β, and interferon-γ on CYP1A1 induction (Barker *et al*, 1992, Calleja *et al*, 1997) since NF-κB is an upstream regulator of these cytokines (Scheidereit, 1998).

2.G.1.b. Direct Effect of NF-κB on AhR

Physical association between the RelA subunit of NF-κB and AhR has been demonstrated by an immunoprecipitation study (Tian *et al*, 1999). It was suggested that the non-activated AhR and NF-κB are retained in the cytoplasm and are kept apart by their association to their respective regulatory proteins [hsp90 associates with AhR (James and Whitlock, 1999) and IκB associates with RelA (Zhong *et al*, 1997)] resulting in compartmentalization. Upon extracellular activation signals, such as TCDD or BNF for AhR, and TNF for NF-κB, the AhR and NF-κB subunits dissociate from their respective regulatory proteins and interact with each other by physical association (Tian *et al*, 1999) producing an inactive complex that prevents AhR from binding to the enhancer sequences of CYP1A1 (Ke *et al*, 2001). This physical association could explain the downregulation of CYP1A1 induction by the activated NF-κB.

2.G.1.c. Effect NF-κB on Histone Acetylation at the *CYP1A1* Promoter.

NF-κB has been demonstrated to inhibit the ligand-induced acetylation of histone H4 at the *CYP1A*1 promoter, especially around the TATA box region. This prevents the AhR/Arnt heterodimer from binding to the XRE and results in downregulation of *CYP1A1* expression (Tian *et al*, 2002). This mechanism was illustrated by using the chromatin imunoprecipitation assay (Ke *et al*, 2001). Histone acetylation is known to enhance transcriptional activation (Strahl and Allis, 2002) which is brought about by assembly of the initiation complex (Ke *et al*, 2001). Silencing of gene expression has been associated with hypoacetylation. Therefore, NF-κB-induced suppression of histone acetylation is associated with silencing of *CYP1A1* gene expression. It has been suggested that the acetylation state of a histone is the result of 2 different intracellular processes; acetylation and deacetylation (Ke *et al*, 2001). Accordingly, the inhibition of the acetylation of histone H4 at the *CYP1A1* promoter could be attributed to either decreased histone acetyl transferase (HAT) activity or increased deacetylation by the histone deacetylase (Ke *et al*, 2001).

2.G.1.d. TNF-α Suppresses *CYP1A1* Transcriptional Elongation

Treatment of mouse Hepatoma (Hepa1c1c7) cells with dioxin resulted in an increase in the phosphorylation of the C-terminal domain of RNA polymerase II (Tian *et al*, 2003). This phosphorylation is essential for *CYP1A1* elongation. Treatment of the same cell line with TNF-α suppressed the phosphorylation of the C-terminus of RNA polymerase II, particularly at serine 2, resulting in interference with *CYP1A1* elongation (Tian *et al*, 2003).

2.G.2. Effect of Inflammation on CYP1A1 Induction

The effect of inflammation on CYPs has been extensively studied in rat hepatocytes (Morgan, 1997) which reflect responses detected *in vivo* in most cases (Morgan, 2001). The response of the body to infection or inflammation has been associated in most cases with suppression of CYPs, particularly in liver (Morgan, 1997). It was suggested that the suppression of CYPs expression during inflammation is not an adaptive or homeostatic response, rather the priority of the liver to assign its transcriptional machinery for synthesis of specific proteins necessary for controlling the

systemic inflammatory response (Morgan, 1989). However, different CYPs isoforms are regulated by different mechanisms and different cytokines (Morgan, 1997). In extrahepatic tissues, the CYPs are preferentially regulated by different inflammatory stimuli (Morgan, 2001). For instance, CYP1A1 is downregulated in brain inflammation whereas CYP2E1 is upregulated in astrocytes (Tindberg *et al*, 1996). Also the intracerebroventricular injection of bacterial lipopolysaccharides (LPS) suppresses CYP1A functional activity (Renton and Nicholson, 2000).

2.G.2.a. Effect of the Reactive Oxygen Species

It has been demonstrated that incubation of human hepatocytes with human serum obtained during the acute phase of infection and inflammation or with rabbit serum from turpentine-injected rabbits decreased the CYP2A1-associated theophylline metabolism without a reduction in CYP1A1 and CYP2A1 protein level (El-Kadi, 2000). Such a reduction in the catalytic activity of these CYPs was partially prevented by addition of antioxidant and exacerbated by antioxidant inhibitors (El-Kadi, 2000). The downregulation of CYPs associated with oxidant injury is a response of the body to prevent further generation of reactive oxygen species and minimize tissue damage (Morgan, 2001). Reactive oxygen intermediates (ROI), such a H_2O_2 (hydrogen peroxide), that are generated during some inflammatory processes might interact with the CYP1A1-associated Fe^{2+} resulting in heme destruction and enzyme inactivation (Karuzina and Archakov, 1994; Archakov *et al*, 1998). An alternative mechanism of CYP1A1-downregulation by reactive oxygen intermediates is mediated via direct phosphorylation of the isoform by kinases resulting in inactivation of the CYPs (Rhee, 1999). ROI, particularly oxygen radicals and hydrogen peroxides, stimulate protein kinase A (Suzuki *et al*, 1997), protein tyrosine kinase (Bae *et al*, 1997; Lowe *et al*, 1998), protein kinase C (Boyer *et al*, 1995), and mitogen-activated protein kinases (Goldstone and Hunt, 1997). The mechanism of the CYP1A1 inactivation by phosphorylation is not yet understood, although phosphorylation enhances the uncoupling of CYP1A1 from NADPH-dependent hydroxylation during xenobiotic metabolism (Mkrtchian and Andersson, 1990).

2.G.2.b. Effect of Reactive Nitrogen Species

Nitric oxide is produced by the inducible NO synthase (iNOS) during inflammatory responses (Morgan, 1997b). Evidence of involvement of NO in regulating

phenobarbital-induced CYP2B1 has been provided by Khatsenko *et al* (1997) when he showed that the administration of the N^G-nitro-L-arginine methyl ester (L-NAME), a nitric oxide synthase inhibitor, to rats simultaneously treated with Phenobarbital (CYP2B1 inducer) and lipopolysaccharide (LPS) prevented the down-regulation of CYP2B1 and CYP2B2 activity, mRNA, and protein. This relationship was further supported by Roberts *et al* (1998) who found that the *in vitro* incubation of CYP2B1 and peroxynitrite resulted in the nitration of tyrosines at either residue 190 or 203 or at both residues of CYP2B1 which coincided with a loss of 2B1-dependent activity. In addition, it has been demonstrated that the addition of nitric oxide to the V79-derived cell lines, which are known to constitutively express rat and human CYP1A1 and CYP1A2, inhibited the CYP1A1 activity in a dose-dependent manner (Stadler *et al*, 1994).

Different mechanisms of NO-associated CYP1A1 downregulation have been proposed. The most commonly accepted one is that nitric oxide binds to the heme moiety of the CYP1A1 forming an iron-nitrosyl complex in rat hepatic cells in a reversible phase, subsequently preventing the binding of oxygen which normally occurs at the catalytic site, and suppression of CYP1A1 functional activity (Wink *et al*, 1993). The same study also showed irreversible inhibition of CYP1A1 and CYP2B1 activity due to destruction of the integrity of the primary structure of hemeprotein, resulting from the action of nitrogen oxides produced from the oxidation of nitric oxide by oxygen. Not only does nitric oxide inhibit the CYP1A1 activity, but also downregulates the CYP1A1 expression by inhibition of CYP1A1 promoter activity as reported by studies on Hepa I cells (Kim and Sheen, 2002).

2.G.2.c. Effect of Inflammatory Mediators on CYP1A1 Expression

The inflammatory mediators or cytokines that are released in inflammatory conditions play an important role in the suppression of CYPs and their mRNAs (Bleau *et al*, 2001). For example, interleukin-6 (IL-6) suppresses CYP1A1, 1A2, 2D, 3A4, and 4A1, and IL-1β depresses 1A2, 2C11, 2D6, 2E1 and 3A *in vitro* (Fukuda *et al*, 1992; Trautwein *et al*, 1992; Donato *et al*, 1997; Parmentier *et al*, 1997). Moreover, TNF-α downregulates *CYP1A1* by inhibiting its transcriptional elongation in mouse Hepatoma cells (Tian *et al*, 2002).

Therefore, in a broad sense, inflammation is mostly associated with downregulation of CYPs by changing the activity and expression levels of different isoforms.

3-Anatomy, Histology and Physiology of Lung

3.A. Anatomy of Lung

Lungs are paired organs that occupy a large space in the thoracic cavity. Each lung is encapsulated by a thin-film membrane called pleura where it is free to move within this pleural sac (Getty, 1975). Generally, the lung has 2 lobes, the right and left, each one receives one of the major bronchi. It consists of a bronchial tree that starts with the major bronchi and ends in the terminal bronchioles (minute bronchi). Following the terminal bronchioles are the lung alveoli, which are sac-like structures (Figure 5) lined by respiratory epithelial cells and capillary endothelial cells. Lung alveoli are the major sites of gas exchange, where most of the blood capillaries are located.

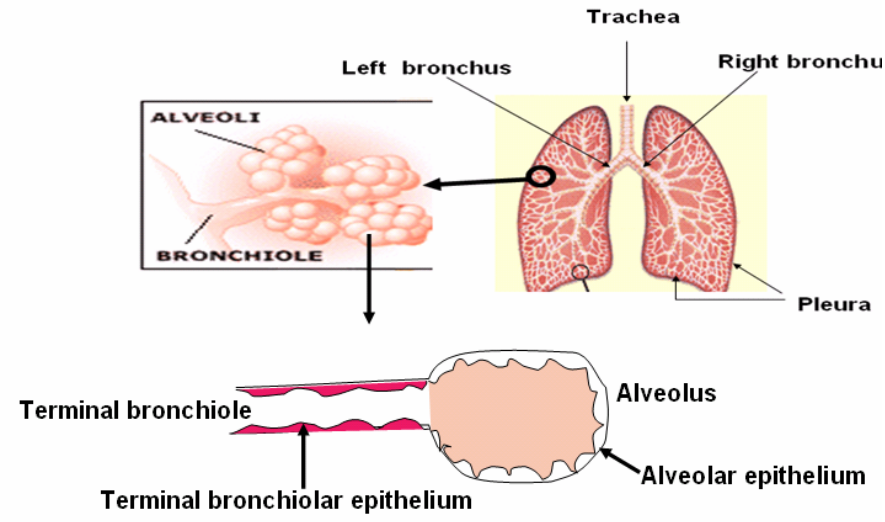

Figure 5: Schematic diagram showing the anatomical structure of lungs. The trachea bifurcates into right and left bronchi. Each major bronchus branches into smaller bronchi until ended by the terminal bronchioles. The terminal bronchioles open into the alveolar duct which leads to the alveoli. The alveoli are sac-like structures consisting of an alveolar wall that encloses the alveolar lumen. The alveolar wall is lined by alveolar epithelium.

(Adapted from: http://www.schoolscience.co.uk/content/4/biology/glaxo/pm3ast1.html)

3.B. Histology of Pulmonary Alveoli

Lung parenchyma is composed of many different cell types (Figure 6) with different pulmonary functions (Sorokin, 1970). The alveolar epithelium consists of 2 morphologically distinct cell types called alveolar type I cells (membranous pneumocytes) and alveolar type II cells (granular pneumocytes), which rest on a basement membrane (Dobbs, 1990, Castranova, 1988). The alveolar epithelial cells have tight intercellular junctions (Schneeberger, 1978). Alveolar type I cells appear long (squamous) with thin cytoplasmic extensions as indicated by transmission electron microscopy (Castranova *et al*, 1988). Alveolar type I cells comprise 96% of the epithelial surface area (Castranova *et al* 1988; Crapo *et al*, 1978) and 8-10 % of all lung cells (Crapo *et al*, 1978). These cells, being thin, facilitate and maximize gas exchange as they reduce the space between the air in alveolar spaces and the pulmonary blood capillaries (Castranova, 1988). On the other hand, AT-II cells are spherical (cuboidal) cells which are about 9 μm in diameter (Jones *et al*, 1982, Haies *et al*, 1981). This size is an intermediate size between the smaller endothelial cells and the larger macrophage and alveolar type I cells (Grapo *et al*, 1982; Crapo *et al*, 1978; Haies *et al*, 1981). These pneumocytes constitute 15 % of all lung cells (Dubbs, 1990) but cover less than 5 % of the alveolar surface (Dobbs, 1990, Castranova, 1988). Clara cells are a third type of epithelial cells present in lungs and are located at the end of the conducting airways near the alveolus and have important nonrespiratory functions (Devereux *et al*,, 1982). These cells are non-ciliated terminal bronchiolar epithelial cells containing extensive endoplasmic reticulum, abundant mitochondria and osmiophilic granules that distinguish them from other epithelial cells (Devereux, 1984; Plopper *et al*, 1980). The Clara cells have extremely high levels of xenobiotic metabolizing enzymes (Boyd, 1977).

Other cells with important biological functions are the alveolar macrophages (AMs). They are considered as part of the innate immunological defense system because they migrate and attack inhaled particles shortly after exposure (Kleinman *et al*, 2003). AMs are free migrating cells localized on the surface of the small airways and alveoli (Weibel, 1973). The reaction of AMs to the inhaled particles consists of progressive attacking steps. Following recognition, the AMs phagocytize these foreign particles in phagolysosomes and try to digest them by releasing lysosomal enzymes into phagocytic

vacuoles (Myrvik and Evan, 1967). Eventually, the digested foreign substances are excreted to the outside medium. Contact of AMs with the inhaled foreign particles or bacteria, results in a release of superoxide anions (Sweeney *et al*, 1981), which can be monitored by the measurement of AM chemiluminescence (Miles *et al*, 1978; Castranova *et al*, 1980).

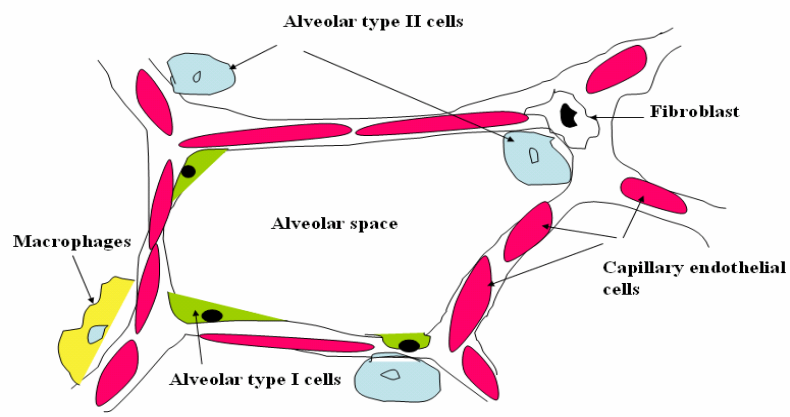

Figure 6: Schematic diagram showing that cells of alveolar wall include AT-II, alveolar type I, fibroblast, macrophages and capillary endothelial cells (Adapted from: http://www.biology.arizona.edu/chh/problem_sets/lung_toxicology/02t.html.)

3.C. Functions of Alveolar Epithelial Cells

The alveolar type I and AT-II cells enclose a space called the alveolar space (Castranova, 1988). Alveolar type I cells, which constitute the majority of alveolar surface help the gas exchange between the pulmonary blood capillaries and the alveolar spaces. The AT-II epithelial cells are multifunctional pneumocytes (Castranova, 1988).

One important function of AT-II cells, is to synthesize and secrete surfactant, which is a mucoid film surrounding the alveolar epithelium (Macklin, 1954). The alveolar lining material (surfactant) is composed of phospholipids, proteins, and carbohydrates (Dobbs and Mason, 1979; Brown and Longmore, 1981) and its major function is to reduce surface tension (Pattle, 1961). A reduction of surface tension is biologically important because it reduces the work required for lung inflation, maintains alveolar stability and prevents alveolar edema (Clements *et al*, 1959; Stub, 1966). AT-II-associated surfactant has been demonstrated to enhance phagocytosis and killing of

bacteria by alveolar macrophage (LaForce *et al*, 1973; Juers *et al* 1976). It also protects the lungs from potentially toxic inhaled particles (Wallace *et al*, 1985).

A second prominent function of AT-II cells occurs during the recovery of lungs from oxidant injury (Castranova, 1988). In contrast to type I cells, which are susceptible to oxidant injury, AT-II cells are resistant to oxidants and physical injuries (Cross, 1974; Crapo *et al*, 1982). Alveolar type I cells seem to be highly sensitive to the pulmonary toxicants because they were damaged first at a cellular level following pulmonary exposure to foreign toxicant (Weibel, 1974). This could be attributed to their relatively large surface area, which may approach 4500 μm^2 (Haies *et al* 1981) and their attenuated cytoplasm (Miller and Hook, 1990). Following injury of alveolar type I cells, AT-II cells proliferate (hyperplasia) (Stanley *et al*, 1992) and differentiate into type I cells in order to repair the alveolar epithelium and maintain the alveolar architecture (Melloni *et al*, 1995; Adamson *et al*, 1988; Thet *et al*, 1984) as shown by pulse label experiments (Castranova 1988). This is necessary because alveolar type I cells are incapable of dividing (Weibel, 1974), and because they are terminally differentiated cells. The process of differentiation of AT-II into type I cells occurs within 2 days of injury (Evans *et al*, 1973). The resistance of AT-II cells to the oxidant injury is attributed to the transport of vitamin C (an antioxidant) into these cells. Castranova *et al* (1983) demonstrated that AT-II cells contained a sodium-ascorbate cotransport system that allows the accumulation of the antioxidant ascorbate in AT-II cells, therefore increasing their resistance to oxidant injury.

In addition to the aforementioned functions, AT-II cells also play an important role in the metabolism of foreign compounds (xenobiotics) such as drugs and environmental pollutants because of their content of CYP monooxygenase system (Devereux *et al*, 1979; Jones *et al*, 1983; Raboveskey *et al*, 1986; Baron and Kawabata, 1983). They are rich in endoplasmic reticulum and sensitive to the exposure of toxic agents (Baron and Kawabata, 1983). Xenobiotic metabolism by AT-II cells is not restricted to inhaled foreign compounds but also includes circulating xenobiotics since these cells are in close proximity to capillary blood supply (Castranova, 1988).

Alveolar macrophages are migratory phagocytic cells located on the surface of the small airways and the alveoli (Weibel, 1973). These cells act as the lung's first line of defense against the toxic effects of inhaled particles, as they play a major role in the protection of lung against these particles. The reaction of alveolar macrophages to the inhaled particles is complex. Upon contact with the particles, AMs release superoxide anion (Sweeney *et al*., 1981), which could be monitored by measurement of chemiluminescence (Miles *et al*, 1978; Castranova *et al*, 1980). Eventually, AMs engulf these foreign particles and attempt to digest them by releasing lysosomal enzymes into phagocytic vacuoles (Myrvik and Evan, 1967).

4-Distribution and Localization of CYP1A1 and Other Isoforms in Pulmonary Alveoli of Different Animal Species

4.A. Human

In humans, CYP1A1 is constitutively expressed in very low level and the intensity of expression varies within different pulmonary cells (Antilla *et al*, 1991). By immunohistochemistry, CYP1A1 is mainly localized in the epithelium of the peripheral airways, the ciliated columnar epithelium of the bronchioles and the cuboidal and columnar cells of the terminal bronchioles (Antilla *et al*, 1991). Immunohistochemical staining was also observed in AT-II cells and in a few cases, within type I cells (Antilla *et al*, 1991). Pulmonary vascular endothelium infrequently showed CYP1A1 immunopositive staining but the alveolar macrophages were always negative (Antilla *et al*, 1991). Another important CYP isoform in humans is CYP1B1. CYP1B1 is regulated through the AhR and its mRNA was detected in liver, lymphocytes, cells of bronchoalveolar lavage and endometrium, but not in lung (Hakkola *et al***,** 1997). However, by immunohistochemistry, CYP1B1 was localized only in a range of malignant tumors, such as tumors of the breast, colon, lung, esophagus, skin, lymph node, brain, and testis and there was no detectable immunostaining for CYP1B1 in normal tissues (Murray *et al*, 1997). Therefore, CYP1B1 seems to be constitutively expressed in tumors (tumor specific) but undetectable in most normal tissue although CYP1B1 mRNA is present (McFadyen *et al*, 2003). Other isoforms, such as CYP2B6, CYP2E1, CYP2J2, and CYP3A5 proteins are expressed in human lung (Hukkanen *et al*, 2002).

4.B. Rodents

In rodents, the CYP activity of the lung has been demonstrated mostly in epithelial and endothelial cells (Pairon *et al*, 1994). CYP protein expression and activity has been identified in three main types of cells: Clara (terminal non-ciliated) cells in the bronchiolar epithelium, AT-II cells in the alveolar spaces, and endothelial cells in the vascular compartment (Serabjit-Singh *et al*, 1980; 1988; Plopper *et al*, 1987; Lacy *et al*, 1992; Jones *et al*, 1983; Kheith *et al*, 1987; Overby *et al*, 1992). Various materials of the lungs have been used to demonstrate the protein expression and activity of CYP isoforms in the lungs of rodents, such as the microsomes (Domin *et al*, 1986; Keith *et al*, 1987; Guengerich *et al*, 1982; Vanderslice *et al*, 1987; Tindberg and Ingelman-sundberg, 1989; Sesardic *et al*, 1990; Carlson and Day, 1992), isolated lung cell fractions of untreated or pretreated animals (Devereux *et al*, 1982; Lacy *et al*, 1992; Jones *et al*, 1983; Chichester *et al*, 1991), and tissue preparation for ultrastructural analysis (Serabjit-Singh *et al*, 1988; Overby *et al*, 1992; Aida *et al*, 1992). The predominant form of CYP in the uninduced rat lung is CYB2B1 (Guengerich *et al*, 1982), which is mainly localized in Clara cells and to a lesser extent in AT-II cells (Baron and Voigt, 1990; Kheith *et al*, 1987). In contrast to lung, the hepatic CYP2B1 is induced by Phenobarbital **(**Kim and Kemper 1997). Other CYP isoforms, such as 1A1 (Pairon *et al*, 1994), 2A3, 3A2, and 4B1, are also expressed in lung but in very small quantities (Foster *et al*, 1986; Voigt *et al*, 1990; Kimura *et al*, 1989; Keith *et al*, 1987; Vanderslice *et al*, 1987). The CYP2E1 protein is another isoform expressed only in rat lungs after being induced by substrates such as acetone or ethanol (Tindberg and Ingelman-Sundberg, 1989; Carlson and Day, 1992).

By immunohistochemistry and *in situ* hybridization techniques, 3-methylchlolantherene (3MC) - induced rat CYP1A1 was localized primarily in Clara cells and AT-II cells, with some labeling observed in other alveolar wall cells. These cells could not be specifically identified microscopically and were believed to be either alveolar type I cells or capillary endothelial cells (Pairon *et al*, 1994). In humans, similar results have been demonstrated without detection of any activity in the endothelial cells (Marcus *et al*, 1990).

4.C. Rabbits

In rabbits, the pulmonary CYP monooxygenase system includes three main isoforms of CYPs; 2B4, 4B1 and 1A1, which were previously classified as forms 2, 5 and 6, respectively (Daniels and Massey, 1992). CYP1A1 was demonstrated by immunohistochemistry in rabbits induced by TCDD using a polyclonal goat anti-rabbit CYP1A1 antibody and was localized mainly in the endothelial cells of the interalveolar septa (Overby *et al*, 1992). Within the endothelial cells, only the perinuclear area associated with endoplasmic reticulum was labeled with the antibody, and no labeling of the plasma membrane was detected (Overby *et al*, 1992). Minimal CYP1A1 labeling was detected in alveolar type I and AT-II cells with absence of macrophage immune reactivity (Overby *et al*, 1992). A dense CYP1A1 staining has been observed in the terminal non-ciliated bronchiolar epithelial (Clara) cells which are considered the primary pulmonary site of cytochrome P-450-dependent monooxygenase activity (Domin *et al*, 1986; Plopper *et al*, 1987; Serabjit-Singh *et al*, 1980). This could be attributed to the enrichment of the Clara cells with large amount of agranular (smooth) endoplasmic reticulum to which the CYPs are associated (Plopper, 1983). Although the CYP1A1 was not detected in the alveolar macrophages of TCDD-induced rabbit by immunohistochemistry (Overby *et al*, 1992), it was detected in the microsomal fraction of alveolar macrophages from rabbits administered with TCDD (Domin *et al*, 1986). While the major constitutive isoform of CYPs in rabbit lung is CYP2B4, this isozyme is present in very low concentrations in the liver of this animal species (Williams *et al*, 1991). However, treatment of rabbits with phenobarbital induces CYP2B4 in liver but has no effect on the levels in lungs (Williams *et al*, 1991). In contrast to CYP2B4, CYP1A1 can be induced in rabbit lungs by beta-naphthoflavone) using a dose of 80 mg/kg by intraperitoneal injection (Daniels and Massey, 1992).

4.D. Food Producing Animals

In food-producing animals, such as sheep and cattle, CYP1A1 is rarely investigated and little information is available about its expression and localization in pulmonary tissue (van't Klooster *et al*, 1993a). Knowledge about the CYP monooxygenase system in agricultural species is not only useful for describing the xenobiotic metabolism comparable to humans, but also extremely important for the risk

assessment of the applied veterinary pharmacotherapy and public health concern, particularly when these animals are considered as a main source of many foods (van't Klooster *et al*, 1993a; 1993b). This is particularly crucial because of the presence of drug residues and/or their metabolites in the foods of animal origin (van't Klooster *et al*, 1993b; Juskevich, 1987). The induction of CYP1A has been observed in cattle treated with pentachlorophenol (PCP), particularly in the liver and lung microsomes of the new born calves which were more responsive to induction than adults (Shull *et al*, 1986). The first CYP isoform purified from sheep lungs was the CYP2B, which was the most abundant form constitutively expressed in sheep lungs (constituting 75 % of the total CYPs) (Williams *et al*, 1991). Moreover, CYP1A1 and CYP2B1 have been induced in sheep hepatic microsomes after a single dose of ivermectin, a common antiparasitic drug in Veterinary Medicine (Skalova *et al*, 2001). In goats, the subcutaneous injection of beta-naphthoflavone (BNF) significantly induced CYP1A1 and CYP2B1 in liver microsomes as assessed by measurement of 7-ethoxyresorufin deethylase (EROD) and 7-pentoxyresorufin deethylase (PROD), respectively (van't Klooster *et al*, 1993b). BNF induces CYP1A1 in cultured hepatocytes isolated from sheep, goat, and cattle (van't Klooster *et al*, 1993b).

5-Pathological Alterations Associated with Respirable Particle Exposure

Lungs, being at the interface between the body and the environment, are major targets of many chemicals. They are exposed to xenobiotics carried by the inspiratory air and the blood (Pairon *et al*, 1994). The response of different alveolar cells to respirable particles is a complex process. Exposure to coal dust, silica, and/or other related inorganic particulates can activate alveolar macrophages to secrete cytokines, such as TNF-α and interleukin-1 (Kelley, 1990), fibronectin (Davies and Erdogdu, 1989), and other soluble mediators that act *in situ* (Kelley, 1990) producing acute cellular injury and initiating lung fibrosis (Davis, 1986). TNF-α plays a key role in the cellular response to particulate inhalation as it enhances the synthesis of other chemokines, such as interleukin-8 (IL-8), macrophage inflammatory protein 2 (MIP-2), MIP-1, and monocyte chemotactic protein 1α (MCP-1α) by alveolar macrophages, epithelial cells, endothelial cells and fibroblasts. In addition, TNF-α stimulates the endothelial expression of the adhesion molecules, such as vascular cell adhesion molecule 1 (VCAM-1), intercellular

adhesion molecule 1 (ICAM-1), and E-selectin. The intravascular inflammatory cells are recruited into the lung interstitium and alveolar spaces by interaction with the endothelial adhesion molecules and chemotactic gradients (Driscoll, 1996) (Figure 7).

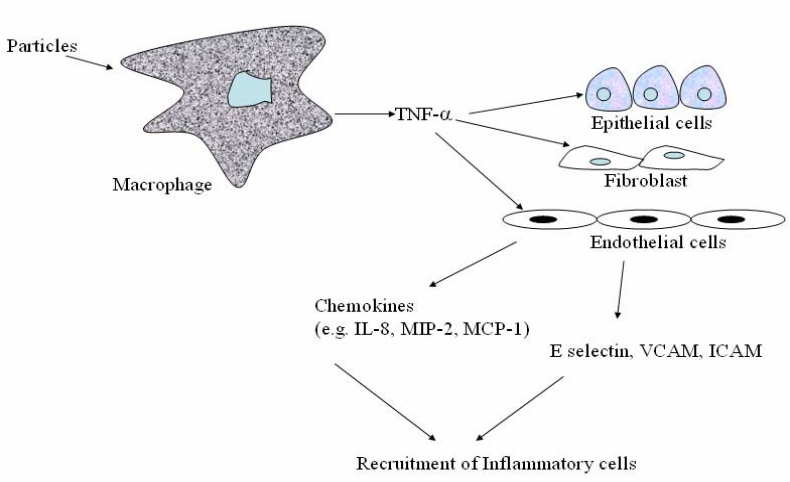

Figure 7. Proposed mechanism of pulmonary inflammation following exposure to respirable particles (Adapted from Driscoll, 1996).

Alveolar type I cells are more vulnerable to toxic and physical injury than AT-II cells (Lee *et al*, 1994). The damage of these cells usually leads to denudation of the subepithelial basement membrane (Evans *et al*, 1973; Adamson *et al*, 1974) with subsequent leakage of the plasma constituents, such as albumin, from the pulmonary vasculature to the alveolar spaces (Crouch, 1990).

AT-II cells generally respond to exposures of respirable particles, such as silica and coal dust, by increasing their number (hyperplasia) and size (hypertrophy) (Panos *et al*, 1990). The mechanism of cellular proliferation in response to particle exposure is unclear. Interestingly, carbon black, which has a minimum cellular toxicity, has been shown to produce a persistent AT-II cellular hyperplasia and neutophilic inflammation in rats (Harkema *et al*, 2003). A possible role of the extracellular signal-regulated kinases (ERKs) was suggested by Albrecht *et al* (2001) when they found a chronic activation of phosphorylated ERKs in immunohistochemical examination of lung sections of coal dust-exposed rats. The release of alveolar macrophage-produced mitogenic factor by activated macrophages is another possible role that enhances the cell cycle proliferation and DNA synthesis in rabbit AT-II cells (Brandes and Finkelstein, 1989). However, other factors in

the bronchoalveolar lavage (BAL) of normal rats have been shown to stimulate the DNA synthesis in the primary culture of rat AT-II cells (Leslie *et al*, 1989). This discrepancy was solved by Panos *et al* (1990) by demonstrating a similar mitogenic effect of BAL fluid collected from normal and silica-treated rats suggesting that other factors may be involved in the silica-associated AT-II hyperplasia. The AT-II hypertrophy associated with particle exposure could be attributed to cellular enlargement during cell division (Miller *et al*, 1986), an increase in cytoplasm during preparatory stage of differentiation and transition from AT-II to type I cells, or edema and degeneration associated with cell death (Miller *et al*, 1986; Baserga, 1985). It is well known that the cell size is increased during DNA synthesis and mitosis (Baserga, 1985) and the cell component should be duplicated during each cell cycle to maintain a uniform cell size between generations (Fraser and Nurse, 1978; Killander and Zetterberg, 1965). Furthermore, during lung injury and particle exposure, the AT-II cells can differentiate into type I cells, which have a volume of 2-5 fold greater than that of AT-II cells but are not considered hypertrophied AT-II cells (Crapo *et al*, 1983).

6-Respirable Particles Affecting Lung

6.A. Coal Dust Particles

6.A.1. Origin and Composition

Coal is produced by progressive coalification of swampy vegetation throughout the world. Although coal is composed mainly of carbon, coal mine dust also contains oxygen, hydrogen, nitrogen, trace elements and inorganic minerals and crystalline silica. Trace elements include copper, cadmium, boron, nickel, antimony, iron, lead, and zinc (Castranova and Ducatman, 1997). Some of these trace elements can be cytotoxic and carcinogenic in experimental models (Castranova and Vallyathan, 2000). The mineral contaminants may include kaolin, quartz, mica, calcite and pyrite. The rank of coal varies according to its carbon contents. As rank increases, the ratio of carbon to other mineral and chemical contaminants increases. Generally, higher rates of pneumoconiosis have been associated with anthracite coal mining than that found in bituminous miners. (Ortmeyer *et al*, 1973; Bunnet *et al*, 1979). This was attributed to the higher surface free radicals in anthracite than bituminous coal (Dalal *et al*, 1990; 1991; and 1995).

Moreover, anthracite has higher crystalline silica than bituminous coal (Wallace *et al*, 1994).

6.A.2. Exposure Conditions

There are two principal types of exposures in mining, surface and underground, that result in pulmonary exposure. Surface exposure usually occurs outdoors with inhalation of low levels of coal mine dust. Underground exposure is more frequently associated with inhalation of a significant amount of coal dust and development of pneumoconiosis. (Castranova and Ducatman, 1997). Mixed exposures are common in underground coal mining. For example, the pulmonary exposure to silica in roof bolters occurs during drilling processes into the noncoal ceiling of mines. Moreover, diesel equipment in coal mines produces mixed exposures to coal dust and diesel particulates (Castranova and Ducatman, 1997).

6.A.3. Pathological Reaction to Coal Mine Dust Exposure

Inhalation of coal mine dust is associated with several diseases in humans such as coal workers' pneumoconiosis (CWP), bronchitis, emphysema, Caplan disease and silicosis (Kleinerman *et al*, 1979; Green and Vallyathan, 1998).

6.A.4. Coal Workers' Pneumoconiosis (CWP)

6.A.4.i. Forms of CWP

CWP is classified according to severity into simple and complicated CWP. Simple CWP is characterized by black dust macules which are usually concentrated in the upper lung lobes. Coal nodules consist of coal dust and dust-laden macrophages usually localized at the bifurcations of respiratory bronchioles. These nodules can be palpable and have a diameter of 2-5 mm. This syndrome can progress to complicated CWP. With increasing time and dust exposure complicated CWP develops, that is, progressive massive fibrosis (PMF). In PMF, the lesions are bigger (1 cm diameter), more numerous, and usually localized in upper and posterior portions of the lungs. These lesions mainly contain increased collagen, coal dust, and inflammatory cells. The Federal Coal Mine Health and Safety Act of 1969 legislatively defined "black lung disease" to include not only CWP but also other chronic pulmonary diseases affecting coal miners,

such as chronic bronchitis and other obstructive pulmonary diseases (Castranova and Ducatman, 1997).

6.A..4.ii. Radiographic Picture of CWP

Simple pneumoconiosis is not always reflected in radiographic changes (Kleinerman *et al*, 1979). The sensitivity of the chest radiograph is affected by many factors, such as the lesion size, background density, contrast effect and thickening of the chest wall (Parkes, 1982; Morgan, 1984). When radiographic changes are present, radiographic opacities 0.001-l.0 cm in diameter may appear and are most frequently round opacities. With progression of CWP, the distribution of the opacities increases. As the PMF develops, there is an increase in the number of irregular opacities as well as an increase in nodular size to exceed 1.0 cm in diameter (Castranova and Ducatman, 1997; Rossiter *et al*, 1967). Chest radiographs are ranked by the size, shape, and profusion of the opacities. In simple CWP, rounded opacities are ranked by increasing size as p, q, and r. A scale of s, t, and u is used to rank irregular opacities. Distribution of lesions is designated as upper, middle, and/or lower lung zones. Profusion, which means increased density of opacities, has a rank of 0, 1, 2, or 3 (Vallyathan *et al*, 1996; Castranova and Ducatman, 1997). It has been demonstrated that profusion category has a direct relationship to dust burden in the lungs. PMF is categorized radiographically as A, B, or C as opacities progressively increased (Castranova and Ducatman, 1997).

6.A.4.iii. Pathology of CWP

The pulmonary pathological changes of CWP range from simple dust accumulation to fibrosis of varying degrees (Green and Vallyathan, 1998). Early coal dust exposure is manifested by aggregation of particles within the cytoplasm of intra-alveolar macrophages and is a marker of recent exposure. With time, the dust is localized around the walls of bronchi, lymphatics, and pulmonary vessels, and in the walls of respiratory bronchioles, without detectable fibrosis. The first distinctive lesion of CWP is the appearance of coal macules that are typically found in the walls of respiratory bronchioles, particularly at bifurcations. The coal dust macule is defined as an aggregation of coal dust-laden alveolar macrophages, in a size that range from 0.5 to 6 mm within the wall of respiratory bronchioles and adjacent alveoli (Vallyathan *et al*, 1996). Coal dust accumulation is accompanied by a variable degree of collagen

deposition. However, at this stage, the macule cannot be palpated (Castranova and Ducatman, 1997). With extended exposure, the fibrotic nodules can develop. As with macules, varying degrees of fibrosis and pigmentation can be found. When there is a central zone of concentric collagen fibers (rather than interlacing bundles of collagen), the nodules should be classified as silicotic nodules. The nodules are defined as an area of fibrosis and are firm when palpated. The nodules are usually located in a background of coal dust macules, however they can be an isolated finding. Nodules can be found in subpleural and peribronchial connective tissues as well as respiratory bronchioles. Focal emphysema is a specific form of emphysema seen in coal miners which is associated with distention and over expansion of alveolar spaces near fibrotic respiratory bronchioles (Castranova and Ducatman, 1997).

6.A.4.iv. Epidemiology of CWP

Epidemiological data suggests a direct relationship between the mass of respirable coal dust and the incidence of CWP in miners (Walton *et al*, 1977). A sequence of events has been supported by the epidemiological data during initiation and progression of CWP, which includes the following steps (Castranova and Ducatman 1997):

i) Coal dust is inhaled and deposited at the bifurcations of the respiratory bronchioles;

(ii) Localized inflammation begins and alveolar macrophages engulf coal dust particle to become dust laden. Aggregation of dust-laden macrophages forms a coal macule;

(iii) Coal macules enlarge and congregate to form coal nodules with further dust deposition and inflammation;

(iv) Pulmonary emphysema may follow when the lesions contract, tearing surrounding tissue; and

(v) Progressive massive fibrosis is the result of subsequent collagen deposition at sites of coal deposition.

6.A.4.v. Progressive Massive Fibrosis (PMF)

PMF is defined as a zone of fibrosis that has a diameter of greater than 1 cm, and can appear as single or multiple lesions (Vallyathan *et al*, 1998). Grossly, PMF lesions appear as hard, black masses which may be round, oval, or irregular but generally with a fairly sharp demarcation from the surrounding parenchyma. PMF often demonstrates

central cavitation that could be detected during sectioning. Microscopically, PMF is recognized either as an amorphous zone of collagen or aggregation of multiple nodules, which commonly co-occur with silicosis. The lesions usually contain a large quantity of coal pigment, cholesterol crystals and debris. PMF is a destructive and progressive lesion that distorts and obliterates functional lung tissue (Castranova and Ducatman, 1997). The PMF-induced distortion of the lung parenchyma is usually accompanied by compensatory emphysema (Vallyathan *et al*, 1996).

6.A.4.vi. Relationship between Coal Dust Exposure and Lung Cancer

Exposure to coal mine dust and the development of CWP has not been associated with lung cancer (Rooke *et al*, 1979). On the contrary, an epidemiologic study of US coal miners suggests that they have a lower than normal risk of lung cancer (Costello *et al*, 1974). Moreover, no relationship has been found between coal dust exposure and lung cancer type (Vallyathan *et al*, 1985). On the other hand, a higher than normal incidence of stomach cancer has been associated with coal dust exposure (Enterline, 1964). Ong *et al*, (1985) proposed a particular mechanism for developing stomach cancer associated with coal dust exposure. Initially, after the coal dust is swallowed and reaches the stomach, it intermixes with nitrite content of the food. The coal-associated organic material then undergoes a nitrosation under the acidic condition in the stomach. This nitrosation product has been demonstrated to induce the neoplastic transformation of a mammalian cell line (Wu *et al*, 1990).

6.A.4.vii. Mechanisms of Coal Dust-Induced Cellular Toxicity

Four main mechanisms of toxicity were proposed for initiation and progression of CWP (Castranova 2000). The first is the direct cytotoxicity of coal dust resulting in cell damage with subsequent release of proteases and lipases. The second mechanism includes over-production of oxidants by alveolar phagocytes, such as macrophages with a rate overwhelming the antioxidant defenses resulting in protein nitrosation and tissue injury. The third mechanism involves the activation of cytokines (chemical mediators) from alveolar epithelium and alveolar macrophages. These mediators recruit excessive numbers of polymorphonuclear leukocytes (PMN) and macrophages into the alveolar spaces with production of more oxidant, enhancing the pulmonary oxidant stress. The fourth mechanism is associated with fibroblast proliferation, enhancement of collagen

synthesis, and induction of pulmonary fibrosis upon stimulation by the growth and fibrogenic factors secreted from alveolar macrophages and alveolar epithelial cells in response to coal dust exposure

6.A.4.vii.a. Direct Cytotoxicity:

Coal dust has been shown by *in vitro* and animal studies to cause hemolysis (red blood cell lysis) and release of lactate dehydrogenase (LDH) from alveolar macrophages (Harrington 1972, and Amadis and Timilar, 1978). The direct cytotoxic effect of coal dust is affected by its metal content, such as nickel (Christian and Nelson, 1978) and iron (Dalal *et al*, 1995). Moreover, coal dust fracturing has been associated with the generation of surface radicals that can injure the biological membranes. However, these radicals are less bioactive that those generated during fracturing of silica (Vallyathan *et al*, 1995).

6.A.4.vii.b. Alveolar Macrophages-Stimulated Oxidant Production

A relationship has been established between the pathogenicity of the coal dust, pulmonary damage, and the ability to enhance oxidant production (Backford *et al*, 1997). Coal mine dust has been demonstrated to stimulate alveolar macrophages to increase the synthesis of reactive oxygen and nitrogen species such as superoxide, hydrogen peroxide, and nitric oxide (Castranova, 2000). These reactive oxygen species (ROS) induce cellular damage and injury (Weiss and Buglo, 1982). Moreover, coal dust may contain stable radicals that can produce ROS in the biological fluids resulting in direct oxidative damage in a non-cellular mechanism (Schins and Borm, 1999).

6.A.4.vii.c. Stimulation of the Proinflammatory Mediators Release

Coal dust exposure in animals elicits pulmonary inflammation that is characterized as infiltration of alveolar macrophages (AM) and polymorphonuclear leucocytes (PMN) in the alveolar spaces (Castranova *et al*, 1985, Bowden and Adamson, 1978). Once the phagocytic cells are recruited into the alveolar spaces, they stimulate the production of chemotactic cytokines and chemokines by AM and AT-II epithelial cells (Driscoll *et al*, 1993). The most common chemotaxins for PMNs are Leukotriene B_4, platelet-activating factor (PAF), and interleukin (IL)-1 (Driscoll, 1997). Tumor necrosis factor alpha (TNF-α) may not have a direct chemoattractant effect. However, it is a

potent chemokine stimulant, with effects on macrophage inflammatory protein (MIP-1 or MIP-2) and cytokine-induced neutrophil chemoattractant (Driscoll *et al*, 1995).

When the PMN are recruited into the alveolar spaces, they are stimulated by several inflammatory cytokines, such as TNF-α, PAF, and IL-1, to increase oxidant production resulting in excessive oxidant burden in the lung. The accumulation of oxidant may overwhelm the antioxidant defenses resulting in lung injury, scarring and fibrosis (Castranova 2000). In oxidative stress, The NF-κB is activated **(**Shukla *et al*, 2000), and upregulates the proinflammatory cytokines such as TNF- α **(**Kim *et al*, 2003) that aggravate the inflammatory process. Moreover, the released TNF- α activates the NF-κB by enhancing the phosphorylation and degradation of the inhibitor IκB as previously mentioned. Although there is little data on NF-κB in coal dust exposure, the NF-κB is activated by TNF- α in silicosis as shown by increasing of its DNA binding activity (Vallyathan *et al*, 1998).

6.A.4.vii.d. Stimulation of Growth and Fibrogenic Factors Production by AM

The fibrogenic factors produced by the alveolar macrophages and pneumocytes under the effect of coal mine dust exposure were detected in the bronchoalveolar lavage (BAL) of miners affected with CWP (Castranova, 2000). The most important of these growth and fibrogenic mediators that promote the lung response to fibrosis was the TNF-α, which has direct proliferative effects and enhances the secretion of platelet derived growth factor (PDGF) (Hajjar *et al*, 1987). Other mediators, such as transforming growth factor (TGF) α and β, and insulin-like growth factor (IGF) are released from AM and epithelial cells, and were found to stimulate the proliferation of mesenchymal cells (Bonner *et al*, 1991; Madtes *et al*, 1988; Moses *et al*, 1990; Rom *et al*, 1988). The glycoprotein, fibronectin, can stimulate fibroblast proliferation and greatly contribute to particle-associated pulmonary fibrosis (Rennard *et al*, 1981; Bitterman *et al*, 1983).

6.B. Crystalline Silica Particles

Exposure to crystalline silica, the crystalline form of silicon dioxide causes severe occupational lung disease in coal miners called silicosis (Castranova and Ducatman, 1997). Silicosis is a chronic inflammatory fibrotic lung disease (Miles *et al*, 1993) that is characterized by the development of silicotic nodules, chronic debilitation, and eventual

death in some cases (Driscoll and Guthrie, 1997). Crystalline silica has several polymorphs; those commonly investigated are the quartz, cristobalite, tridymite, coesite, and stishovite. The most toxic forms of crystalline silica are tridymite and cristobalite followed by quartz (Seaton, 1984). Chemically, silica is composed mainly of silicon dioxide (SiO_2) and some other cations may occur in trace amounts, such as aluminium, iron, and titanium. The iron content of silica may be involved in the production of reactive oxygen radicals through a Fenton-type reaction (Goodglick and Kane, 1986; Mossman and March, 1989) ($Fe^{3+} \longrightarrow Fe^{2+} + e^-$) that may greatly contribute to silica cytotoxicity (Razzaboni and Bolsaitis, 1990).

6.B.1. Mechanisms of Silica-Induced Cytotoxicity and Fibrosis

The cytotoxic effect of the silica is attributable to 4 major mechanisms. These mechanisms have been discussed in detail under the coal dust effect. However, in silicosis, the cytotoxic effect is more robust than coal dust for the following reasons:

1- The silanol group (SiOH), which is uniquely present on the surface of silica particulate, acts as an H donor. Therefore, it interacts with the biological membranes by forming a hydrogen bond resulting in injuries of these membranes (Nash *et al*, 1966). This was suggested because the polyvinylpyrilidine-N-oxide was found to reduce the silica toxicity by acting as proton acceptor, consequently protecting the biological membranes from the surface SiOH group.

2- The presence of the negative surface charge of the SiO^- group is crucial for silica-induced cytotoxicity (Nolan *et al*, 1999; Castranova and Vallyathan, 2000). This negative group could enhance the interaction of silica with the scavenger receptors on the surface of alveolar macrophages (Nolan *et al*, 1981; Kobzek, 1985).

3- Silica radicals, such as $Si^{\cdot}$ and $SiO^{\cdot}$, are usually produced at the fracture planes during fracturing of silica (Vallyathan *et al*, 1988). These radicals may participate in induction of oxidative stress, particularly when they come in contact with aqueous medium that results in the production of hydroxyl radicals (Vallyathan *et al*, 1988). It has been demonstrated that lipid peroxidation has a direct relationship with the hydroxyl radicals produced by silica *in vitro* (Vallyathan *et al*, 1988; Dalal *et al*, 1991) and *in vivo* (Castranova *et al*, 1996; Vallyathan, 1995).

4- The presence of surface iron in silica augments the production of hydroxyl radicals by silica exposure and enhances the cytotoxicity *in vivo* and *in vitro* (Vallyathan *et al*, 1988; Castranova *et al*, 1997).

6.B.2. Pathological and Inflammatory Responses to Silica Exposure

Pulmonary cytotoxicity in silicosis has been demonstrated on a large scale in animals and humans (Holland, 1990; Saffioti and Stinson, 1988, Green and Vallyathan, 1995). Different clinical types of silicosis have been identified based upon the intensity and the period of exposure or upon the chest radiographic picture (Driscoll and Guthrie, 1997; Green and Vallyathan, 1995, Ziskind *et al*, 1986; Seaton, 1984).

Radiologically, simple silicosis and progressive massive fibrosis can be identified. Simple silicosis is characterized by the presence of small opacities (silicotic nodules) (Ziskind *et al*., 1986; and Seaton, 1984) with a diameter of less than 10 mm (Weissman and Wagner, 2002) without respiratory impairment unless accompanied by tuberculosis (Snider, 1978 and Craighead *et al*., 1988). Simple silicosis may develop into progressive massive fibrosis (PMF) when congregation of these silicotic nodules occurs followed by destruction of lung tissue and a significant disturbance in lung function (Snider, 1978). Until now, 3 different types of silicosis are recognized: chronic, accelerated, and acute (Weissman and Wagner, 2002). The occurrence and development of these forms is determined by the amount of exposure and the total cumulative silica inhalation (Green and Vallyathan, 1995; Ziskind *et al*, 1986; Seaton, 1984). Chronic silicosis is characterized by the appearance of simple silicotic nodules 10-30 years post exposure (Weissman and Wagner, 2002) because it usually progresses very slowly. However, in some cases, nodules may congregate to form PMF (Weissman and Wagner, 2002). Accelerated silicosis, which develops in less than 10 years after exposure to silica (Weissman and Wagner, 2002), is accompanied by a rapid progression to PMF, severe lung dysfunction, and is life threatening (Ziskind, 1986; Seaton, 1984). Acute silicosis, on the other hand, is the form that develops very rapidly [(a few weeks to 5 years post exposure (Weissman and Wagner, 2002)] after exposure to high concentrations of silica (Banks *et al*, 19981; Suratt *et al*, 1977; Xipell, 1977) and is associated with severe alveolar and interstitial inflammation, alveolar proteinosis, and rapid respiratory failure (Driscoll and Guthrie, 1997).

7-Difference between CWP and Silicosis

CWP was originally thought to be a variant form of silicosis because of the similarity of chest radiographs of coal miners and silicotic people. A differentiation between CWP and silicosis was first proposed by Collis and Gilchrist (1928). They reported that Welsh stevedores who trimmed coal in the holds of ships developed nodules in the chest which were indistinguishable from those of underground coal miners. Histological examination of autopsied lungs from these coal trimmers showed lung lesions distinct from the characteristic whorled nodules of silicosis (Gouph, 1940). In 1947, Heppleston demonstrated that the histological pulmonary lesions in coal trimmers were similar to those in underground coal miners. In 1954, he showed that, these pulmonary lesions, in contrast to silicosis, consisted of black stellate dust macules surrounded by dilated respiratory bronchioles. In general, silicosis is more progressive than CWP and may initiate, develop and progress more rapidly (Scarisbrick, 2002).

8-Interaction Between PAH, AhR and Apoptotic Pathways

8.A. Role of AhR in Cellular Apoptosis

Apoptosis, or programmed cell death is a genetically-controlled process that occurs as a response of the cell to environmental (such as radiation) and developmental (e.g. embryogenesis) stimuli ending by programmed death of the cells (Wylie, 1980; Orren *et al*, 1997). Therefore, apoptosis is a negative selection mechanism by which the organism gets rid of damaged or unneeded cells (Buckley, 1998). Apoptosis plays an important role in tissue remodeling (Stanley *et al*, 1992) and eliminating cells that are excessively developed, improperly developed, or genetically damaged (Thompson, 1995). For example, the remodeling of certain epithelial cells, such as AT-II cells (Bardales *et al*, 1996) during the repair process following acute lung injury was attributed solely to the occurrence of apoptosis in these cells (Polunovsky *et al*, 1993).

Cellular death by apoptosis has characteristic hallmarks that start with condensation of the cytoplasm, loss of the plasma membrane microvilli, and nuclear condensation followed by fragmentation (Buckley, 1998). Apoptosis can be differentiated from necrosis by the presence of activated endogenous proteases, disruption of the cytoskeleton, cell shrinkage and formation of membrane blebbing, condensation of the

nucleus with DNA fragmentation forming oligonucleosomes, and elimination of the damaged cells without any inflammatory response (Thompson, 1995).

Apoptotic pathways initiate via different entry sites, such as death receptor (receptor pathway) or mitochondria (mitochondrial pathway) (Fulda, and Debtain, 2002). Both pathways result in the activation of effector caspases (**c**ysteine **asp**artate protea**ses**) (Kaufmann and Earshaw, 2000). The receptor pathway is associated with stimulation of death receptors of the tumor necrosis factor (TNF) receptor (TNFR) superfamily such as CD95 (APO1/Fas) resulting in receptor aggregation and recruitment of the adaptor molecule Fas-associated death domain (FADD) and caspase-8 (Sprick *et al*, 2000). The end result is the activation of caspase-8 that initiates apoptosis by direct cleavage of downstream effector caspases (Peter and Krammer, 1989). In the mitochondrial pathway, apoptogenic factors such as apoptosis inducing factor (AIF), cytochrome *c*, and caspase-2 or caspase-9 are released from mitochondria into the cytoplasm to activate caspase-3 by the formation of apoptosome complex (cytochrome *c*/Apaf-1/caspase-9) (Kroemer and Reed, 2000). This is followed by a downstream mitochondrial activation of caspase-8 resulting in further cleavage of effector caspases and apoptosis (Fulda, and Debtain, 2002) (Figure 8). Bax is a member of Bcl-2 family that comprises different proteins involved in controlling apoptosis and induced by a variety of stimuli (Desagher *et al*, 1999). Bax interacts with Bid, another preapoptotic protein belonging to Bcl-2 family resulting in conformational changes that drive Bax to translocate from cytosol to the mitochondria, increasing the release of cytochrome c and initiating apoptosis (Aiba-Masago *et al*, 2002) (Figure 8). However, Bax may be expressed in many tissues without demonstration of any apoptotic features (Olive and Ferrer, 1999, Penault-Llorca *et al*, 1998) suggesting that Bax has other cell functions (Aiba-Masago at al, 2002). Peptide caspase inhibitors Z-Asp-Ch_z-DCB and zVAD-fmk have been shown to inhibit apoptosis induced by overexpression of Bax in COS-7 cells suggesting that Bax induces apoptosis in a caspase-dependent mechanism (Kitanaka *et al*, 1997).

The DNA fragmentation associated with apoptosis was demonstrated by agarose gel electrophoresis that showed a ladder appearance at 200 base-pair intervals (Compton, 1992). More recently, Gavrieli *et al*, (1992) were able to localize the DNA fragmentation by visualization of apoptosis *in situ* using routine immunohistochemistry of paraffin

embedded tissue sections. This *in situ* apoptosis assay (ISAA) depends upon the binding of the terminal deoxynucleotide transferase to the $3^{/}$-OH end of the fragmented DNA and incorporating biotinylated deoxyuridine at the sites of DNA breaks. The localization of apoptosis was then visualized by binding of fluorescein- or peroxidase labeled avidine (Bardales, 1996; Gouchuico *et al*, 1997). The ISAA, which is also described as terminal deoxynucleotidyl transferase-mediated dUTP nick end labeling (TUNEL) proved more sensitive than the laddering assay in detecting apoptosis in different cells (Hagimoto *et al*, 1997).

Exposure of female mice to PAHs enhanced the expression of Bax in the oocyte, which was accompanied by induction of apoptosis. This was confirmed by the prevention of PAHs-mediated ovarian damage by selectively antagonizing the AhR by α-naphthoflavone (Shiromizu and Mattison, 1985; Mattison and Nightingale, 1980) or inactivation of Bax (Matikainen *et al*, 2001).

Apoptosis is considered the main cellular mechanism through which oocyte depletion is induced under both physiological and pathological conditions (Morita and Tilly, 1999; Perez *et al* 1997; 1999; Morita *et al* 2000; Pru and Tilly, 2001). Computer-based scanning of the promoter sequences of a number of regulatory genes involved in apoptosis showed that mouse Bax promoter has two core AhR response elements (AhRE1 and AhRE2) (Matikainen *et al*, 2001). In addition, increasing Bax mRNA levels and accumulation of its protein in quiescent (primordial) and early growing (primary) oocytes followed a single intraperitoneal injection of 9,10-dimethylbenz[a]anthracene (DMBA), a prototypical PAH (Matikainen *et al*, 2001). It is possible that Bax expression is directly regulated by the PAH-activated AhR which is indicated by the simultaneous expression of both AhR and Arnt in oocytes (Matikainen *et al*, 2001).

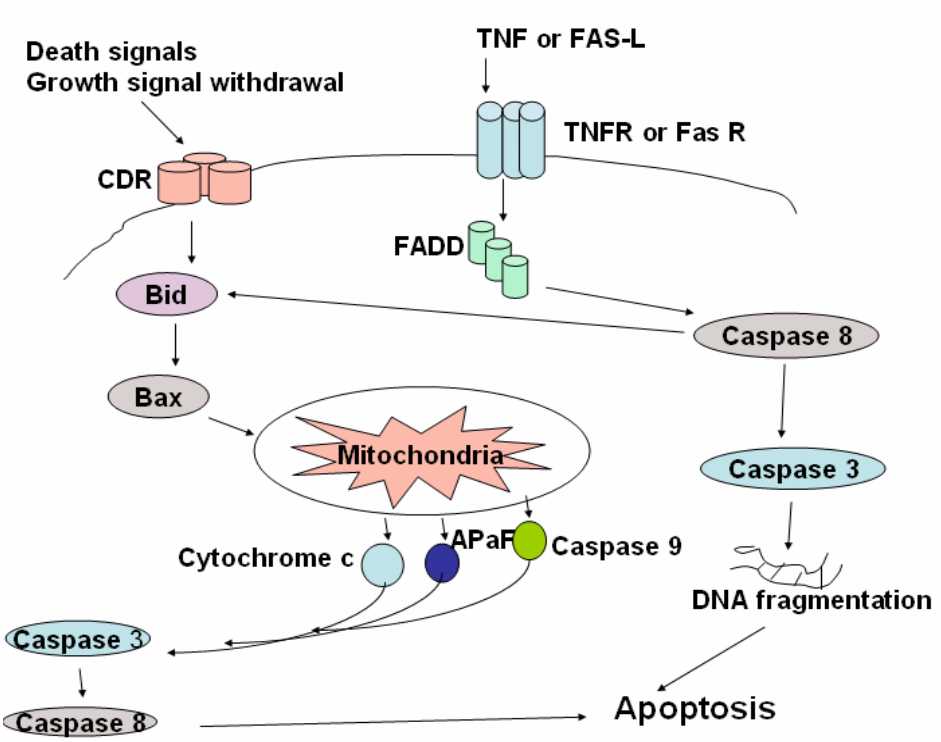

Figure 8. Diagram showing the apoptotic pathway through receptor dependent and mitochondrial dependent mechanisms (adapted from Fulda and Debtain, 2002; Spickle *et al*, 2000; Kroemer and Reed, 2000).

Although apoptosis remained detectable in Hepa-1 cells after blocking the CYP1A1 activity by 1-aminobenzotriazole (Mann *et al*, 1999), the MCF-7 human breast cancer cells are resistant to the dimethylbenz(a)anthracene-induced apoptosis due to reduction of CYP1A1 expression (Ciolino *et al*, 2002). The role of CYP1A1 in induction of dimethylbenz(a)anthracene-induced apoptosis in MCF-7 was attributed to its metabolization of this compound into a genotoxic forms that are able to bind to DNA leading to apoptosis (Ciolino *et al*, 2002).

8.B. Role of AhR in Cellular Proliferation

Interestingly, the AhR increases cellular proliferation (hyperplasia) by stimulating c-myc expression (Kim *et al*, 2000). The proposed mechanism involves the association of the AhR with the Rel A subunit of the NF-κB producing a complex that was able to cotransactivate the c-myc expression in non-malignant MCF-10F breast epithelial and malignant Hs578T breast cancer cells (Kim *et al*, 2000).

9-Role of AT-II Cell Apoptosis in Remodeling of Lung Parenchyma

Apoptosis or programmed cell death is known to play a role in tissue remodeling, as shown by remodeling of lung mesenchymal cells during the reparative phase of acute lung injury in humans (Polunovsky *et al*, 1993). Apoptosis is responsible for resolution of AT-II cell hyperplasia in patients with acute lung injury (Bardales *et al*, 1996). AT-II cell proliferation can be induced in different animal models by exposure to oxygen, ozone, asbestos, LPS (Ulich *et al*, 1994) silica (Albrecht *et al*, 2001; Friemann *et al*, 1999; Williams *et al*, 1993; Panos *et al*, 1990), coal dust (Friemann *et al*, 1999) and carbon black (Harkema *et al*, 2003). Recently, apoptosis has been demonstrated in the human epithelial cell line A459 and primary rat AT-II cells following exposure to ambient air particles of different sizes (Hetland *et al*, 2003).

10- Modification of CYP1A1-Induced Carcinogenesis by Exposure to Particles

The effect of respirable particles, such as silica and coal dust, on CYP1A1 induction has been studied to improve risk assessment for lung cancers in smoking coal miners. In one epidemiological study, the lung cancer risk in smoking miners was not significantly different or even less than other smoking populations (Costello *et al*, 1974). Recent epidemiologic studies have suggested that lung cancer in coal mine workers may not be detected because of the healthy worker-survivor effect (Albrecht *et al*, 2002).

The International Agency for Research in Cancer (IARC), has classified crystalline silica, in the form of quartz or cristobalite, as a carcinogen (IARC, 1997). Nine of the studies done by the IARC showed a higher risk of human lung cancer associated with silicosis (Castranova and Vallyathan, 2000). Previous findings were suspicious about the carcinogenicity of silica because of the limited evidence of carcinogenicity in humans, although there was sufficient evidence for carcinogenicity in animals (Holland, 1990).

It has been demonstrated that intratracheal exposure to silica alone without exposure to CYP1A1 inducers enhances the CYP1A1-dependent enzymatic activity (7-ethoxyresorufin-o-deethylase, EROD) in rat lung microsomal fraction (Miles *et al*, 1993). A recent case control study showed that occupational exposure to coal dust significantly enhanced the lung cancer risk in women (Rachtan, 2002). However, lung cancer was

mostly absent in people exposed concomitantly to silica and other lung carcinogens, such as PAH of cigarette smoke (Cocco *et al*, 2002). Based upon abundant epidemiological studies, Chechoway and Franzblau (2000) came up with the conclusion that risk assessment should interpret and manipulate silicosis and lung cancer as distinct entities whose cause/effect relationships are not necessarily associated.

The CYP1A1 induction is sometimes modified in mixed exposures relative to single exposures. For example, exposure to kerosene soot significantly increased the induction of CYP in rat lung; however, the co-exposure of the kerosene and chrysolite (asbestos) simultaneously significantly depleted the microsomal content of CYPs (Arif *et al*, 1994). Also, exposure to occupational crystalline silica dust decreased the activity of the CYP1A1-dependent enzymatic process, 7-ethoxyresorufin-*O*-dethylase (EROD), in rat lungs (Battelli *et al*, 1999) and rabbit lungs (Ghanem *et al*, 2003) exposed to a potent CYP1A1 inducer, beta-naphthoflavone. Furthermore, EROD activity was suppressed in a dose-dependent manner by intratracheal exposure to respirable, poorly soluble, coal dust particles in rats (Ghanem *et al*, 2003).

11-Pattern of CYP1A1 Expression in Cellular Proliferation

The CYP1A1-dependent enzymatic activity, EROD, was undetectable in proliferating cultures of mouse lung epithelial cells, but the level became detectable once cultures were confluent (Reiners *et al*, 1992). It was suggested that EROD expression was regulated as a function of the proliferative process of the cell culture. An inverse relationship between cellular proliferation and CYP expression was suggested by the observation that proliferative regeneration of hepatic cells following partial hepatectomy was associated with lower CYP protein levels and activities than normal liver (Hino *et al*, 1974; Presta *et al*, 1980; Klinger and Karge, 1987; Ronis *et al*, 1992). It seems that hepatic cells are allocated to replication, rather than transcription, with a main function of DNA being proliferate and regenerate the cells after hepatectomy (Liddle *et al*, 1989; Waxman, 1989; Morgan *et al*; 1985; Steer, 1995). Moreover, an inverse relationship exists between another form of CYP, CYP2B1 apoenzyme, and the proliferation level of AT-II cells, as previously concluded (Lag *et al*, 1996). The CY2B1 apoenzyme was lowest in AT-II cell culture during the most active proliferative stage, which coincided

with presence of largest number of cells in S-phase and highest proliferating cell nuclear antigen (PCNA) expression (Lag *et al*, 1996).

CHAPTER 3
RESPIRABLE COAL DUST PARTICLES MODIFY CYTOCHROME P4501A1 (CYP1A1) EXPRESSION IN RAT ALVEOLI

ABSTRACT

Cytochrome P450 1A1 (CYP1A1) plays a critical role in the metabolism of cigarette smoke-containing organic compounds, such as polycyclic aromatic hydrocarbons (PAHs), producing highly reactive intermediates that bind to cellular DNA and trigger lung tumors. Epidemiological studies report that coal miners, most of whom are smokers, have a lower risk of developing lung cancer than non-miner smokers (Costello *et al*, 1974). Therefore, we hypothesized that exposure to coal mine dust (CD) might be a modifying factor for development of pulmonary carcinogenesis by altering cell-specific CYP1A1 induction. To investigate this hypothesis, we evaluated the ability of CD particles (less than 5 microns) to prevent induction and activity of pulmonary CYP1A1. For that purpose, male, Sprague Dawley rats (220-270g) were intratracheally instilled with 0, 2.5, 10, 20, 40 mg coal dust/rat or vehicle (saline). Eleven days later, the pulmonary CYP1A1 was induced in all rats by intraperitoneal (IP) injection of β-naphthoflavone (BNF: 50mg/kg IP), as a well-known potent CYP1A1 inducer. After 3 days, rats were sacrificed and the metabolic activity of CYP1A1 was measured as 7-ethoxyresorufin-O-deethylase (EROD) activity in fresh lung microsomes. The amount of CYP1A1 protein in lung microsomes was quantified by Western blot using a polyclonal rabbit anti-rat CYP1A1 antibody. Cell-specific expression of CYP1A1 was quantified by dual immunofluorescent staining of CYP1A1 and cytokeratins 8/18, cytoskeletal proteins highly expressed in alveolar type II (AT-II) cells. Our data showed a dose-dependent suppression of EROD activity by CD exposure (r^2= 0.399, p=0.0028). Western blot CYP1A1 protein was significantly lower in rats exposed to the highest dose (40 mg/rat) of CD and BNF than rats treated with BNF alone (p=0.031). Immunoflourescent examination showed a significant reduction of CYP1A1 area colocalized in AT-II cells in rats exposed to CD 20 and 40 mg and BNF compared to rats treated with BNF alone. These findings suggest that CD exposure modifies BNF-mediated CYP1A1 induction by altering its cell specific localization in pulmonary alveoli and interferes with CYP1A1 metabolic activity.

INTRODUCTION

Studies of CYPs have recently received a great interest because these enzymes play critical roles in metabolism of drugs, carcinogens, dietary xenobiotics and steroid hormones (James and Whitlock 1999). The CYP proteins are heme-containing proteins, which are members of a gene super-family that contains almost 1000 members in species ranging from bacteria to plants and animals (Hasler *et al*, 1999). Cytochrome P4501A1 (CYP1A1) has garnered particular interest because of its involvement in the conversion of organic compounds, like polycyclic aromatic hydrocarbons (PAH) in cigarette smoke, into carcinogenic intermediate species (Crespi *et al*, 1989; Shimada *et al*, 1989; Eaton *et al*, 1995) that can initiate lung cancer development. Moreover, the expression of CYP1A1 can be induced at the transcriptional level by its substrates. The transcriptional regulation of the CYP1A1 gene by polycyclic aromatic hydrocarbons (PAH) is mediated through ligand-dependent activation of the aryl hydrocarbon receptor (AhR), which translocates to the nucleus upon activation, dimerizes to the aryl hydrocarbon receptor nuclear translocator (Arnt) protein and binds to the xenobiotic responsive element (XRE) in the regulatory region of the CYP1A1 gene (Ma and Whitlock 1997; Tian *et al,* 1999,)

Coal is a fossil fuel mined all over the world. Coal mine dust generated during underground coal mining results in significant respiratory exposure to coal miners. In addition to the carbon, which is the main component of coal, it also contains oxygen, nitrogen, hydrogen, and trace elements, including non-coal minerals. The trace elements may include copper, nickel, cadmium, boron, antimony iron, lead, and zinc (Sorenson *et al,* 1974). Some of these trace elements can be cytotoxic and carcinogenic in experimental models (Castranova 2000). Mineral contaminants include quartz, kaolin, mica, pyrite and calcite (Parkes, 1994). Coal dust inhalation is associated with development of a respiratory disease of coal miners called coal workers' pneumoconiosis (CWP). CWP is categorized according to severity into simple and complicated CWP. In the simple form, black dust macules appear and consist of dust-laden macrophages concentrated near respiratory bronchioles. In complicated CWP, also described as progressive massive fibrosis (PMF), the nodules are larger (exceeding 1 cm diameter), and more numerous. These nodules contain increased amount of collagen, coal dust, and inflammatory cells (Castranova, 2000).

Epidemiological studies demonstrated that lung cancer in coal miners occurs less frequently than in general population after adjustment for age and smoking (Meijers *et al*, 1991; Kuempel, 1995). Instead, coal dust exposure is associated with lung scarring (pulmonary fibrosis) and accumulation of particles in dust-laden alveolar macrophages (Castranova, 2000). Most of the studies of lung cancer in coal miners are difficult to interpret because most of the miners are smokers. This means that they are exposed to a mixed exposure of the coal dust particles and the carcinogenic compounds of cigarette smoke. Recent studies from our laboratory suggest that exposure to another occupational dust, crystalline silica, decreases the activity of the CYP1A1-dependent enzymatic process, 7-ethoxyresorufin-*O*-dethylase (EROD), in rat lungs exposed to a potent CYP1A1 inducer, beta-naphthoflavone (Battelli *et al*, 1999). Silicosis in rats is also associated with the appearance of new population of alveolar epithelial cells without detectable expression of CYP1A1 or CYP2B1, even after exposure to inducers of CYP1A1 (Battelli *et al*, 1999; Levy *et al*, 1997). If other fibrogenic inhaled particulates, such as coal dust, also reduce the activity of carcinogen-activating CYP1A1-dependent enzymatic processes, the expected result would be a reduction in the lung cancer attributable to chemical carcinogens activated by CYP1A1, such as the PAH in cigarette smoke. Therefore, we investigated the effect of coal dust inhalation on the metabolism of chemical carcinogens in lungs of rats. These studies will help determine if the effect of silica on CYP1A1 is a unique feature of silica dust or is a characteristic of pulmonary exposure to other respirable particles, which cause alveolar epithelial cell hypertrophy and hyperplasia, such as coal dust. For that purpose, we designed a dose response experiment in rats to investigate the dose-dependent effect of CD. We injected beta-naphthoflavone (BNF) of the PAH family, as a potent and specific CYP1A1 inducer (Lee *et al*, 1998). The study utilized the immunofluorescent localization of critical proteins and morphometric analysis of immunofluorescent-stained tissue to investigate the effect of coal dust on the expression of CYP1A1 in the deep lung. We also determined the CYP1A1-dependent enzymatic activity in lung microsomes. Lungs from the same rats were microscopically examined to determine histopathological alterations associated with changes in cell specific protein expression. The amount of CYP1A1 protein in the lung microsomes of control and exposed rats was determined by Western blot analysis using

polyclonal rabbit anti-rat CYP1A1 antibodies. To our knowledge, we demonstrated for the first time that CD exposure inhibits the PAH-induced CYP1A1-dependent enzymatic activity in a dose responsive fashion. This suppression was also observed in pulmonary alveoli of CD exposed rats in immunofluorescent-stained section. In addition, the amount of CYP1A1 detected by western blot in lung microsomes was also diminished.

MATERIALS AND METHODS

Animals

Male Sprague-Dawley rats (~220-270g) were purchased from Hilltop Labs (Scottsdale, PA). Upon arrival, the rats were kept in an AAALAC-approved barrier animal facility at NIOSH. Food and water were supplied *ad libitum.* Rats were housed in Shoebox cages on autoclaved hardwood and cellulose (Alpha-Dri) bedding in HEPA filtered laminar-flow, ventilated cage racks (Thoren). Rats were allowed to acclimatize in their cages for at least 7 days before the experiment.

Experimental Design

By using a research randomizer program (www.randomizer.org), rats were randomized into five groups, of 4 rats each. Each group was intratracheally (IT) instilled with 0, 2.5, 10, 20, or 40 mg CD /rat (~ 0, 1, 4, 8, and 16 mg/100 gm BW) suspended in sterile saline. Eleven days later, rats were intraperitoneally (IP) injected with the CYP1A1 inducer beta-naphthoflavone (BNF) (50 mg/kg BW) suspended in filtered corn oil. Three days after BNF injection, rats were euthanized and the right lung lobes were homogenized for collecting the lung microsomes whereas the left lungs were inflated with 10% neutral buffer formalin for histopathology.

Coal Dust Particles:

The size of these particles was less than 5 microns with surface area 7.4 m^2/g. The particles contained 0.34 % total iron of which 0.119 % is surface iron. The particles were weighed, placed in a scintillation vial, covered with foil and heat sterilized in an oven at 160 ºC for 2 hours. Coal dust suspensions were prepared from heat-sterilized samples using non-pyrogenic sterile saline (Abbott Laboratories, North Chicago).

Intratracheal Instillation

The coal dust particles were suspended in sterile saline at a concentration of 8.3, 33.3, 66.6, and 133.3 mg/ml. Rats received either 0.3 ml of this suspension (~2.5, 10, 20, and 40 mg/rat) or equivalent dose of saline (vehicle). The rats were anesthetized by intraperitoneal (IP) injection of sodium methohexital (Brevital, Eli Lilly Indianapolis, IN) and were intratracheally instilled using a 20-gauge, 4-inch ball-tipped animal feeding needle as previously described (Porter *et al*, 2002)

Beta-Naphthoflavone (BNF) Preparation

Solutions of 5 % BNF (Sigma, St. Louis, MO) in corn oil (50 mg/ml) were prepared one day before intraperitoneal (IP) injection. Prior to use, the corn oil was filtered with non-pyrogenic Acrodisc 25 mm syringe filter (0.2 μm in diameter) (Pall Gelman sciences, Ann Arbor, MI) to assure sterility. The solution suspension was vortexed until the particles were evenly suspended and then sonicated in Ultronics sonicator (Mahwa, NJ) for 15 minutes before injection. BNF solutions were injected once, IP, at a dose of 50 mg/kg 3 days before sacrifice.

Euthanasia

Euthanasia was induced by IP injection of 0.5 ml 26% sodium pentobarbital (Sleepaway®, Fort Dodge Animal Health, Fort Dodge, IA) 2 weeks after CD exposure.

Necropsy

The lungs and attached organs including tracheobronchial lymph node, thymus, heart, aorta, and esophagus were removed. The right lung lobes were collected and weighed at necropsy for microsomal preparation while the left lung lobe was inflated with 3 cc of 10% neutral buffered formalin (NBF). Tracheobronchial lymph nodes, liver, spleen, and right and left kidneys were also fixed in 10 % NBF. Fixed tissues were trimmed the same day, routinely processed in a tissue processor and embedded in paraffin the following morning. Tissue sections of left lung were stained with Hemotoxylin and Eosin (H&E). Additional 5-micrometer sections were used for immunofluorescence.

Microsomal Preparation

Lung microsomes were prepared for determination of EROD activity as an indicator of the CYP1A1-dependent enzymatic activity, 7-pentoxyresorufin-*O*-deethylase (PROD) activity as an indicator of the CYP2B1-dependent enzymatic activity, and for Western blot analysis of CYP1A1 and CYP2B1 proteins. Microsomes were prepared as previously described (Flowers and Miles, 1991; Ma *et al*, 2002). At the necropsy, the right lung lobes were weighed and chopped 4 times with a Mc1Iwain tissue chopper (Mickle Engineering Co., Gomshall, Surrey, UK) set at slice thickness of 0.5 mm. Then, the chopped lung tissues were suspended in ice-cold incubation medium (145 mM KCL, 1.9 mM KH_2PO_4, 8.1 mM K_2HPO_4, 30 mM Tris-HCL, and 3 mM Mg Cl_2; pH 7.4) at a ratio of 1gm lung to 4 ml incubation medium. The suspended solution was homogenized using a Teflon-glass Potter-Elvejhem Homogenizer (Emerson, NJ) through 16 complete passes. The cell nuclei and debris were removed by centrifugation of the homogenate at 2500 rpm for 10 minutes in a Sorvall Model RC2-B refrigerated centrifuge (Ivan Sorvall Co., Northwalk, CT). Mitochondria were slowly deposited by three sequential centrifugations for 20 minutes each at 5,000, 9,000, and 13,000 rpm to reduce the mitochondrial contamination of the microsomes. The resulting supernatant was ultra-centrifuged at 40,000 rpm for 75 minutes in a Beckman Model L5-50 Ultracentrifuge (Beckman Instruments, Palo Alto, CA) to get the microsomal fraction (Figure 1). The pellet was re-suspended in the incubation medium in a ratio equal to the original lung weight (i.e. 1gm lung/ 1ml medium) and frozen at -80C until assayed.

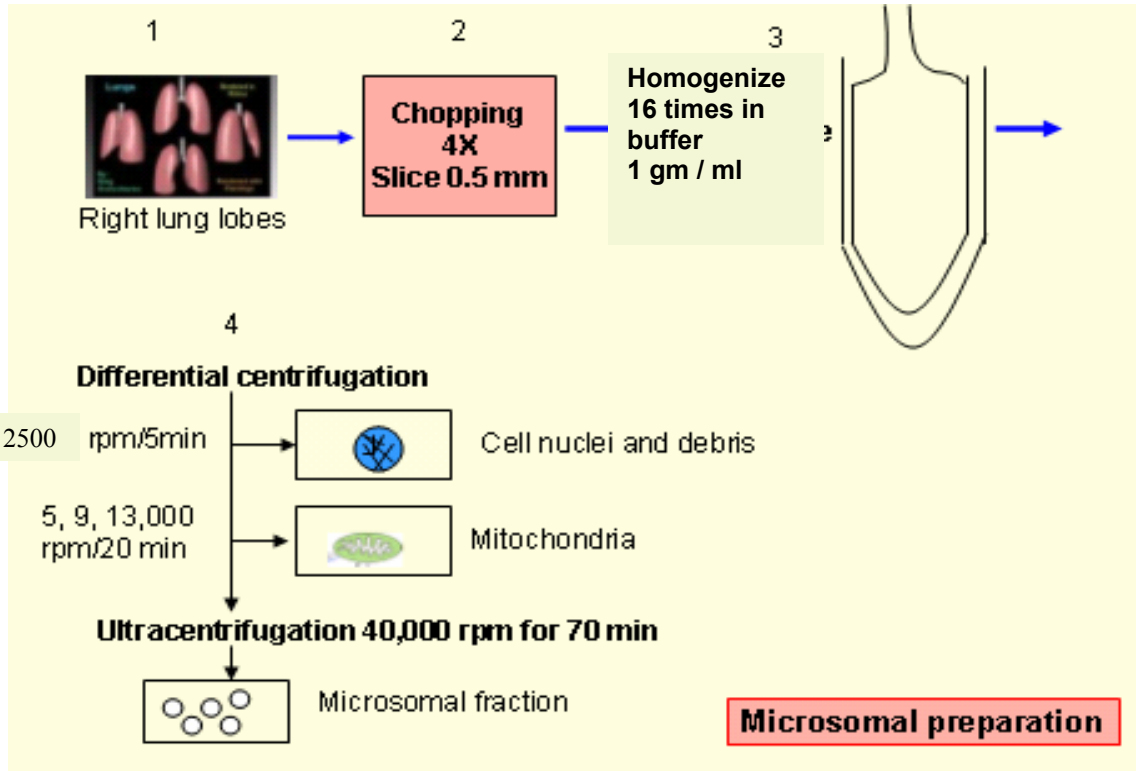

Figure 1. Four main steps involved in the microsomal preparation of rat lungs. The process included (1) Collecting the right lung lobes, (2) Chopping the lungs, (3) Homogenizing lungs, and (4) Centrifugation of lung homogenate to remove the cellular and nuclear debris and to reduce the mitochondrial contamination of the microsomal fraction

Determination of the Total Lung Proteins

The protein content of lung microsomes was measured by the bicinchoninic acid (BCA) method as previously described (Smith *et al*, 1985, Ma *et al*, 2002) using the BCA protein assay kit (Pierce, Rockford, IL) in a spectra Max 250 Spectrophotometer (Molecular Devices Corporation, Sunnyvale, California). Bovine serum albumin was used as the standard.

Measurement of EROD and PROD activities

EROD and PROD activities were measured as previously described (Burke *et al*, 1985 and Ma *et al*, 2002) using a luminescence spectrometer model LS-50 (Perkin-Elmer, Norwalk, CT). A 10 μM concentration of 7-ethoxyresorufin (Sigma, St. Louis, MO) solution prepared from 2.35 μg 7-ethoxyresorufin in 1 ml DMSO was used for the standard curve following each run. EROD and PROD activities were expressed as picomoles of the produced resorufin per minute per milligram microsomal protein (pmol/min/mg protein).

Western Blot Analysis

Western Blot analysis of lung microsomes was conducted as previously described (Ma *et al*, 2002). Each gel received 75 μg of microsomal protein for CYP1A1 and 20 μg for CYP2B1. The nitrocellulose membrane was probed using a polyclonal rabbit anti-rat CYP1A1 antibody (Xenotech, Kansas city, KS) or a monoclonal mouse anti-rat CYP2B1 antibody (Xenotech) at 4ºC overnight. Blocking of non-specific binding was made by incubating the membrane with a solution of 1% dry milk in tris-buffered saline/tween (TBS/T) for 1 hour at room temperature with rocking. The membranes were then incubated for 1 hour at room temperature with a goat anti-rabbit antibody (Santa Cruz Biotech. Inc., Santa Cruz, CA) for CYP1A1 or goat anti-mouse antibody (Santa Cruz Biotech. Inc., Santa Cruz, CA) for CYP2B1. For positive control, liver microsomes of BNF-treated rat (Xenotech) were used for CYP1A1 or liver microsomes of phenobarbital-treated rats (Amersham, Piscataway, NJ) for CYP2B1. The CYP1A1 and CYP2B1 proteins were detected by enhanced chemiluminescence (ECL) reagent kit (Amersham). The x-ray films (Fuji Film Corp., LTD., Tokyo, Japan) containing protein bands were scanned by the Eagle Eye II scanner (Stratagene, La Jolla, California 92037)

with Eagle Sight software. The scanned images were quantified by ImageQuant software version 5.1 (Molecular Dynamics, Sunnyvale, CA). The quantification of western blot by this software calculates the volume under the surface area created by a 3-D plot of the pixel locations and pixel intensities. Each sample was quantified three times, and then the averages of the values were used to calculate the individual measurement. The data were expressed as a percentage of the CYP1A1 or CYP2B1 positive controls.

Dual Immunofluorescence Technique

Paraffin-embedded, formalin-fixed sections from the left lung lobe were used for immunofluorescent detection of CYP1A1 and cytokeratins 8/18, which are cytoskeletal proteins used as markers of AT-II cells (Kasper *et al*, 1993). Briefly, immunofluorescence was a two-day procedure (Figure 2**)** where in the first day the slides were first heated in the oven at 60 ºC for 10 to 20 minutes. The slides were deparaffinized and rehydrated in xylene in 3 sequential 6 minute immersions, a 3 minute immersion in 100 % alcohol, 3 minutes in 90 % alcohol, 3 minutes in 80 % alcohol, and 5 minutes in distilled water. The antigenicity of hidden epitopes was retrieved using 0.01M disodium ethylenediamine tetraacetate (Fischer Scientific, Fair Lawn, New Jersey), pH 8 in a microwave heating procedure. Specifically, slides in the EDTA solution were heated for 1 minute and 45 seconds in the microwave on high and then for 6 minutes on defrost. EDTA solution was then added to replenish the solution which had been evaporated and the slides were reheated for 6 additional minutes on defrost. To avoid the non-specific binding of the primary antibodies, the slides were blocked with 5 % BSA in PBS (IgG free) (Sigma) for 10 minutes at room temperature (RT). Then the slides were rinsed with distilled water and blocked with 5% pig serum in PBS (Biomeda Corporation, Foster city, CA) for 10 minutes at RT. The slides were then rinsed with distilled water and primary antibodies were applied. We used a polyclonal Guinea pig anti-cytokeratins 8/18 antibody (RDI, Flanders, NJ) for staining of cytokeratins 8/18 at a 1:50 dilution in PBS. For CYP 1A1 staining, a polyclonal, affinity purified, highly cross-absorbed rabbit anti-rat CYP1A1 antibody (Xenotech,) was used at a 1:5 dilution. Both primary antibodies were applied by utilizing the capillarity generated between each pair of slides in a microprobe holder (Fischer Scientific). The slides were kept at room temperature overnight during which the primary antibodies were allowed to bind to the antigen

(CYP1A1 and cytokeratins 8/18). On the second day, the slides were incubated in the oven at 37 ºC for 2 hours after which they were thoroughly rinsed with distilled water and the secondary antibodies were dropped onto the slides. A FITC-labeled, donkey anti-Guinea pig IgG (Research Diagnostic Inc., Flanders, NJ) was used to detect cytokeratins 8/18 at a 1:50 dilution with PBS. For CYP1A1 detection, Alexa 594-conjugated goat anti-rabbit antibody (Molecular probes, Eugene, Oregon) was applied at a dilution of 1:20 with PBS. The secondary antibodies were allowed to bind to the primary antibodies for 2 hours in the dark. For the negative control, the primary antibodies were omitted and replaced by rabbit serum. Slides were rinsed with distilled water, cover slips were applied using gel mount (Biomeda Corp., Foster City, CA), and the slides were allowed to dry for 2 hours. Ten images were captured using a digital camera (Quantix Photometrics, Roper Scientific Inc, Trenton, NJ) fitted on an Olympus photomicroscope (OlympusAX70, Olympus American Inc., Lake Success, NY) by a researcher blinded to the exposure status. For each slide, 5 images were captured from proximal alveolar regions (PAR) where most of the dust particles tend to accumulate (Nikula *et al*, 1997). Another 5 images were obtained from random alveolar (RA) regions, which were not located near visible alveolar ducts. The aim of selecting those 2 areas is to assure sampling of the alveolar regions representative of the site of coal dust particle deposition. Five images were also captured from the terminal bronchiolar region to count the number of CYP1A1-positive bronchiolar epithelial cells. The digital camera settings for contrast, brightness, and gamma were held constant for all slides. The staining was described as being specific due to the absence of background staining, distinct cellular localization of CYP1A1 and cytokeratins 8/18, and absence of the staining in the negative control slides where rabbit serum was applied instead of the primary antibodies.

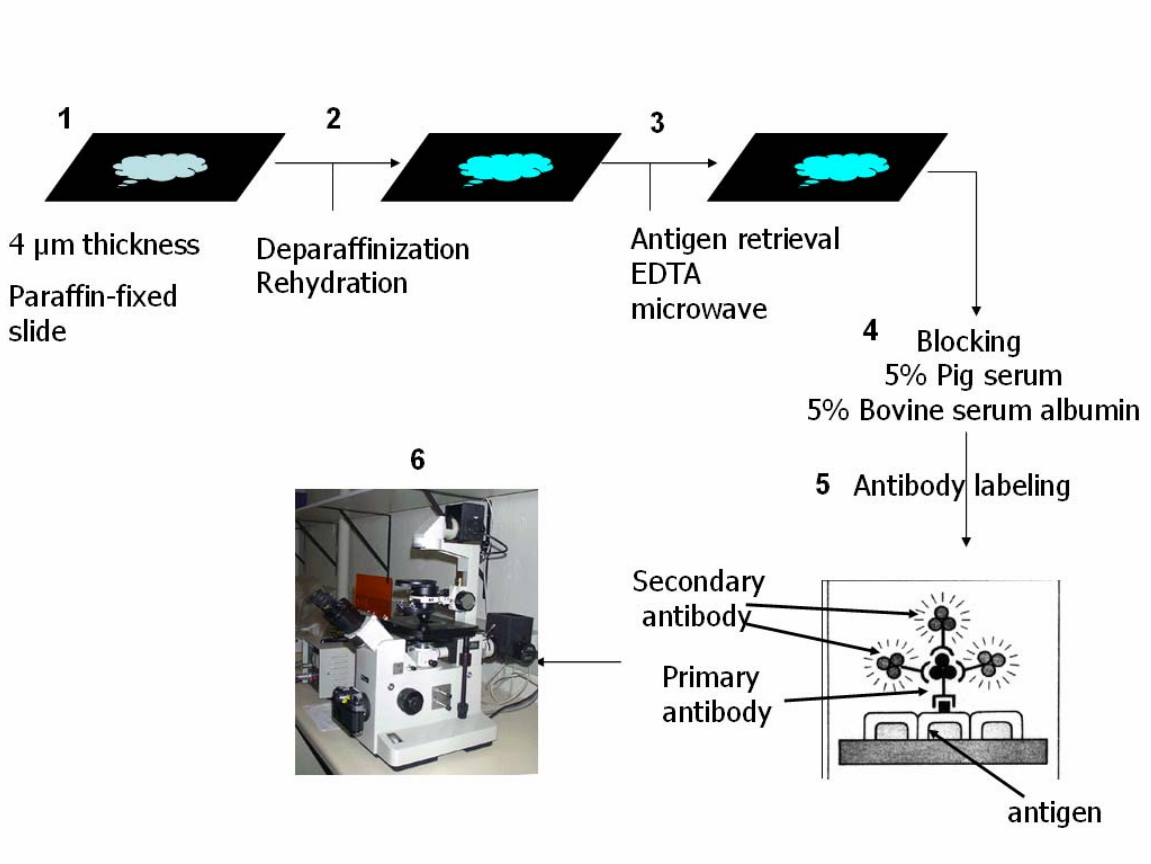

Figure 2. Immunofluorescent technique for staining tissue sections. The procedure included:

1- Preparation of tissue section of 4 µm thickness from paraffin embedded tissue.

2- Deparafinization and rehydration of tissue sections by emersion in xylene and alcohol.

3- Retrieval of protein epitopes by using EDTA and microwave heating.

4- Blocking the non-specific antibody binding by pig serum and bovine serum albumin.

5- Addition of the primary antibody to allow binding to the antigen then labeling the primary antibody with fluorescent-conjugated secondary antibody.

6- Examination of the fluorescent emission from the secondary antibody under fluorescent microscope at standard settings.

Quantification of CYP1A1 and Cytokeratins 8/18 by Morphometric Analysis

The lung area occupied by red fluorescence (representing CYP1A1 expression), green fluorescence [representing cytokeratins 8/18, which are cytoskeletal proteins highly expressed in primitive epithelia such as the cuboidal AT-II cells (Kasper *et al*, 1993)], and colocalized (concomitantly occurring) red and green fluorescence were quantified by using commercial morphometry software (Metamorph Universal Image Corp.). The area of CYP1A1 colocalized with cytokeratins 8/18 in AT-II cells was obtained by the following formula:

$$C = R \times T \text{ where;}$$

C stands for the area of CYP1A1 that co-expressed (colocalized) with cytokeratins 8/18 in AT-II cells,

R stands for the percent of CYP1A1 expressed in AT-II cells measured by the Metamorph software, and

T stands for the total CYP1A1 area expressed in the whole alveolar septum (including AT-II and alveolar non-type II cells) measured by the Metamorph software.

Moreover, the proportional CYP1A1 expression in AT-II cells, which is the relative area of CYP1A1 to cytokeratins 8/18 expression, was calculated from the following formula:

$$P = \frac{R \times T}{G} \text{ where;}$$

C, R, and T as defined above and,

G is the total green area of cytokeratins 8/18 expressed in AT-II cells.

P is the proportional CYP1A1 expression within areas occupied by the AT-II marker, and adjusts for increases associated with AT-II hyperplasia.

By this method, we were able to analyze the expression pattern in AT-II cells. Moreover, the hyperplasia of AT-II cells was also determined by measuring the area containing the FITC expression (green area), which represents the expression of cytoskeletal proteins 8/18 by AT-II cells. The threshold ranges for red and green colors were held constant during morphometric analysis of all images.

Histopathology:

Slides were interpreted by a board-certified veterinary pathologist blinded to the exposure status of the individual slides. Changes assessed in each slide included: AT-II cell hyperplasia and hypertrophy, alveolitis (inflammation), and hyperplasia of bronchus-associated lymph tissue. Histopathologic changes were scored for severity and distribution from zero to five as previously described (Hubbs *et al*, 1997). Briefly, severity was scored as none (0), minimal (1), mild (2), moderate (3), marked (4), or severe (5). Distribution was scored as none (0), focal (1), locally extensive (2), multifocal (3), multifocal and coalescent (4), or severe (5). The pathology score is the sum of the severity and distribution score.

Statistical Analyses

The dose responsive effects of coal dust instillation on EROD, PROD, and Western blot for CYP1A1 and CYP2B1 were assessed using linear regression analysis. Pairwise comparisons of each dose to the control group were analyzed using one-way analysis of variance followed by Dunnett's test. AT-II hyperplasia and hypertrophy based on immunofluorescence were analyzed using one-way analysis of variance followed by Dunnett's test to compare each dose to the control group. Pathology scores were analyzed using the nonparametric Kruskal-Wallis test followed by the Wilcoxon Rank-sum test for pairwise comparisons. All differences were considered statistically significant at $P<0.05$.

RESULTS

Effect of Coal Dust Exposure on EROD and PROD

The IT instillation of coal dust suppressed the CYP1A1-dependent enzymatic activity (EROD) in a dose-dependent fashion (r^2=0.399, p=0.0028) (Figure 3). Rats exposed to 40 mg/rat CD with BNF had a significant lower EROD activity than those exposed to control saline with BNF (p=0.036). Similarly, CYB2B1-dependent enzymatic activity (PROD), the major CYP isoform in rat lungs, showed a dose-dependent reduction by CD exposure using linear regression (r^2= 0.458, P=0.001). PROD was significantly reduced in rats exposed to 20 and 40 mg/rat CD with BNF compared to control, saline with BNF (p 0.017) (Figure 4).

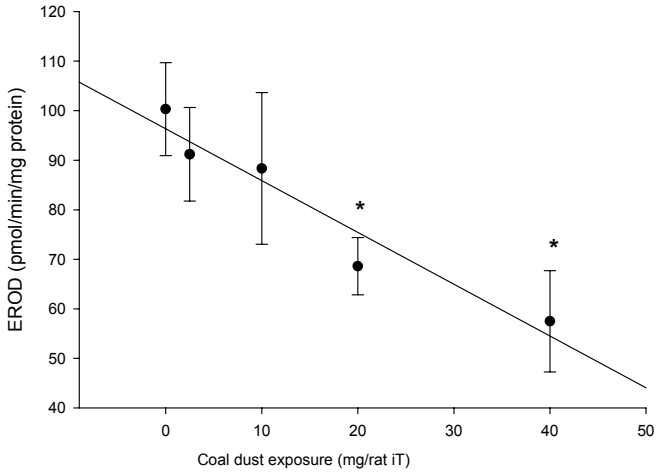

Figure 3. BNF-induced CYP1A1-dependent enzymatic activity (EROD) is suppressed in a dose dependent fashion by intratracheal exposure of rats to 0, 2.5, 10, 20, or 40 mg coal dust suspended in the vehicle (saline). EROD activity is significantly reduced at 40 mg/rat CD exposure comparing to the control saline. Values are means and standard error of 4 rats /group. EROD was measured as pmol/min/mg microsomal protein. All rats received 50 mg/kg BNF IP 3 days before sacrifice. The linear regression best fit curve showing the reduction of EROD activity with increasing CD exposure. * Significantly different from control at $p<0.05$.

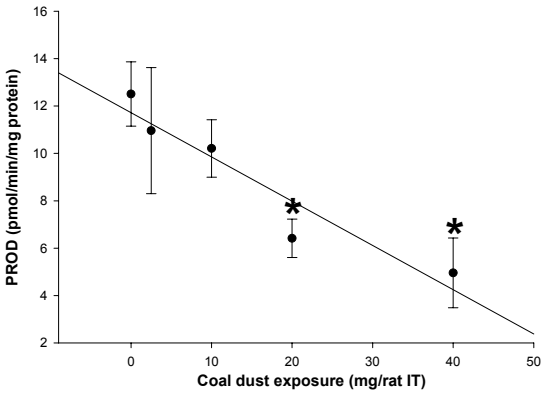

Figure 4. Lung microsomal CYP2B1-dependent enzymatic activity (PROD) is reduced in a dose-dependent manner by CD exposure. Values are means and standard error of 4 rats /group. PROD was measured as pmol/min/mg microsomal protein. All rats also received IP BNF (50mg/kg) 3 days prior to sacrifice. The linear regression best fit curve showing the reduction of PROD activity with increasing CD exposure. * Significantly different from control at $p<0.05$.

Western Blot Analysis

CYP1A1

A representative Western blot of the pulmonary microsomal preparations is shown in Figure 5A. The results were expressed as the percentage of the CYP1A1 positive control. The amount of CYP1A1 quantified by Western blot in CD and BNF-exposed was less than in rats exposed to BNF without CD. Groups treated with the highest dose of CD (40mg/rat) showed a significant reduction of CYP1A1 protein compared to control ($p=0.03$) (Figure 5A and B).

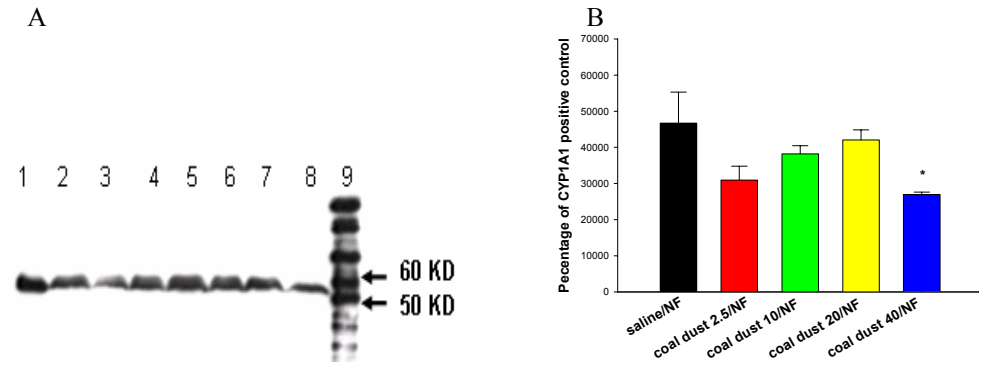

Figure 5. In A, a sample of Western blot showing significant repression of CYP1A1 protein in lung microsomes by coal dust exposure (p=0.029) at high dose of CD (40mg/rat) analyzed by linear regression. Microsomal protein (75 μg) from a positive control (liver microsomes of BNF-treated rats) (lane 1), pulmonary microsomes from BNF-treated rats (lane 2 & 4) and CD and BNF-exposed rats (2.5mg CD lane 3, 10mg CD lane 5, 20mg CD lanes 6 &7, and 40 mg CD lane 8) were subjected to SDS gel electrophoresis using Tris-glycine SDS running buffer and blotted to nitrocellulose membranes. The membranes were probed with rabbit anti-rat CYP1A1 antibody overnight at 4ºC then goat anti-rabbit antibody as described in the materials and methods. Lane 9 is the molecular weight standard. In B, the data from multiple Western blots is expressed as the percentage of CYP1A1 positive control from quantification of four different samples from each exposure group. The values represent means ± SE, n=4. *significantly different from control group at $P < 0.05$.

CYP2B1

The CYP2B1 protein, the major isoform of CYP subfamily in the rat lung, was measured in the lung microsomes. CYB2B1 is not inducible by BNF in rat lungs but can be induced in liver by phenobarbitals. The amount of lung CYP2B1 detected by Western blot was numerically, but not significantly, less in CD-exposed rats than control rats (6A and B). The results were expressed as the percentage of CYP2B1 positive control.

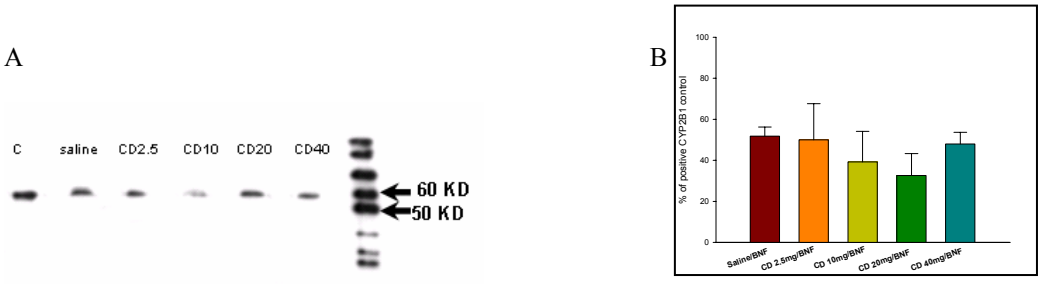

Figure 6. The effect of coal dust on CYP2B1 in the lungs of BNF-exposed rats assessed by Western blot using linear regression analysis. Microsomal protein (20 μg) from control rats (saline and BNF) and exposed (CD and BNF) rats were subjected to SDS gel electrophoresis using Tris-glycine SDS running buffer and blotted against nitrocellulose membrane. The membranes were probed with mouse anti-rat CYP2B1 antibody overnight at 4ºC then goat anti-mouse antibody as described in the materials and methods. The amount of lung CYP2B1 detected by Western blot is decreased, although not significantly, by coal dust exposure. In A, the first lane (c) is the positive CYP2B1 control (liver microsomes of Phenobarbital-treated rats), the last lane is the molecular weight standard, while all other treatments are indicated above the lanes. In B, 4 different samples for each treatment were quantified and the data expressed as a percentage of positive CYB2B1 control. Values are means ± SE, n=4.

Effect of CD Exposure on Histopathological Changes of Lung Alveoli

AT-II cell hyperplasia (increased cell number) and hypertrophy (increased cell size), alveolitis (alveolar inflammation), and lymphoid hyperplasia of tracheobronchial lymph node were the major histopathological changes assessed in sections stained by H and E. Accumulation of dust-laden macrophages in the alveolar spaces was a noteworthy finding in coal dust exposed alveoli (Figure 7). Rats exposed to CD (2.5, 10, 20, and 40mg/rat) showed significant hyperplasia and hypertrophy of AT-II cells compared to control ($p<0.001$ in all treatment doses); Figure 8. In addition, alveolitis (alveolar inflammation) was significantly increased in rats exposed to 2.5, 10, 20, and 40mg/rat CD ($p=0.01$, $p=0.006$, $p=0.002$, $p=0.002$, respectively) (Figure 8)

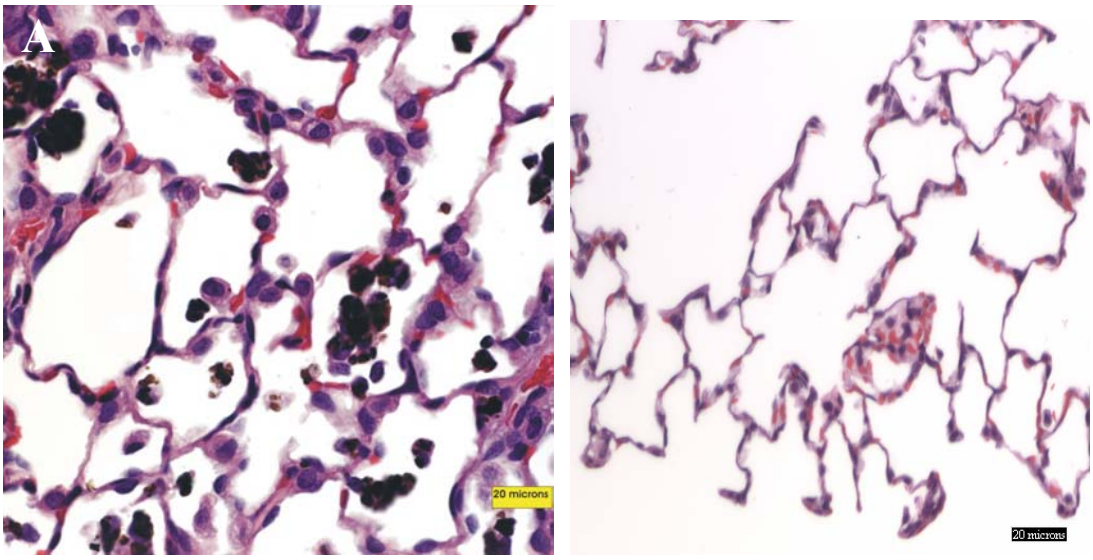

Figure 7. Microphotograph of tissue section stained with H & E showing AT-II cellular hyperplasia and hypertrophy. Dust-laden macrophages are also shown as dark spots in the alveolar spaces. These histopathological changes are absent in control (B). The bar is 20 μm.

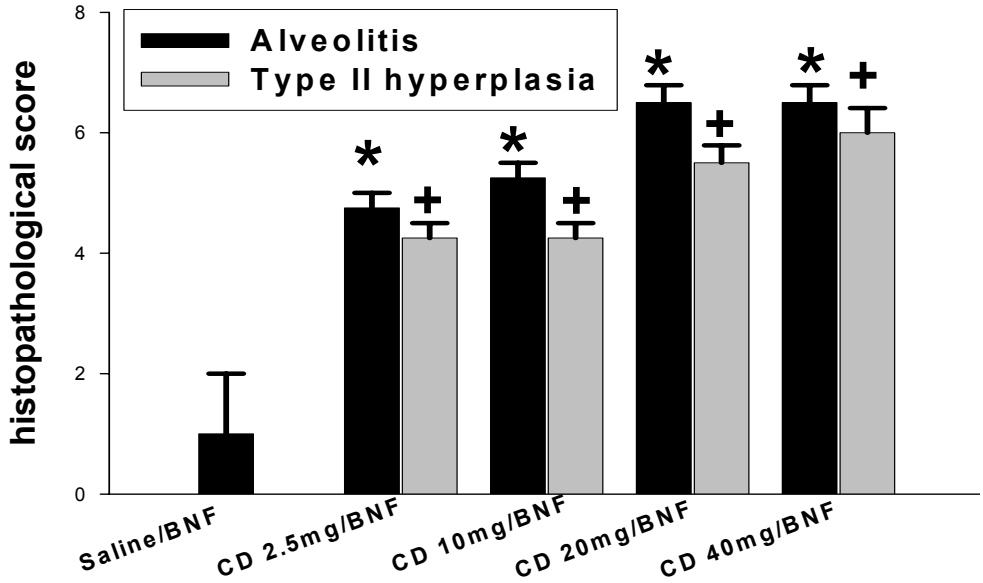

Figure 8: Histopathological changes in rat lungs after intratracheal exposure to coal dust. Changes were scored for severity and distribution of alveolitis and AT-II hyperplasia and hypertrophy as described in the material and methods. * indicates that alveolitis is significantly higher than control (saline/BNF) at $p < 0.05$. + indicates that AT-II hyperplasia and hypertrophy are significantly higher than control (saline/BNF) at $p < 0.05$. Data were analyzed by the non-parametric Kruskal-Wallis test followed by Wilcoxon Rank-Sum test for pairwise comparisons. Values are means ± SE, n=4.

Results of dual Immunofluorescence:

The result of immunofluorescent changes by CD exposure is summarized in Table 1.

I-Pattern of CYP1A1 Expression in Alveolar Region of the Lung

A specific pattern of rat CYP1A1 expression was observed in the alveolar region of the lung by immunofluorescence examination. In rats exposed to BNF alone (control rats), the CYP1A1 expression (red-labeled area in Figure 9) was mostly localized to the endothelium of the pulmonary vasculature and in cells of the alveolar septum. Statistically, areas of CYP1A1 expression were significantly smaller in AT-II cells than in other cells (NT-II cells) of the alveolar septum ($p=0.003$) (Figure 9B and C).

II-Pattern of Cytokeratins 8/18 Expression in the Alveolar Region of the Lung

The green fluorescent Cytokeratins 8/18 were clearly expressed in the cytoplasm of cuboidal cells that were mainly localized on the corners of the alveolar septum (Figure 9A). These cells have the plump morphology characteristic of AT-II cells of the alveolar septa. No green fluorescence was visualized in the other types of cells of the alveolar septum, which were then designated as alveolar NT-II cells (Figure 9A).

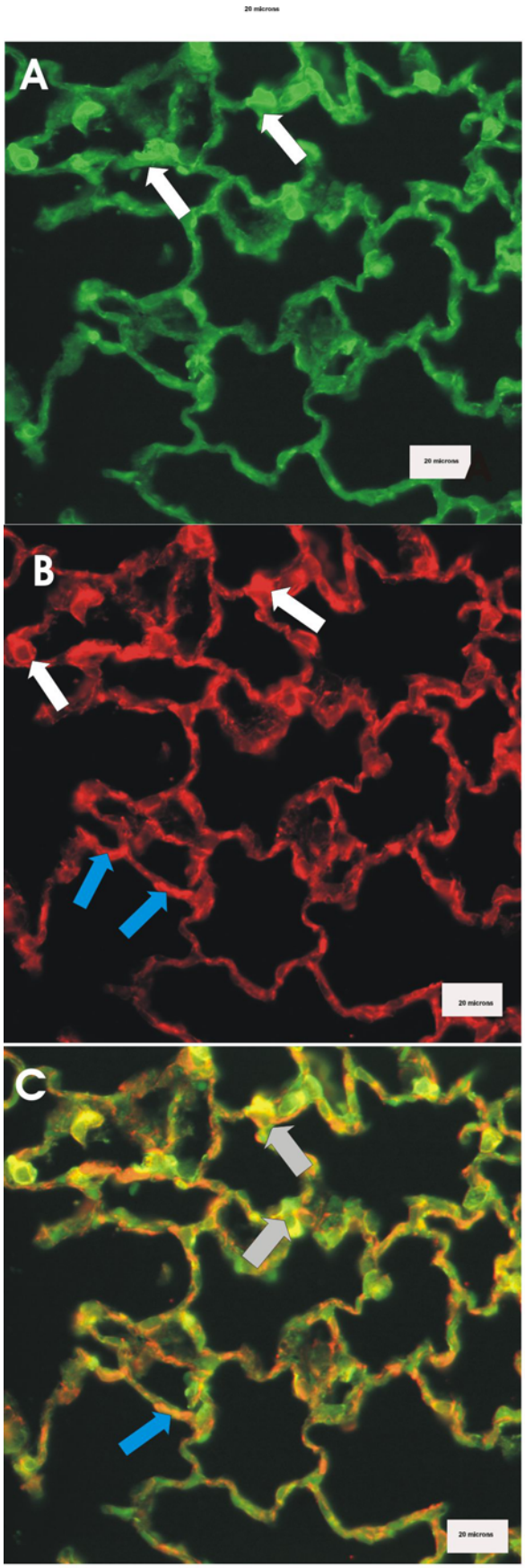

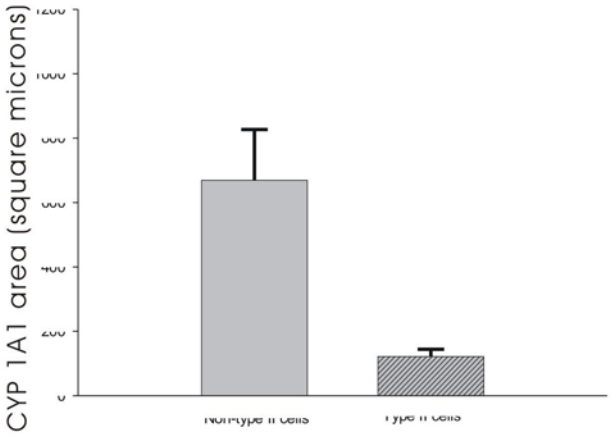

Figure 9. Immunofluorescence staining of pulmonary CYP1A1 and cytokeratins 8/18 of rat alveoli. A. The green color shown represents the staining of cytokeratins 8/18 expressed in AT-II cells, which appear as plumb cells at the corners of the alveoli (white arrows). B. The red fluorescence stains the areas of CYP1A1 expression in alveolar NT-II (blue arrows) and AT-II cells (white arrows). In C, the green and red colors were combined to visualize the concomitant localization (colocalization) of red CYP1A1 and green cytokeratins 8/18 within AT-II cells that gives rise to yellow color (gray arrows). The double labeling image (C) shows that CYP1A1 expression in AT-II cells is less than expression in alveolar NT-II cells. This reduction was significant as illustrated by morphometric analysis (D). * Indicates significant difference from CYP1A1expression in alveolar NT-II cells at $p < 0.05$. Magnification is digital 40 X. Reference bar is 20 micrometers.

III-Effect of CD on AT-II Cell Proliferation by Immunofluorescent Examination

The area of expression of cytoskeletal proteins (cytokeratins 8/18), which are highly expressed in the cytoplasm of AT-II was quantified morphometrically and expressed as square micrometer. In the proximal alveolar (PA) regions, this area was significantly larger in rats exposed to 20 and 40 mg CD/rat and BNF than control (Figure 10A), indicating hyperplasia and hypertrophy of AT-II cells (p= 0.027 and p=0.02, respectively) (Figure 10 A and 11B). On the contrary, no significant change of AT-II hyperplasia and hypertrophy was detected in the random alveolar (RA) regions of CD-exposed rats compared to control (Figure 10B and Figure 12B,).

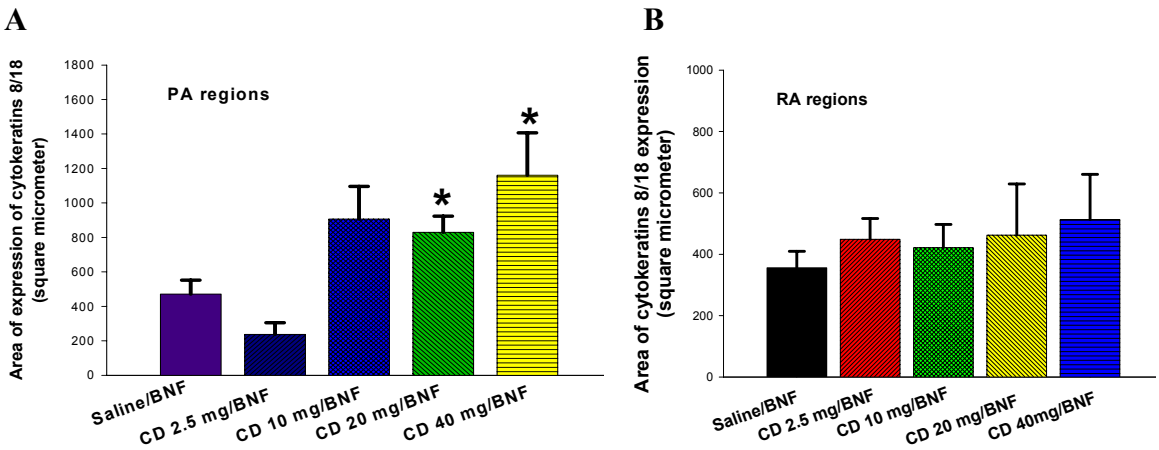

Figure 10. Morphometric quantification of area of cytokeratins 8/18 expression in AT-II cells. In A, the area was quantified in the PA regions and showed a significant increase of cytokeratins 8/18 expression in rats exposed to 20 and 40 mg/rat coal dust and BNF compared to control. In B, no significant change was detected in cytokeratins 8/18 expression of the RA regions of rats exposed to CD vs. control. Data were analyzed by one way analysis of variance followed by Dunnett's test. * indicates significant difference from control at $p<0.05$. Values are means ± SE, n=4.

IV-Effect of CD exposure on CYP1A1 Expression by Alveolar Non-Type II (NT-II) Cells

1-CYP1A1 Expression by Alveolar NT-II Cells in Saline vs. Coal Dust Exposed Rats:

A- In proximal Alveolar (PA) Regions

The area of expression of CYP1A1 (measured in square micrometer) by alveolar NT-II cells (all cells in the alveolar septum except for AT-II cells) of PA regions (regions of coal dust accumulation) was significantly lowered in groups exposed to 20 mg and 40

mg/rat CD and BNF compared to BNF control group (p=0.007, p=0.008, respectively) (Figure 11A). This was indicated by the reduction of the red-labeled area that is not co-expressed with green-labeled area (NT-II cells stained red only for CYP1A1) as shown in Figures 12A and B.

B- In Random Alveolar (RA) Regions

No significant change was detected in the area of CYP1A1 expression by alveolar NT-II cells of RA regions (regions of minimum particle aggregation) of groups exposed to CD and BNF compared to control group. This result was illustrated by morphometric quantification of CYP1A1 expression in alveolar NT-II cells where none of the cytokeratins 8/18 were localized with CYP1A1 (Figure 11B and Figure13A and B).

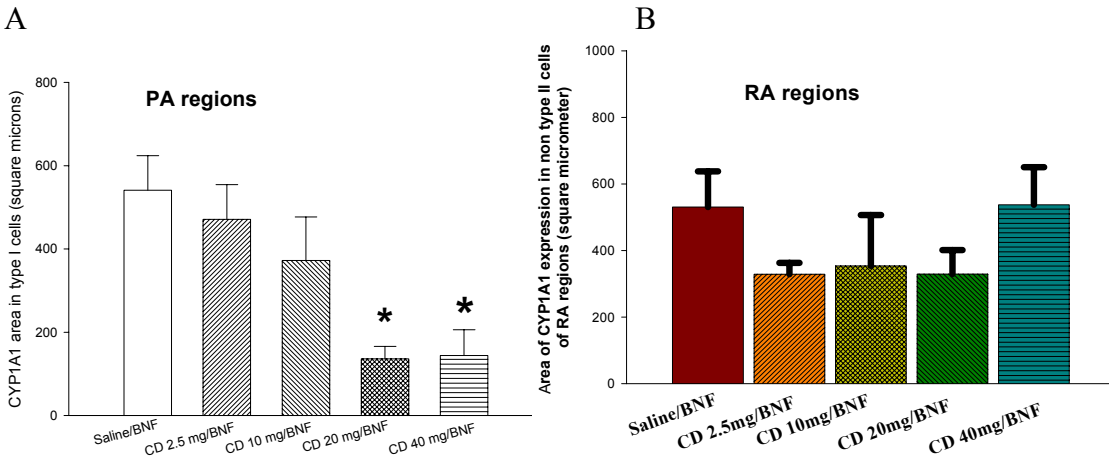

Figure 11. Morphometric quantification of immunofluorescent-stained sections for CYP1A1 and cytokeratins 8/18 of NT-II cells of the PA and RA regions of control and CD-exposed rats. In A, the CYP1A1 expression area in alveolar NT-II cells is significantly reduced in groups exposed to 20 and 40 mg/kg CD and BNF compared to that exposed to BNF alone. However in B, no significant changes in the area of CYP1A1 expression in NT-II cells of the RA regions of CD-exposed rats compared to control. Values are means ± SE, n=4. * Significantly different from control at $p<0.05$.

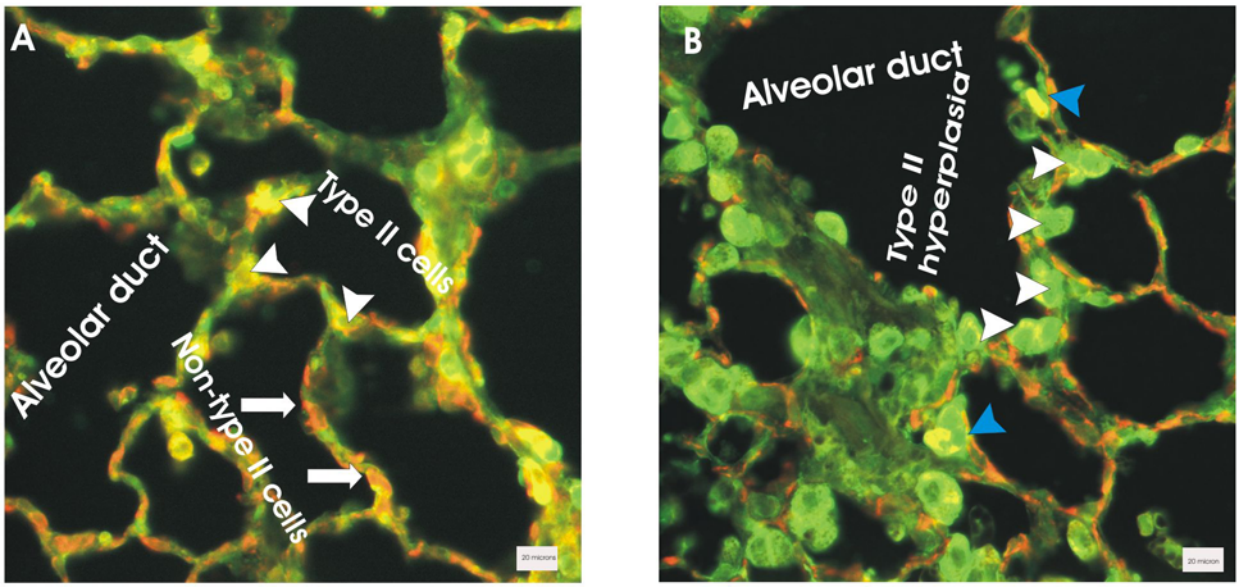

Figure 12. Representative immunofluorescence images of PA regions of a BNF-treated (A) and BNF and 40 mg CD-exposed rats (B) showing reduction of CYP1A1 expression in AT-II and NT-II cells by CD exposure. In A, the CYP1A1 (red fluorescence) is expressed in the flattened NT-II cells, which constitute the majority of alveolar septum architecture and in AT-II cells (green fluorescence; yellow color represent co-localization of red and green fluorescence), which are cuboidal cells mainly located at the corners of the alveoli. In B, the CYP1A1 expression in both types of alveolar cells was significantly reduced as shown by reduction of red color and yellow color in the alveolar septum. AT-II cell hyperplasia and hypertrophy is also evident in CD-exposed rats (B) (white arrows) that appear with a small amount of CYP1A1 expression as shown by tiny yellow signal in their cytoplasm (blue arrows). (40 X magnification). Reference bar is 20 micrometer.

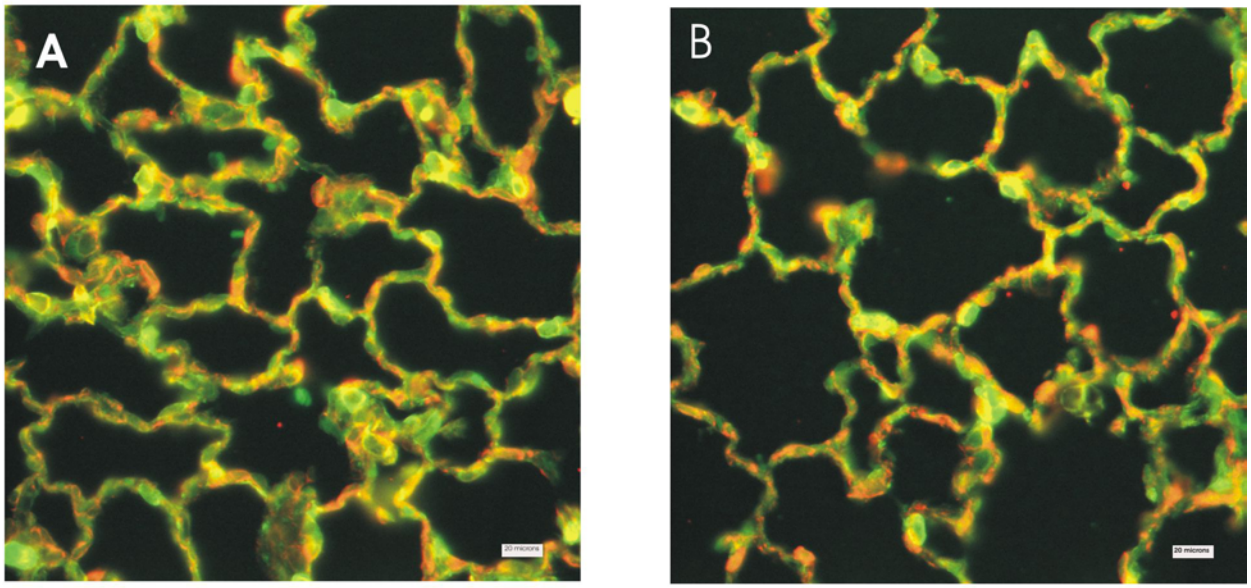

Figure 13. Representative immunofluorescence images of pulmonary CYP1A1 and cytokeratins 8/18 of RA regions (with no visible alveolar duct present) of a BNF-exposed rat (A) and a rat exposed to BNF and the highest dose (40mg/rat) of CD (B). No significant differences were apparent between BNF and CD-exposed when compared with BNF-exposed rats regarding CYP1A1 expression in AT-II and NT-II cells. 40 X magnification. Reference bar is 20 micrometer.

***2-CYP1A1 Expression by Alveolar NT-II Cells in PA Regions vs. RA Regions of CD-Exposed Rats*:**

CYP1A1 expression by alveolar NT-II cells was compared in 2 different alveolar regions, the proximal versus random alveolar regions. The area of CYP1A1 expression measured in alveolar NT-II cells of PA regions was significantly reduced compared to the RA region in rats exposed to 20 and 40 mg/kg CD and BNF (p=0.048, p=0.022, respectively) (Figure14).

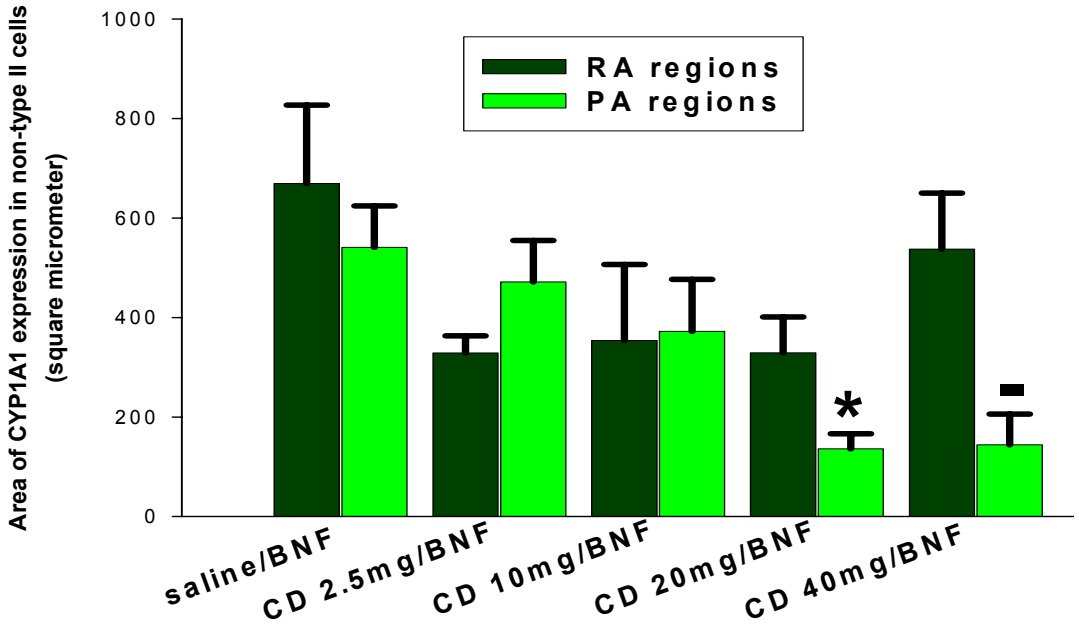

Figure 14. Morphometric quantification of CYP1A1 expression in NT-II cells of PA regions vs. RA regions. The area was measured in square micrometer. * indicates that CYP1A1 expression is significantly lower in NT-II cells of PA regions compared to RA regions in rats exposed to 20 mg/rat CD and BNF at $p<0.05$. ▬ indicates that CYP1A1 expression is significantly lower in NT-II cells of PA regions compared to RA regions in rats exposed to 40 mg/rat CD and BNF at $p<0.05$. Values are means ± SE, n=4.

V-Effect of CD Exposure on CYP1A1 Expression by AT-II Cells

1-CYP1A1 Expression by AT-II Cells in CD-Exposed Rats vs. Control in the PA Regions

A- Relative Area (proportion) of CYP1A1 Expression in green AT-II Cells

The relative area of red fluorescent CYP1A1 expression to the green fluorescent area of cytokeratins 8/18 expression was calculated by the formula described in the materials and methods section, and was designated as proportional CYP1A1 expression,

which determines the amount of CYP1A1 expression within AT-II cells with correction for changes in AT-II cell number. The proportional CYP1A1 expression in AT-II cells of PA regions was significantly reduced in rats exposed to 20 mg (p=0.005) and 40 mg (p=0.003) CD and BNF compared to control (Figure 15A).

B- Area of CYP1A1 Colocalized with Cytokeratins 8/18 in AT-II Cells

The expression of CYP1A1 in AT-II cells is visualized as a yellow fluorescence due to concomitant expression of the red-fluorescent CYP1A1 and green-fluorescent cytokeratins 8/18 (Figure 9C). The expression (co-localization) of CYP1A1 in AT- II cells of the PA regions measured in μm^2 was significantly lowered in rats exposed to 20 mg/rat (p=0.007) and 40 mg/rat (p=0.002) CD and BNF compared to control (Figure 15B). This was indicated by the reduction of the red areas that colocalized (co-expressed) with green areas in rats receiving higher exposures of CD (Figure12B).

A B

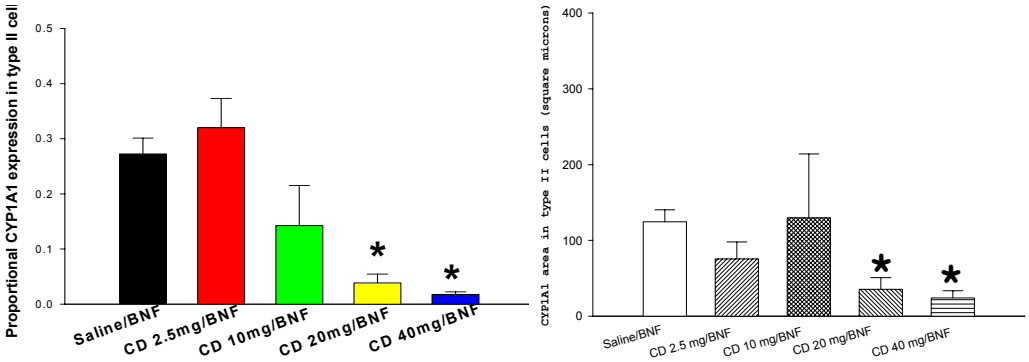

Figure 15. Morphometric quantification of proportional CYP1A1 expression (A) and colocalization area (B) in AT-II cells. In A, * indicates significant reduction of fractional CYP1A1 expression in AT-II cells in the PA regions of rats exposed to 20 and 40 mg/rat CD with BNF compared to the PA region of BNF-treated rats at $p<0.05$. in B, * indicates significant reduction of area of CYP1A1 expression in AT-II cells (colocalization area) in PA region exposed to 20 and 40 mg/rat CD with BNF compared to control at $p<0.05$.

***2-CYP1A1 Expression by AT-II cells in CD-Exposed Rats vs. Control* in RA Regions**

The expression of CYP1A1 in AT-II cells (either the co-localization or the proportional expression) was not significantly affected by CD exposure in RA regions (data not shown).

***3-CYP1A1 Expression by AT-II Cells in PA Regions vs. RA Regions of CD-Exposed Rats*:**

The area of CYP1A1 expression measured in AT-II cells showed no significant changes in PA regions when compared to RA regions in CD-exposed groups compared with BNF-exposed groups (data not shown)

IV-Effect of CD Exposure on CYP1A1 Expression in the Whole Alveolar septum:

The area of CYP1A1 expression was measured in the alveolar septum as a total red area, which represent the expression by all different types of cells at the septum. A significant reduction was detected with 20 and 40 mg/rat CD in PA regions (Figure 16A). However, there was no change observed in RA regions (Figure 16B). In addition, in rats exposed to 20 and 40 mg of CD, CYP1A1 expression in RA regions was significantly less than in PA regions (Figure 17).

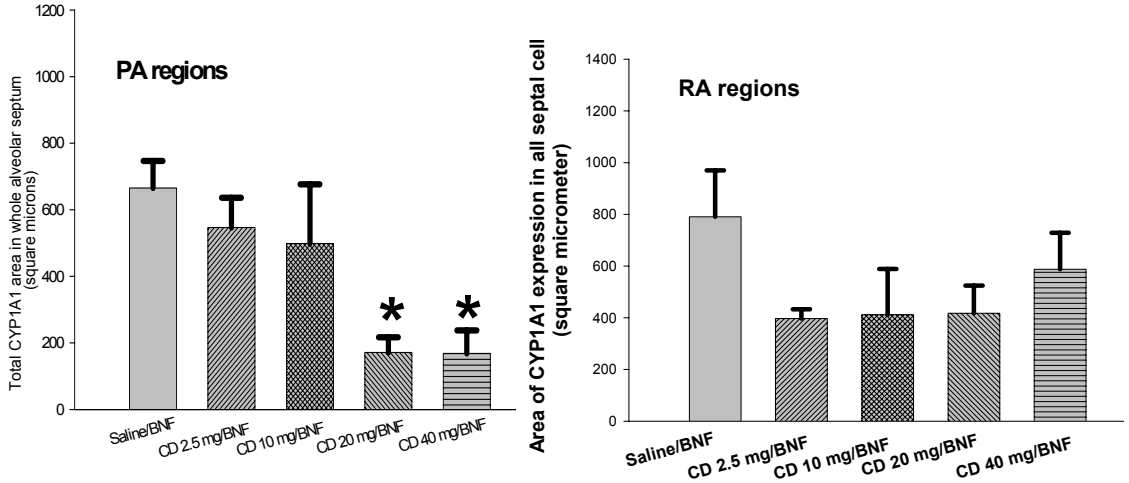

Figure 16. Morphometric analysis of area of CYP1A1 expression in the whole alveolar septal cells of the PA (A) and RA (B) regions. In A, the total CYP1A1 area localized in PA regions lung alveoli of rats exposed to 20 and 40 mg CD and BNF is significantly lower than BNF-exposed . In B, however, no significant change is observed Values represent means ± SE (n=4). *Significantly different from control saline/BNF at $P<0.05$.

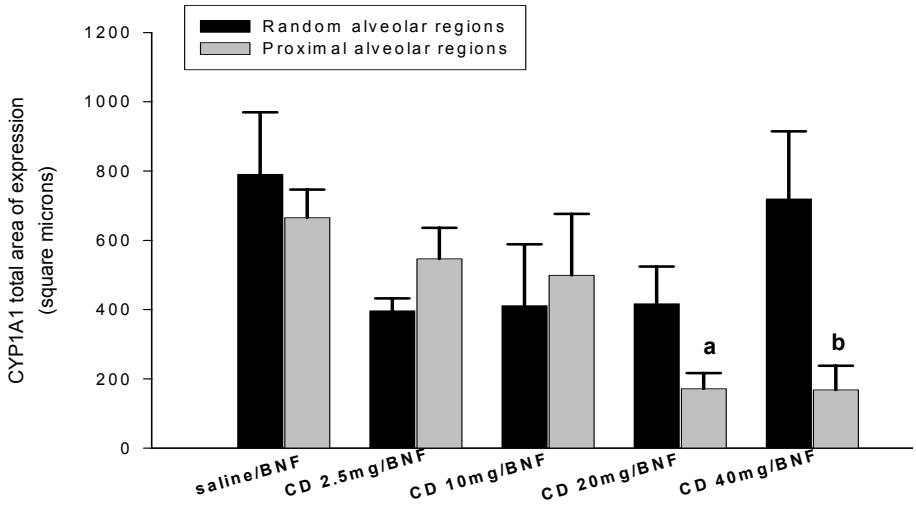

Figure 17: Quantitative analysis of the total alveolar area expressing CYP1A1 in PA regions vs. RA regions. The total CYP1A1 area expressed in all alveolar cells of PA regions is significantly decreased in rats exposed to 20 and 40 mg CD and BNF compared to that of the RA regions. The letter a above the bar indicates a significant difference from RA regions of rats exposed to 20 mg CD and BNF at $p<0.05$. the letter b above the bar indicates a significant difference from RA regions of rats exposed to 40 mg CD and BNF at $p<0.05$. Values represent means ± SE (n=4).

IIV-Effect of CD on CYP1A1 Expression by the Non-Ciliated Bronchiolar Epithelial (Clara) Cells

The number of the CYP1A1-positive non-ciliated bronchiolar epithelial cells was counted per micrometer of the basement membrane. No significant change in the number of CYP1A1-positively stained cells was observed in BNF and CD-exposed rats compared to BNF-exposed rats (Figure 18 and 19).

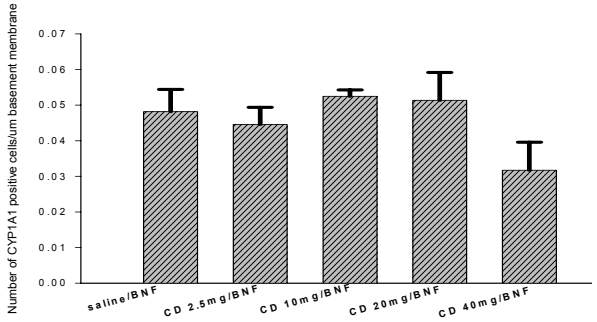

Figure 18. Effect of CD exposure on CYP1A1 expression by terminal non-ciliated bronchiolar (Clara) cells. The number of Clara cells positive for the CYP1A1 immunofluorescent signal per μm of basement membrane showing no significant difference between CD exposed rats and control. Values represent means ± SE (n=4).

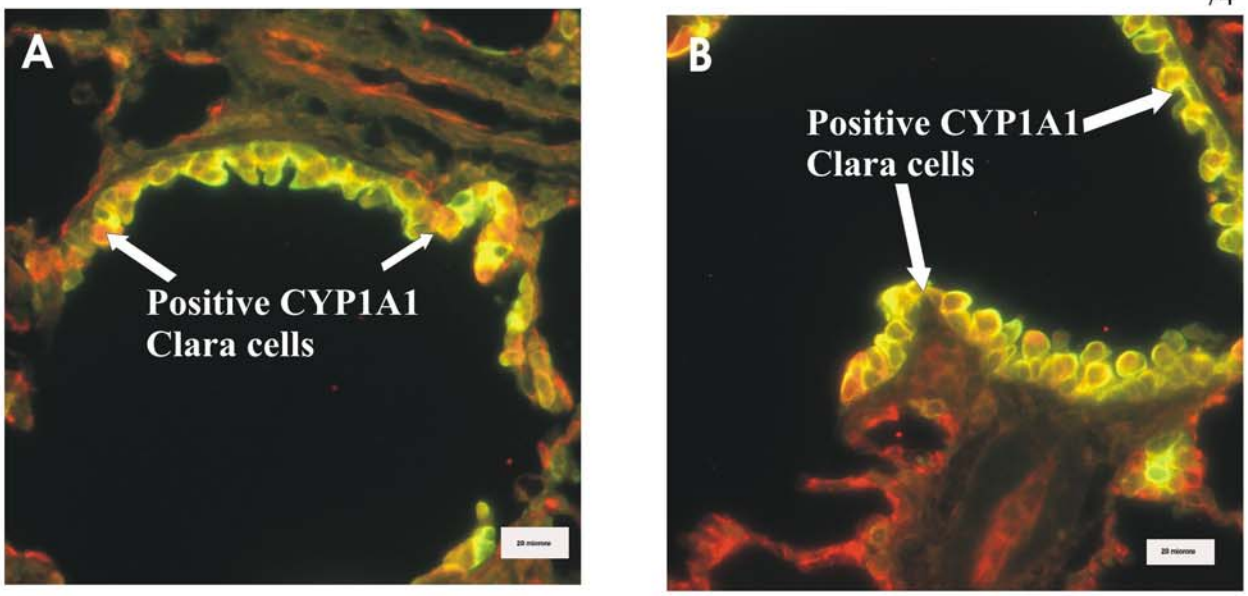

Figure 19. CYP1A1 expression in terminal non-ciliated bronchiolar epithelial (Clara) cells of BNF-induced rats. The number of CYP1A1-positive Clara cells was counted per micrometer of basement membrane. No significant difference was detected in BNF and CD-exposed rats (A) compared to BNF-treated rats. Reference bar is 20 micrometer.

Table 1. Summary of morphometric quantification of immunofluorescent-stained sections against CYP1A1 and cytokeratins 8/18 in rat lungs exposed to coal dust.

	saline		CD 2.5 mg		CD 10 mg		CD 20 mg		CD 40 mg	
Region / **parameter**	**PA**	**RA**	**PA**	**RA**	**PA**	**RA**	**PA**	**RA**	**PA**	**RA**
Cytokeratins 8/18 expression	471.1 ± 152.6	509.1 ± 133.7	236.7 ± 152.6	44.8 ± 133.7	907.2 ± 152.6	421.2 ± 133.7	829.5* ± 152.6	462.4 ± 133.7	1160* ± 152.6	512.8 ± 133.7
Area of CYP1A1 in AT-II cells (μm^2)	124.5 ± 40.4	79.2 ± 54.5	75.5 ± 40.4	67.7 ± 54.5	129.9 ± 40.4	57.3 ± 54.5	35.4 ± 40.4	87.8 ± 54.5	24.0 ± 40.4	181.9 ± 54.5
proportional CYP1A1 expression in AT-II cells	0.274 ± 0.043	0.260	0.319 ± 0.043	0.163	0.141 ± 0.043	0.175	0.039* ± 0.043	0.187	0018* ± 0.043	0.275
Area of CYP1A1 in NT-II cells (μm^2)	540.9 ± 76.86	711.5 ± 127	471.2 ± 76.86	328.8 ± 127	372.1 ± 76.86	353.9 ± 127	136.1*☼ ± 76.86	328.9 ± 127	144.2*☼ ± 76.86	537.2 ± 127
Area of CYP1A1 in all alveolar cells (μm^2)	665.4 ± 103.0	575.0 ± 173.6	546.8 ± 103.0	396.4 ± 173.6	498.7 ± 103.0	411.3 ± 173.6	171.4 *☼ ± 103.0	416.8 ± 173.6	168.2*☼ ± 103.0	719.2 ± 173.6
CYP1A1 positive Clara cells/µm	0.0482 ± 0.0062		0.0446 ± 0.00482		0.0525 ± 0.0018		0.0513 ± 0.00784		0.0317 ± 0.00785	

The values presented are means ± SE, n=4. * means significant difference from the control (saline) regarding the same region. ☼ indicates significant difference of PA regions from RA regions of the same treatment group.

DISCUSSION

Some epidemiological studies report that coal miners, primarily smokers, have a lower risk of developing lung cancer compared with control non-miners (Costello *et al*, 1974). Moreover, lung cancer risk in workers exposed to the more toxic particles, such as silica, was mostly absent when workers were concurrently exposed to other workplace lung carcinogens, such as polycyclic aromatic hydrocarbons (PAHs) (Cocco *et al*, 2001). Such data concerning lung cancer in miners are difficult to interpret because miners are exposed to a mixture of environmental pollutants; such as the coal dust particles and the PAH in cigarette smoke

Using rats with induced CYP1A1, as it is in cigarette smokers, our EROD data showed that coal dust exposure suppressed induced CYP1A1 activity in a dose-dependent fashion (Figure 3). Previous studies in our laboratory showed that IT exposure of rat lungs to crystalline silica (20mg/rat) significantly suppressed induced EROD activity (Battelli *et al*, 1999). Although coal dust is less cytotoxic than silica (Castranova, 2000), it is able to inhibit the CYP1A1-dependent enzymatic activity (EROD) in a dose responsive manner suggesting that CD particles are among the toxic respirable compounds, that include silica, that interfere with CYP1A1 metabolic activity in rat lungs. Western blot analysis was performed using a polyclonal rabbit anti-rat CYP1A1 antibody to detect CYP1A1 protein expression in the lung microsomes. The amount of CYP1A1 protein in the gel was reduced at all doses of CD treatment, but was significant only in the highest dose (40 mg/rat) (Figure 5A and B). This suggested that the reduction in the CYP1A1 activity upon exposure to CD is partly attributed to the reduction of CYP1A1 expression and protein synthesis by different pulmonary cells.

The activity of CYP2B1, measured in lung microsomes as PROD activity, showed a dose-dependent reduction by exposure to coal dust (Figure 4). CYP2B1 is the major constitutive isoform of cytochrome P450s in rat lungs (Martin *et al*, 1993; Guengerich *et al*, 1982). CYP2B1 expression is not inducible in the rat lung (Guengerich *et al*, 1982). BNF, a specific CYP1A1 inducer, significantly up-regulates CYP1A1 expression in the lung parenchyma (Lee *et al*, 1998, Jones *et al*, 1983, and Sesardic *et al*, 1990). Western blot analysis for CYP2B1 showed a reduction of the protein, albeit not

significant, in BNF and CD-exposed rats compared to rats receiving BNF alone. This suggested that CD exposure modified not only the CYP1A1 expression and activity but also the activity of CYP2B1 in the rat lung.

Cell-specific expression and localization of CYP1A1 were studied by immunofluorescence followed by quantification using morphometric analysis. Immunofluorescence was employed in this study because preliminary studies indicated that it was more sensitive than enzymatic immunohistochemistry and useful for localizing the sites of pulmonary CYP1A1 through double labeling (Battelli *et al*, 2001). Morphometric analysis of immunofluorescent-stained sections for CYP1A1 demonstrated that within the alveolar septum, CYP1A1 expression area was generally localized to flattened cells morphologically suggestive of alveolar type I cells (Figure 9D). By using colocalization to sites of cytokeratins 8/18 expression to determine AT-II CYP1A1 expression, it was demonstrated that most of the alveolar area expressing CYP1A1 is not occupied by AT-II cells. This was not surprising because alveolar type I epithelial cells cover greater than 90% of the internal surface area of the lungs (Wang *et al*, 2002; Gonzalez and Dobbs, 1998) whereas type II epithelial cells account for less than 10% (Castranova *et al*, 1988). Moreover, it has been observed by in situ hybridization in the lungs of 3-methylcholanthere-induced rats that CYP1A1 labeling was visualized in other alveolar wall cells that could be either capillary endothelial cells or alveolar type I pneumocytes (Pairon *et al*, 1994). An overall reduction of CYP1A1 expression within the alveolar septum was observed in BNF-induced rats exposed to 20 mg and 40 mg CD/rat compared to those exposed to BNF induction and saline. These results were consistent with EROD activity, suggesting that both CYP1A1 protein expression in the alveolus and its metabolic function throughout the lung are suppressed by CD exposure. Localization of CYP1A1 in terminal non-ciliated bronchiolar epithelial (Clara) cells was also investigated because Clara cells are considered the major area of CYP1A1 expression in lungs since they are rich in agranular endoplasmic reticulum (Plopper, 1983) where CYP1A1 is localized. The number of CYP1A1-positive cells was counted per micrometer of the basement membrane. This number did show a significant change in rats exposed to CD and BNF compared to the control. This result suggested that CD modified CYP1A1 expression at the alveolar rather than the bronchiolar level,

presumably because the CD particles tend to aggregate in alveolar regions adjacent to the alveolar duct.

Previous morphometric studies demonstrated that the alveolar tissue represents 87% of the total lung volume in rats where the volume of alveolar type I cells is more than twice that of alveolar type II cells (Carpo *et al*, 1983 and Perkinton, *et al*, 1982). Following lung injury at the alveolar level, the damage of type I pneumocytes is repaired by progenitor alveolar type II cells that can proliferate and regenerate the damaged alveolar surface and may differentiate into type I cells, thus reconstituting the alveolar architecture (Melloni *et al*, 1995; Wang *et al*, 2002). The hypertrophy and hyperplasia of AT-II cells were obvious in immunofluorescence (Figure 12B) and histopathology (Figure 7A). Despite the increasing numbers (hyperplasia) and size (hypertrophy) of AT-II cells, AT-II cell-specific CYP1A1 expression decreased as many of these cells were devoid of detectable CYP1A1 (Figure 12B). This suggested that coal dust exposure was associated with the appearance of new populations of AT-II cells but that many of these cells did not contain detectable amounts of CYP1A1. A number of investigators have reported that CYP activities and the level of CYP apoproteins decreased after partial hepatectomy and regeneration of hepatic cells (Hino *et al*, 1974; Presta *et al*, 1980; Klinger and Karge, 1987; Ronis *et al*, 1992). The priority of hepatic cell function during regeneration is the key factor where the replication, but not the transcription, is the main function of DNA regenerating the cells (Liddle *et al*, 1989, Waxman, 1989, Morgan *et al*, 1985, and Steer, 1995). One possible explanation for our findings may be that like regenerating hepatocytes, AT-II cells during the hyperplasia and hypertrophy, are mainly devoted to proliferation and not to expressing CYP1A1. Consistent with that were the higher levels of CYP2B1 protein expression and mRNA in freshly isolated AT-II cells, but these levels diminished in the cell culture (Lag *et al*, 1996).

Histopathological changes assessed in stained sections showed that CD exposure enhanced the pulmonary inflammatory response (Figure 7B and 8). Lung inflammation was characterized by intra-alveolar and interstitial accumulation of macrophages and rare neutrophils. The dust-laden macrophages were enlarged and often aggregated in clumps of two or more cells. The alveolar inflammation was often centered around alveolar ducts where CD particles were deposited. These findings were consistent to those described by

Nikula *et al*, (1997). It has been demonstrated that the ability of the liver to metabolize drugs in rodents is impaired following inflammatory stimuli that are accompanied by a depletion of total hepatic CYP content and a declined microsomal metabolism of drug substrates (Ghezzi *et al*, 1986; Bissell and Hammaker, 1976). In other similar studies, the experimentally-induced inflammatory reactions resulted in a reduction of the microsomal CYP concentration and their metabolizing activity in the liver (Beck and whitehouse, 1974; Mahu and Feldman 1984; Endo *et al*, 1981; Baer and Green, 1981). In addition, exposure of cultured hepatocytes to inflammatory stimuli decreased the total microsomal CYP, CYP-catalyzed enzyme activities, and levels of CYP proteins and mRNAs (Morgan, 1997). Although relatively little data describes the effect of inflammation on extrahepatic CYP expression and some evidence suggests that extrahepatic CYPs are likely to be differentially regulated by different inflammatory stimuli (Morgan, 2001). The CD-induced pulmonary inflammation shown in our experiment was associated with suppression of pulmonary CYP1A1 induction and CYP2B1expression and activity in the rats. Studies of possible roles of pro-inflammatory mediators are underway.

In conclusion, our data showed for the first time that CD exposure had a modifying effect on the BNF-induced CYP1A1 expression via altering its cell specific localization in rat lung. CD was able to suppress the activity and expression of CYP1A1 as demonstrated by the dose-dependent reduction of EROD activity and diminution of CYP1A1 apoprotein measured by Western blot analysis. Not only was CYP1A1 induction modified by CD exposure, but the activity of another CYP isoform, CYP2B1, was suppressed in a dose-dependent fashion. The overall results suggested that coal dust exposure was a complex modifier of the CYP1A1 induction in rat lungs and had the ability to trigger pulmonary inflammation and reduction of CYP1A1 induction and activity.

CHAPTER 4
SUPPRESSION OF RABBIT PULMONARY CYP1A1 INDUCTION BY RESPIRABLE CRYSTALLINE SILICA

ABSTRACT

Silicosis is an inflammatory and fibrosing occupational lung disease which is also associated with increased risk of developing lung cancer. However, inflammation interferes with the biological activation of polycyclic aromatic hydrocarbon (PAH) procarcinogens to ultimate carcinogens by cytochrome P450 1A1 (CYP1A1). In addition, the carcinogenic effects of crystalline silica and cigarette smoke, which contains PAHs, are subadditive in some epidemiologic studies. Investigating the modifying effect of silicosis on PAH metabolism will facilitate interpretation of epidemiologic studies of mixed exposures to cigarette smoke and crystalline silica. We have, therefore, investigated the hypothesis that acute and chronic silicosis can modify PAH-induced pulmonary carcinogenesis by altering cell specific induction of pulmonary CYP1A1. Acute or chronic silicosis were induced in male New Zealand White rabbits by intratracheal instillation of 300 mg respirable crystalline silica 2 weeks or 1 year prior to sacrifice, respectively. Chronic silicosis was principally localized to one side of the lung to minimize the signs of respiratory diseases. Control rabbits received intratracheal instillation of saline. CYP1A1 was induced in all exposure groups by intraperitoneal injection of beta-naphthofalvone (BNF, 80mg/kg IP) 2 and 3 days prior to sacrifice. CYP1A1 function as assessed by 7-ethoxyresorufin-O-deethylase (EROD) activity was significantly lower in BNF-exposed rabbits with acute ($p=0.01$) or chronic ($p=0.02$) silicosis than in rabbits receiving BNF alone. By Western blot, CYP1A1 protein was significantly reduced in acute ($p=0.02$) but not chronic silicosis. Cell specific expression of CYP1A1 was assessed in sections of lung by immunofluorescent double labeling for CYP1A1 and cytokeratins 8/18, cytoskeletal proteins expressed in Alveolar type II (AT-II) and airway epithelial cells. In the alveolus, total septal expression of CYP1A1 per unit area was decreased in both acute and chronic silicosis. In terminal bronchioles, both acute and chronic silicosis resulted in a decrease in the number of Clara cells expressing CYP1A1 per mm basement membrane. These results suggest that silicosis suppresses the

induction of CYP1A1 activity and alters the alveolar and bronchiolar cellular expression of CYP1A1 in rabbits.

INTRODUCTION

CYP1A1 is the microsomal enzyme responsible for the bioactivation of pro-carcinogenic compounds such as benzo[a]pyerene, producing biologically active intermediates that bind to the DNA to produce adducts and lung cancer (Gelboin, 1980; Crepsi *et al*, 1989; Shimada *et al*, 1989; Anttila *et al*, 1991; Eaton *et al*, 1995). CYP1A1 is associated with the endoplasmic reticulum of many cells, particularly those of xenobiotic-metabolizing organs such as liver and lungs (Anttila *et al*, 1991). It is well known that CYP1A1 is induced via an aryl hydrocarbon receptor (AhR)-ligand binding mechanism. The binding of a ligand, such as a PAH, causes dissociation of a 90-KDa heat-shock protein (Hsp90) and other cytoplasmic factors such as the AhR-interacting protein (AIP) (Ma and Whitlock, 1997) from the AhR in the cytoplasm, which leads to translocation of the AhR to the nucleus where it dimerizes with another structurally related protein, AhR nuclear translocator (Arnt). This heterodimer binds to the xenobiotic responsive element (XRE) in the regulatory region of the CYP1A1 gene initiating its expression and induction (Takahashi *et al*, 1996; Abbot *et al*, 1999; Ke *et al*, 2001; Hayashi *et a*., 1994). The promoter region of CYP1A1 assumes a particular nucleosomal configuration in un-induced cells that could explain its barely detectable constitutive expression (Morgan and Whitlock, 1992; Whitlock, 1999). Upon induction, the CYP1A1 promoter undergoes a change in chromatin structure and loss of the nucleosomal configuration that facilitates the attachment of promoter-binding proteins (Wu and Whitlock, 1992). The changes in the chromatin structure and configuration at the CYP1A1 promoter area are AhR-dependent and Arnt-dependent processes (Whitlock, 1999).

Silicosis is an occupational lung disease resulting from exposure to the crystalline form of the mineral silicon dioxide or silica (Driscoll and Guthrie, 1997). Silicosis is characterized by inflammation and fibrosis in the lower respiratory tract. Because silica is one of the most abundant minerals in the earth's crust, there are significant opportunities for exposure particularly in occupations or activities involving cutting, shaping, or polishing of rock. The increase in silicosis during the past years is mainly attributed to the

development of tools and processes that generate high concentrations of fine particles (<10μm in diameter), which are able to penetrate into the deep lung tissues, and elicit their toxic effects (Craighead *et al*, 1998; Castranova *et al*, 1996; Peters 1986). Crystalline silica is toxic to a wide range of animal species including humans (Holland, 1990; Saffiotti and Stinson, 1988; Green and Vallyathan, 1995). In humans, there are different forms of silica-induced lung disease differentiated according to the nature and progression of the lung pathology (Driscoll and Guthrie, 1997). Radiologically, simple and progressive massive fibrosis can be identified. Simple silicosis is characterized by the presence of small opacities (silicotic nodules) (Ziskind *et al*, 1986; Seaton, 1984) with a diameter of less than 10 mm (Weissman and Wagner, 2001) without respiratory impairment unless accompanied by tuberculosis (Snider, 1978; Craighead *et al*, 1988). Simple silicosis may develop into progressive massive fibrosis (PMF) when congregation of these silicotic nodules occurs followed by destruction of lung tissue and a significant disturbance in lung function (Snider, 1978). Different types of silicosis are recognized; chronic, accelerated, and acute silicosis (Weissman and Wagner, 2002). The occurrence and development of these forms is determined by the amount of exposure and the total cumulative silica inhalation (Green and Vallyathan, 1995; Ziskind *et al*, 1986; Seaton, 1984). Chronic silicosis is characterized by the appearance of simple silicotic nodules 10-30 years post exposure (Weissman and Wagner, 2002) because it usually progresses very slowly. However, in some cases, nodules may congregate to form PMF (Weissman and Wagner, 2001). Accelerated silicosis, which develops in less than 10 years after exposure to silica (Weissman and Wagner, 2002), is accompanied by a rapid progression to PMF, severe lung dysfunction, and is life threatening (Ziskind, 1986; Seaton, 1984). Acute silicosis, on the other hand, is the form that develops very rapidly [a few weeks to 5 years post exposure (Weissman and Wagner, 2002)] after exposure to high concentrations of silica and is associated with severe alveolar and interstitial inflammation, alveolar proteinosis, and rapid respiratory failure (Driscoll and Guthrie, 1997).

In a recent study by Cocco and co-workers, (Cocco *et al*, 2001) who worked with modifications of silica-associated lung cancer by other workplace lung carcinogens, lung cancer risk in miners exposed to respirable silica alone was higher than those exposed to silica and PAH. The effect of crystalline silica exposure on the CYP1A1- mediated

metabolism of pulmonary chemical carcinogens, such as those in cigarette smoke is unclear. Addressing this effect is biologically important because many chemical carcinogens, such as PAHs in cigarette smoke are metabolized in the lung by CYP1A1 enzyme systems to produce more active carcinogens (Crepsi *et al*, 1989; Shimada *et al*, 1989; Eaton *et al*, 1995) that may result in an increased risk of developing lung cancer. Recent studies from our laboratory suggest that silicosis decreases the activity of CYP1A1-dependent enzymatic activity, 7-ethoxyresorufin-O-deethylase (EROD), in the lungs of rats exposed to a potent CYP1A1 inducer, beta-naphthoflavone (Battelli *et al*., 1999). Cell specific studies on CYP1A1 expression and localization showed that silicosis led to the appearance of a new population of hypertrophied and hyperplastic alveolar epithelial cells without immunohistochemically detectable CYP1A1 or CYP2B1 (Levy *et al*, 1995; Battelli *et al*, 1999).

However, a debate concerning the species differences between rats and humans regarding their response to inhaled particles has emerged (Mauderly, 1997). Moreover, the pattern of particle retention as well as the lung tissue response to respirable particles in rats may not be predictive of those of primates who are exposed to poorly soluble particles particularly at high occupational exposures (Nikula *et al*, 1997). Such debates necessitate the need for investigating the effect of respirable crystalline silica on the induction of the carcinogen-activating system, CYP1A1, in the lung by conducting a study on a non-rodent model. Rabbits were used to investigate our hypothesis because a model of rabbit silicosis has been previously established (Dale, 1973a; 1973b; Wallace *et al*, 2002). Moreover, a high degree of homology between rabbits and human has been reported regarding the critical proteins involved in CYP1A1 induction process, such as the AhR and Arnt. (Takahashi *et al*, 1996). Based upon the homology studies of AhR and Arnt between rabbit and human, and the existence of a rabbit model of silicosis, the rabbits were a suitable non-rodent model to illustrate the effect of silicosis on the carcinogen-metabolizing enzymatic activity of CYP1A1.

In this study, we have investigated the hypothesis that acute and chronic silicosis can alter cell-specific induction of CYP1A1 in the lung, thus modifying the metabolism of carcinogenic polycyclic aromatic hydrocarbons in the lung. To avoid concerns about differences between human and rodent pulmonary responses to respirable particles, we

have investigated this hypothesis using a well-established rabbit model of silicosis Wallace *et al*, 2002). In this model, silicosis progresses with time to produce a fibrosing lung disease which occasionally includes silicotic nodules which are remarkably similar to the human silicotic nodules, the pathognomonic lesion of silicosis in man. By using a partially localized model of chronic silicosis, clinical disease was prevented which permitted maintenance of these rabbits for a year. A more generalized model of silicosis was used to model acute silicosis and was directly comparable to our previous rat studies. Because constitutive CYP1A1 expression is extremely low in both animals and man and because CYP1A1 activity is induced in people who smoke, CYP1A1 activity was induced in all rabbits in the study using the model polycyclic aromatic hydrocarbon, BNF. We have used antibodies to cytokeratins 8/18, proteins which are highly expressed in airway epithelium and AT-II cells to help localize sites of expression of CYPIA1 within the deep lung by immunofluorescence and have found that alveolar expression of CYP1A1 is principally localized in cells that are not AT-II cells, that the area of cells expressing CYP1Al in the alveolus is reduced in both acute and chronic silicosis and that the number of CYP1A1 expressing Clara cells per mm basement membrane is reduced in both acute and chronic silicosis. Acute, but not chronic, silicosis caused statistically significant reductions in the amount of induced CYPIA1 as determined by Western blot. However, CYP1A1-dependent EROD activity induction was reduced by both acute and chronic silicosis. Our findings support the hypothesis that acute and chronic silicosis decrease CYP1Al induction and modify the cell-specific expression of CYP1A1 in the rabbit lung.

MATERIALS AND METHODS

Rabbit Treatment and Experimental Procedure

Male New Zealand White rabbits (3-5 kg) were housed in the AAALAC-approved Laboratory animal facility of Health Sciences Center of West Virginia University. They were fed commercial rabbit pellets and provided water *ad libitum*. All procedures were approved by WVU-ACUC under protocol number 9911-06. Ten of these rabbits were designated for chronic exposure and were exposed to a single dose of silica or saline using a predominantly unilateral model with lesser distribution to additional lobes according to a previously published procedure (Wallace *et al*, 2002). A year later, 7

additional rabbits were randomized into 2 groups, which were intratracheally exposed to silica or saline and kept for 2 weeks as a model of acute exposure (i.e. in the chronic model, rabbits were exposed once and kept for 380 days, while in the acute model, they were kept for only 2 weeks). In the acute model, both lung lobes (right and left) were diffusely exposed to silica to be comparable to previous rat studies. All rabbits, in both acute and chronic models, were exposed to a single dose of crystalline silica suspension (300 mg/rabbit in saline). CYP1A1 was induced in all rabbits by intraperitoneal (IP) administration of 2 doses of BNF of 80mg/kg each suspended in sterile filtered corn oil 3 and 2 days before sacrificing.

Preparation of Silica for IT Instillation

Silica particles (< 5 microns) were weighed into scintillation vials, autoclaved at 23 PSI, 250 ºF, for 30 minutes on the dry cycle. Rabbits exposed to silica received 300 milligrams of heat-sterilized silica particles suspended in 3.0 ml non-pyrogenic saline (0.9% sodium chloride, Abbott Laboratories, North Chicago, IL) and vortexed to achieve a uniformly distributed suspension before IT instillation. The silica suspension used in the study was endotoxin-free as shown by endotoxin analysis using the Limulus Amebocyte Lysate assay (BioWhittaker; Walkersville, MD) as previously described (Olenchock and Stephen, 1990; Porter *et al*, 1999).

Intratracheal Instillation (IT) in Rabbits

Rabbits were first weighed and anesthesized by intramuscular (IM) administration of ketamine hydrochloride (Ketaset, Fort Dodge, IA) 5 mg/kg and xylazine hydrochloride (Rompun, Bayer Pharma, West Haven, CT) 100 mg/kg. After induction of anesthesia, which was marked by absence of palpebral reflex, an endotracheal tube of 3.0 mm external diameter was placed into the trachea under the guidance of a laryngoscope (Anesthesia Medical Specialties, Inc., Santa Fe Spring, CA) that was inserted through the mouth until the arytenoid cartilages were visualized. The presence of the endotracheal tube in the trachea was verified by feeling the expiratory air expelled out of its proximal tip. A long polyethylene cannula with a 1.44 mm outer diameter (Becton Dickinson and Company, Sparks, MD) was passed through the lumen of the endotracheal tube into the trachea. A syringe containing saline or silica suspension was attached to the cannula and the plunger was slowly pressed down. For acute silicosis, the cannula was inserted to the

level of trachea and the rabbit was kept upright on the sternum. In chronic silicosis, the model was predominantly unilateral where the intubated rabbit was placed on its right side, the cannula was blindly inserted until it lodged in a bronchus, and then exposed (Wallace *et al*, 2002). The acute exposure method was directly comparable to rat intratracheal instillation. The chronic exposure method exposed both sides of the lung (Wallace *et al*, 2002), but because severe lesions were limited to one side of the lung, long-term humane maintenance of these rabbits was possible. Because the technique for chronic exposure involves the blind passage of a cannula, the most affected lobes will not always be in the same site. The advantage over bronchoscopy is less trauma, more rapid recovery from anesthesia, and involvement of many lobes in mild disease with the more severe lesions localized so that the rabbits remain healthy throughout the study but the disadvantage is that the localization of the more severe silicotic lesions varies.

Necropsy

Rabbits were humanely killed by intravenous injection of pentobarbital (Pentobarbital Sodium, Med-Pharmex, Inc., Pomona, CA) 1.5 ml/rabbit, followed exsanguination via the abdominal aorta. The lungs and attached organs including tracheobronchial lymph nodes, thymus, heart, aorta, and esophagus were removed. At necropsy, the right lung lobes were tied off, removed, and placed on ice for microsome preparation. The left lung lobes were inflated with 30 ml of 10% neutral buffer formalin (NBF) to prepare formalin fixed tissues for histopathology and immunofluorescence. The fixed tissues were trimmed later the same day, and processed on a Hypercenter XP tissue processor (Thermo Shandon, Pittsburgh, PA) over night. The processed tissues were embedded in paraffin the following morning. Sections were routinely stained with hematoxylin and eosin (H&E) and with trichrome stain. In addition, five-micrometer-thick sections were placed on Probe On Plus^{Tm} slides (Fischer Scientific, Pittsburgh, PA) for immunofluorescent double-labeling. In all rabbits, sampling for histopathology involves areas with obvious gross lesions. Due to the presence of silicotic nodules in the right lung lobes of two rabbits from the chronic silica-exposed group, the right lung lobes from these two rabbits containing the gross morphologic changes of silicosis were used for histopathologic examination, while the left lung lobes were used for microsome preparation.

Microsome Isolation

All steps of microsomal preparation were carried out at -4ºC to avoid possible loss of microsomal activity. Microsomes were prepared as previously described (Ma *et al*, 2001; Flowers and Miles, 1991). Briefly, after necropsy, the right lung lobes (except for the 2 rabbits in the chronic exposure group where the left lung lobes were used) were weighed and chopped 4 times with a MacIlwain tissue chopper (Mickle Engineering Co., Gomshall, Surrey, UK) set at slice thickness of 0.5 mm. The minced lung tissues were suspended in 4 times the lung weight of ice-cold incubation medium(1.9 mM KH_2PO_4,145 mM KCL, 30 mM Tris-HCL, 8.1 mM K_2HPO_4, and 3 mM Mg Cl_2; pH 7.4) and homogenized by using a Teflon-glass Potter-Elvejhem homogenizer (Emerson, NJ) through 16 complete passes. Differential centrifugation of the homogenate was used to obtain the microsomal pellets. First, the cell nuclei and debris were sedimented by centrifugation at 2500 rpm for 10 minutes in a Sorvall Model RC2-B refrigerated centrifuge (Ivan Sorvall Co., Northwalk, CT). To reduce the mitochondrial contamination of the microsomes, Mitochondria were slowly sedimented by three sequential centrifugations at 5,000, 9,000, and 13,000 rpm for 20 minutes each. To collect the microsomal pellets, the supernatant was ultra-centrifuged for 75 minutes at 40,000 rpm in a Beckman Model L5-50 Ultracentrifuge (Beckman Instruments, Palo Alto, CA). The microsomal pellets were re-suspended in the incubation medium at a ratio equal to the original lung weight (1gm lung/ 1ml medium) and frozen at -80 ºC until use.

Determination of the Total Lung Proteins

The BCA (bicinchoninic acid) method was used to determine the protein content of lung microsomes as previously described (Ma *et al*, 2002; Smith *et al*, 1985) using the BCA protein assay kit (Pierce, Rockford, IL) and a spectra Max 250 Spectrophotometer (Molecular Devices Corporation, Sunnyvale, California). Bovine serum albumin was used as the standard.

Western Blot Analysis

The CYP1A1 protein in lung microsomes was determined by Western blot analysis as previously described (Ma *et al*, 2002). Briefly, 60 μg of the lung microsomal proteins, as measured by BCA method, were subjected to polyacrylamide gel

electrophoresis followed by electroblotting of the gel to a nitrocellulose membrane based on the manufacturer's instruction (Invitrogen Corporation, Carlsbad, CA). The protein transferred to the nitrocellulose membrane was detected by overnight incubation with a polyclonal goat anti-rabbit CYP1A1 antibody (Oxford, Oxford, MI) at 4 ºC. The membrane was then incubated with a donkey anti-goat IgG-HRP (horse radish peroxidase) conjugated secondary antibody (Santa Cruz Biotech. Inc., Santa Cruz, CA) for 1 hour at room temperature. Liver microsomes of a BNF-treated rat (Xenotech, Kansas city, KS) were used for a CYP1A1 positive control. The ECL MW (molecular weight) marker (Invitrogen Life Technology, Carlsbad, CA) was used to determine the size of the CYP1A1 band. CYP1A1 protein bound to the membrane was detected by the enhanced chemiluminescence (ECL) method using the ECL detection reagent kit (Amersham, Piscataway, NJ). Super RX Fuji Medical X-ray film (Fuji Film Corp., LTD., Tokyo, Japan) was then exposed at room temperature to the membrane. The intensity of the bands on the X ray film was measured by the Strategen Eagle Eye II scanner (La Jolla, California) with Eagle Sight software. The density on the scanned images was measured using ImageQuant software version 5.1 (Molecular Dynamics, Sunnyvale, CA). Each sample was quantified three times to get the averages of the individual measurement, then the averages were used for statistical analyses. The Western blot results were expressed as a percentage of the CYP1A1 positive control.

Measurement of the CYP1A1- and CYP2B4-Dependent Enzymatic Activities (EROD and PROD)

Measurement of EROD and 7-pentoxyresorufin-*O*-deethylase (PROD) activities were conducted as previously described, using 150 and 300 µl of microsomal suspension (Ma, *et al*, 2002; Burke *et al*, 1985), respectively (suspension was prepared by adding an amount of buffer equal to original lung weight). PROD is a measure of CYP2B4 activity (Cawley *et al*, 2001). The CYP2B4 in rabbits is analogous to rat CYP2B1 (Oesch-Bartlomowicz and Oesch, 2003). It is the major constitutively expressed CYP in rabbit lung but is present in very minute quantities in liver (Serabjit-Singh *et al*, 1979; Parandoosh *et al*, 1987). A standard curve was made after each assay by using a standard solution of 2.35 µg of 7-ethoxyresorufin dissolved in 1 ml DMSO to get a 10 mM concentration. EROD and PROD activities were measured by a luminescence

spectrometer model LS-50 (Perkin-Elmer, Norwalk, CT) that measures the formation of fluorescent resorufin catalyzed by CYP1A1 or CYP2B4 activities. EROD and PROD activities were expressed as picomoles of the produced resorufin per minute per milligram microsomal protein (pmol/min/mg protein).

Dual Immunofluorescence Technique for CYP1A1 and Cytokeratins 8/18

The formalin-fixed paraffin-embedded sections of left lung lobe were used for double-label immunofluorescence. Immunofluorescence was conducted to localize the CYP1A1 protein within alveolar and terminal non-ciliated bronchiolar cells (Clara). In addition, immunofluorescence identified alveolar type II (AT-II) cells by localizing the cytokeratins 8/18, which are cytoskeletal proteins expressed mainly in primitive epithelial cells such as AT-II cells and airway epithelium. The double-label Immunofluorescence was a two-day procedure. During the first day, the slides were heated and routinely deparaffinized in xylene and rehydrated in alcohol as previously described (Dey *et al*, 1999). To maximize the antibody binding, the antigen was retrieved by using 0.01M disodium ethylenediamine tetraacetate (EDTA) (Fischer Scientific, Fair Lawn, New Jersey), pH 8.0. Slides immersed in EDTA solution were heated for one minute and 45 seconds on high in a microwave followed by 2 defrosting cycles of 6 minutes each. Tissue slides were blocked with a filtered [(Acrodisc syringe filter with 0.2 μm pore diameter (Pall Corporation, Ann Arbor, MI)], freshly prepared solution of 5 % BSA (IgG free) (Sigma, St Louis, MO) in PBS (Ca^{++} and Mg^{++} free) (Sigma, St Louis, MO) for 10 minutes at room temperature (RT) to minimize the non-specific binding of the primary antibodies. Additional blocking was applied by dropping of 5% fresh pig serum (Biomeda Corporation, Foster City, CA) in PBS on slides for 10 minutes at RT. The slides were then rinsed and incubated with a primary antibody mixture with a final dilution of 1:50 of the polyclonal Guinea pig anti-cytokeratins 8/18 antibody (Research Diagnostic Inc., Flanders, NJ) and the polyclonal goat anti-rabbit CYP1A1 antibody (Oxford biomedical Research, Inc., Oxford, MI). The primary antibody mixture was applied by holding the slides in pairs in a microprobe holder (Fischer Scientific, Fair Lawn, NJ) and allowing the capillary action between each pair to pull the mixture onto the slides. The microprobe holder carrying slides was placed in a humidity chamber and incubated overnight at room temperature to allow binding of the primary antibodies to the

antigen (CYP1A1 and Cytokeratins 8/18). On the second day, the humidity chamber containing the microprobe holder was incubated in the oven at 37 ºC for 2 hours. The excess and unconjugated primary antibodies were washed off by thorough rinsing with distilled water. Then, a mixture of the secondary antibodies was applied by dropping on the slides. The mixture was produced by equal volumes of a polyclonal FITC-conjugated donkey anti-Guinea pig antibody (Research Diagnostic Inc.) at a dilution of 1:50 with PBS, and Alexa 594-conjugated rabbit anti-goat antibody (Molecular probes, Eugene, OR) for CYP1A1, diluted 1:20 with PBS. Before application, the mixture was centrifuged for 5 minutes at 2000 rpm and the supernatant dropped onto the slides, and the slides were incubated for 2 hours at RT in the dark. After rinsing the slides, cover slips were applied using gel mount (Biomeda Corp., Foster City, CA) and slides were allowed to dry for 2 hours. For the negative control, the same procedure was applied except that the primary antibodies were replaced by rabbit serum (BioGenex, San Ramon, CA).

Slides were examined using a fluorescent photomicroscope (OlympusAX70, Olympus American Inc., Lake Success, NY) and images were captured using the 40x objective and a Quantix cooled digital camera (Photometrics, Tucson, AZ) with QED camera plugin software (QED Imaging, Inc., Pittsburgh, PA). Fifteen images were captured per slide; five of which were taken from proximal alveolar (PA) regions located adjacent to the alveolar duct where most of the silica particles tend to accumulate (Warheit, 1989**)**. The purpose of these samples was to assure that images were captured from representative alveolar regions with silica deposition. Another five images were obtained from random alveolar (RA) regions where no visible alveolar ducts are located. An additional five images were obtained from the terminal bronchioles which are lined by non-ciliated bronchiolar epithelial (Clara) cells. Since normal alveolar structure granulomas and nodular fibrosis, areas showing granulomas and nodular fibrosis were avoided during capture of images. The exposure settings of the digital camera were held constant for during capture of images from all slides. For green fluorescence, a FITC filter cube with an excitation wave length of 460-500nm was used. For red fluorescence, a Texas Red filter cube with an excitation wave length of 432.5-487.5nm was used.

Morphometric Analysis

A specific software program (MetaMorph Universal Imaging Corp., Downingtown, PA) was employed to quantify and measure the area in μm^2 of the red fluorescence that represents CYP1A1 protein and the green fluorescence that represents cytokeratins 8/18. Morphometric analysis was conducted on digital images captured using a 40x objective producing a microscopic field with an area of 34466.1 μm^2. The threshold range for positive red or green fluorescence was constant throughout the analysis process of all images. These thresholds were selected to measure the area occupied by cells expressing green fluorescence in the cytoplasm (which in the alveolus indicates AT-II cells), the area of cells demonstrating red fluorescent labeling of CYP1A1 in the alveolar septum, and the co-localization of these proteins. The morphometric analysis quantified the following:

A-Quantification of CYP1A1 Expression in Alveolar Cells that are not AT-II Cells:

We have designated the alveolar cells without cytokeratins 8/18 expression as alveolar non-type II (NT-II) cells. These cells are identified by their low affinity for cytokeratins 8/18 staining, which is specific for primitive epithelial cells such as airway epithelium and AT-II cells (Kasper, 1993). In the double labeled sections, cells expressing CYP1A1 fluoresce red. By morphometric analysis, the percent of CYP1A1 that is not concomitantly stained with cytokeratins 8/18; that is the percent of area of CYP1A1 expression in NT-II cells was estimated. To calculate the area of CYP1A1 expressed within NT-II cells, we multiplied this percent by the total red (CYP1A1) area within alveolar septum. The resulting area was expressed in μm^2.

B-Quantification of CYP1A1 Expression in AT-II:

By the aid of morphometric analysis, the CYP1A1 co-expression (co-localization) in AT-II was quantified. Colocalization means concomitant expression of CYP1A1 and cytokeratins 8/18 in AT-II. Two estimates were obtained to express this co-localization in AT-II cells:

1-The Area of CYP1A1 Colocalized to Cytokeratins 8/18:

This area was estimated, in a similar way as in alveolar non-type (NT-II) cells, by multiplying the percentage of CYP1A1 that concurrently stained with cytokeratins 8/18 by the total septal expression of CYP1A1. This area was expressed in μm^2.

2- The Proportional CYP1A1 Expression in AT-II Cells

Proportional CYP1A1 expression is a ratio of the area of CYP1A1 expressed in AT-II to the total area of AT-II cells. This calculation was necessary because respirable particles often cause AT-II cell hyperplasia in the lung. Thus the proportional CYP1A1 expression in AT-II cells corrects for increases in CYP1A1 in AT-II cells resulting from simple increase in the number and area of lung occupied by AT-II cells. This fraction was calculated from the following formula:

$$F = \frac{P \times R}{G} \quad \text{where;}$$

F= proportional CYP1A1 expression in AT-II

P= percentage of CYP1A1 colocalized to cytokeratins 8/18 (estimated by morphometry)

R= red area (total) of CYP1A1 in alveolar septum (measured by morphometry)

G= green area (total) of AT-II in alveolar septum (quantified by morphometry)

C-Determination of AT-II Cell Hypertrophy and Hyperplasia:

AT-II cell hypertrophy and hyperplasia were quantified by measuring the total area of green fluorescence in the alveolar septum expressed in each 40x field (34466.1 μm^2).

D-Determination of CYP1A1 Pattern of Expression in Clara Cells

The non-ciliated terminal bronchiolar (Clara) cells that stained positively for CYP1A1 (red) were counted per micrometer of the basement membrane. Morphometric settings helped standardize detection of positive cells consistently to avoid false positive or false negative results. Therefore, this morphometric analysis provided a direct way to determine the effect of silica particle exposure on the expression pattern of CYP1A1 in AT-II cells, non-AT-II, and Clara cells.

Immunofluorescence analysis was used to compare the cell-specific localization of CYP1A1 in silica and BNF-exposed groups versus the control (BNF only) group.

Within the alveolus, cell-specific CYP1A1 has been compared in the PA regions (which are exposed to more silica) and the RA regions (which are random alveolar samples, and thus receive variable and lower silica exposure).

Histopathology:

Tissue sections from control and silica-exposed lungs were routinely stained with hemotoxylin and eosin (H&E) for histopathology. The stained slides were examined and interpreted by a board-certified veterinary pathologist while blinded to the exposure status of the individual rabbit. The changes of interest to be evaluated were: alveolitis (inflammation), AT-II cells hyperplasia and hypertrophy, and hyperplasia of bronchus associated lymph tissue. The histopathologic changes were converted to quantitative scores based upon the severity and distribution of the morphologic changes as previously described (Hubbs *et al*, 1997). The pathology score for each slide is the sum of the severity and distribution scores and the pathology score for each lung is the mean pathology score for each slide from that lung (Table 1).

Table 1. Scoring system for histopathological changes caused by exposure of rabbit lungs to silica.

Score	Severity	Distribution
0	None	None
1	Minimal	Focal
2	Mild	Locally extensive
3	Moderate	Multifocal
4	Marked	Multifocal and coalescent
5	Severe	Severe

Statistical Analyses

All analyses were performed with SAS version 8.2 and using Proc Mixed. Comparisons between saline treated and silica treated rabbits were performed using one-way analyses of variance. Comparisons of CYP1A1 immunostaining between cell types, and comparisons between compartments within the alveoli were performed using a 2 factor repeated measures analysis of variance (treatment by cell type and treatment by

compartment). All pairwise comparisons were performed with Fisher's LSD. All results were considered statistically significant at $p<0.05$.

RESULTS

Activities of CYP1A1 and CYP2B4

EROD (indicator of CYP1A1-dependent enzymatic activity) measured as pmol/min/mg of microsomal proteins was significantly reduced in rabbits with acute ($p=0.011$) and chronic silicosis ($p=0.0453$) exposed to BNF compared to rabbits exposed to BNF alone (Figure 1A and B, respectively). Acute exposure to silica particulates significantly lowered ($p=0.0099$) the PROD activity (Figure1C) while chronic exposure failed to induce any effect on the CYP2B4-dependent enzymatic activity (Figure 1D).

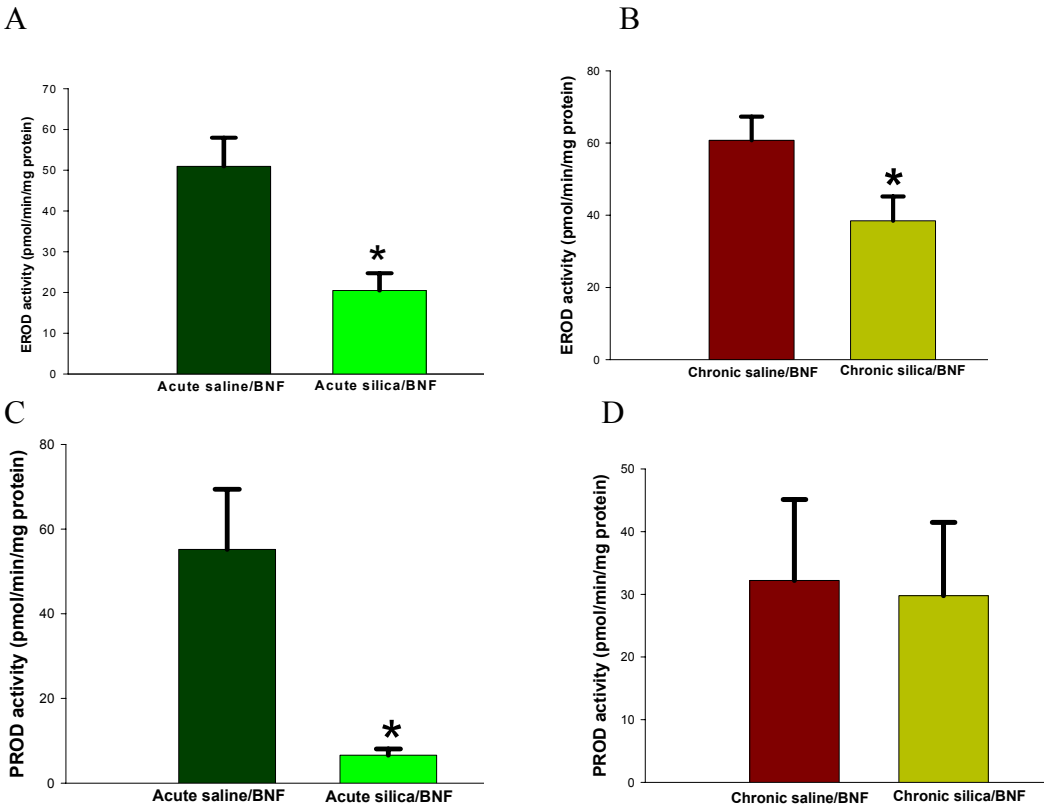

Figure 1. Effect of silicosis on EROD and PROD activities. EROD and PROD activities are expressed as pmol/min/mg protein. Acute silicosis significantly suppresses the BNF-induced-EROD (A) and PROD (C) activity. Chronic silicosis inhibits EROD activity (B) and does not have any effect on PROD activity (D). * indicates significant difference from control (rabbits received BNF alone) at $p<0.05$.

Western Blot Analysis

Western blot analysis demonstrated a reduction, albeit not significant, in CYP1A1 protein in the lungs of BNF-treated rabbits with acute silicosis when compared to the lungs of rabbits exposed to BNF alone (Figure 2A and B). In chronic silicosis, no change was observed (Figure 3A and B).

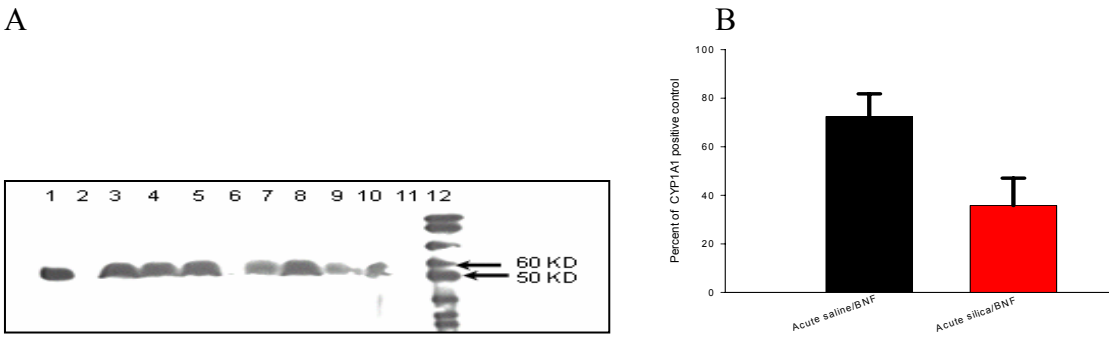

Figure 2. Western blot analysis of CYP1A1 in lung microsomes of rabbits with acute silicosis. 60 µg of microsomal protein were subjected to SDS gel electrophoresis using Tris-glycine SDS running buffer and blotted to nitrocellulose membrane. The membranes were probed with goat anti-rabbit CYP1A1 antibody overnight at 4 ºC. then donkey anti-goat IgG-HRP was used to visualize the bands. In A, Lane 1 is a positive control, while lane 12 is the molecular weight standard. Lanes 3, 4, and 5 are controls (acute saline/BNF), whereas lanes 7, 8, 9 and 10 are acute silica/BNF. Lanes 2 and 6 are empty. In B, the data expressed as the percentage of positive CYP1A1 control resulted from quantifying of western blot of control and silica treated rabbits.

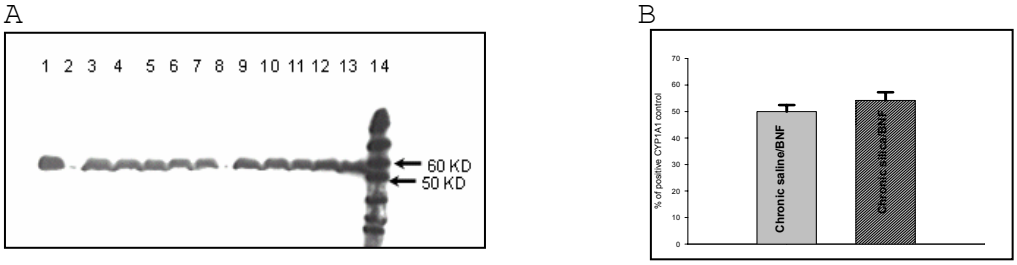

Figure 3. Western blot analysis of CYP1A1 in lung microsomes of rabbits exposed to chronic silicosis. Lane 1 is a positive control, while lane 14 is the molecular weight (MW) standard. Lanes 3, 4, 5, 6, 7 are control (chronic saline/BNF), while lanes 9, 10, 11, 12, and 13 are chronic silica/BNF. Lanes 2 and 8 are empty. In B, the Western analysis data were quantified and expressed as the percentage of positive CYP1A1 control. No significant change of CYP1A1 protein expression was observed in chronic silicosis (silica/BNF) exposure versus control (saline/BNF).

Dual Immunofluorescence for CYP1A1 and Cytokeratins 8/18

A- General Distribution of CYP1A1 in the Rabbit Alveolus

AT-II (AT-II) cells were identified as green fluorescent (due to the markers, cytokeratins 8/18) plump cells localized at the corners of the alveoli, whereas NT-II cells were visualized as flattened cells without green fluorescence occupying the majority of alveolar septum using immunofluorescence visualization and a narrow beam FITC filter cube for excitation. Cells expressing CYP1A1 fluoresced red using a Texas Red filter cube for excitation. Superimposition of the red and green fluorescent images permitted determination of where CYP1A1 was expressed in the same sites as cytokeratins 8/18 (Figure 4).

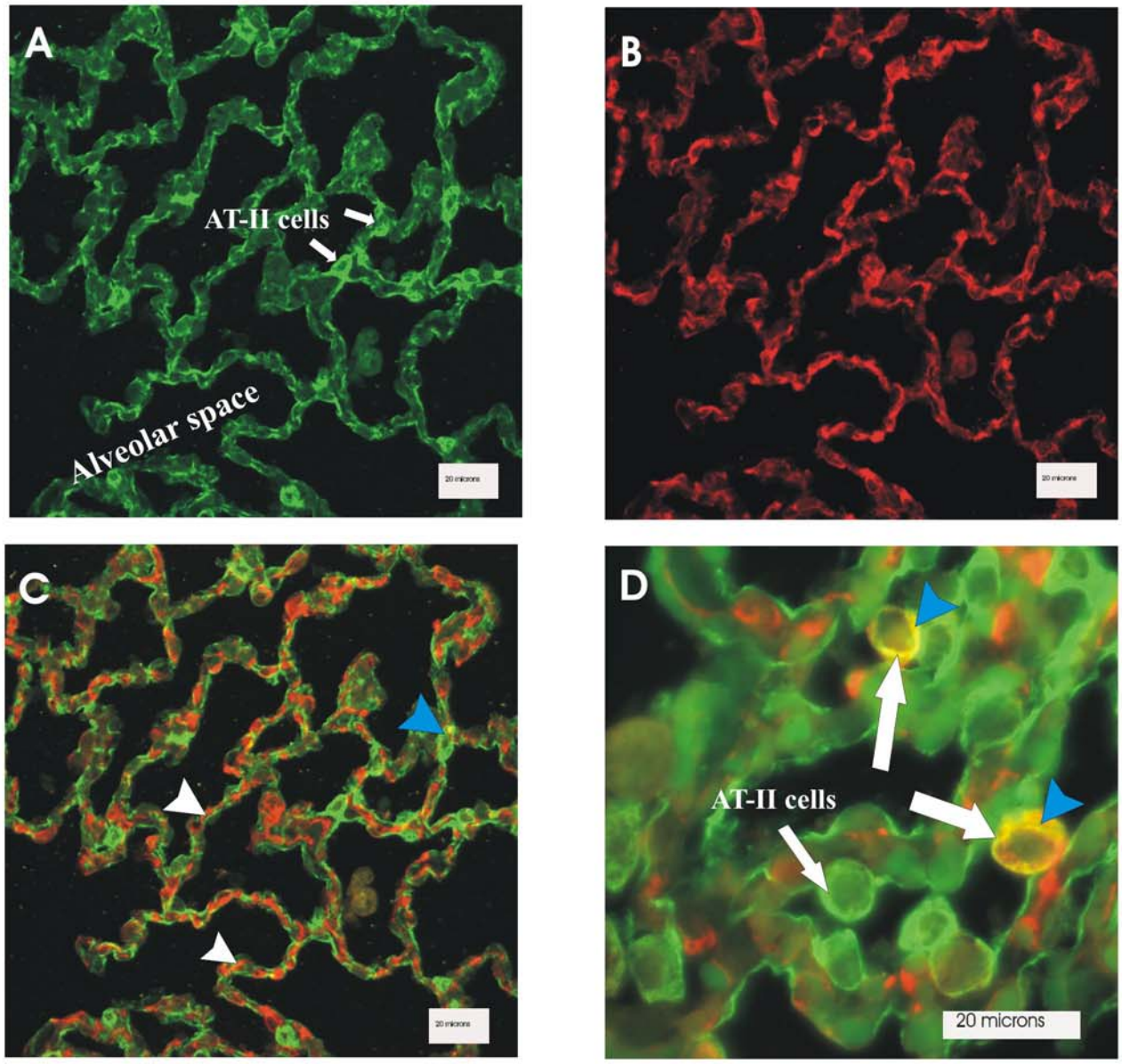

Figure 4. Immunofluorescence staining for CYP1A1 and cytokeratins 8/18 of rabbit alveoli. The CYP1A1 is probed with goat anti-rabbit CYP1A1 antibody while the cytokeratins 8/18 is probed by Guinea pig anti-cytokeratins 8/18 antibody. In the alveolus of rabbits receiving BNF, the cells containing cytokeratins 8/18 fluoresce green (A) and are AT-II cells (cuboidal cells at the corners of alveoli); cells containing CYP1A1 stain red (B);when the images in A and B are superimposed, cells containing both stain yellow (C). The combined image of red and green (C) showing that the red signals (CYP1A1) are mainly localized in the flattened NT-II cells (white arrow heads) of the alveolar septum while a small amount of CYP1A1 is localized in AT-II cells (yellow color-blue arrow head). In D, the image is shown with a higher magnification. Reference bar is 20 micrometer.

Quantification of CYP1A1 by morphometric analysis of proximal alveolar (PA) regions revealed its cell specific expression and localization within the alveolus. The area of CYP1A1 expression within AT-II cells was significantly lower than that of NT-II cells in all groups (acute saline/BNF, acute silica/BNF, chronic saline/BNF, and chronic silica/BNF groups) with p values 0.0001, <0.0001, 0.0006, and 0.0171, respectively (Figure 5A and C and Figure 6A and C, respectively). A similar pattern of expression has been found in random alveolar (RA) regions where area of AT-II cells expressing CYP1A1 is significantly lower than NT-II cells in all groups with p values 0.0097, < 0.0001, 0.0045, and <0.0001, respectively (Figure 5B and D and Figure 6A and D).

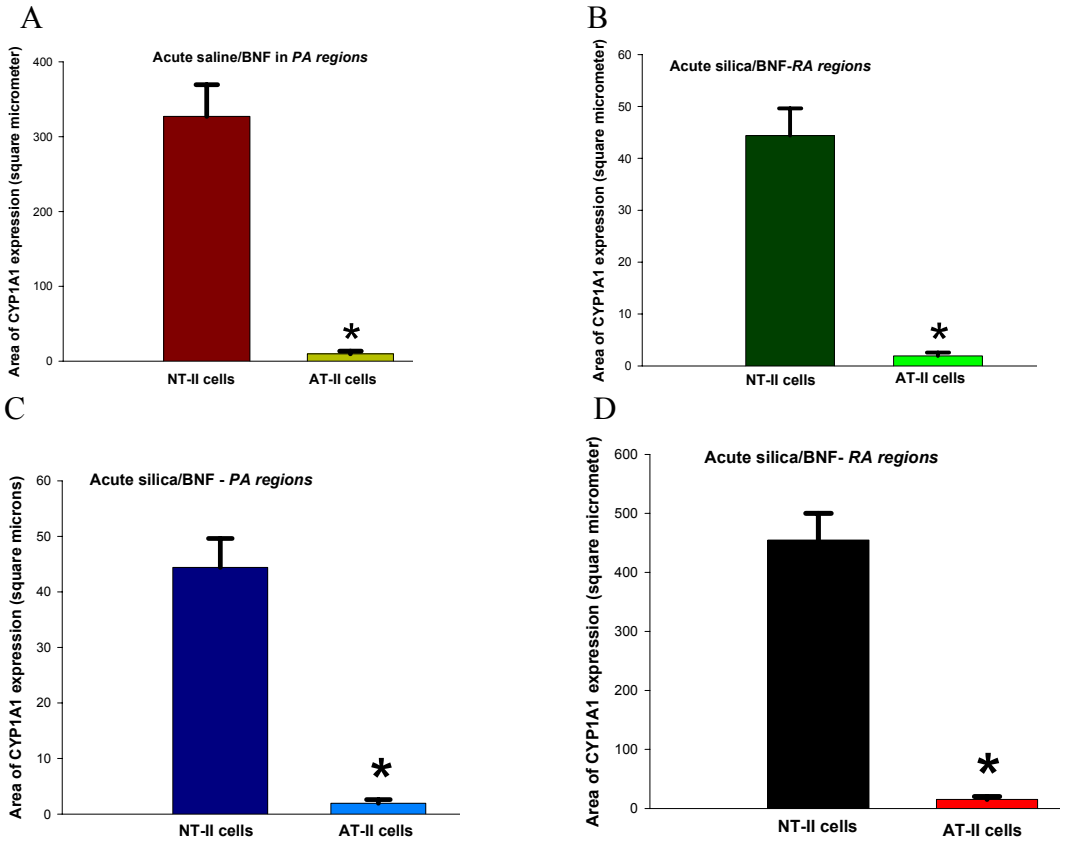

Figure 5. Morphometric quantification analysis of CYP1A1 immunofluorecence in AT-II cells versus NT-II cells of PA and RA regions BNF-treated rabbits acutely exposed to saline or silica. The area of CYP1A1 expression within these cells is expressed in square micrometer. * indicates significant difference from area of CYP1A1 expression in NT-II cells at P<0.05.

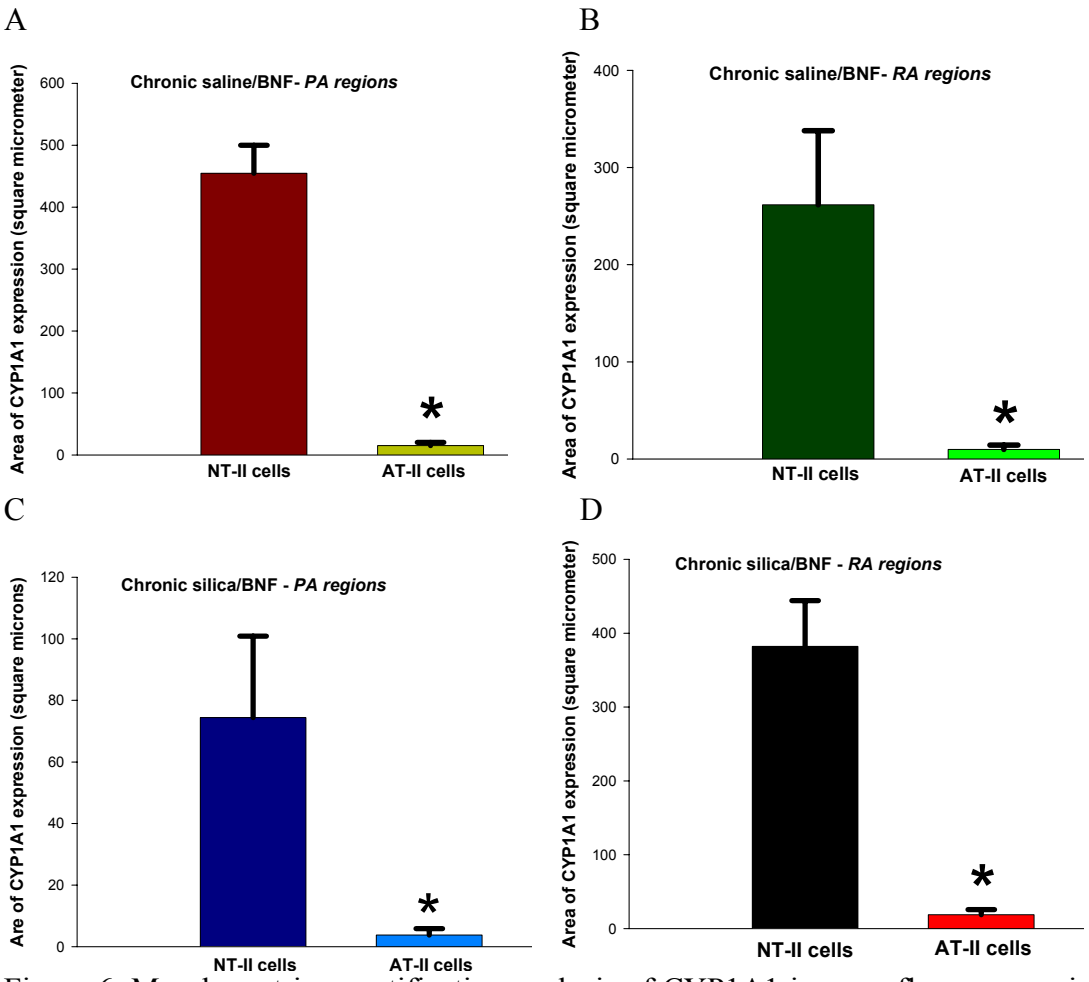

Figure 6. Morphometric quantification analysis of CYP1A1 immunofluorescence in AT-II cells versus NT-II cells of PA and RA regions BNF-treated rabbits chronically exposed to saline or silica. The area of CYP1A1 expression within these cells is expressed in square micrometer. * indicates significant difference from area of CYP1A1 expression in NT-II cells at $P<0.05$.

B- Effect of Acute and Chronic Silicosis on CYP1A1 Expression by NT-II Cells in PA and RA Regions.

In immunofluorescent-stained slides, the area of CYP1A1 expression quantified by morphometric analysis within NT-II cells of the PA regions was significantly reduced in rabbits acutely exposed to silica and BNF when compared to the control saline/BNF ($p=0.0005$). The area of CYP1A1 expression within NT-II cells of RA regions of rabbits acutely exposed to silica and BNF did not show a significant change compared to the control saline/BNF (Figure 7A). A comparison of CYP1A1 expression within NT-II cells in the PA versus the RA regions indicated a significant reduction in the PA regions of rabbits acutely exposed to silica and BNF compared to the RA regions ($p=0.0006$) (Figure 7A).

In rabbits with chronic silicosis and BNF, the area of CYP1A1 expression quantified by morphometric analysis within NT-II cells of the PA regions was significantly reduced when compared to control saline/BNF ($p=0.0066$) (Figure 7B). However, the area of CYP1A1 expression within NT-II cells of RA regions of rabbits chronically exposed to silica and BNF did not show a significant change compared to the control saline/BNF. A comparison of CYP1A1 expression within NT-II cells in the PA versus the RA regions indicated a significant reduction in the PA regions of rabbits chronically exposed to silica and BNF compared to RA regions ($p=0.0243$) (Figure 7B). Results of CYP1A1 expression in NT-II cells are summarized in Table 2.

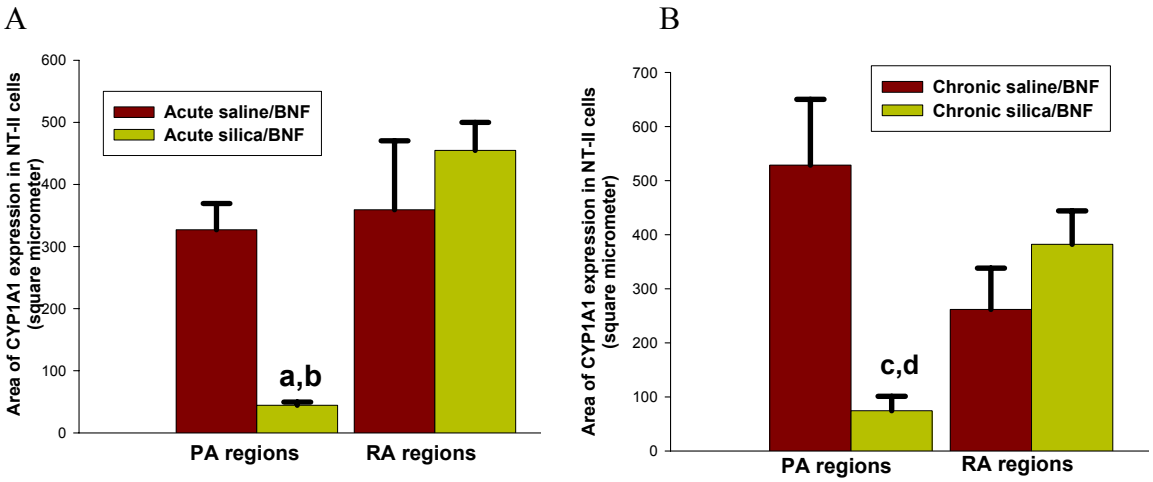

Figure 7. Morphometric quantification analysis of area of CYP1A1 expression measured in μm^2 within NT-II cells of the PA regions and RA regions in acute and chronic silicosis. In A, the area of CYP1A1 expression within NT-II cells of the PA regions is significantly lower in rabbits acutely exposed to silica and BNF than the control saline/BNF (indicated by a above the bar). Also, the area of CYP1A1 expression within NT-II cells of the PA regions is significantly lower than the RA regions in rabbits acutely exposed to silica and BNF (indicated by b above the bar). In B, the area of CYP1A1 expression within NT-II cells of the PA regions is significantly lower in rabbits chronically exposed to silica and BNF than the control saline/BNF (indicated by c above the bar). Also, the area of CYP1A1 expression within NT-II cells of the PA regions is significantly lower than the RA regions in rabbits chronically exposed to silica and BNF (indicated by d above the bar). In RA regions, no significant change is observed between acute and chronic silica with BNF compared to the control (saline/BNF). The letters a, b, c, and d indicate significant difference at <0.05.

Table 2. Effect of silica exposure on CYP1A1 expression in NT-II cells of rabbit alveoli.

Exposure	PA regions (μm^2)	RA regions (μm^2)
Acute saline with BNF	327.068 ± 42.257	359.223 ± 110.968
Acute silica with BNF	44.417 ± 5.212[a,b]	454.661 ± 45.39
Chronic saline with BNF	528.445 ± 121.904	261.624 ± 76.238
Chronic silica with BNF	74.385 ± 26.452[c,d]	382.002 ± 61.984

Values represent means ± SE, (n=3-5).
Superscript a indicates significant difference from acute saline with BNF of PA regions at p<0.05.
Superscript b indicates significant difference from acute silica with BNF of RA regions at p<0.05.
Superscript c indicates significant difference from chronic saline with BNF of PA regions at p<0.05.
Superscript d indicates significant difference from chronic silica with BNF of RA regions at p<0.05.

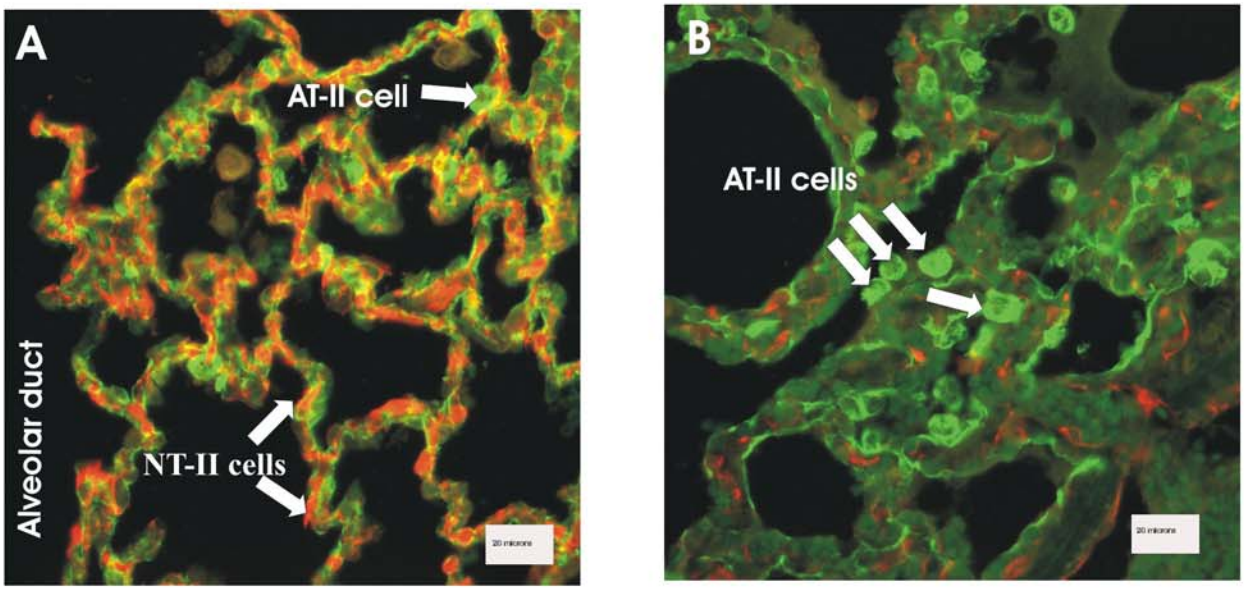

Figure 8. Immunofluorescent image showing a decrease in the area of CYP1A1 expression in non-type II (NT-II) cells of the PA regions of rabbit alveolus with acute silica and BNF (B) compared to rabbits with acute saline and BNF (A). In acute silicosis, the alveolar type II (AT-II) cells showed an increase in the number (hyperplasia) and size (hypertrophy). Reference bar is 20 micrometer.

C- ***Effect of Silica Exposure on CYP1A1 Expression in AT-II***

1- Proportional CYP1A1 Expression in AT-II Cells

The proportional expression of CYP1A1 in AT-II cells was calculated by a formula described in the Materials and Methods and measures expression of CYP1A1 in AT-II cells corrected for increases in AT-II area. In acute silicosis with BNF, the proportional CYP1A1 expression in AT-II cells of PA regions was significantly lower ($p=0.0293$) than control saline with BNF (Figure 9A). Although, in rabbits exposed to acute silica and BNF, the proportional CYP1A1 expression in AT-II cells of PA regions was lower than that of RA regions (Figure 9A, Table 3), this reduction was not statistically significant.

In chronic silicosis (chronic silica/BNF), by contrast, the proportional CYP1A1 expression in AT-II cells of the PA regions was not statistically distinguishable from expression in the PA regions of the control saline/BNF but significantly lower than expression in the RA regions of chronic silicosis/BNF (Figures 9B, Table 3).

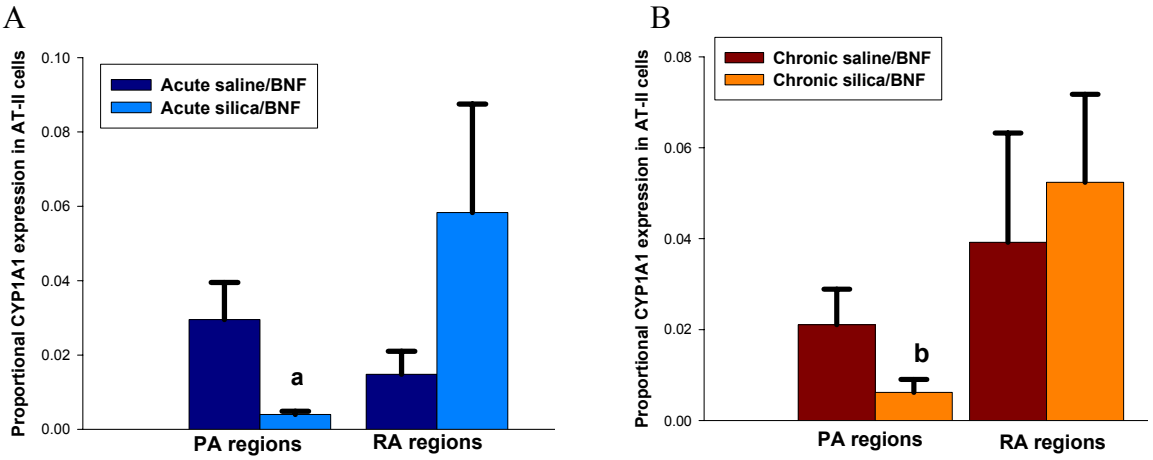

Figure 9. Morphometric analysis of proportional CYP1A1 expression in AT-II cells in immunofluorescent-stained sections of rabbit lungs with acute and chronic silicosis. In A, the proportional CYP1A1 expression within AT-II cells of PA regions is significantly reduced in acute silicosis/BNF compared to control saline/BNF (as designated by the letter a above the bar). In B, the proportional CYP1A1 expression within AT-II cells of PA regions of chronic silicosis/BNF is significantly reduced compared to RA regions (as designated by the letter b above the bar), but no significant change is observed when compared to control saline/BNF. Values are means ± SE. The letters a and b indicate significant difference at <0.05.

Table 3. Effect of acute and chronic silicosis on proportional CYP1A1 expression in AT-II cells of rabbit alveoli.

Exposure	PA regions	RA regions
Acute saline with BNF	0.0295± 0.0100	0.0148 ± 0.00622
Acute silica with BNF	0.00399 ± 0.000888[a]	0.0583 ± 0.0292
Chronic saline with BNF	0.208 ± 0.19	0.0392 ± 0.0241
Chronic silica with BNF	0.00618 ± 0.00285[b]	0.0524 ± 0.0193

Values are presented as means and SE
[a] indicates significant difference from acute saline with BNF in PA regions at $p<0.05$.
[b] indicates significant difference from chronic silicosis with BNF in the RA regions at $p<0.05$

2- Area of CYP1A1 Colocalized (Co-Expressed) to Cytokeratins 8/18

The area of CYP1A1 concomitantly expressed (colocalized) with cytokeratins 8/18 per unit area of AT-II cells of PA regions was decreased and bordered ion statistical significance ($p=0.0507$) in rabbits acutely exposed to silica and BNF compared to control rabbits (acute saline/BNF exposure) (Figures 10A and 11, Table 4). This area was significantly reduced when compared to RA regions of rabbits exposed to acute silica and BNF ($p=0.0475$) (Figure 10A, Table 4). In chronic silicosis with BNF, the area of CYP1A1 expression colocalized in AT-II cells was significantly decreased in the PA region and compared to the RA regions and was reduced, albeit not significantly compared to the control saline/BNF (Figure 10B, Table 4). In areas where granulomatous inflammation and silicotic nodules were localized, the positive CYP1A1 cells were completely absent (Figure 11C). These regions were not included in the morphometric quantification.

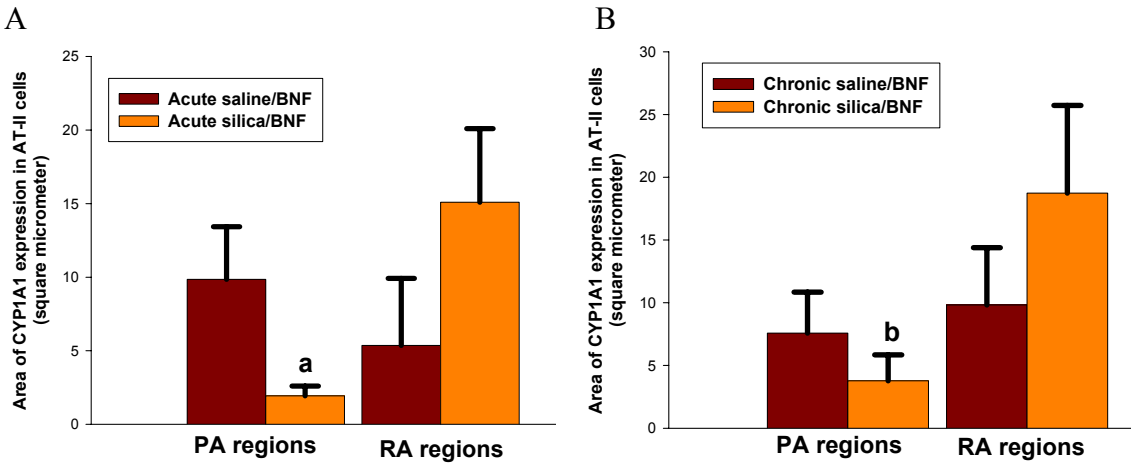

Figure 10. Morphometric quantification of area of CYP1A1 expression colocalized to cytokeratins 8/18 in BNF-induced rabbits affected with acute and chronic silicosis. In A, the letter a above the bar indicates that acute silicosis/BNF significantly reduced CYP1A1 co-localization area in the PA regions compared to that in the RA regions. In B, the letter b above the bar designates a significant reduction of CYP1A1 co-localization area in PA regions compared to RA regions in rabbit alveoli with chronic silicosis/BNF. a, b, and c indicate significant difference at $p<0.05$.

Table 4. Effect of silicosis on CYP1A1 colocalization in AT-II cells.

Exposure	PA regions (μm^2)	RA regions (μm^2)
Acute saline with BNF	9.8515± 3.5771	5.362 ± 4.558
Acute silica with BNF	1.7618 ± 0.4897[a]	15.091 ± 5.002
Chronic saline with BNF	7.578 ± 3.264	9.83 ± 4.569
Chronic silica with BNF	3.776 ± 2.066[b]	18.733 ± 6.995

Values represent means ± SE, (n=3-5).

[a] indicates significant difference from acute silica with BNF of RA regions at $p<0.05$.

[b] indicates significant difference from chronic silica with BNF of RA regions at $p<0.05$.

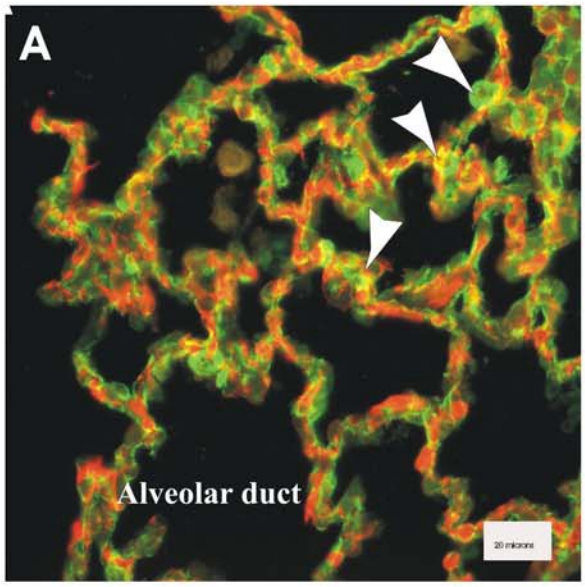

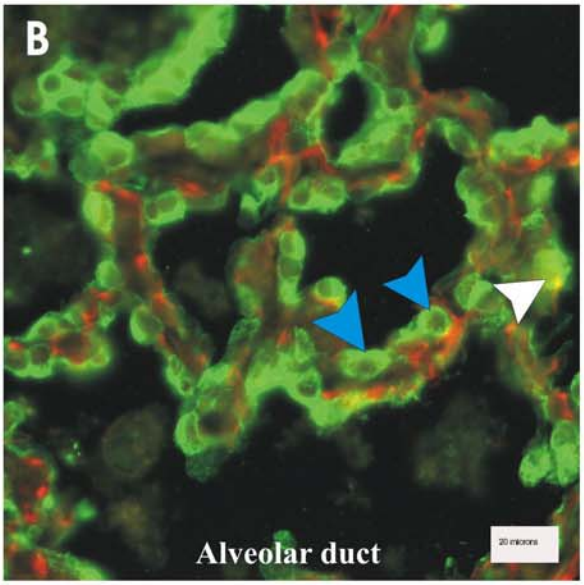

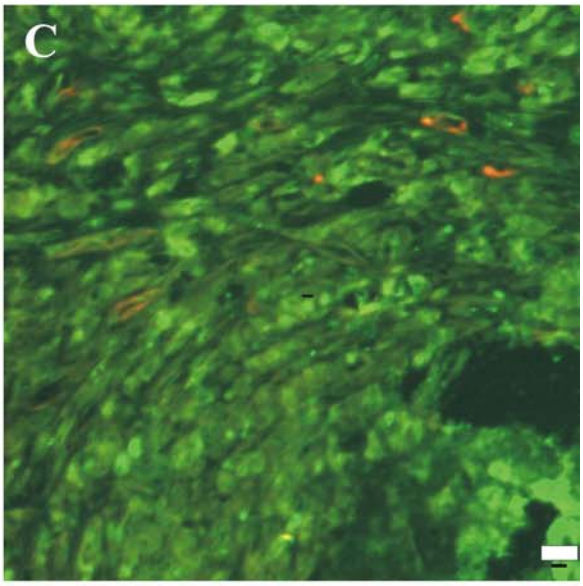

Figure 11. Immunofluorescence images of PA regions of rabbit alveoli showing a reduction of CYP1A1 expression area in AT-II cells (yellow area, white arrow head) in rabbits acutely exposed to silica (B) compared to control saline (A). In B, hyperplasia and hypertrophy of AT-II cells are evident (blue arrow head). In C, silicotic nodules appear with absence of normal alveolar cell population and CYP1A1 expression. Reference bar is 20 micrometer.

D-Effect of Silicosis on Total CYP1A1 Expression in the Alveolar Septum

The total red-labeled area of CYP1A1 expression in the alveolar septum (both AT-II and NT-II cells) of PA regions showed a significant reduction in both acute and chronic silicosis compared to the control saline (p=0.0007; 0.0069, respectively) and that of the RA regions (p=0.0006; p=0.0219, respectively) (Figure 12A and B, Table 4).

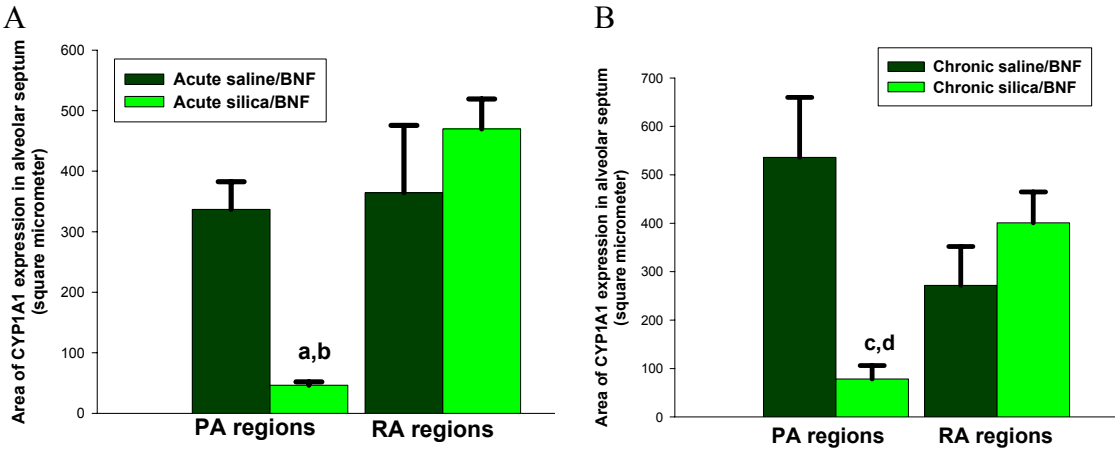

Figure 12. Morphometric assessment of the total area of CYP1A1 expressed in all cells of the alveolar septum. In A, the letter a above the bar indicates that the area of CYP1A1 expression in the alveolar septum of PA regions in acute silicosis/BNF is significantly lower than control (acute) saline/BNF. A b above the bar indicates that the area of CYP1A1 expression in the alveolar septum of PA regions in acute silicosis/BNF is significantly lower than that of RA regions. In B, the letter c above the bar indicates that the area of CYP1A1 expression in the alveolar septum of PA regions in chronic silicosis/BNF is significantly lower than control (chronic saline/BNF). A d above the bar indicates that the area of CYP1A1 expression in the alveolar septum of PA regions in chronic silicosis/BNF is significantly lower than that of RA regions. Values are means ± SE and significance level was set at $p<0.05$.

Table 5. Effect of acute and chronic silicosis on total CYP1A1 expression in alveolar septal cells

Exposure	PA regions (	Random alveolar regions
Acute saline with BNF	336.92 ± 45.818	364.584 ± 111.134
Acute silica with BNF	46.353 ± 5.466[a,b]	469.752 ± 49.67
Chronic saline with BNF	536.023 ± 123.951	271.453 ± 80.366
Chronic silica with BNF	78.161 ± 27.931[c,d]	400.735 ± 64.027

Values are the means of expression area (μm^2) ± SE (n=3-5)
[a] indicates significant difference from PA regions of acute saline with BNF of at $p<0.05$.
[b] indicate significant difference from RA regions of acute silica with BNF at $p<0.05$.
[c] indicates significant difference from PA regions of chronic saline with BNF at $p<0.05$.
[d] indicates significant difference from RA regions of chronic silica with BNF at $p<0.05$.

E- Silica Exposure Produced AT-II Cell Hypertrophy and Hyperplasia

Rabbit silicosis caused AT-II cell hyperplasia and hypertrophy, which was significant in chronic silicosis/BNF compared to control saline/BNF ($p=0.046$) (Figure 13A and B). Since cytokeratins 8/18 was indicated by green immunofluorescence, AT-II hypertrophy and hyperplasia was indirectly calculated from the measurement of the total green fluorescent areas in the alveolar septum (Figure 11).

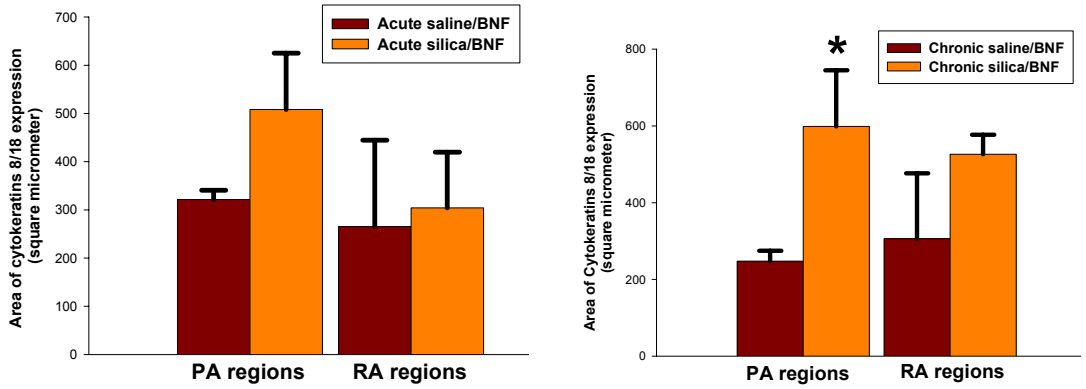

Figure 13. Morphometric analysis of immunofluorescent-stained sections showing the effect of rabbit silicosis on hypertrophy and hyperplasia of AT-II cells. The area of cytokeratins 8/18 is measured in square micrometer as indicator of type AT-II cell hyperplasia and hypertrophy. Values are means ± SE. * significantly different from chronic saline/BNF at $p<0.05$.

F-Acute and Chronic Silicosis Significantly Decreased CYP1A1 Expression in the Terminal Non-Ciliated Bronchiolar (Clara) Cells:

The number of CYP1A1 immunoreactive Clara cells exceeding the red fluorescent threshold for 1A1 expression was counted and standardized per micrometer of the basement membrane. Clara cells were identified as a group of adjacent columnar non-ciliated airway epithelial cells resting on the basement membrane of the terminal bronchioles which stain green with cytokeratins 8/18 (Figure 14). They were differentiated from the cuboidal AT-II cells, which are usually found in the alveolar septa, by their morphology and location. Both acute and chronic exposure of rabbits to silica resulted in a highly significant reduction of CYP1A1 positive Clara cells per µm basement membrane compared to control ($p=0.0005$, $p=0.00057$, respectively) (Figures 14, 15).

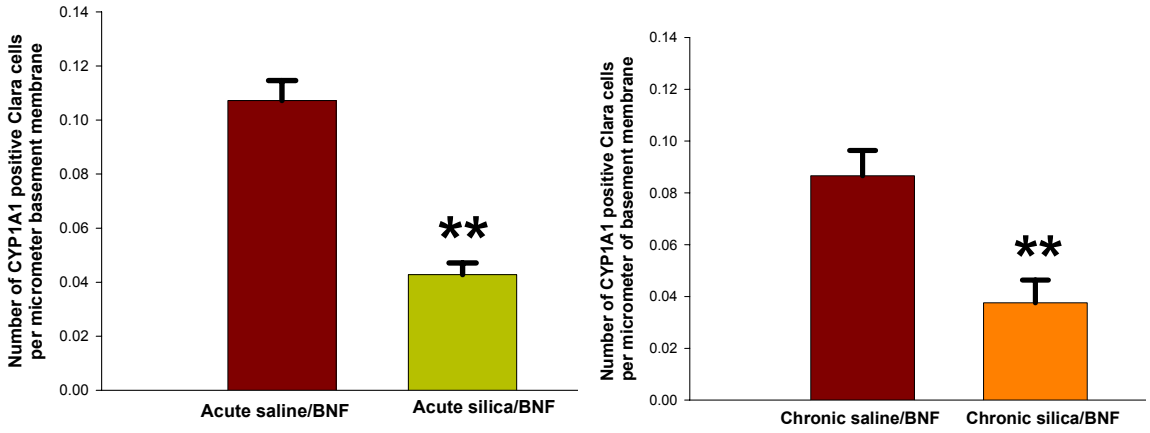

Figure 14: Effect of silicosis on CYP1A1 expression in rabbit non-ciliated terminal bronchiolar (Clara) cells. In A, ** indicates a highly significant reduction of the number of CYP1A1-positive Clara cells in acute silicosis and BNF than the control saline and BNF ($p<0.001$). In B, ** indicates a highly significant reduction of the number of CYP1A1-positive Clara cells in chronic silicosis and BNF compared to the control saline and BNF ($p<0.001$). Values presented as mean ± SE. the significance level is set at $p<0.001$

Figure 15: A sample of immunofluorescent image of the PA regions showing CYP1A1 expression in Clara cells next to alveolar duct. The number of positive Clara cells standardized per micrometer of basement membrane in rabbits with acute silicosis (B) is less than those in control (A). Reference bar is 20 micrometer.

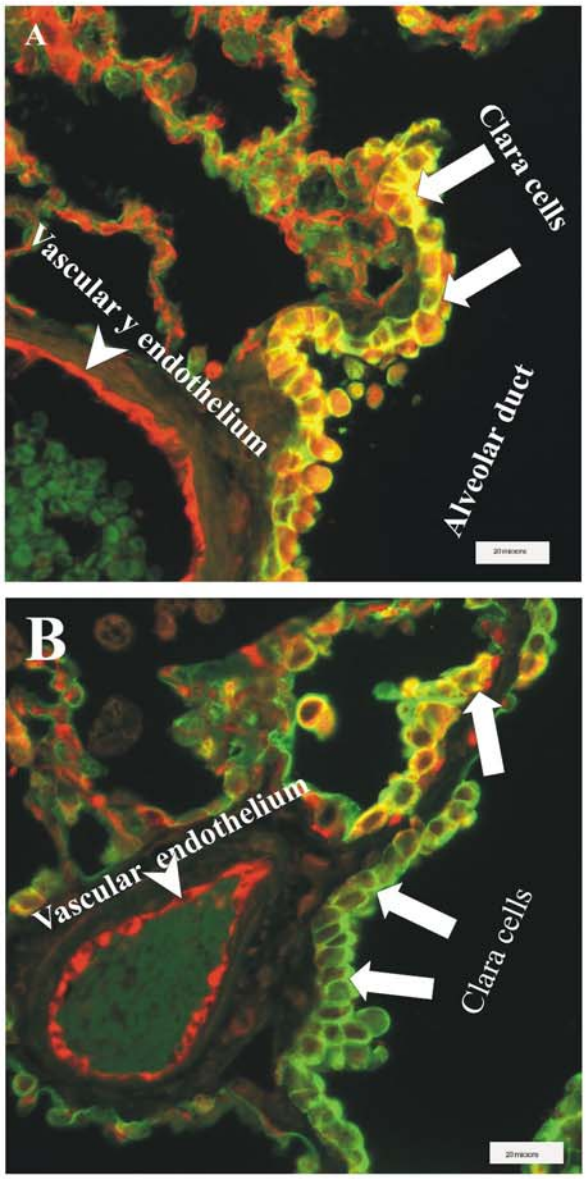

Histopathological Changes

Tissue sections from control and silica-exposed rabbits were stained with hematoxylin and eosin (H & E) and the histopathological changes were assessed and scored (Figure 16). Histopathological changes include AT-II hyperplasia and hypertrophy, pulmonary inflammation which was mostly histiocytic and suppurative to necrogranulomatous bronchointerstitial pneumonia with thickening of the alveolar wall (Figure 17). Alveolar lipoproteinosis was one of the common findings in silica-exposed rabbit alveoli. In some rabbit lungs with silicosis, silicotic nodules appear as centrically arranged collagen fibers surrounding necrotic foci (Figure 17B). These histopathological changes were absent in the control rabbits (Figure 17 C).

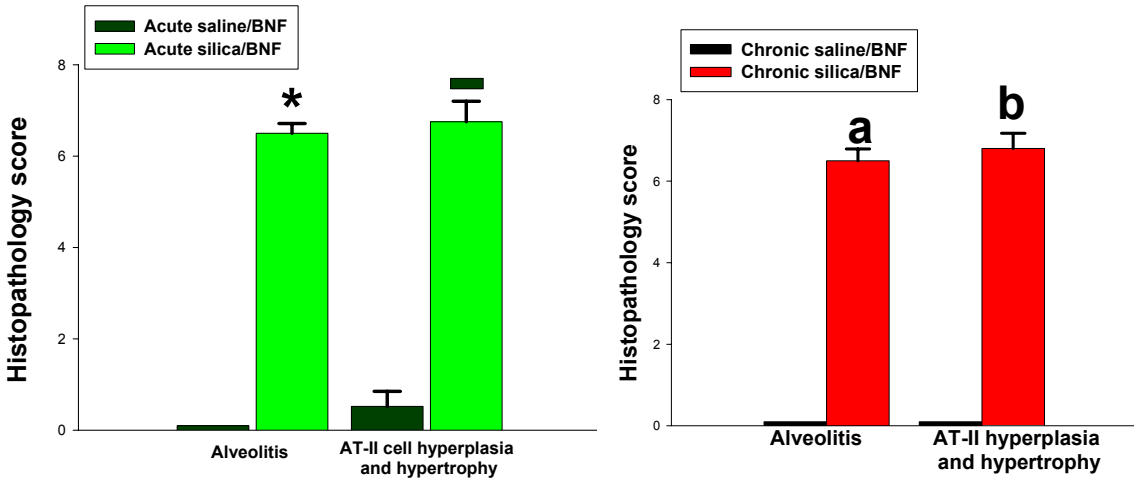

Figure 16: Alveolitis and AT-II cell hyperplasia and hypertrophy scored in H & E-stained tissue sections. Both alveolitis and AT-II changes were significantly higher in rabbit alveoli acutely and chronically exposed to silica particulate compared to control. * and ▬ indicate that in rabbits exposed to acute silicosis and BNF, alveolitis and AT-II changes are significantly different from control (acute saline/BNF), respectively. a and b indicate that in rabbits exposed to chronic silicosis and BNF, alveolitis and AT-II changes are significantly different from control (chronic saline/BNF), respectively. Results represent mean ± SE. All results are statistically significant at $p<0.05$.

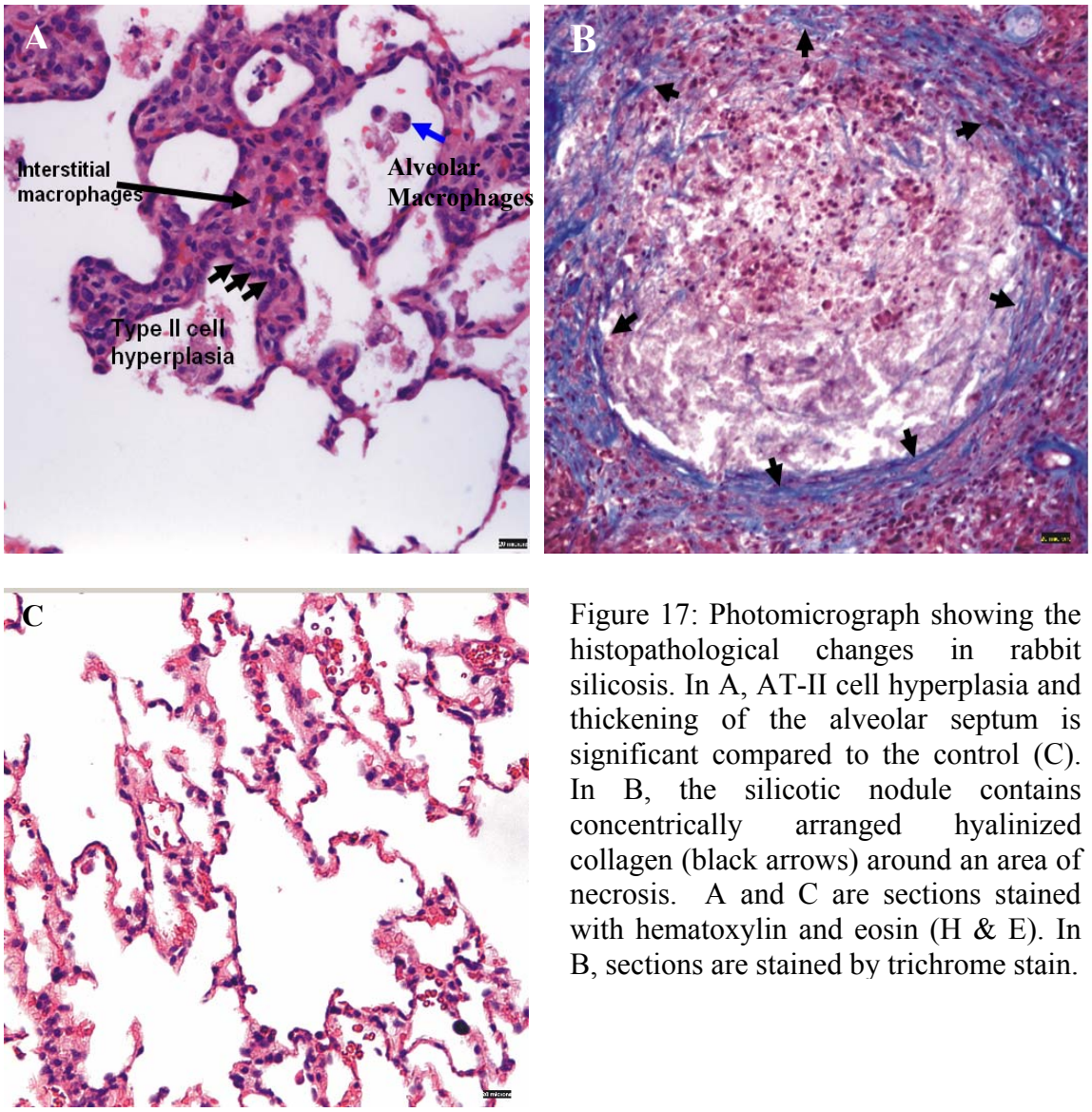

Figure 17: Photomicrograph showing the histopathological changes in rabbit silicosis. In A, AT-II cell hyperplasia and thickening of the alveolar septum is significant compared to the control (C). In B, the silicotic nodule contains concentrically arranged hyalinized collagen (black arrows) around an area of necrosis. A and C are sections stained with hematoxylin and eosin (H & E). In B, sections are stained by trichrome stain.

DISCUSSION

This study investigates the modifying effect of silicosis on the polycyclic aromatic hydrocarbon-associated induction and cell-specific localization of CYP1A1 in the rabbit lung by exposure to silica. The use of the rabbit as a non-rodent model for this particular study has several advantages. First, rabbit and human AhR and Arnt, which are the 2 main proteins involved in CYP1A1 induction and gene expression, are highly conserved between these two species (Takahashi *et al,* 1996). Moreover, a recent study suggests that rabbit, as well as mouse, are among the species with CYP1A1 that is comparable to human as determined by the inhibition of EROD activity in the lung microsomes of these species by the antiserum to human CYP1A (Bogaards, *et al,* 2000). Therefore, this suggests that the results of rabbit studies, particularly those investigating the modification and alteration of CYP1A1 expression by exposure to environmental toxicants could be comparable to the human response to these compounds. Second, the rabbit as a non-rodent model helps resolve the debate concerning the use of the rat, to investigate genetic and histopathological changes associated with particle exposures in human lungs. Third, CYP1A1 is one of the major isoforms of CYP present in the lungs of rabbit (Daniels and Massey, 1992). Fourth, CYP1A1 occurs in an amount of 1 to 3% of total CYP in pulmonary microsomes prepared from untreated rabbits. However, intraperitoneal injection of BNF produces a several fold induction of the CYP1A1 with associated induction of EROD activity in rabbits (Serabjit-Sinh *et al,* 1983; Philpot *et al,* 1985). For all these reasons, rabbits were selected to fulfill the objectives of our study. In our experiment, CYP1A1 was induced in rabbits by intraperitoneal (IP) injection of a representative polycyclic aromatic hydrocarbon, BNF, (80 mg/kg) in corn oil as previously determined (Mathews *et al,* 1985; Daniels and Massey 1992). BNF induces CYP1A1 through a mechanism identical to the benzo(a)pyrene in cigarette smoke by binding the aryl hydrocarbon receptors (AhR) (Ma and Whitlock, 1997) resulting several fold increase in CYP1A1 content and EROD activity (Serabijt-Singh *et al* 1983; Philpot *et al*, 1985).

Exposure to silica alone, without exposure to CYP1A1 inducers (such as BNF) has been associated with increased CYP1A1-metabolic activity, EROD, in rats (Miles *et al*, 1993, 1994). However, the effect of mixed exposure was not investigated in the

previous study. At least one epidemiological study of mixed exposure to silica and PAH concluded that lung cancer risk was higher among people exposed to silica than those exposed to silica and other lung carcinogens, such as PAH (Cocco *et al*, 2001). This suggests that silicosis may modify PAH-associated carcinogenesis. Because, CYP1A1 activity is associated with an increased risk of lung cancer in smokers (Anttila *et al*, 2001) and because smokers have induced CYP1A1 (Alexandrov *et al*, 2002; Willey *et al*, 1997), the effect of silicosis on CYP1A1 induction is important. EROD is a reaction catalyzed in rabbits by CYP1A1 (Serabjit-Singh *et al*, 1979; Devereux *et al*, 1989). Our data showed that CYP1A1-dependent EROD activity induction by BNF was significantly suppressed by acute and chronic silicosis (Figure 1A and B).

To further investigate the effect of silica on BNF-induced CYP1A1 apoprotein induction in rabbit lungs, Western blot analysis of lung microsomes was conducted using goat anti-rabbit CYP1A1 antibody. We found a reduction of CYP1A1 protein in acute silicosis compared to control (Figure 2A and B). This result supports downregulation of the protein as well as activity by exposure to silica. In chronic silicosis, Western blot did not show any change in the CYP1A1 protein compared to control (Figure 3A and B) although the EROD activity was significantly reduced (Figure 1B). This observation suggests that silica exposure in rabbits downregulates the induced pulmonary CYP1A1 in a posttranscriptional process in which the enzyme protein is expressed, as shown in the Western blot, but not active as shown in the suppressed EROD activity. A similar result was obtained by Paton and Renton (1998) when they had a significant reduction of EROD activity of Hepa 1 cells upon addition of tumor necrosis factor alpha directly to the cell, while the Western blot CYP1A1 protein showed no change. It is also possible that EROD activity is more sensitive indicator of changes of changes in CYP1A1 than western blot. It is noteworthy to mention that chronic silicosis models was induced in rabbits by a more localized exposure procedure to prevent respiratory impairment, and accordingly, the acute and chronic models can not be compared to each other but each one can be compared to its control. However, taken together, these results suggest that exposure of rabbits to crystalline silica suppresses BNF-induced CYP1A1 activity.

PROD activity was also measured as an indicator of CYP2B4 activity in the lungs. PROD is a specific indicator of the CYP2B4 activity (Cawley *et al*, 2001). The

CYP2B4 in rabbits is the analog of rat CYP2B1 (Oesch-Bartlomowicz and Oesch, 2003) which is the major isoform of CYP in rodents (Martin *et al*, 1993). Similar to rat CYP2B1, rabbit CY2B4 is constitutively expressed in lung tissue in high levels and considered the major CYP isoform in rabbit lung, but present in very minute quantity in liver (Serabjit-Singh *et al*, 1979; Parandoosh *et al*, 1987). Statistically, PROD was significantly lowered in rabbits with acute silicosis and BNF compared to the control (Figure 1C). However, no significant change in PROD activity was observed in lung microsomes from chronic silicotic rabbits (Figure 1D) compared to control. The significant reduction of PROD activity in acute silicosis suggests that downregulation of CYP activity in acute silicosis involves multiple isoforms.

In order to determine the pattern of CYP1A1 expression by different alveolar cells upon acute and chronic exposure to crystalline silica, cell-specific localization of CYP1A1 protein has been analyzed by double-labeling immunofluorescence. The dual immunofluorescence includes a double staining of the CYP1A1 protein and cytokeratins 8/18 proteins, which are cytoskeletal proteins expressed in primitive epithelial cells of the lungs, such as alveolar AT-II cells and used as markers for these cells (Kasper *et al*, 1993). A characteristic pattern of CYP1A1 expression has been detected by morphometric analysis of immunofluorescence in rabbit alveoli. Apparently, the NT-II cells (all alveolar cells except type II) in PA regions and RA regions, which were identified as cytokeratins 8/18 negative alveolar cells, significantly express CYP1A1 protein more than AT-II cells, which were identified by their plump shape, and protrusion into alveolar lumen and positive immunofluorescence for cytokeratins 8/18 (Figure 4A&B, 5, and 6). That observation suggests that alveolar AT-II cells are not the major cell types involved in CYP1A1 expression in rabbit alveolus; other alveolar septal cells are responsible for more area of CYP1A1 protein expression. Our findings are consistent with those of Domin *et al*, 1986 who demonstrated that the majority of pulmonary CYP1A1 (isoform 6) in rabbit lungs is localized in cells other than AT-II cells, Clara cells, or the alveolar macrophage. In rabbits exposed to 2,3,7,8- tetrachlorodibenzo-*p*-dioxin (TCDD), an inducer of CYP1A1, the immunopositive areas of CYP1A1 expression in the interalveolar septa were the capillary endothelium, with a minimum labeling of type I and AT-II cells (Overby *et al*, 1992). On the contrary, rat CYP2B1

isoform has been localized and concentrated mainly within alveolar type I cells because the selective destruction of these cells by trialkylphosphothiolates resulted in a marked loss of the enzyme (Dinsdale and Verschoyle, 2001).

Hyperplasia and hypertrophy of AT-II cells were evident in acute and chronic exposures, compared to control as shown by the increase in the area of green fluorescence for cytokeratins 8/18 per alveolar microscopic field in AT-II cells of the alveolar septum (Figure 13) and by the histopathological examination. These findings are in agreement with those of Miller *et al* (1990), who demonstrated approximately two fold increase in the number of AT-II cells following silica exposure. The increased number (hyperplasia) and size (hypertrophy) of alveolar AT-II cells were not associated with a parallel increase of CYP1A1 expression in these cells. Indeed, per unit area of alveolar AT-II cells, CYP1A1 expression (proportional CYP1A1 expression) was significantly decreased in acute silicosis compared to control saline (Figure 9). This observation suggests that many of the hyperplastic and hypertrophic alveolar AT-II cells appearing in rabbit lungs following exposure to silica do not express detectable levels of CYP1A1. This result is consistent with a previous rat study in our laboratory, which demonstrated that intrapulmonary exposure to silica lead to appearance of new population of AT-II cells without a detectable amount of CYP1A1 protein expression (Battelli *et al*, 1999). The response of alveolar AT-II cells to silica exposure has been extensively studied because these cells perform many vital functions in the lungs and increase in response to dust exposure (Miles *et al*, 1993). AT-II cells play an important role in synthesis and secretion of surfactant (Castranova, 1988) which increases surface tension (Pattle, 1955; Clements, 1957) and protects lungs from potentially toxic respirable particles (Castranova *et al*, 1988, Wallace *et al*, 1985) while contributory to the pathogenicity of acute silicosis (Lesur *et al,* 1995). AT-II cells are also involved in repairing alveolar epithelium by their differentiation into alveolar type I cells (Miller *et al*, 1990; Castranova *et al*, 1988). The alveolar AT-II cell population of the lung has been found to be very sensitive to the deposition of toxicants in the distal lung, and respond in two major ways upon exposure. Damage to the type I alveolar epithelial cells stimulates AT-II cell proliferation, which subsequently differentiate to repopulate the injured type I cells and reconstitute the alveolar architecture (Miller and Hook, 1990; Melloni *et al,* 1995;

Wang *et al,* 2002; Sutherland *et al,* 2001). The second portion of the AT-II cell population may become enlarged in size (hypertrophic) (Miller and Hook, 1990). Moreover, AT-II cells, being rich in endoplasmic reticulum (Baron and Kawabata, 1983) and CYP monooxygenase system, are generally believed to be involved in metabolism of foreign compounds (xenobiotics) (Devereux *et al*, 1979; Jones *et al*, 1983; Baron and Kawabata, 1983; Rabovsky *et al,* 1986). However in our study, we found that the major area of the alveolus containing induced CYP1A1 was not the AT-II cells. In our study, we found that these hypertrophied and hyperplastic AT-II cells are frequently devoid of detectable CYP1A1. In addition, in acute silicosis the proportional expression of CYP1A1 in AT-II cells is reduced.

The mechanisms involved in the reduction of CYP1A1 expression in AT-II cells following silica-induced proliferation are incompletely investigated. However, the inverse relationship between AT-II cell hyperplasia and CYP expression that we have observed *in vivo* is consistent with *in vitro* findings from previous studies. Lag *et al* (1996) concluded that an inverse relationship could exist between CYP2B1 apoenzyme expression and the proliferation level of AT-II cells. That conclusion was based upon the observation that CYP2B1 apoenzyme was lowest in alveolar AT-II cell cultures during the most active proliferative stage, which coincided with presence of largest proportions of cells in S-phase and highest proliferating cell nuclear antigen (PCNA) expression. Similarly, the CYP1A1-dependent enzymatic activity, EROD, was undetectable in proliferating cultures of mouse lung epithelial cells, but the level became detectable once cultures were confluent (Reiners *et al*, 1992). It was suggested that EROD expression was regulated as a function of the proliferative process of the cell culture. An inverse relationship between cellular proliferation and CYP expression was also suggested by the observation that proliferative regeneration of hepatic cells following partial hepatectomy was associated with lower P450s protein levels and activities than normal liver (Hino *et al,* 1974; Presta *et al,* 1980; Klinger and Karge, 1987; and Ronis *et al,* 1992). It seems that hepatic cells are allocated to replication, rather than transcription, as a main function of DNA to proliferate and regenerate the cells after hepatectomy (Liddle *et al,* 1989, Waxman, 1989; Morgan *et al,* 1985; Steer, T.C. (1995). Similarly, alveolar AT-II cells

may repair the damaged alveolar epithelium by proliferating and regenerating the injured alveolar wall instead of expressing CYP1A1.

A more detailed cell-specific localization and morphometric quantification demonstrated that the area of alveolar NT-II cells expressing CYP1A1 was significantly decreased in both acute and chronic silicosis compared to control and compared to the internal control regions (RA regions) where few silica particles deposited (Figure 7, Table 2). This finding suggested that silica exposure not only altered the induction of CYP1A1 expression in AT-II cells, but also affected the alveolar NT-II cells. The overall effect for the alveolus was significant reduction of the alveolar area expressing CYP1A1 in the whole alveolar septum in acute and chronic silicosis in PA regions compared to control and to RA regions (Figure 12, Table 4).

Clara cells are considered the predominant nonciliated cell type at the terminal bronchiolar epithelium (Widdicombe and Pack, 1982; Plopper, 1983). They serve as an important site for xenobiotic metabolism in the distal lung (Boyd, 1977; Boyd *et al*, 1978; Boyd *et al*, 1980). For this reason, we counted the number of CYP1A1 positive staining cells and standardized that number per micrometer of the basement membrane. Rabbit silicosis, either acute or chronic, in BNF-treated rabbits significantly reduced the number of CYP1A1 immunoreactive Clara cells in the terminal bronchiolar regions compared to BNF treatment alone (Figure 14 and 15). This may contribute to the reduction in EROD activity in silicosis.

The inflammatory effects of silica on rabbit alveoli have been demonstrated by assessing the histopathological changes. Both acute and chronic silicosis produced a significant pulmonary inflammation and AT-II hyperplasia and hypertrophy as shown in Figure 16. Previous studies on rat showed that the pulmonary reaction to the inhalation of crystalline silica resulted in lung damage, inflammation, and hypertrophy and hyperplasia of AT-II cells (Miller *et al*, 1986; Miller et al, 1990; Castranova *et al*, 2002). In our study, the positive CYP1A1 immunoreactive cells completely disappeared in areas with granulomatous inflammation associated with rabbit silicosis (Figure 11C). Although these regions were not quantified morphometrically because of the absence of normal

alveolar cell populations, they may also contribute to the total reduction of the CYP1A1 activity measured by EROD assay by replacing normal parenchyma.

A number of investigators studying the effect of the inflammatory response on hepatic CYP metabolic activity concluded that the acute inflammatory reaction caused by subcutaneous injection of turpentine (Kobusch *et al*, 1986), bacterial lipopolysaccharide (LPS) (Morgan, 1989) and viral and bacterial infection (El-Kadi and Du Souich, 1998) depressed the constitutive hepatic CYP. It was also suggested that the inhibition in the metabolism was attributed to the inflammation itself (or to its consequences) and not to the inflammatory agents (Parent *et al*, 1992). Previous studies by Ke and co-investigators (Ke *et al*, 2001) have demonstrated that the proinflammatory mediators, such as tumor necrosis factor-α (TNF-α) that were released in response to lipopolysaccharide exposure downregulated the CYP1A1 *in vitro*. Their results showed that TNF-α inhibited the ligand-induced acetylation of histone H4 at the promoter region of CYP1A1 gene and consequently prevented CYP1A1 induction in Hepa1c1c7 cells. In addition, they demonstrated that nuclear factor kappa B (NF-κB) interacted with AhR and thus interfere with AhR-mediated CYP1A1 induction. The effect of the mixed exposure to crystalline silica and CYP1A1-inducers, such as BNF on CYP1A1 expression and activity has been investigated only in our laboratory (Battelli *et al*, 1999). Our previous findings in rats indicated that silica produced a significant reduction of the induced CYP1A1 enzymatic activity (EROD). The current study indicated that such findings were not unique to the rat. In rabbit with acute and chronic silicosis, the induction of CYP1A1 activity by BNF was inhibited. Our study suggested that AT-II cells and Clara cells in silicotic rabbits expressed CYP1A1 less frequently than did controls. Thus, one mechanism of modifying CYP1A1 induction in silicosis, appeared to be decreased CYP1A1 expression in both cells of the terminal bronchiolar and alveolar septum.

In conclusion, our data strongly suggests that rabbit silicosis is a modifying factor for CYP1A1 induction in rabbits. Factors associated with downregulation of CYP1A1 induction *in vivo* include altering the cell specific localization of the apoprotein in the alveolus and terminal bronchioles. Silicosis, both acute and chronic, inhibited the induced-CYP1A1 enzymatic activity (EROD). This inhibitory effect on cytochrome P450 isoforms is not limited to CYP1A1 induction. PROD activity which is associated with

CYP2B4, is also decreased with silica exposure. Suppression of CYP1A1 induction is associated with reduction of protein expressed in Clara cells, AT-II cells, and other cells of the alveolar septum, as assessed by quantitative immunofluorescence microscopy. CYP1A1 was not the only CYP isoform modified by exposure to crystalline silica, but at least one other CYP isoform, CYP2B4, also underwent suppression.

CHAPTER 5
SUPPRESSION OF SHEEP PULMONARY CYP1A1 INDUCTION BY INTRATRACHEAL EXPOSURE TO RESPIRABLE COAL DUST PARTICLES

ABSTRACT

A non-rodent model was used to investigate the effect of coal dust (CD) exposure on CYP1A1 induction and localization in the lung. Since pulmonary effects of silica are similar in sheep and humans (Larivee *et al*, 1990), lambs were used in this study. Therefore, we investigated the hypothesis that CD exposure in sheep modifies CYP1A1 metabolic activity and localization in pulmonary cells. To investigate this hypothesis, the right apical lobes of 9 Katahdin crossbred lambs were instilled with 500 mg coal dust (<5 microns) using a flexible fiberoptic bronchoscope. Lambs were sacrificed 8 weeks after exposure. All lambs received 50mg/kg of the CYP1A1 inducer, BNF, suspended in corn oil or corn oil by intraperitoneal injection, 2 and 3 days prior to sacrifice. Bronchoalveolar lavage (BAL) fluid, microsomes and formalin-fixed lung tissue were collected from the instilled right tracheal bronchial lobes and the uninstalled left apical lobes. CYP1A1-dependent EROD activity and CYP2B-dependent PROD activity were significantly reduced in the microsomes of CD-exposed tracheal bronchial lobes relative to the uninstalled left lobes or the right tracheal bronchial lobes of sheep receiving BNF alone. In addition, the cellular expression of CYP1A1 in alveolar type II cells, non-type II cells, and whole alveolar septum was significantly reduced in sheep exposed to CD and BNF compared to those receiving BNF alone. These results further support our hypothesis that CD exposure modifies the induction and cellular localization of CYP1A1 protein.

INTRODUCTION

In the previous 2 chapters, we have demonstrated suppression of CYP1A1 induction and its dependent enzymatic activity (EROD) by pulmonary exposures to respirable coal dust (in rats) and crystalline silica (in rabbits). In addition, coal dust and silica particles respectively suppressed the enzymatic activity (PROD) of the CYP2B isoforms in rat and rabbit lungs. However, there is a scientific debate concerning the comparability of rat and human pulmonary responses to respirable particles of low toxicity, such as coal dust (International Life Science Institute (ILSI) Risk Science

Institute Workshop Participants, 2000). In this study, we used the lamb as a non-rodent model to establish the relationship between pneumoconiosis, caused by coal dust deposition in sheep lungs, and alteration in xenobiotic metabolism. Specifically, we have examined the activity, quantity, and localization of CYP1A1, the CYP isoform which activates some polycyclic aromatic hydrocarbons, such as those in cigarette smoke. In addition, we have studied the activity of CYP2B. CYP2B is the major constitutively expressed CYP member in sheep lung, which is analogous to CYP2B1 and CYP2B4 in rats and rabbits, respectively (Williams *et al*, 1991). Sheep were selected as a model because their pulmonary response to respirable crystalline silica, another cause of pneumoconiosis, is similar to that observed in humans (Begin *et al*, 1989, Larivee *et al*, 1990). Sheep lungs are larger, which permits directed exposure and the use of internal control lobes, an important advantages in an outbred species.

A literature search dealing with the effect of environmental toxicants, such as PAHs, on sheep CYP1A1 did not reveal any studies. However, some studies have investigated the effect of commonly used veterinary pharmaceuticals, such as ivermectin, on CYP1A1, 1A2, 2B and 3A because of the role of these isoforms in drug metabolism in farm and cloven-hoofed animals (Skalova *et al*, 2001). The sheep cDNA coding region of CYP1A1 has an 85 % homology to human CYP1A1 (Hazinski *et al*, 1995). Therefore, sheep appear to be an appropriate model to studying the effect of xenobiotics, such as PAHs, on CYP1A1-associated carcinogenic pathways. Our results showed a reduction of the CYP1A1-dependent (EROD) and CYP2B-dependent (PROD) enzymatic activities in lung microsomes of sheep exposed to a CD particle suspension and BNF (CYP1A1 inducer). These results were further supported by Western blot analysis for CYP1A1 protein and immunofluorescence examination of tissue sections stained for CYP1A1 and cytokeratins 8/18 (AT-II markers).

MATERIALS AND METHODS

Sheep

Eleven Katahdin crossbred castrated male lambs weighing 17-30 kg at the start of the study were used. The lambs were housed in the Food Animal Research Facility (FARF) of West Virginia University. Lambs were fed Alfagreen Supreme Dehydrated alfalfa pellets (containing 17% crude protein, 1.5% crude fat and 30% crude fibers), with

ad libitum supply of water. The lambs were kept in pens for 3 weeks prior to exposure for acclimatization. During this period, they were examined physically for pulse and respiratory rates. In addition, the body temperature and capillary refill time were examined and all parameters were within normal range. To assure parasite-free lambs, ivermectin was injected subcutaneously 3 weeks before instillation. Lungs were examined by auscultation to assure normal lung sounds before coal dust instillations. Complete blood counts were taken from each lamb and were within normal limits.

Experimental Design:

Lambs were randomized into a coal-dust exposed and a control group using a randomizing program (www.randomized.com). The right apical lobe of each lung was instilled with CD or saline and the left apical lobes served as internal controls. The lambs were exposed in groups of two to three each day over an eight day period. The lambs were sacrificed eight weeks after exposure based upon the results of a preliminary coal dust instillation experiment. All lambs were subcutaneously injected with 10 mg/kg Tilmicosin antibiotic (Mycotil, Eli Lilly, Indianapolis, IN) one day after instillation of the final lamb as a prophylaxis against pulmonary infections. Three and two days before sacrifice, lambs were intraperitoneally (IP) injected with 50 mg/kg beta-naphthoflavone (BNF), to induce pulmonary CYP1A1.

Preparation of Particle Suspension

Coal dust particles (< 5 micrometer in diameter, 500 mg/lamb) were heat sterilized for 2 h at 160 ºC. The particles used in this study contained 0.34 % total iron of which 0.119 % was surface iron. The coal dust suspension was prepared by addition of 15 ml sterilized saline to 500 mg coal dust and vortexed. The suspension was drawn into a sterile syringe attached to a 1 mm diameter polyethylene tube and inserted into an endoscope (Jorgensen Laboratories Inc., Loveland, CO). The whole amount was instilled in the right tracheal bronchial lobe. In the control group, only 15 ml of the sterile saline was instilled into the same lobe under the guidance of the fiberoptic bronchoscope.

Intratracheal Instillation of Particles Using Flexible Fiberoptic Bronchoscope

Lambs were anesthetized by intramuscular injection of a combination of ketamine hydrochloride (Keta-ject, Phoenix Laboratories Inc., St. Joseph, MO 64503) 11 - 15

mg/kg and xylazine hydrochloride (Xyla-ject. Phoenix Laboratories Inc., St. Joseph, MO) 0.22 mg/kg. When the lambs were in surgical plane anesthesia (manifested by absence of the palpebral reflex), they were placed in a dorsal recumbency with the head extended down the surgical table to facilitate the passage of the bronchoscope tube into the trachea. A mouth speculum (Ideal Instruments, Detroit, IL) was modified by cutting into 2 halves and one half was inserted and fixed *in situ* by a piece of gauze to avoid damage to the bronchoscope tube. Cetacaine spray (Cetylite Industries, Inc., Pennsauken, NJ) was spayed in the pharynx to minimize pain and the swallowing reflex. An alcohol-sterilized flexible fiberoptic bronchoscope (Jorgensen Laboratories Inc., Loveland, CO) with a 5-mm external diameter was inserted though the speculum into the trachea by passage into the laryngeal orifice. Positioning was confirmed by visualization of the tracheal rings and a cough reflex. Once the bronchoscope was in the trachea, the lambs were turned into sternal recumbency followed by further insertion of the endoscopic tube until the orifice of the right tracheal bronchus appeared (just before the major bifurcation). At this point, the distal tip of the endoscope was tilted toward the orifice, and a 1-mm diameter polyethylene cannula (Becton Dickinson and Company, Sparks, MD) was inserted through the working channel of the endoscope directly into the right tracheal bronchus orifice through which the coal dust suspension was instilled into the lumen of the mainstem bronchus of the right apical lobe. After the coal dust suspension instillation, 5-10 cc of air was instilled into the mainstem bronchus. Importantly, in sheep, the right apical lobe is divided into 2 segments, the cranial segment and the caudal segment, each one receives a separate bronchus from the mainstem right tracheal bronchus (Getty, 1975). In our instillation procedure, the CD was instilled in the mainstem tracheal bronchus so that both segments were exposed. Post instillation, lambs were kept on the right side to allow settling of particle suspension within the instilled lobe. To facilitate anesthetic recovery, yohimbine hydrochloride (Yobine, LLOYD Laboratories, Shenandoah, OH) was injected IV (0.2-0.4 mg/kg) after the lambs were placed in the recovery stall.

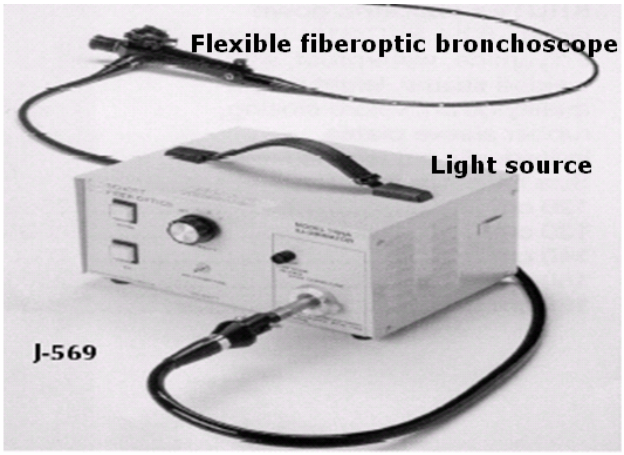

Figure 1: The flexible fiberoptic bronchoscope (JorVet 569) used in the study attached to the light source (Jorgensen Laboratories Inc., Loveland, CO)

Lamb Necropsy

Lambs were euthanized by intravenous injection of Sodium pentobarbital (Sleepaway®, Fort Dodge Animal Health, Fort Dodge, Iowa) 26 mg/lb. Under deep surgical plane anesthesia, the abdomen was incised along the midline and the abdominal aorta was transected to assure exsanguination. The entire lung was weighed and the right tracheal bronchial lobe and the left apical lobe were separately weighed. Both lobes were lavaged with PBS solution to collect the bronchoalveolar lavage fluid (BALF) as described later. Following lavage, 10 % of each lobe, by weight was excised for microsome preparation and the other 90 % was fixed by airway perfusion with a volume of 3 ml/gm of 10 % neutral buffered formalin (NBF). The amount of NBF used was calculated form the following formula:

$$\frac{\text{Wt of lavaged lobe portion for histopathology}}{\text{Wt of the total lavaged lobe}} \times \text{wt of the unlavaged lobe} \times 3 = \text{mls of NBF}$$

The formalin fixed tissues were trimmed later that day to prepare 4µm-thick tissue sections for histopathology and immunofluorescence.

Certain criteria were set to include a lamb in the study. Any lamb that did not meet any one of these criteria was excluded. These criteria were:

1- Absence of pulmonary infections.

2- Presence of coal dust particles in the instilled lobe.

3- Absence of technical difficulties that may result in partial instillation of the designated amount of CD

Two lambs were intended to be in the study but, due to failure to meet with the previous inclusion criteria, they were excluded. One of the lambs instilled with saline showed a bacterial pneumonia associated with translocation of bacteria and plant material from the esophagus/pharynx to the right apical lobe. Another lamb (supposed to be instilled with coal dust) was excluded because it showed no coal dust deposition by gross examination of lung tissue, inspection of tissue sediments during microsomal preparation, and microscopic examination of BAL and had minimal deposition noted histologically. That lamb had coughed powerfully during instillation, dislodging the bronchoscope. Therefore, that lamb was excluded. All the lambs were castrated males but a single testicle was identified in one lamb that was determined histologically to be immature, as it contained no spermatogonia. The lamb with the single immature testicle was included in the experiment due to the internal control incorporated in the design.

Preparation of Sheep Lung Microsomes

The microsomal fraction of lung homogenate was obtained by differential centrifugation method as previously described (Flowers and Miles, 1991; Ma *et al*, 2002). These microsomes were used for measuring the CYP1A1 and CYP2B1-dependent enzymatic activities (EROD and PROD, respectively). In addition, lung microsomes were subjected to electrophoresis to determine the CYP1A1 protein by western blot analysis.

Determination of the Total Lung Proteins

The total amount of protein content of lungs was measured in the microsomal suspension spectrophotometrically using the bicinchoninic acid (BCA) method as previously described (Smith *et al*, 1985; Ma *et al*, 2002) according to the direction of the BCA protein assay kit (Pierce, Rockford, IL) in a spectra Max 250 Spectrophotometer (Molecular Devices Corporation, Sunnyvale, California). Bovine serum albumin was used for the standard curve. Protein was measured as mg/ml.

Determination of CYP1A1- and CYP2B-Dependent Enzymatic Activities (EROD and PROD)

Spectrophotometric assays for measuring EROD and PROD metabolic activities were performed as previously described (Burke *et al*, 1985 and Ma *et al*, 2002) using a luminescence spectrometer model LS-50 (Perkin-Elmer, Norwalk, CT) and 7-ethoxyresorufin (7-ER) (Sigma, St. Louis, MO) as the standard. The 7-ER was used at a concentration of 10 μM that was prepared by dissolving 2.35 μg 7-ER in 1 ml DMSO. EROD and PROD activities were expressed as picomoles of the produced resorufin per minute per milligram microsomal protein (pmol/min/mg protein) as previously described (Ma *et al*, 2002).

Immunofluorescence Double Labeling

The tissue sections were stained to identify CYP1A1 and cytokeratins 8/18. The technique was basically the same as in rats (chapter 2). However, the tissue sections were incubated with the primary antibodies for 48 h instead of overnight in rat immunofluorescence. The primary antibodies were a polyclonal rabbit anti-rat CYP1A1 (Xenotech) diluted 1:5 with PBS and a polyclonal Guinea pig anti-cytokeratins 8/18 (RDI) diluted 1:50 with PBS. Rabbit serum was applied as a negative control, and the primary antibodies were omitted. After 48 h incubation at room temperature, the slides were incubated for additional 2 h at 37 ºC. The slides were then thoroughly washed to remove un-conjugated primary antibodies and then the secondary antibodies were dropped onto the slides. The secondary antibodies were a mixture of a FITC-labeled, donkey anti-Guinea pig IgG (Research Diagnostic Inc., Flanders, NJ) diluted 1:50 with PBS and Alexa 594-conjugated goat anti-rabbit antibody (Molecular probes, Eugene, Oregon) diluted 1:20 with PBS. The slides were incubated with the secondary antibodies for two h in the dark at room temperature. The slides were visualized using a fluorescent photomicroscope (OlympusAX70, Olympus American Inc., Lake Success, NY) and images were captured using the 40x objective and a Quantix cooled digital camera (Photometrics, Tucson, AZ) with QED camera plugin software (QED Imaging, Inc., Pittsburgh, PA). Five images were captured per slide from the proximal alveolar (PA)

regions, where most of the CD particle tend to localize near the terminal bronchioles and alveolar ducts.

Mophometry

Immunofluorescence morphometric analysis using Metamorph software (MetaMorph, Universal Imaging Corp., Downingtown, PA) was conducted on images captured from the proximal alveolar (PA) regions where CD accumulation was observed and from the same areas in control sheep. A representative slide from each lobe, where most of CD was grossly observed, was stained for immunofluorescence. Five images were captured per slide from completely perfused areas of the lung, where the alveoli were fully distended. The digital images were captured using a 40x objective producing a microscopic field with an area of 34466.1 μm^2. The captured images were quantified as previously described in chapters 3 and 4 to assess the localization of CYP1A1 in different alveolar epithelial cells. Briefly, the area of CYP1A1 expression was quantified in AT-II cells, NT-II cells, and the entire alveolar septum. The proportional CYP1A1 expression in AT-II cells was calculated as previously described in chapter 3. AT-II cell hyperplasia and hypertrophy were assessed by measuring the area of cytokeratins 8/18 expression.

Western Blot Analysis

The amount of CYP1A1 apoprotein in lung microsomes was determined by Western blot as previously described (Ma *et al*, 2002) with minor adaptation. A Novex Tris glycine gel with 15 small wells, (Invitrogen Corporation, Carlsbad, CA), and 30 µg of microsomal proteins were subjected to SDS gel electrophoresis for 90 min at 120 volts followed by transfer to a nitrocellulose membrane (blotting) for another 90 minutes at 25 volts. Liver microsomes of BNF-treated rat (Xenotech, Kansas city, KS) were used as a positive control. The membranes containing protein bands were identified by using a primary polyclonal rabbit anti- rat CYP1A1 antibody (Xenotech, Kansas city, KS) for overnight incubation at 4 ºC. Then, the membranes were washed and blocked for 1 h at room temperature with rocking with a 5% solution of dry milk in tris-buffered saline/tween (TBS/tween). After blocking, the membranes were washed and incubated for 1 h with a HRP (horse radish peroxidase)-conjugated goat anti-rabbit IgG (Santa Cruz Biotech. Inc., Santa Cruz, CA) at room temperature. Super RX Fuji Medical X-ray film was then exposed to the membranes at room temperature. Band intensity developed on

the X ray film was measured by the Eagle Eye II scanner with Eagle Sight software (Strategene, La Jolla, California). The density on the scanned images was measured using ImageQuant software version 5.1 (Molecular Dynamics, Sunnyvale, CA). Each image was quantified three times, the average of which was used for statistical analysis. After quantification, the data were presented as a percentage of the CYP1A1 positive control.

Bronchoalveolar Lavage Fluid (BALF) Analysis

Both the right apical (exposed) and left apical (internal control) lobes were lavaged using ice-cold PBS (Ca^{++} and Mg^{++} free). Three consecutive lung lavages were performed in which the first lavage was collected by using 2 ml/gm lung while the subsequent 2 lavages were conducted by using 2.7 ml/gm lung weight. In the last 2 lavages, the PBS fluid was flushed in and out of the lobes through a cannula and a 60-ml plastic syringe. The lobes were excised from the rest of lung and the incision site was clamped off by digital pressure during BAL collection process. Nevertheless, some of the lavage fluid was lost due to incision of the lung tissue which reduced the recovery of the fluid. Therefore, the BAL differential is considered more accurate that the total BAL cell yield.

The BALF analysis was conducted as previously described (Porter *et al*, 1999). Briefly, the first BAL fluid was kept separate from the subsequent lavages and centrifuged at 500 x g for 10 min at 4 ºC to collect the BAL cells. The acellular supernatant was decanted and used for analysis as BAL fluid (BALF). Cells of the subsequent BAL were collected by centrifugation and the acellular supernatant lavages were decanted and discarded. BAL cells from the first and second lavages were combined, re-suspended in HEPES buffer (145 mM KCL, 1.0 mM $CaCl_2$, 5.5 mM D-glucose, 10 mM N-2-hydroxyethylepiperazine-N-2-ethanesulfonic acid: pH 7.4), centrifuged at 500 x g for 10 min at 4 ºC, and the supernatant was discarded. The cell pellet was resuspended in HEPES buffer and kept in ice.

BAL Cell Count and Differential Count

To assess pulmonary inflammation associated with coal dust instillation, the alveolar macrophages (AM) and the polymorphonuclear leucocytes (PMN) were counted

by using a coulter multisizer II and AccuComp software (coulter Electronics, Hialeah, Fl) as previously described (Castranova *et al*, 1990). Cytospin preparations of BAL cells of 1 x 10^5 total phagocytes (AM and PMN) suspended in 200 µl HEPES-buffered solution were prepared by using a Shandon Elliot cytocentrifuge (800 rpm for 5 minutes). The cytospin preparations were stained with modified Wright-Giemsa stain as previously described, and cell differentials were determined by light microscopy (Porter *et al*, 2002a). To calculate the differential cell counts, the total cell count (PM-PMN) obtained from Coulter Counter was multiplied by the cell percentage differentials from the cytospin preparations. In addition, the percentage of alveolar macrophages containing phagocytized coal dust particles was determined for each lamb.

BALF Albumin Concentration

The albumin concentrations in the BALF reflect the integrity of the blood-pulmonary epithelial cell barrier. The BALF albumin was measured as previously described (Porter *et al*, 2002a) by using a Cobas Fara II analyzer (Roche Diagnostic systems, Montclair, NJ). The albumin was determined colorimetrically, based upon its binding to bromocresol green (Doumas *et al*, 1971), at 658 nm using a commercial assay kit (albumin BCG diagnostic kit, Sigma Chemical Company, St Louis, MO).

BALF Lactate Dehyrogenase (LDH)

Lactate dehydrogenase activity was measured in the BALF as an indicator of cytotoxicity, by detection of the reduction of NAD^+ associated with LDH catalyzed oxidation of lactate to pyruvate at 340 nm (Gay *et al*, 1969) using a commercial assay kit (Roche Diagnostics Systems, Montclair, NJ) as previously described (Porter *et al*, 2002a).

Alveolar Macrophage (AM) Chemiluminescence (CL)

AM chemiluminescence (AM CL) is a marker of increased production of reactive oxygen and nitrogen species by AM. In this assay, the use of unopsonized zymosan permits the measurement of chemiluminescence emitted from stimulated AM only (Castranova, 1987) and not PMN chemiluminescence (Hill, 1977; Allen, 1977). The assay was conducted in a total volume of 0.25 ml of HEPES-buffered medium as previously described (Porter *et al*, 2002a).

Nitric Oxide Dependent AM CL

To determine the NO-dependent chemiluminesecence released from AM in response to particle exposure, the zymosan-stimulated chemiluminescence from cells preincubated with 1 mM nitro-L-arginine methyl ester (L-NAME, a nonselective NOS inhibitor (Vaughan *et al*, 2003)) was subtracted from zymozan-stimulated chemiluminescence from cells without nitro-L-arginine methyl ester as previously described (Porter *et al*, 2002b).

Differential Blood Count

Blood samples were collected from all sheep to monitor the changes in blood status before and after CD instillation until sacrifice. Blood collection was conducted once after sheep arrival at the pens, 1 day before instillation, and 1, 3, 5, 7, 14, 28, 42, and 56 days after instillation. Differential blood count was performed using a Cell-DYN® 3500 R (Abbot Diagnostics, Santa Clara, California). Hematocrit values were measured by using microhematocrit tubes and microhematocrit centrifuge.

Statistical Analyses

All analyses were performed with SAS version 8.2 and using Proc Mixed. In the comparison between CYP1A1 localization between AT-II cells and NT-II cells, in sheep exposed to BNF only, the model was the two factor repeated measures analysis of variance. In all other cases, where data of right exposed lobe were compared to the control and to the left unexposed lobes, the model was single factor repeated measures analysis of variance. All pairwise comparisons were performed using a pooled variance estimate and Fisher's LSD (Least Significant Difference). All results were considered statistically significant at $p<0.05$.

RESULTS

The coal dust deposition was observed in the right apical lobe as black spots (Figure 2A) indicating a successful instillation.

A B

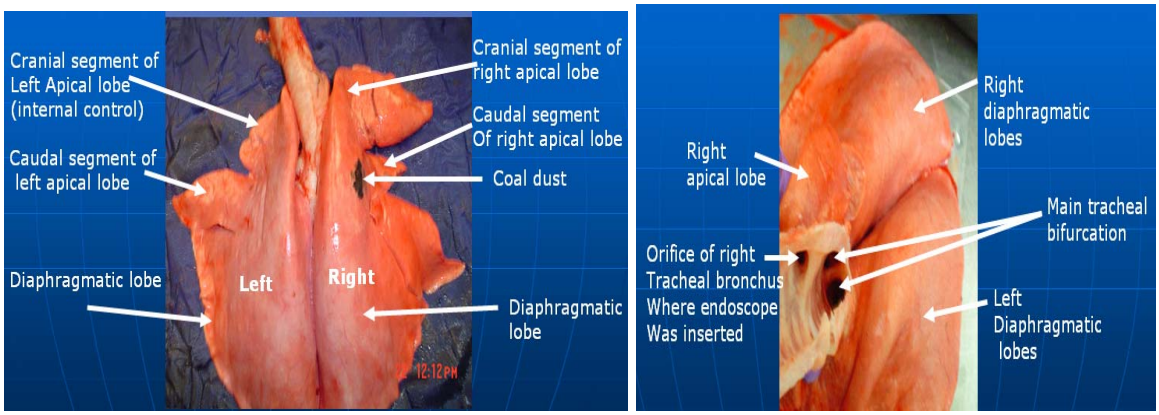

Figure 2: Photographs of sheep lung showing (A) the deposition of coal dust particles in the caudal segment of the right apical lobe and the cranial segment of the left apical lobe as an internal control. In B, the orifice of the tracheal bronchus where the endoscope was inserted is shown.

1- 7-Ethoxyyresorufin-O-Deethylase (EROD) Activity

The CYP1A1-dependent enzymatic activity (EROD), measured per mg microsomal protein was significantly reduced ($p=0.0166$) in lambs exposed to CD and BNF compared to those exposed to BNF alone. Moreover, EROD was significantly reduced ($p=0.0265$) in microsomes prepared from the CD-instilled lobe (right lobe) compared to the un-instilled lobe (left lobe) (Figure 3B).

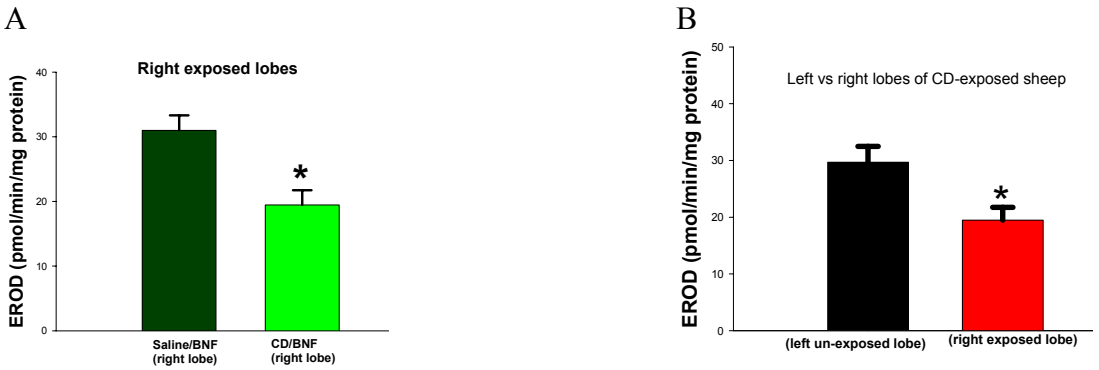

Figure 3. Effect of CD exposure on pulmonary EROD activity in lambs. In A, EROD is significantly reduced in lambs exposed to CD and BNF compared to lambs with BNF alone. In B, EROD activity is significantly reduced in CD-exposed lobes compared to the control unexposed lobes. * Significantly different at $p<0.05$.

2- 7-Pentoxyresorufin-O-Deethylase (PROD) Activity

The CYP2B-dependent enzymatic activity (PROD) was significantly lowered ($p=0.042$) in CD-exposed lambs with BNF compared to control (Figure 4A). Compared to the non-instilled lobe, PROD activity was reduced to less than 50 % in the CD-exposed lobe (Figure 4B) but did not reach a statistically significant difference.

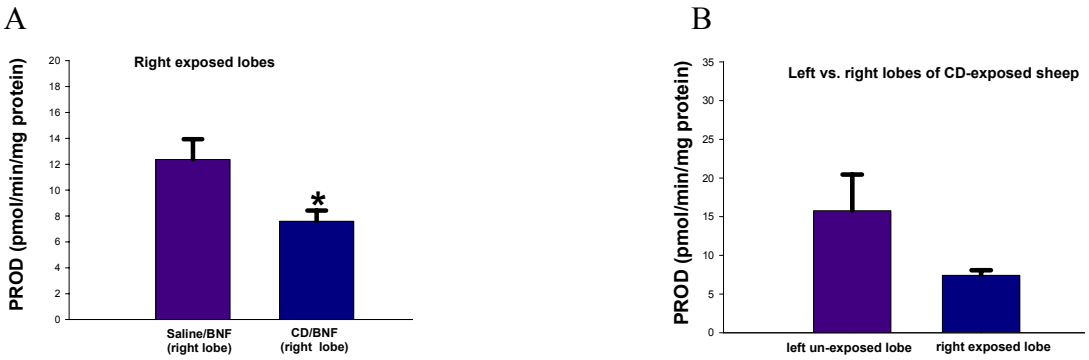

Figure 3. Effect of CD exposure on pulmonary PROD activity in lambs. In A, PROD is significantly reduced in lambs exposed to CD and BNF compared to lambs with BNF alone. In B, PROD activity is reduced 50 % in CD-exposed lobes compared to the control unexposed lobes. * Significantly different at $p<0.05$.

3-Western Blot Analysis

CYP1A1 protein bands of right exposed lobes (Figure 5A) and left unexposed lobes (Figure 5B) were quantified and expressed as percentage of positive CYP1A1 control. The CYP1A1 apoprotein measured in lung microsomes by Western blot was not significantly reduced in lambs exposed to CD and BNF compared to control ($p=0.2$)

(Figure 5C) and in the CD-exposed lobes compared to the control unexposed lobes (p=0.5) (Figure 5D).

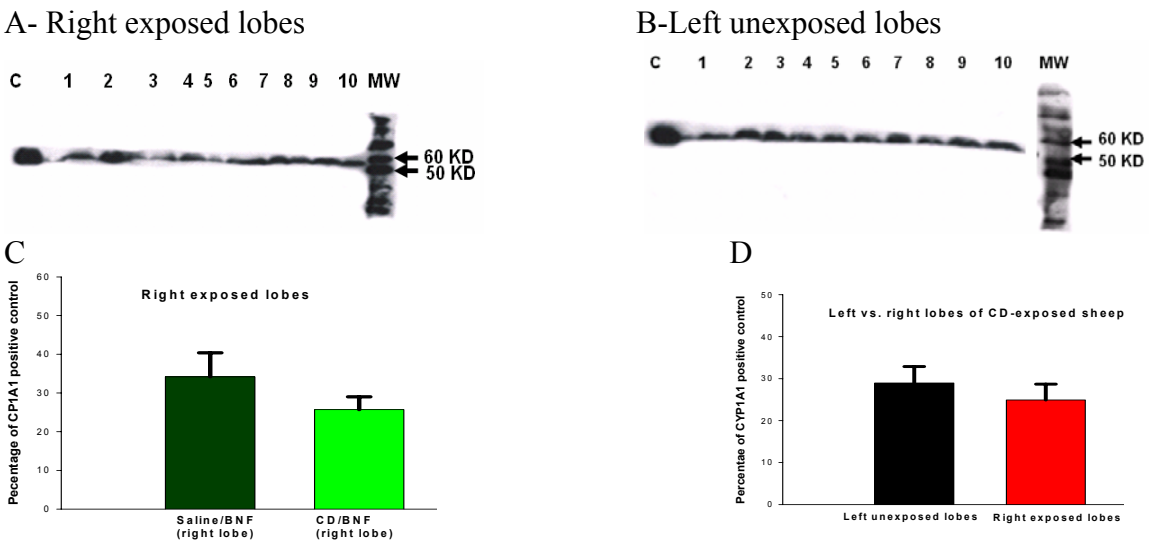

Figure 5. Effect of CD exposure on CYP1A1 protein measured by Western blot. 30 µg microsomal proteins were subjected to SDS-PAGE and electroblotted to a nitrocellulose membrane. The membrane was primed by a polyclonal rabbit CYP1A1 as described in the materials and methods. The results are expressed as a percentage of CYP1A1 positive control. CYP1A1 protein is lower in lambs exposed to CD and BNF than control (C). The CD-exposed lobes have a lower amount of CYP1A1 protein compared to the unexposed lobes (D). In A, lanes 1-5 are for right lobes of control (exposed to saline) and lanes 6-10 are for right lobes of CD-exposed lambs. In B, lanes 1-5 are for left unexposed lobes of the control and 6-10 are for the left unexposed lobes of the CD group. C is the positive CYP1A1 control and MW is the molecular weight standard.

4-Immunofluorescence Double Labeling for CYP1A1 and Cytokeratins 8/18

A- Distribution of CYP1A1 in BNF-Induced Sheep.

Sheep CYP1A1 was visualized as red fluorescence in alveolar type II cells, non-type II cells, and endothelial cells of the alveolar septum (Figure 7). However, the area of CYP1A1 quantified in alveolar non-type II (NT-II) cells is significantly greater than that in alveolar type II (AT-II) cells of the left ($p=0.009$) (Figure 6A) and right ($p<0.001$) (Figure 6B) apical lobes of the BNF-induced sheep.

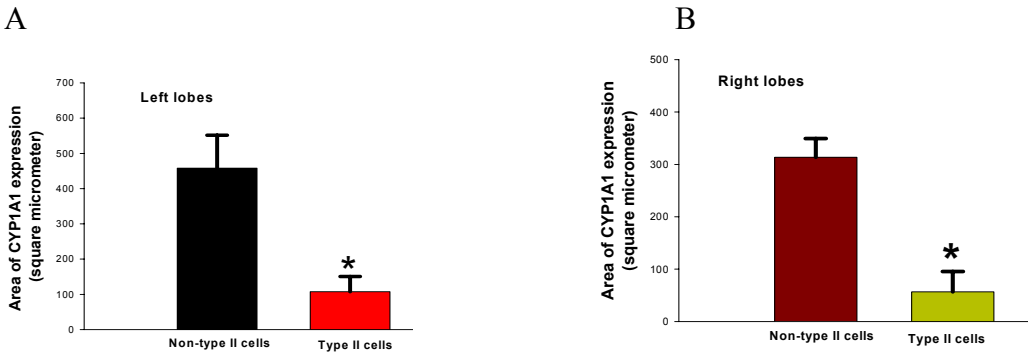

Figure 6. Morphometric analysis showing the distribution of CYP1A1 in sheep lung. In A, the area of CYP1A1 expression in non-type II cells is significantly larger compared to CYP1A1 area in type II cells of the alveolus of left lung lobes. In B, the area of CYP1A1 expression in non-type II cells is significantly larger, compared to CYP1A1 area in type II cells of the alveolus of left lung lobes. * Significantly different at $p<0.05$. Data are means ± SE, n=5 in the saline exposed group and 4 in the CD-exposed group.

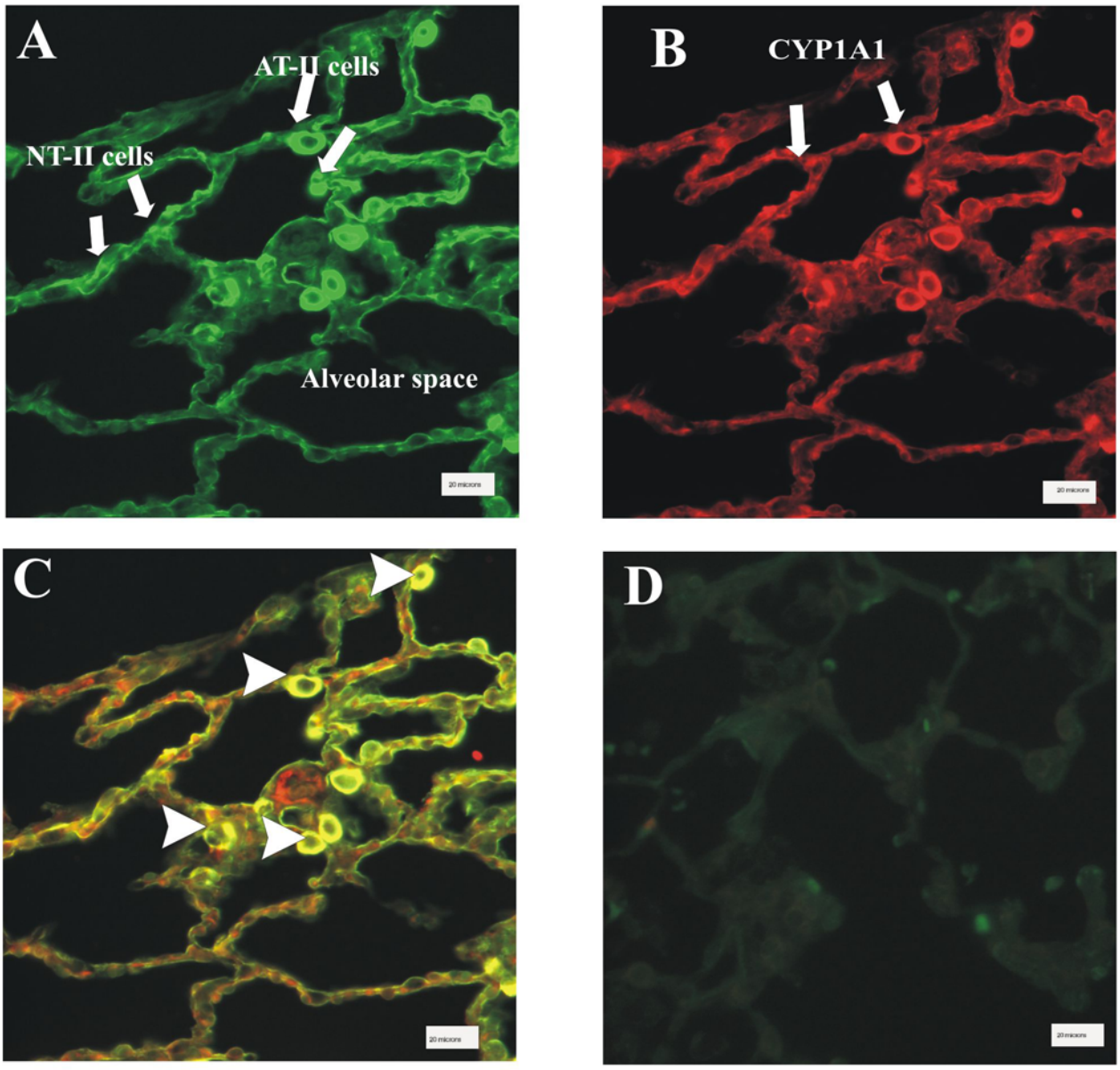

Representative images of immunofluorescent-stained tissue section against CYP1A1 and cytokeratins 8/18 in sheep treated with BNF alone showing the general distribution pattern of CYP1A1 in sheep. In A, the green fluorescence is for the cytokeratins 8/18 and marks primarily alveolar type II cells that appear cuboidal in shape and located at the corners of alveolar septa. Cells that do not express cytokeratins 8/18 are not green and are usually elongated cells. In B, the red fluorescence indicates the sites of CYP1A1 expression. In C, the 2 images in A and B are superimposed to determine the CYP1A1 that is co-localized with cytokeratins 8/18. Therefore cells expressing both CYP1A1 and cytokeratins 8/18 stain yellow. In D, the negative control demonstrates absence of specific fluorescence for CYP1A1 and cytokeratins 8/18, indicating the high specificity of the staining procedure. Bar is 20 micrometers.

B- CYP1A1 Induction is Suppressed in the Alveolus of CD-Instilled Sheep

Morphometric quantification of the CYP1A1 area of expression in lamb alveolus has been conducted in the CD-exposed and control sheep to assess the effect of CD instillation on the CYP1A1 induction. CYP1A1 area was quantified in alveolar type II cells, non-type II cells, and the entire alveolar septum.

a- In Alveolar Type II (AT-II) Cells

The proportional CYP1A1 expression in AT-II cells, which adjusted for the increased area of AT-II cell, showed a highly significant reduction ($p<0.001$) in sheep exposed to CD and BNF compared to those receiving BNF alone (Figure 8A). When compared to the left unexposed (internal control) lobes, the right lobes exposed to CD also showed a significant diminution ($p=0.01$) of proportional CYP1A1 expression in AT-II cells (Figure 8B). In addition, the area of CYP1A1 co-localized (co-expressed) with cytokeratins 8/18 marker in AT-II cells was smaller, albeit not significantly, in sheep exposed to CD and BNF than BNF alone (Figure 8C). Furthermore, the area of CYP1A1 that co-localized with cytokeratins 8/18 was also smaller in the CD-exposed right lobes compared to the unexposed left lobes (Figure 8D), but these differences were also not significantly different.

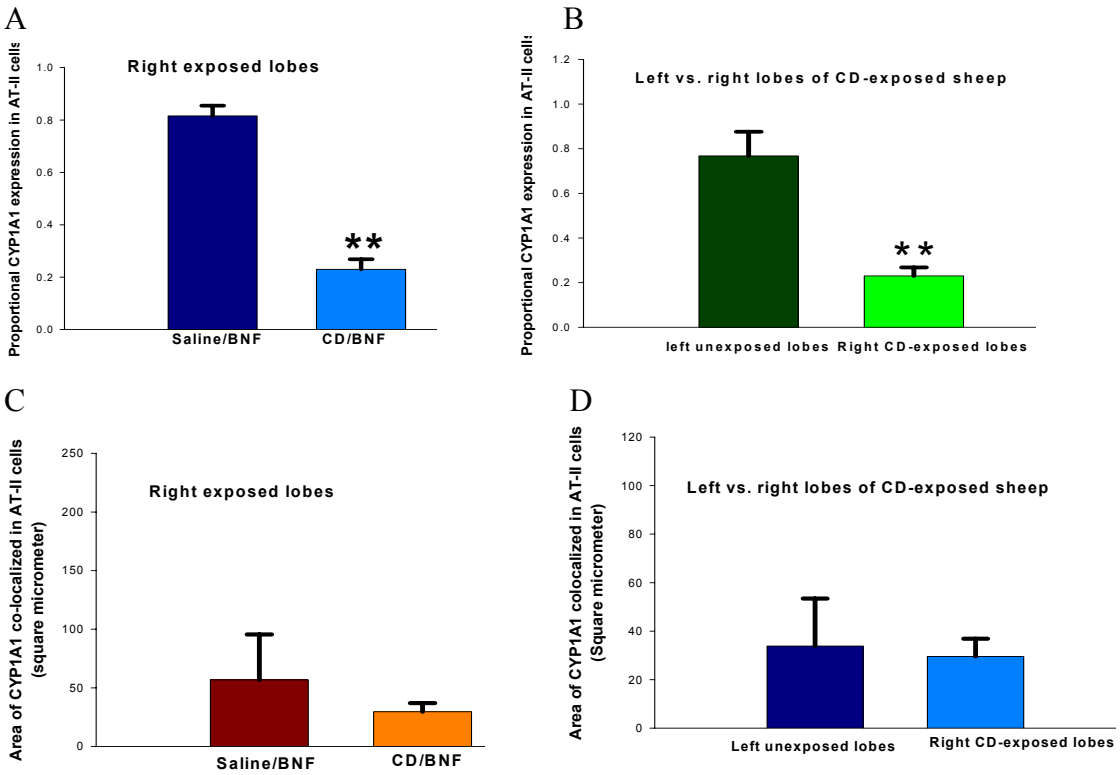

Figure 8. Morphometric quantification of CYP1A1 expression in AT- II cells. In A, there is a highly significant reduction of the proportional CYP1A1 expression in AT-II cells of CD-exposed lambs with BNF compared BNF alone. In B, the proportional CYP1A1 expression in AT-II cells of the CD-exposed lobes is highly significantly decreased compared to the left unexposed lobes. In C the proportional CYP1A1 expression is reduced in CD-exposed sheep with BNF compared to BNF alone. In D, the proportional CYP1A1 expression is reduced in CD-exposed lobes compared the left unexposed lobes. ** significantly different at $p<0.001$.

b- Alveolar Non-Type II (NT-II) Cells

Cells in the alveolar septum that do not express cytokeratins 8/18 (AT-II makers) are not type II cells and are designated here as alveolar non-type II (NT-II) cells. These cells are usually thin, elongated and often contain immunofluorescence CYP1A1. The area of CYP1A1 expression in these cells is significantly diminished in alveolar septum of sheep exposed to CD and BNF compared to BNF alone ($p=0.0015$) (Figure 9A). In addition, the area of CYP1A1 expression in NT-II cells is significantly reduced in alveolar septum right lobes exposed to CD compared to the left unexposed lobes of the CD-exposed sheep ($p<0.0299$) (Figure 9B).

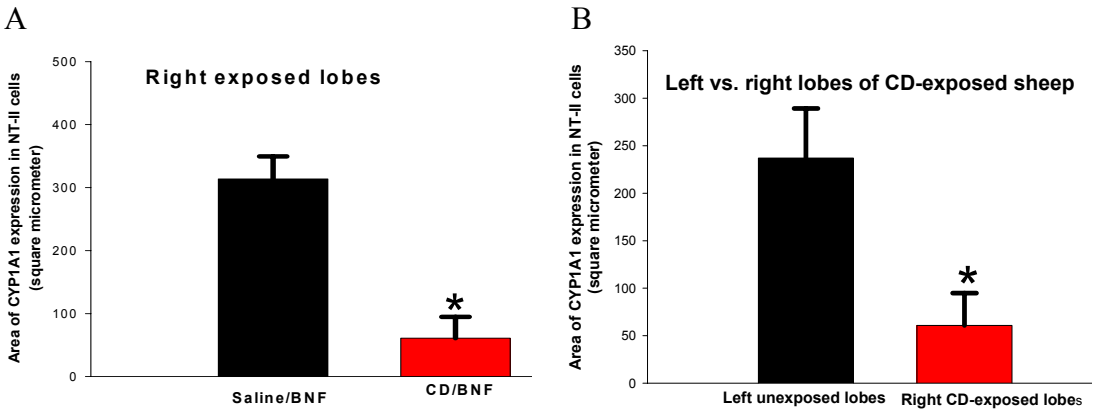

Figure 9. Morphometric quantification of the area of CYP1A1 expression in NT-II cells. In A, the area of CYP1A1 expression, measure in μm^2 is significantly reduced in CD-exposed sheep with BNF compared to BNF alone. In B, the area of CYP1A1 expression in NT-II cells of the CD and BNF-exposed right lobes is significantly lower than the left unexposed lobes exposed to BNF alone.* significantly different at $p<0.05$.

c- Total CYP1A1 Expression in the Whole Alveolar Septum of Sheep

The total area of CYP1A1 expression in alveolar septum includes expression in AT-II cells and NT-II cells. This area showed significant reduction in sheep exposed to CD and BNF compared to sheep that received BNF alone ($p=0.006$) (Figures 10A and 11). Moreover, in BNF-treated sheep, the area of CYP1A1 expression in the alveolar septal cells of the right lobes exposed to CD is reduced by 65.3 % compared to the left unexposed lobes of the CD-exposed sheep (Figure 10B).

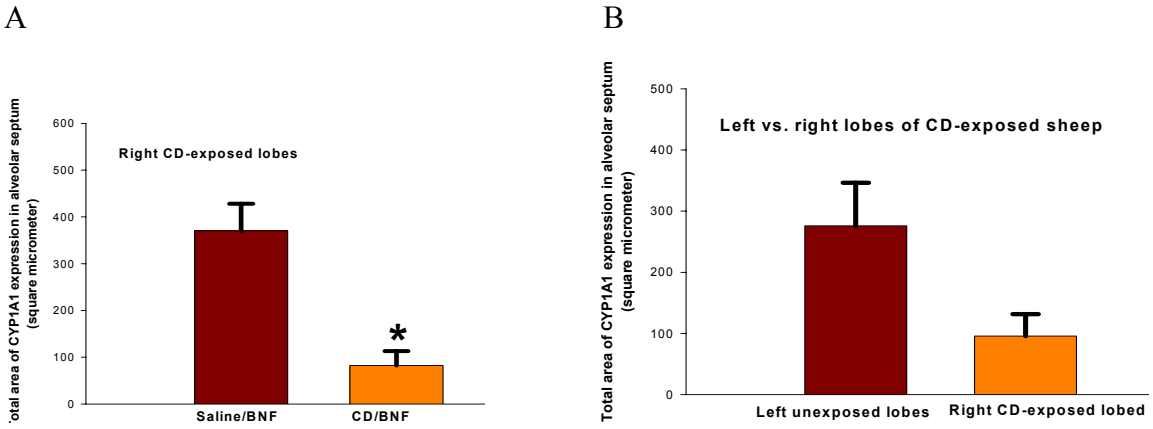

Figure 10. Morphometric quantification of the total CYP1A1 expression in alveolar septum. In A, the total area of CYP1A1 expression in the alveolus, expressed as μm^2 of CD-exposed sheep with BNF is significantly lower than BNF alone. In B, the area of CYP1A1 expression in the alveolus of right CD-exposed lobes is reduced by 65.3 % compared to the left unexposed lobes of CD-exposed sheep. * significantly different at $p<0.05$.

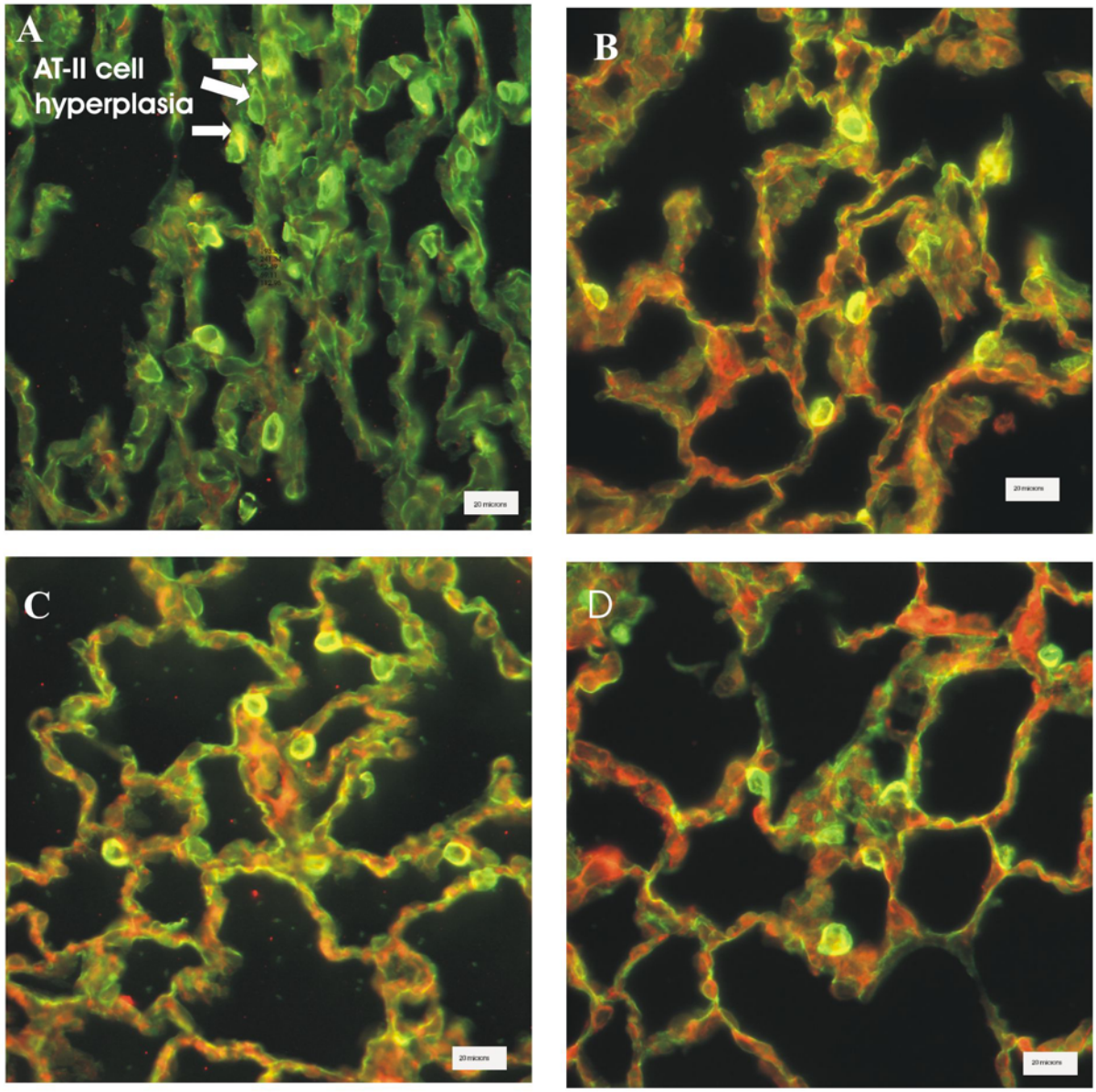

Figure 11. Representative images of immunofluorescent-stained sections showing the suppression of CYP1A1 expression in the alveolus of CD-exposed lung of BNF-induced sheep. The red fluorescence of CYP1A1 is reduced in the AT-II cells, NT-II cells, and the entire alveolar septum in CD-exposed lung lobe (A) compared to the unexposed left lobe (B) of the CD-exposed sheep and compared to sheep injected with BNF alone (C). In D, the CYP1A1 expression in the left (un-instilled) lobe of control sheep does not show any a difference compared to the right (saline-instilled) lobe. Alveolar type II hyerplasia and hypertrophy is shown in CD-exposed lobes (A). Reference bar is 20 micrometers.

C-Effect of CD Exposure on Alveolar Type II (AT-II) Cell Hyperplasia in Sheep

The area of AT-II cells, as indicated by lung area with green fluorescence due to cytokeratins 8/18 expression, was quantified morphometrically. The area of AT-II cells was increased in the alveolus of sheep exposed to CD and BNF compared to BNF alone, albeit not significantly. The area of cytokeratins 8/18 expression in the alveolus of the right CD-exposed lobe was also numerically, but not significantly, increased relative to the left unexposed lobe (Figure 12). AT-II cell hyperplasia and hypertrophy were visualized in fluorescent-stained sections of CD exposed sheep (Figure 12).

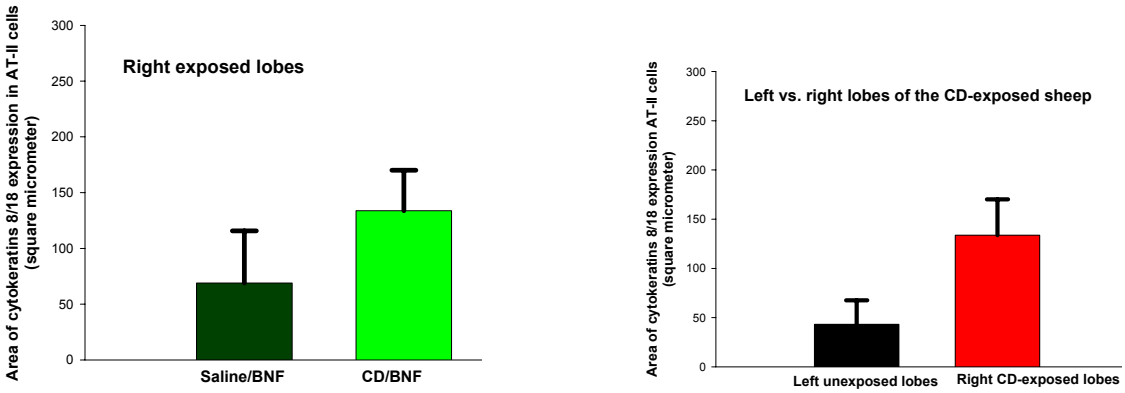

Figure 12. Morphometric quantification of the cytokeratins 8/18 expression in alveoli of CD exposed and control sheep. In A, the area of cytokeratins 8/18 expression is numerically higher in CD-exposed sheep with BNF compared to control. In B, the area of cytokeratins 8/18 expression is numerically, but not significantly increased in CD exposed right lobes compared to the left unexposed lobes. Results represent means ± SE, n=5 in the saline exposed group and 4 in the CD-exposed group.

4-Results of BAL Fluid Analysis

A- BAL Cell Differentials

a- Alveolar Macrophages (AM)

The number of BAL AMs was not significantly increased in the CD-instilled right lobe compared to the left lobes instilled with saline (Figure 13A) or the uninstalled left lobes (Figure 13C). Cell differentials of cytospin preparation showed a significant increase in the percentage of AM in CD-exposed right lobes compared to the right lobes instilled with saline (p= 0.0008) (Figure 13B) or the unexposed left lobes (p=0.0318) (Figure 13D). While no CD-laden AM was observed in saline exposed groups or the left

unexposed lobes, an average of 44.5% of the AM counted in the BAL of CD-exposed sheep contained coal dust particles (range 23 to 73 %).

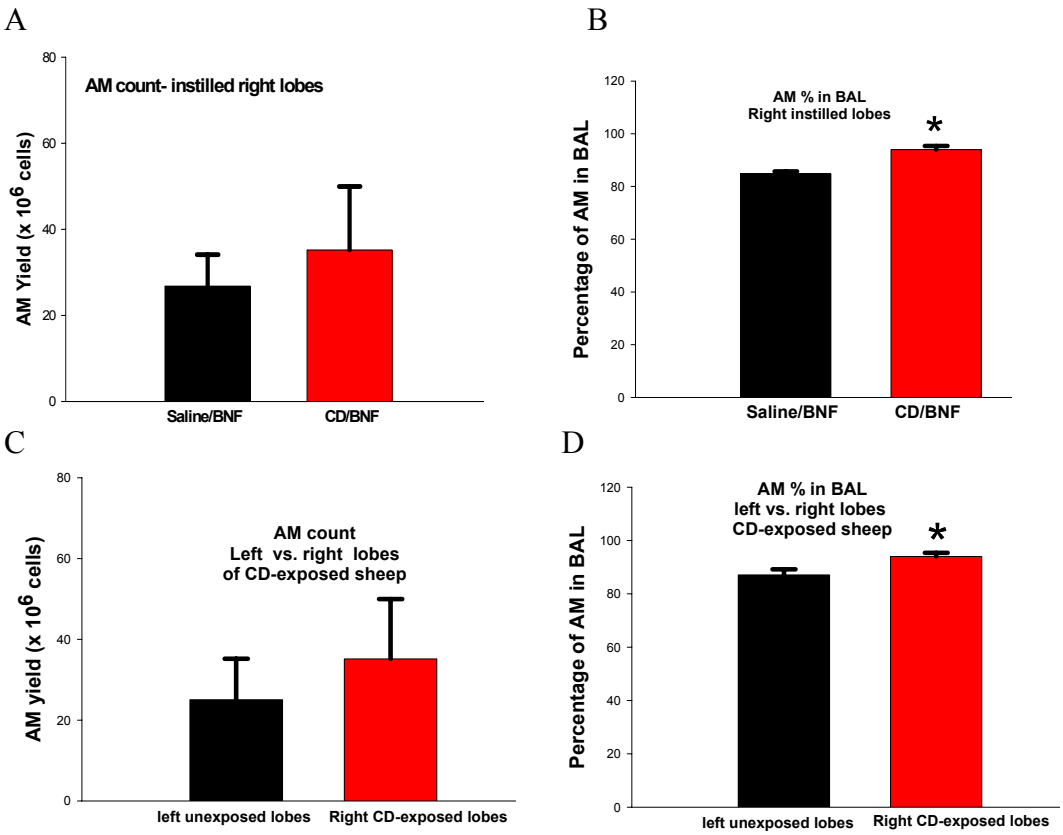

Figure 13. Differential count of BAL cells. The AM yield is higher in CD-exposed right apical lobe than saline-exposed lobe (A) or left uninstilled (unexposed lobes) (C). The percentage of AM is significantly higher in CD-exposed right apical lobe than saline-exposed lobe (B) or left uninstilled (unexposed lobes) (D). Results represent means ± SE, n=5 in the saline exposed group and 4 in the CD-exposed group.

b- Polymorphonuclear Leucocytes (PMN)

The PMN yield in CD-exposed right lobes was not significantly higher than the right lobes exposed to saline (Figure 14A) or the uninstilled left lobes (Figure 14C). Cell differentials of cytospin preparation exhibited a significant increase in the percentage of AM in CD-exposed right lobes compared to the right lobes instilled with saline ($p=0.047$) (Figure 14B) or the uninstalled left lobes ($p=0.04$) (Figure 14D). These results suggest that the CD-exposed lobes exhibit higher phagocytic cell percentage.

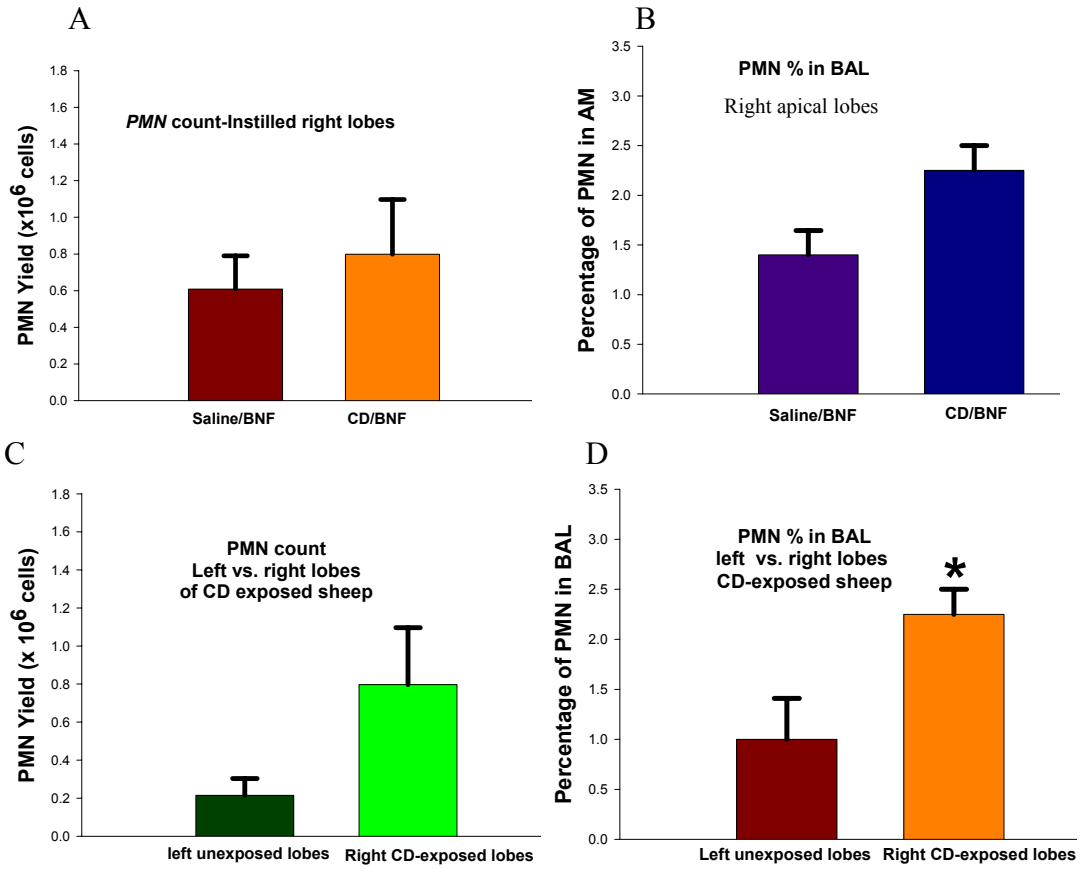

Figure 14. Differential cell count of the BAL. The PMN yield is non-significantly higher in CD-exposed tracheal bronchial lobe than saline-exposed lobe (A) and left uninstilled (unexposed lobes) (C). The percentage of PMN is significantly higher in CD-exposed tracheal bronchial lobe than saline-exposed lobe (B) or left uninstilled (unexposed lobes) (D). Results represent means ± SE, n=5 in the saline exposed group and 4 in the CD-exposed group.

B- BAL Fluid Albumin

The albumin measured in the BAL fluid was not significantly increased in CD-exposed right lobes compared to the saline-exposed right lobes (Figure 15A) and to the left uninstilled lobes (Figure 15B).

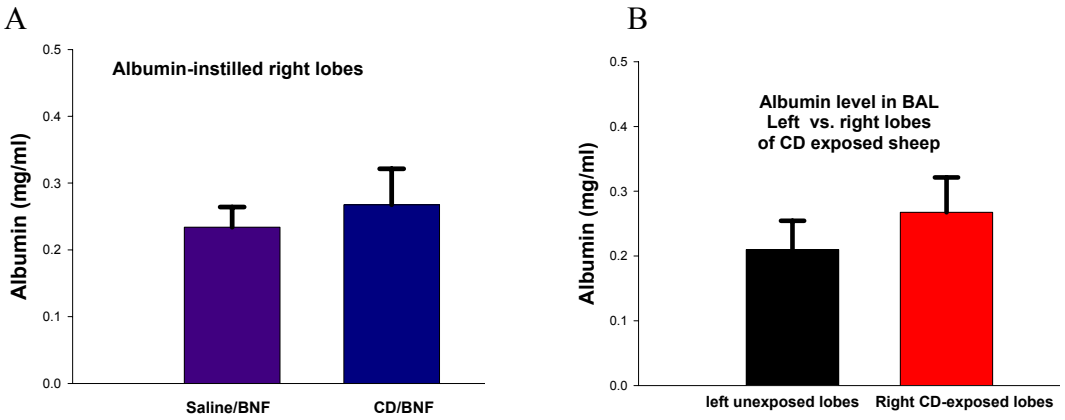

Figure 15. Albumin levels in BAL of CD-exposed lobes are not significantly increased compared to saline exposed (A) or left unexposed lobes (B). Results are means ± SE, n= 5 in the saline exposed group and 4 in the CD-exposed group.

C- LDH in BAL Fluid

The LDH concentration in BAL of CD-exposed tracheal bronchial lobes was not significantly higher than saline-exposed lobes (Figure 16A) or left uninstilled lobes (Figure 16B).

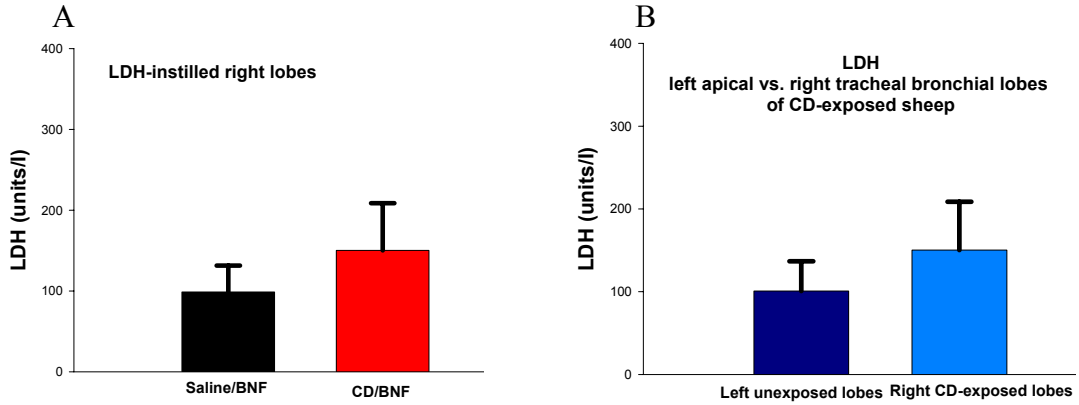

Figure 16. BAL fluid LDH levels are not significantly increased in right tracheal bronchial lobes exposed to CD compared to the right lobes exposed to saline (A) or left unexposed lobes (B). Data shown are means ± SE, n= 5 in the saline exposed group and 4 in the CD-exposed group.

D-AM-Dependent (CL) and NO-Dependent AM (CL)

No change was seen in AM-dependent CL and NO-dependent AM CL in BAL samples of CD-exposed lambs compared to the controls (data not shown).

5- Differential Blood Count (Total Leucocytic Count)

The neutrophil, monocyte, and total leucocyte counts for both CD-exposed and control sheep were temporarily increased the day after the instillation and then gradually decreased the following days to reach almost the resting stage on the day of sacrifice (Figure 17A, B, and C, respectively). In addition, the hematocrit values do not show significant difference between CD-exposed sheep and controls (data not shown) at any time period (data not shown).

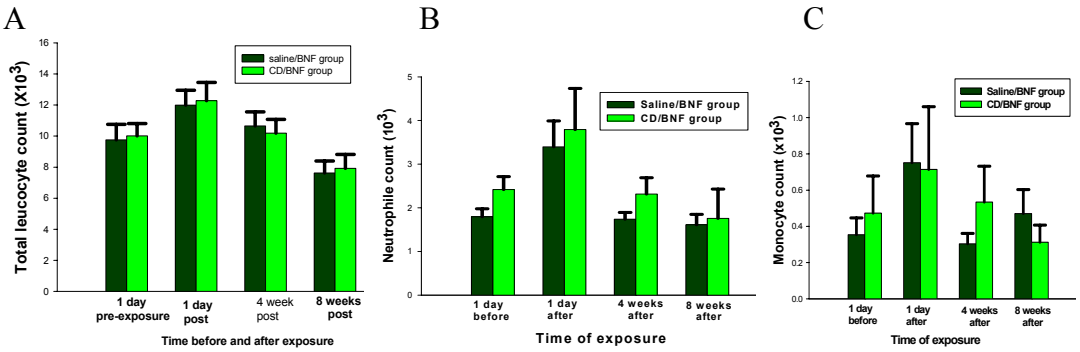

Figure 17. The total leucocyte count (A), neutrophil count (B), or monocyte count (C) exhibits a brief increase one day after instillation then reduced gradually to resting levels at the time of sacrifice for both CD-exposed and control group. Data shown are means ± SE, n= 5 in the saline exposed group and 4 in the CD-exposed group.

6- Histopathological Changes

Histopathological changes of CD-exposed lung lobes included bronchointerstitial pneumonia with accumulation of dust-laden alveolar macrophages, mainly in the interstitial tissue with only occasional foci of alveolar histiocytosis, a finding expected in a lavaged lung. These changes were irregularly distributed but consistently present in the instilled right apical lobes. Thus, bronchointerstitial pneumonia with particle-laden interstitial macrophages was observed in the right apical lobe of all instilled lambs but was not present in all sections of this lobe in the instilled lambs. Bronchointerstitial pneumonia was not seen in the control lambs (Figure 18 C and D). AT-II cell hyperplasia and hypertrophy was also observed in CD-exposed lobes (Figure 18A and B).

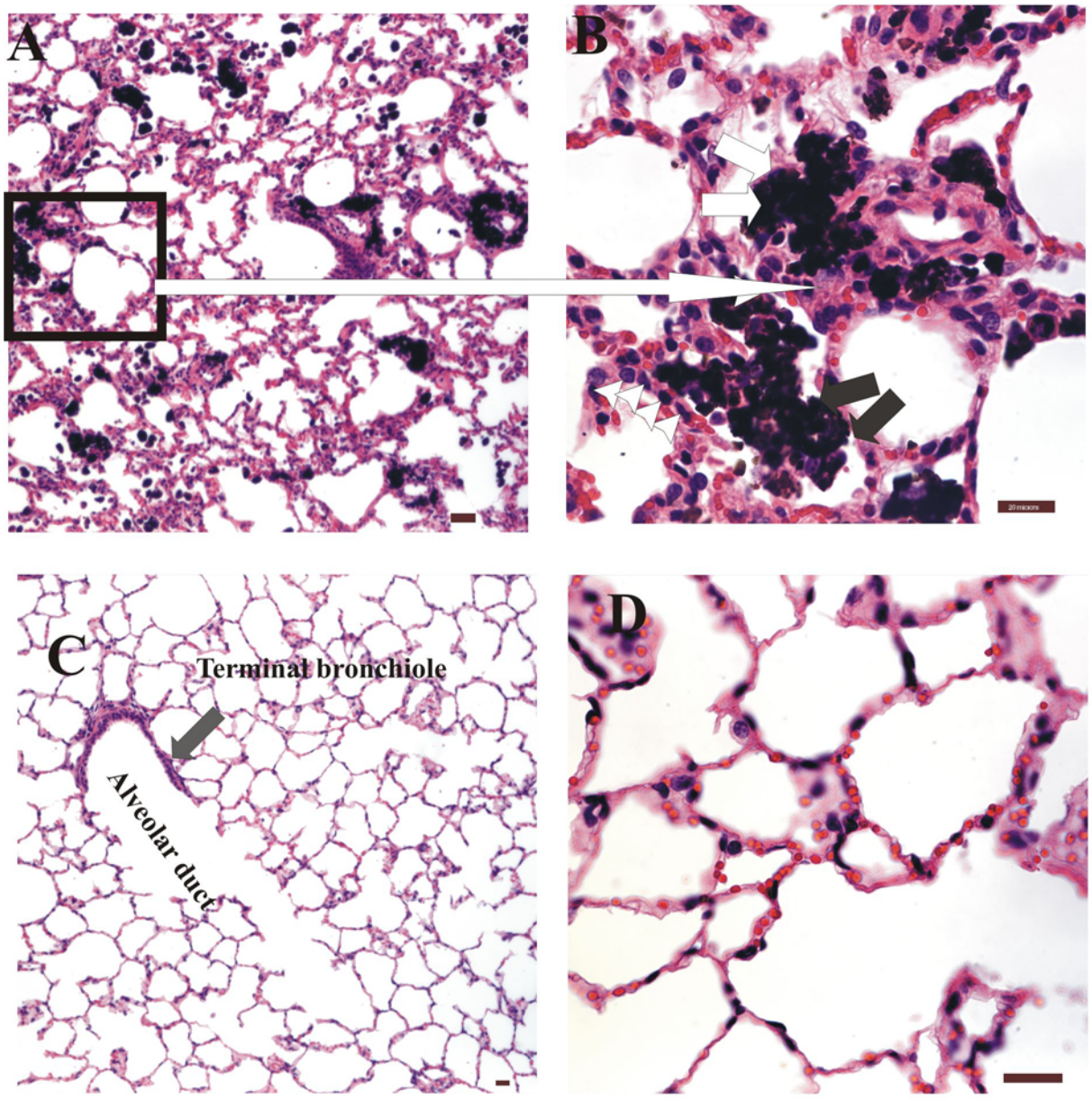

Figure 18. Photomicrograph of lung tissue sections of lambs stained with Hematoxylin and Eosin showing the histopathological changes in CD exposed lobes. Bronchointerstitial pneumonia is shown in A and B with accumulation of dust-laden AM in the interstitial tissues (arrows). AT-II cell hyperplasia and hypertrophy is also shown (arrow heads). Alveolar macrophages also contain abundant coal dust particles (black arrows). In the control (C and D), no histopathological changes appear within the alveoli. The bar is 20 μm.

DISCUSSION

In this study, we investigated the modifying effect of respirable coal dust particles on CYP1A1 induction in BNF-exposed sheep. The response of sheep lung to CD particles, in regard to CYP1A1 expression, was similar to that of the other 2 species, rats and rabbits that have been investigated in the previous chapters. The model of CWP in sheep was based upon a previous model of sheep silicosis (Begin *et al*, 1989). However, the CD suspension was instilled only one time and the sheep were kept for eight weeks before sacrifice. The response of sheep lung to respirable particles, such as quartz, is similar to the human response, particularly in cellular cytotoxicity (Larivee *et al*, 1990).

The results indicated that the intratracheal instillation of CD significantly inhibited the CYP1A1-dependent metabolic activity (EROD) lung microsomes (Figure 1). This effect was localized only in the lobes that were instilled with CD (right lobes). However, in the left lobes, which were not exposed to CD particle suspension, there was no change in the activity, suggesting that the CD exposure inhibited the CYP1A1 metabolic activity locally and the effect did not extend to include the neighboring lung lobes. Along with CYP1A1 activity, another CYP isoform, CYP2B, was measured. CYP2B is the major constitutive isoform of CYP family in sheep lungs (Williams *et al*, 1991). The CYP2B-dependent enzymatic activity (PROD) showed a significant diminution in lung microsomes prepared from lung of sheep exposed to CD and BNF compared to BNF alone (Figure 2). This result suggested that, CD not only inhibited the activity of BNF-induced CYP1A1 in sheep lung, but the inhibitory effect also included another CYP isoform, constitutively expressed in sheep lungs.

To assess the effect of CD exposure on CYP1A1 induction, the CYP1A1 protein was measured by Western blot. The amount of CYP1A1 protein measured by Western blot was reduced, albeit not significantly, in the CD-exposed lobes compared to unexposed lobes (Figure 3). Although the reduction was not significant, the general trend seemed to be suppressive as shown in Figure B.

The suppressive effect of the CD on CYP1A1 induction in sheep lungs was further demonstrated by immunofluorescence double labeling. By using this technique, the CYP1A1 expression in different pulmonary epithelial cells was investigated. We used

cytokeratins 8/18, which are cytoskeletal proteins highly expressed in primitive epithelial cells, to recognize the AT-II cells (Kasper *et al*, 1993) in the lung alveolus. Accordingly, the cellular components of the stained lung tissue section were divided into 2 distinct populations using indirect immunofluorescence with a primary anti-cytokeratins 8/18 antibody and a green FITC-labeled secondary antibody. One population stained distinctively green and those were AT-II cells (Figure 5A). The others did not stain green and were designated as NT-II cells. The CYP1A1 has been visualized in alveolar type II cells and NT-II cells. However, by morphometry, the area of CYP1A1 expression measured in NT-II cells, where no green fluorescence was visualized, was significantly higher than that area in AT-II cells. This result suggests that in the alveolus, AT-II cells are not the major sites of CYP1A1 induction and NT- II cells are important sites of CYP1A1 induction. In addition, there is a general deficit in the literature regarding the localization of inducible CYP1A1 in ruminant lungs. The majority of literature in ruminant CYPs concentrates on the inducibility of CYP1A1 in the liver of goat (van't Klooster *et al*, 1993), or cattle (Shull *et al*, 1986) and this study is the first, to our knowledge to report the distribution pattern of CYP1A1 in sheep lungs.

The CD instillation in sheep significantly reduced the area of CYP1A1 expression in AT-II cells (Figure 6), NT-II cells (Figure 7) and the entire alveolar septum (Figure 9). Therefore, one mechanism of suppression of BNF-induced CYP1A1 by CD exposure appears to be inhibition of CYP1A1 expression in different alveolar septal cells. These results are not surprising and are comparable to those seen in rats exposed to coal dust and rabbits exposed to silica. While increased size (hypertrophy) and number (hyperplasia) of AT-II cells were not significant in this study, they were increased numerically which is consistent with studies in other species. The area of CYP1A1 expression in AT-II cells, relative to the total area of AT-II cells showed a significant reduction suggesting that the new hyperplastic AT-II cells do not express CYP1A1 in proportion to their number and size. This result supports our findings in rats that CD exposure leads to production of a new population of alveolar type II cells with decreased CYP1A1 expression. The mechanism of downregulation of CYP1A1 associated with cellular proliferation should be further investigated. However, in the rat liver with hyperplastic nodules, induced by diethylnitrosamine and partial hepatectomy, the total

amount of microsomal CYP enzymes was reduced 50% compared to the control (Degawa *et al*, 1995). Moreover, the inducibility of CYP1A by inducers decreases slightly in the rat liver bearing hyperplastic nodules (Degawa *et al*, 1995). Consistent with that, the inducibility of CYP1A1 by BNF was markedly reduced in early lung hyperplastic foci associated with urethane exposure and the lung carcinomas were devoid of expression of CYP1A1 protein (Forkert *et al*, 1998). All of these previous studies suggest that CYP protein is downregulated in proliferating cells - - a finding which is consistent with the downregulation of CYP1A1 induction and CYP2B in our study of CD-exposed lambs.

To assess the local inflammatory reaction of sheep lung in response to the inhaled CD particles, the AM and PMN were counted in BAL. The percentage of AM and PMN showed a modest, but significant increase. This result suggests that an inflammatory process accompanied the CD instillation in sheep. Interstitial pneumonia with accumulation of dust-laden AM in the interstitial tissue were the hallmarks of histopathological changes in lung sections of CD-exposed lobes in sheep. In spite of the local inflammatory reaction, no systemic reaction was observed as there was no significant change in the neutrophil count, monocyte count, or total leucocyte count between CD-exposed and control sheep. This result suggests that CD instillation into a localized region of the lung is not associated with a systemic reaction in lambs at the dose instilled (500 mg/sheep). The local inflammatory process was also associated with non-significant enhancement of LDH (marker of cytotoxicity) and albumin levels (marker of pulmonary-blood barrier in the lung) of the CD-exposed group compared to control. This suggests that CD exposure in sheep is associated with an inflammatory response, which involves the interstitium consistently.

In conclusion, the general response of sheep lung to the CD-mediated suppression of BNF-induced CYP1A1 is similar to that observed in rats. The sheep results are also comparable to the CYP1A1-downregulation observed in acute and chronic silicosis in rabbits. Therefore, if the suppression of CYP1A1 by particle exposure occurs in 3 animal species (rats, rabbits, and sheep), it is also likely to happen in any other species, such as the human.

CHAPTER 6
SOME MECHANISTIC INTERACTIONS ASSOCIATED WITH PARTICLE-MEDIATED SUPPRESSION OF CYP1A1 INDUCTION IN RATS

ABSTRACT

CYP1A1 induction was suppressed by pulmonary exposure to coal dust and crystalline silica. However, the mechanism of induction suppression was not completely elucidated. Therefore, we investigated some of the alterations associated with suppression of BNF- induced CYP1A1 in rat lungs. We hypothesize that the inflammatory response and induction of apoptotic proteins are two potential mechanisms associated with CYP1A1 downregulation. To investigate this hypothesis, male Sprague Dawley (SD) rats were intratracheally (IT) exposed to 2.5, 10, 20, and 40 mg/rat coal dust (<5 μm) or vehicle (saline). Three days prior to sacrifice, rats were intraperitoneally (IP) injected with 50 mg/kg BNF (CYP1A1 inducer). At necropsy, bronchoalveolar lavage (BAL) was collected to evaluate pulmonary inflammation by measuring BAL alveolar macrophage (AM) and polymorphonuclear (PMN) cell counts, AM chemiluminescence (CL), and nitric oxide (NO)-dependent AM CL. Pulmonary cytotoxicity was assessed by measuring the BAL lactate dehydrogenase (LDH). In a parallel experiment, immunofluorescence triple labeling was conducted to identify the interaction between CYP1A1, cytokeratins 8/18, and Bax expression. BAL analysis showed a dose-responsive enhancement of PMN and LDH by CD exposure (r^2=0.661, $p<0.0001$; r^2=0.174, $p= 0.0139$ respectively), a significant increase of AM count in all groups exposed to CD and BNF compared to control BNF-treated rats, and a significant enhancement of NO-dependent AM CL in rats exposed to the highest dose (40 mg/rat) of CD and BNF compared to rats treated with BNF alone ($p= 0.004$). Immunofluorescence (IF) triple labeling showed an inverse relationship between CYP1A1 expression and Bax expression in alveolar type II cells. Because Bax is a pre-apoptotic protein, we investigated the role of Bax expression and apoptosis on the CD-mediated suppression of CYP1A1 induction. To explore this mechanism, male SD rats (50-70 gm) were IT instilled with 40 mg/kg coal dust or vehicle (saline). At days 0, 5, 9, 10, 11, 12, 13 post instillation, rats were IP injected with the pan-caspase inhibitor, Q-VD-OPH (20mg/kg), or vehicle (DMSO). Three days before sacrifice, all rats were administered BNF IP (50 mg/kg). EROD and PROD activities

were measured in microsomes of the right lobe. Histopathology, IF for CYP1A1, cytokeratins 8/18, and Bax, as well as TUNEL assays were conducted on tissue sections of the left lobes. EROD and PROD were significantly lower in CD-exposed rats compared to control. CD-exposed rats with caspase inhibitor did not show statistical difference in PROD and EROD activities compared to DMSO-injected rats. By IF, the area of CYP1A1 expression within alveolar septum of CD and BNF exposed rats was significantly lower than rats exposed to BNF without CD, but was unaffected by caspase inhibition with Q-VD-OPH. In single label IF, Bax expression measured as area (μm^2) or number of cells/field was significantly lower in CD-exposed rats with Q-VD-OPH than CD-exposed rats with DMSO, but significantly higher than saline-exposed rats with Q-VD-OPH. TUNEL assay showed a significant increase of percentage of apoptotic cells in CD-exposed rats with BNF compared to rats receiving BNF alone. CD-exposed rats with Q-VD-OPH had a significant reduction of percentage of apoptotic cells compared to the CD-exposed rats with DMSO. Taken together, these results suggest that CD exposure enhances the pulmonary inflammatory response in a dose-dependent manner, upregulates the Bax expression in AT-II cell, and induces apoptosis in lung cells. CYP1A1 induction and activity was not significantly affected by the Q-VD-OPH-mediated inhibition of caspases but caspase inhibition decreased Bax expression and apoptosis. This suggests that CD-associated suppression of CYP1A1 is associated with inflammation and associated with, but not caused by, Bax expression.

INTRODUCTION

The pathogenesis and mechanisms of suppression of CYP1A1 induction by intra-pulmonary deposition of respirable particles are important processes in understanding the modification of the xenobiotic-associated lung cancer by downregulation of pulmonary enzymatic systems. In the previous 3 chapters, we have demonstrated a downregulation of CYP1A1 protein expression and its dependent activity, EROD by pulmonary exposure to CD and silica. At the cellular level, the suppression of induction was demonstrated in alveolar type II cells, non type II cells, and the entire alveolar septum in three animal species, rats, rabbits and sheep. However, the mechanisms associated with this cellular behavior in response to particle exposure were not entirely clear. Pulmonary inflammation and lipoproteinosis were demonstrated by histopathological examination of

particle-exposed lung tissue and were associated with reduced CYP1A1 induction. In this study, we investigated the inflammatory response to CD exposure by examining bronchoalveolar lavage (BAL) fluid collected from rats exposed to coal dust particles. We examined the relationship between increasing levels of inflammation and increased suppression of CYP1A1 induction. Since the sensitivity of tissue to apoptosis is increased when expression of cell-death regulator proteins, such as Bax is upregulated (Guinee *et al*, 1997), we also investigated the relationship between the upregulation of Bax expression and apoptosis induction in alveolar cells and the CD-mediated suppression of CYP1A1 induction.

Apoptosis is programmed cell death that is essential for homeostasis (Wang *et al*, 2002) and tissue remodeling (Stanley *et al*, 1992). Apoptosis helps eliminate cells that have improperly developed, have been produced in excess, or have sustained genetic damage (Thompson, 1995). Apoptosis is characterized by cell shrinkage, nuclear condensation, DNA fragmentation, cytoplasmic blebbing and formation of apoptotic bodies (Wyllie *et al*, 1980). Because the plasma membrane is intact during programmed cell death, there is limited tissue injury and inflammation (Savill *et al*, 1993). Two common mechanisms are associated with cellular apoptosis: receptor-dependent and mitochondrial-dependent (Mayer and Oberbauer, 2003). The receptor-dependent mechanism is mediated through specific receptors, such as tumor necrosis factor receptors (TNFR). Stimulation of these receptors by extracellular stimuli, such as cytokine release or an inflammatory process, results in recruitment and activation of caspase 8. Activated caspase 8 can activate a cascade of downstream caspases that eventually produce DNA fragmentation and apoptosis (Peter and Krammer, 1989). In the mitochondrial pathway, intrinsic stimuli, such as ischemia and ionizing radiation (Mayer and Oberbauer, 2003) enhance the release of apoptotic proteins, such as caspase 9, or apoptosis inducing factor (AIF) from the mitochondrial outer membrane. These apoptotic factors activate caspase 8 and caspase 3, resulting in apoptosis (Peter and Krammer, 1989). Some pre-apoptotic proteins, such as Bax, may be activated and translocated from cytosol to mitochondria, enhancing the release of cytochrome c and stimulating the mitochondrial-induced apoptotic mechanism (Aiba-Masago *et al*, 2002).

In our coal dust response study, we demonstrated a dose-dependent increase of Bax expression in alveolar cells by CD exposure. On the other hand, our previous experiments showed a reduction of CYP1A1 expression in alveolar cells by CD exposure. This suggests an association between increased Bax expression and reduced CYP1A1 induction. In addition, the Bax gene has 2 AhR response elements that play a role in PAH-mediated apoptosis of ovarian oocytes in mice (Matikainen *et al*, 2002). Since agents triggering pulmonary inflammation, such as silica (Lim et al, 1999; Lyer et al, 1996) and bleomycin (Kuwano et al, 2000), can also induce apoptosis of lung cells, we investigated the effect of CD, which also triggers lung inflammation, on alveolar cell apoptosis. Because apoptosis can be inhibited by specific caspase inhibitors, such as zVAD-fmk (Kitamaka *et al*, 1997) and Q-VD-OPH (Rebbaa *et al,* 2003), we investigated the effect of caspase inhibition on suppression of Bax-associated apoptosis and CYP1A1 induction. We demonstrated that CD increases the number of apoptotic lung cells, and the caspase inhibitor, Q-VD-OPH inhibits both Bax expression and apoptosis. However, the suppression of CYP1A1 by CD exposure was not reversed by injection of the caspase inhibitor, suggesting that the suppression occurs by a mechanism other than Bax expression or apoptosis of pulmonary cells.

MATERIAL AND METHODS

Experimental Design

In the coal dust dose response experiment**,** 40 male SD rats (220-270 gm body weight at time of exposure) were randomized into 5 groups (8 rats/group) by a randomizer program (www.randomizer.org). Rats were exposed to 2.5, 10, 20, or 40 mg/kg CD suspended in sterile saline or saline by intratracheal instillation (IT). Eleven days later, BNF was administered IP as a suspension in sterile corn oil at a dose of 50 mg/kg for CYP1A1 induction. Three days after the BNF injection, rats were euthanized and BAL was collected as described later.

In the caspase inhibitor (Q-VD-OPH) experiment, 24 male SD rats, (~67-93 gm body weight at time of exposure) were randomized into 4 groups (Table 1) using a randomizer program (www.randomizer.org). Rats were IT instilled with 40 mg/rat CD suspended in 0.3 ml saline or saline. On the day of the exposure, rats were injected with the caspase inhibitor, Q-VD-OPD dissolved in dimethylsulfoxide (DMSO) or the vehicle

with a dose of 15 mg/kg. The initial dose of caspase inhibitor or the vehicle was then followed by subsequent doses of 10 mg/kg injected at days 5, 9, 10, 11, 12, and 13 post exposures. Eleven days post instillation, all rats received 50 mg/kg BNF suspended in corn oil as a CYP1A1 inducer by IP administration. Rats were euthanized on day 14.

Group	**Group size (n)**	**CD or saline (IT)**	**Q-VD-OPH or DMSO (IP)**	**BNF (IP)**
Group 1	6	Saline	DMSO	BNF
Group 2	5	Saline	Q-VD-OPH	BNF
Group 3	7	CD	DMSO	BNF
Group 4	6	CD	Q-VD-OPH	BNF

Table 1. The treatment groups, group size and type of treatment in the caspase inhibitor study. The number of rats per group was selected based upon a power analysis, utilizing results of previous experiments.

Preparation of CD Suspension

The CD particulates used in the study are less than 5 microns in diameter with a surface area of 7.4 m^2/g. The particles contained 0.34 % total iron of which 0.119 % is surface iron. The particles were heat sterilized in an oven at 160 ºC for 2 h. Coal dust suspensions were made up daily from heat sterilized samples using pyrogen-free, sterile 0.9% saline (Abbott Laboratories, North Chicago). Suspensions were vortexed directly after preparation and shaken well before instillation.

Intratracheal Instillation

The CD particles were suspended in sterile saline at a concentration of 8.3, 33.3, 66.6, and 133.3 mg/ml. Rats received either 0.3 ml of this suspension (~2.5, 10, 20, and 40 mg/rat) or 0.3 ml of saline (vehicle). The IT instillation was conducted as previously described (Porter *et al*, 2002). Briefly, rats in the CD response experiment were anesthetized by intraperitoneal (IP) injection of sodium methohexital (Brevital, Eli Lilly Indianapolis, IN) and were intratracheally instilled using a 20-gauge, 4-inch ball-tipped animal feeding needle. Rats in the caspase experiment were instilled using the same

procedure except that an 18 gauge, 1.5 inch animal feeding needle was used for the instillation

Preparation and Injection of Caspase Inhibitor, Q-VD-OPH

The Q-VD-OPH (Quinoline-Val-Asp (Ome)-VH2-OPH) (Enzyme Systems Products, Inc., Livermore, CA), is a broad spectrum caspase inhibitor with potent antiapoptotic properties (Caserta *et al,* 2003). The mechanism of action depends upon the formation of an irreversible thioester bond between the active site cysteine of the caspase and the aspartic acid residue in the inhibitor (Melnikov et al, 2003). The Q-VD-OPH was injected in rats to block the caspase-dependent apoptosis in pulmonary cells. Solutions of 2 % of the pan-caspase inhibitor were prepared in endotoxin-free dimethyl sulphoxide (DMSO) (Sigma Chemical Co., St. Louis, MO). Rats received 15 mg/kg in the first injections (day 0) and 10 mg/kg in the following injections (days 5, 9, 10, 11, 12, and 13 post exposure) by IP administration.

Preparation of BNF

To prepare BNF suspension, the vehicle (corn oil) was sterilized by filtering with non-pyrogenic Acrodisc 25 mm syringe filter (0.2 μm in diameter) (Pall Gelman sciences, Ann Arbor, MI). Solutions of 5 % BNF (Sigma, St. Louis, MO) in sterilized corn oil (50 mg/ml) were prepared 24 h before injection. The suspension was vortexed and then sonicated 15 minutes in Ultronics sonicator (Mahwa, NJ). BNF solutions were injected IP 72 h before sacrifice.

Necropsy of Rats

Rats were euthanized by IP injection of 0.5 ml 26% sodium pentobarbital (Sleepaway®, Fort Dodge Animal Health, Fort Dodge, IA). The abdomen was opened by incision in the midline and the lungs and attached organs, including tracheobronchial lymph node, thymus, heart, aorta, and esophagus, were removed. The right mainstem bronchus was ligated and the lung lobes were collected and immediately placed in ice for isolation of microsomes. The left lung lobe was inflated with 3.0 mls of 10% neutral buffered formalin (NBF). Tracheobronchial lymph nodes, liver, spleen, and right and left kidneys were also fixed in 10 % NBF. Fixed tissues were trimmed the same day, routinely processed in a tissue processor and embedded in paraffin the following

morning. For histopathoological examination, tissue sections of left lungs were stained with hematoxylin and eosin (H&E) for histopathology. Additional 5-micrometer sections were used for immunofluorescence.

Microsome Preparation

Microsomes were prepared as previously described (Flowers and Miles, 1991; Ma *et al*, 2002). Steps of microsomal preparation in rats are described in chapter 3.

Determination of the Total Lung Proteins

The protein content of lung microsomes was measured by the bicinchoninic acid (BCA) method as previously described (Smith et al, 1985, Ma et al, 2002) using the BCA protein assay kit (Pierce, Rockford, IL) in a spectra Max 250 Spectrophotometer (Molecular Devices Corporation, Sunnyvale, California). Bovine serum albumin was used as the standard.

Measurement of EROD and PROD Activities

EROD and PROD activities were measured as previously described (Burke *et al*, 1985 and Ma *et al*, 2002) using a luminescence spectrometer model LS-50 (Perkin-Elmer, Norwalk, CT). A 10 μM concentration of 7-ethoxyresorufin (Sigma, St. Louis, MO) solution prepared from 2.35 μg 7-ethoxyresorufin in 1 ml DMSO was used for the standard curve following each run. EROD and PROD activities were expressed as picomoles of the resorufin produced during the reaction per minute per milligram microsomal protein (pmol/min/mg protein).

Western Blot Analysis

Western Blot analysis of lung microsomes was conducted as previously described (Ma *et al*, 2002). Using a 15-well Novex tris glycine gel (Invitrogen Life Technologies, Carlsbad, CA), 30 micrograms of microsomal protein were loaded and subjected to a SDS gel electrophoresis and blotted against nitrocellulose membrane (Invitrogen Life Technologies, Carlsbad, CA). The nitrocellulose membrane was incubated with a polyclonal rabbit anti-rat CYP1A1 antibody (Xenotech, Kansas city, KS) or a monoclonal mouse anti-rat CYP2B1 antibody (Xenotech) at 4ºC overnight. The non-specific binding was blocked by addition of 1% dry milk in tris-buffered saline/tween (TBS/T) for 1 h at room temperature with rocking. The membranes were then incubated

with a goat anti-rabbit antibody (Santa Cruz Biotech. Inc., Santa Cruz, CA) for CYP1A1 detection or goat anti-mouse antibody (Santa Cruz Biotech. Inc., Santa Cruz, CA) for CYP2B1 detection for 1 h at room temperature with rocking. For the positive control, liver microsomes of BNF-treated rats (Xenotech) were used for CYP1A1 or liver microsomes of phenobarbital-treated rats (Amersham, Piscataway, NJ) for CYP2B1. The CYP1A1 and CYP2B1 proteins were detected by an enhanced chemiluminescence (ECL) reagent kit (Amersham). The X-ray films (Fuji Film Corp., LTD., Tokyo, Japan) containing protein bands were scanned by the Eagle Eye II scanner (Stratagene, La Jolla, California) with Eagle Sight software. The scanned images were quantified by ImageQuant software version 5.1 (Molecular Dynamics, Sunnyvale, CA). The values were expressed as a percentage of the CYP1A1 or CYP2B1 positive controls.

Immunofluorescence Techniques

1- Single Label Immunofluorescence for Bax.

Single label immunofluorecence for Bax was conducted as described in previous chapters with minor modification. Briefly, the slides were heated in the oven at 60 ºC for 15 minutes. The slides were deparaffinized and rehydrated in xylene in 3 sequential 6-minute immersions, a 3 minute immersion in 100 % alcohol, 3 minutes in 90 % alcohol, 3 minutes in 80 % alcohol, and 5 minutes in distilled water. The antigen was retrieved by 0.01M disodium ethylenediamine tetraacetate (Fischer Scientific, Fair Lawn, New Jersey 07410), pH 8.0 in a microwave heating procedure. Non-specific binding was blocked by 5 % BSA in PBS (IgG free) (Sigma) for 10 minutes at room temperature (RT) followed by 5% pig serum in PBS (Biomeda Corporation Foster City, CA) for 10 minutes at RT. The slides were then rinsed with distilled water and a polyclonal affinity purified rabbit anti-Bax antibody (Santa Cruz Biotechnology Inc., Santa Cruz, CA) was applied overnight at a dilution of 1:20 with phosphate buffer saline (PBS) at room temperature. For the negative control, one slide was incubated with non-immune rabbit serum (BioGenex, San Ramon, CA). To maximize the antibody binding, slides were incubated for 2 h at 37 ºC the following day after which slides were washed and Alexa 594-conjugated goat anti-rabbit antibody (Molecular probes, Eugene, Oregon) was applied for 2 h at RT in the dark.

2- Double Label Immunofluorescence for CYP1A1 and Cytokeratins 8/18

The double-label immunofluorescence was carried out by the same method described in chapter one.

3- Triple Label Immunofluorescence for Bax, CYP1A1 and Cytokeratins 8/18

Triple label immunofluorescence for Bax, CYP1A1, and cytokeratins 8/18 was conducted to localize the expression of Bax and CYP1A1 in AT-II cells (with cytokeratins 8/18 marker) or NT-II cells. The technique was similar to the single label and double label procedure. The only difference was the application of three polyclonal antibodies for Bax, CYP1A1, and cytokeratins 8/18, which were added to the same slide simultaneously. For Bax, a polyclonal affinity purified rabbit Bax antibody (Santa Cruz Biotechnology Inc., Santa Cruz, CA) was applied at a dilution of 1: 20 with PBS. For CYP1A1, a polyclonal affinity purified goat antibody (Santa Cruz Biotechnology Inc., Santa Cruz, CA) was applied at a dilution of 1:10 with the diluted Bax antibody. For cytokeratins 8/18, a polyclonal Guinea pig anti-cytokeratins 8/18 (Research Diagnostic, Inc., Flanders, NJ) was applied at a dilution of 1:5 with the diluted mixture of and Bax CYP1A1 antibodies. The mixture of the polyclonal antibodies was applied by the aid of capillarity between folded slides and kept in the humidity chamber overnight at RT. For the negative control, one slide was incubated with rabbit serum (BioGenex, San Ramon, CA). On the second day and after 2 h incubation of the slides at 37 ºC, a mixture of appropriate secondary antibodies was applied on the slides for 2 h at RT in the dark. This mixture contains an Alexa 594-conjugated donkey anti-rabbit (Eugene molecular probe), Alexa 350-conjugated donkey anti-goat (Molecular Probes), and FITC-labeled donkey anti-G pig (Research Diagnostic, Inc., Flanders, NJ) antibodies for detection of Bax, CYP1A1, and cytokeratins 8/18, respectively.

Morphometry of Immunofluorescence

In all kinds of immunofluorescence, single, dual, or triple, five images were captured from the proximal alveolar (PA) regions, where most of the instilled particles were deposited. PA regions are areas of the lung that are located next to visible alveolar ducts. PA regions are different from random alveolar (RA) regions, which are areas without visible alveolar ducts. We concentrated on immunofluorescence in alveolus

rather than airways because we have previously demonstrated that in CD-exposed rats, changes in CYP1A1 expression principally occur in the alveolus. The threshold ranges for red (Bax), blue (CYP1A1) and green (cytokeratins 8/18) fluorescence were held constant throughout the morphometric analysis of all images. The slides were examined under a fluorescent photomicroscope (Olympus AX70, Olympus American Inc., Lake Success, NY) and images were captured using the 40x objective and a Quantix cooled digital camera (Photometrics, Tucson, AZ) with QED camera plugin software (QED Imaging, Inc., Pittsburgh, PA).

1- Morphometry for Immunofluorescence of Bax Alone (Single Label)

The area of Bax expression in the alveolar septum was measured by commercial morphometry software (Metamorph Universal Image Corp., Downingtown, PA) and expressed as μm^2. In addition, the number of cells expressing Bax in the tissue sections was counted and expressed as number per 40x field.

2- Morphometry for Double Label Immunofluorescence

Morphometry of images captured from slides stained for CYP1A1 and cytokeratins 8/18 was conducted by the same method described in the previous chapters.

3- ***Morphometry for Triple Label Immunofluorescence***

The morphometric analysis of immunofluorescence triple labeling for Bax, CYP1A1, and cytokeratins 8/18 was mainly intended to investigate the sites of localization of CYP1A1 and Bax expression and investigate the effect of caspase inhibition on the expression of both proteins. Quantification of triple-label immunofluorescence includes the following:

A- Quantification of Bax Expression in the Entire alveolar Septum

The total red area (representing Bax) expressed in the whole alveolar septum (including AT-II and NT-II cells) per 40x field was directly quantified by commercial morphometry software (Metamorph Universal Image Corp.). The total Bax area was expressed in μm^2 and designated as Q.

B- Quantification of CYP1A1 Expression in the Entire Alveolar Septum

The total blue area (representing CYP1A1) expressed in the whole alveolar septum (including AT-II and NT-II cells) per 40x field was measured directly by the commercial morphometry software (Metamorph Universal Image Corp.). The total CYP1A1 area was expressed in μm^2 and designated as T.

C- Quantification of Cytokeratins 8/18 Expression in the Entire Alveolar Septum

The total green area (representing cytokeratins 8/18) per 40x field was measured as an indicator of AT-II cell hypertrophy and hyperplasia. This area was also measured by the commercial morphometry software (Metamorph Universal Image Corp.) and expressed in μm^2.

D- Quantification of Bax Expression in AT-II Cells

The area of Bax expression in AT-II cells was quantified and expressed as μm^2 by measuring the red area (representing Bax) colocalized to the green area (representing cytokeratins 8/18 in AT-II cells) by the following mathematical formula:

$$A = P \times Q \text{ where;}$$

A is the area of Bax that co-expressed (colocalized) with cytokeratins 8/18 in alveolar type II cells,

P is the percent of Bax expressed in type II cells measured by the Metamorph software, and

Q is the total Bax area expressed in the whole alveolar septum (including alveolar type II and non-type II cells) measured by Metamorph software as in A.

In addition to the area measured, the number of type II cells expressing Bax was counted per field.

E-Calculating the Proportional Bax Expression Colocalized Within AT- II Cells

The proportional colocalization of Bax within type II cells was obtained by the following calculation:

$$\frac{A \text{ (The area of Bax colocalized in type II cells as calculated in D, expressed as } \mu m^2)}{\text{Total green area of cytokeratins 8/18 expression, expressed as } \mu m^2}$$

This calculation helped to investigate the relationship of Bax expression in the AT-II cells. Because AT-II cells increased in number and size in CD exposure, this estimate was normalized Bax expression per area of AT-II cells.

F-Quantification of the area of CYP1A1 Colocalized with Bax

The area of blue color (representing CYP1A1) colocalized (co-expressed) with red area (representing Bax) expressed as μm^2 was calculated from the following formula:

M=G x Q where;

M is the area of CYP1A1 that co-expressed (colocalized) with Bax

G is the percentage of CYP1A1 expression colocalized with Bax when measured by the Metamorph software, and

Q is the total Bax area expressed in the whole alveolar septum (including alveolar type II and non-type II cells) measured by Metamorph software as in A.

G- Calculating the Proportional CYP1A1 Colocalized Within Bax Area

The proportional CYP1A1 expression within Bax area was calculated by the following formula:

$$\frac{M \text{ (the area of CYP1A1 colocalized with Bax as calculated in E, expressed as } \mu m^2)}{Q \text{ (the total area of Bax expression, expressed as } \mu m^2)}$$

This measurement is very important as it reflects the changes in CYP1A1 expression relative to Bax expression in CD exposure.

H-Quantification of CYP1A1 Colocalized with Cytokeratins 8/18 (in AT-II Cells).

The area of CYP1A1 colocalized with cytokeratins 8/18 in AT-II cells (expressed as μm^2) was obtained by the following formula:

C = R x T where;

C is the area of CYP1A1 that co-expressed (colocalized) with cytokeratins 8/18 in alveolar type II cells,

R is the percent of CYP1A1 expressed in type II cells measured by the Metamorph software, and

T is for the total CYP1A1 area expressed in the whole alveolar septum (including alveolar type II and non-type II cells) measured by the Metamorph software.

I- Proportional CYP1A1 Expression in AT-II Cells

The proportional CYP1A1 expression in AT-II cells was calculated as follows.

$$\frac{C \text{ (the area of CYP1A1 colocalized with cytokeratins 8/18, expressed as } \mu m^2)}{\text{Total green area of cytokeratins 8/18 expression, expressed as } \mu m^2}$$

This measurement reflects the CYP1A1 expression in AT-II cells but adjusts for area increases associated with the hypertrophy and hyperplasia of AT-II cells.

J- Counting AT-II cells with Colocalized CYP1A1 and Bax

Since CD exposure was associated with AT-II hyperplasia, the number of AT-II cells that concomitantly express both CYP1A1 and Bax was counted per field of triple-stained sections and the percentage of these cells from the total number of AT-II cells was calculated as follows:

$$\frac{\text{Number of AT-II cells with Bax and CYP1A1}}{\text{Total number of AT-II cells}} \times 100$$

This percentage adjusts the number of cells expressing both Bax and CYP1A1 for the increased number of AT-II cells associated with CD exposure.

TUNEL Assay

Apoptosis of pulmonary cells was determined by terminal deoxynucleotidyl transferase-mediated dUTP nick end-labeling (TUNEL) assay using a TUNEL assay kit (Promega, Madison, WI) as previously described (Wang *et al*, 2002). In this apoptotic detection system, the fragmented DNA of apoptotic cells is measured by catalytically incorporating fluorescein-12-dUTP at the 3′- OH end of the DNA using the enzyme Terminal Deoxynucleotidyl Transferase (TdT) to form a polymeric tail in a TdT-mediated dUTP Nick-End labeling process as previously described (Gavrieli *et al*, 1992). Briefly, the formalin-fixed, paraffin embedded lung sections were deparaffinized by 3 sequential immersions in xylene, 3 minute each followed by rehydration with ethanol (100%, 95%, and 80%), 3 minutes each. The slides were then incubated with protease type 1 (Sigma) diluted with PBS at a concentration of 4%. For a positive control, a positive control slide was prepared by incubating the slide with DNase 1 (Sigma Aldrich

Co, St. Louis, MO) for 30 minutes at room temperature. All slides were then incubated with the equilibration buffer for 10 minutes, during which the reaction mix per slide was prepared by addition of 10 µl of the nucleotide mix to 90 µl equilibration buffer and 2µl terminal deoxynucleotidyl transferase (TdT) enzyme, according to the manufacturer instruction. For negative control, the 2 µl of TdT was replaced by 2 µl distilled water in the fluorescein-12-dUTP reaction mix. The slides were then incubated for 1 h at 37 ºC in the dark. Propidium iodide (100 µl/slide) (Sigma) was applied for 2 minutes as a counter stain, after which slides were rinsed in distilled water and cover slipped using anti-fade Gel/Mount (Biomeda, Foster City, CA) and kept at 4 ºC in the dark until examined. The slides were examined under a fluorescent photomicroscope (Olympus AX70, Olympus American Inc., Lake Success, NY) and images were captured using the 40x objective and a Quantix cooled digital camera (Photometrics, Tucson, AZ) with QED camera plugin software (QED Imaging, Inc., Pittsburgh, PA). Five images were randomly captured from PA regions and another five images were randomly captured from the RA regions. The number of positive and negative (normal) cells per field was counted. The results were expressed as a percentage of the positive apoptotic cells.

Bronchoalveolar Lavage (BAL) and Cell Differentials

Lungs were lavaged and cells collected as previously described (Hubbs et al, 2001). To assess pulmonary inflammation, cell counts of alveolar macrophages (AM) and polymophonuclear leukocytes (PMN) were obtained using a Coulter Multisizer II (Coulter Electronics, Hialeah, FL) as previously described (Castranova *et al*, 1990)

BAL Fluid Albumin Concentration

BAL fluid albumin concentrations were determined as an indicator of the integrity of the blood-pulmonary barrier. BAL fluid albumin was measured colorimetrically at 628 nm based on albumin binding to bromcresol green (Doumas *et al*, 1971) using a commercial assay kit (Albumin BCG diagnostic kit, Sigma Chemical Company, St. Louis, MO) and a COBAS MIRA Analyzer (Roche Diagnostic Systems, Montclair, NJ).

BAL Fluid Lactate Dehydrogenase Activity

BAL fluid lactate dehydrogenase (LDH) activities were determined as a marker of cytotoxicity, and were determined by monitoring the LDH catalyzed oxidation of lactate

to pyruvate coupled with the reduction of AAD^+ at 340 nm (Gay *et al*, 1968) using a commercial assay kit (Roche Diagnostics Systems, Montclair, NJ) and a COBAS MIRA Analyzer (Roche Diagnostic Systems, Montclair, NJ).

Zymosan-Stimulated AM Chemiluminescence

AM chemiluminescence was determined as an indicator of reactive oxygen and nitrogen species production by AM. The use of unopsonized zymosan in the chemiluminescence assay allows only AM chemiluminescence to be measured, because unopsonized zymosan stimulates AM chemiluminescence (Castranova *et al*, 1987) but not PMN chemiluminescence (Hill, 1977; Allen, 1977). The assay was conducted in a total volume of 0.50 ml HEPES buffer. Resting AM chemiluminescence was determined by incubating 1.0 x 10^6 AM/ml at 37°C for 20 minutes, followed by the addition of 5-amino-2,3-dihydro-1,4-phthalazinedione (luminol) to a final concentration of 0.08 μg/ml followed by the measurement of chemiluminescence. To determine zymosan-stimulated chemiluminescence, unopsonized zymosan was added to a final concentration of 2 mg/ml immediately prior to the measurement of chemiluminescence. All chemiluminescence measurements were made with an automated luminometer (Berthold Autolumat LB 953, Gaithersburg, MD) at 390-620 nm for 15 minutes. The integral of counts per minute versus time was calculated. Zymosan-stimulated (total) chemiluminescence was calculated as the cpm in the zymosan-stimulated sample minus the cpm in the resting sample. 1400W (N-(3-aminomethyl)benzyl)acetamidine•HCl), an inhibitor of nitric oxide synthase, was used to determine the component of zymosan-stimulated (total) chemiluminescence that is attributable to reactive nitrogen species. 1400W sensitive chemiluminescence was determined by subtracting the zymosan-stimulated chemiluminescence from cells pre-incubated with 1 mM 1400W from the zymosan-stimulated (total) chemiluminescence from AM without 1400W.

Histopathology

Tissue sections from control and CD- exposed lungs were routinely stained with hematoxylin and eosin (H&E) to assess histopathological changes. The changes were evaluated by a board-certified veterinary pathologist while blinded to the exposure status. The changes of interest that have been evaluated were: alveolitis (alveolar inflammation),

and AT-II cell hyperplasia and hypertrophy. The histopathologic changes were scored on a scale ranging from 0 to 5 for each of the severity and distribution scores to produce a sum pathology score of 0 to 10 for each slide, as previously described (Hubbs *et al*, 1997).

Statistical Analyses

The dose responsive effects of coal dust instillation on quantity of AMs, PMNs, levels of albumin, LDH, AM CL, NO-dependent CL for BAL fluid, Bax area and cells with Bax/field, we used Proc Reg for the regression analysis. All analyses were performed with SAS version 8.2 and using Proc Mixed or using Proc Reg. In all other CD response study comparisons, where we compared between groups, the model was single factor repeated measures analysis of variance. In the case of comparison between PA with RA, the model was three factors repeated measures analysis of variance. In all other caspase inhibitor study comparisons, where we compared between groups, the model was two factors repeated measures analysis of variance. All pairwise comparisons were performed using a pooled variance estimate and Fisher's LSD (Least Significant Difference). All results were considered statistically significant at $p<0.05$.

RESULTS

Effect of CD Exposure on Bronchoalveolar Lavage Fluid (BALF) Analysis

CD-exposed rats had a dose-dependent increase in polmorphonuclear leucocytes (PMN) (r^2=0.974, p= 0.002) (Figure 1A). The alveolar macrophage (AM) count was significantly increased in the BALF of all rats exposed to CD and BNF compared to rats treated with BNF alone (Figure 1B). AM CL and NO-dependent CL were significantly increased in rats exposed to 40 mg CD and BNF compared to rats treated with BNF alone (Figures 2A and B, respectively). The intrapulmonary deposition of CD particles produced pulmonary cytotoxicity manifested by elevation of LDH activity in a dose-dependent fashion (r^2=0.963, p=0.003) (Figure 3A). The blood barrier in the lung was also damaged in CD- exposed groups as shown by elevation of BALF albumin, which was statistically significant following exposures to 20 and 40 mg/kg CD and BNF compared to BNF alone (Figure 3B).

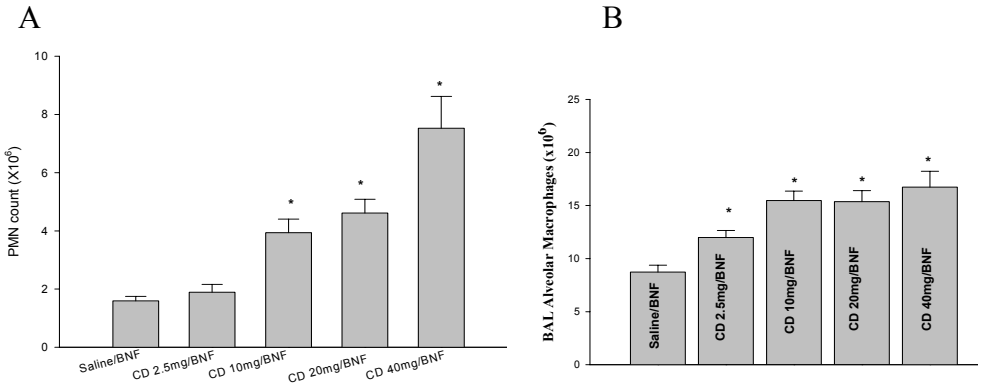

Figure 1. CD exposure increased the BALF PMN count in a dose-dependent manner (A). A significant PMN increase is shown in rats exposed to 10, 20, and 40 mg/rat CD and BNF compared to control saline and BNF. Alveolar macrophages cell count was significantly higher in all groups exposed to CD and BNF compared to the control saline with BNF (B). The bars are values of means and SE for each treatment. *Significantly different from control group at $P < 0.05$.

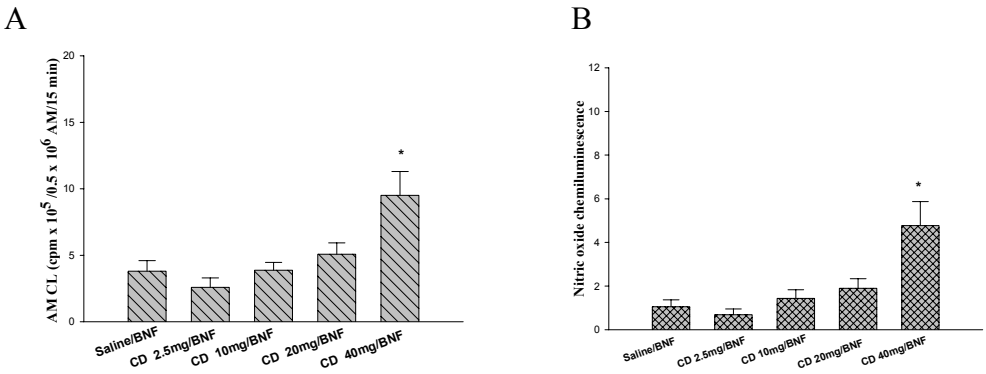

Figure 2. In A, AM CL was significantly higher in rats exposed to 40 mg CD and BNF compared to control saline and BNF. In B, the NO-dependent AM CL was also significantly increased in rats exposed to CD 40 mg and BNF compared to control saline and BNF. The bars are values of means and SE for each treatment. *Significantly different from control group at $P < 0.05$.

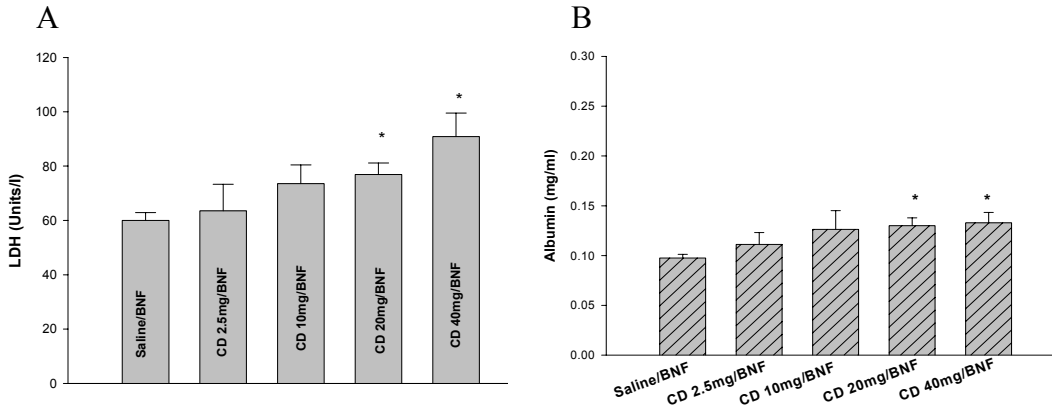

Figure 3. The effect of coal dust exposure on pulmonary cytotoxicity and vascular leakage in BNF-exposed rats. In A, CD exposure causes a dose-dependent increase in LDH that indicates pulmonary cytotoxicity (r^2=0.963, p=0.003). In B, CD increased BAL albumin in all CD-exposed rats that was statistically significant in rats exposed to 20mg and 40 mg/rat CD compared to control indicating pulmonary vascular damage. *Significantly different from control group at $P < 0.05$.

Effect of CD Exposure on Bax Expression in Lung Cells

By using single label immunofluorescence, Bax was mainly localized within cell cytoplasm (Figure 5). The area of Bax expression quantified by morphometric analysis was increased in a dose-dependent manner by CD exposure in rats (r^2= 0.6541, p<0.001). In addition, the average number of lung cells expressing Bax counted per field was increased in a dose-dependent fashion by the CD exposure (r^2= 0.903, p<0.001) (Figure 4).

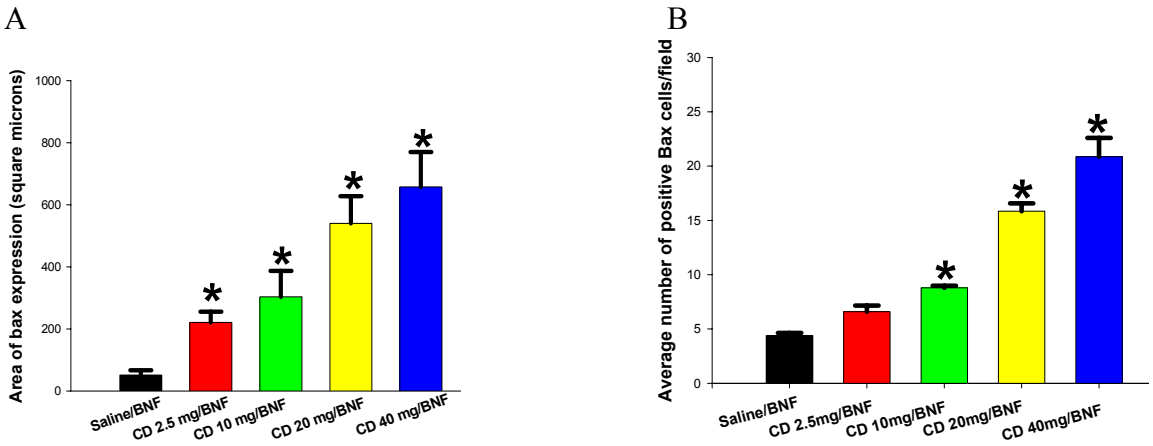

Figure 4. Bax expression is enhanced in a dose dependent manner by CD exposure in rats. In A, the area of Bax expression in lung cells measured in μm^2 is increasing in a dose responsive fashion by exposure to 2.5, 10, 20, and 40 mg/rat CD. Similarly, the number of positive cells for Bax is increased in a dose dependent manner by exposure to 2.5, 10, 20, and 40 mg/rat CD. * significantly different from saline/BNF at $p<0.05$.

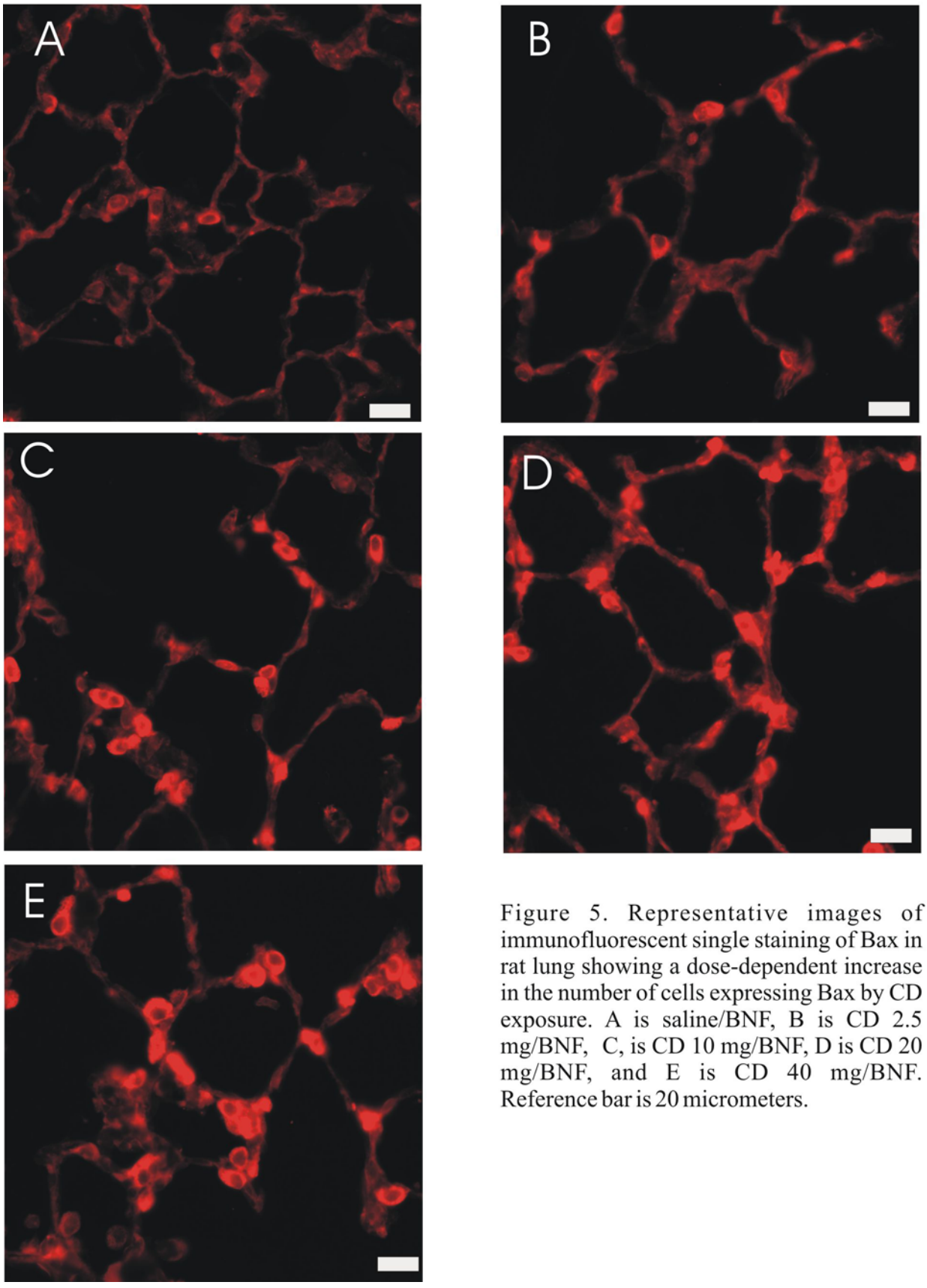

Figure 5. Representative images of immunofluorescent single staining of Bax in rat lung showing a dose-dependent increase in the number of cells expressing Bax by CD exposure. A is saline/BNF, B is CD 2.5 mg/BNF, C, is CD 10 mg/BNF, D is CD 20 mg/BNF, and E is CD 40 mg/BNF. Reference bar is 20 micrometers.

Relationship Between Bax Expression and CYP1A1 Induction

To investigate a relationship between Bax expression and the suppression of CYP1A1 induction mediated by CD exposure, tissue sections were labeled for Bax, CYP1A1 and cytokeratins 8/18 (AT-II markers) (immunofluorescence triple labeling). In this procedure, cells containing CYP1A1 fluoresce blue, cells containing Bax fluoresce red, and cells containing cytokeratins 8/18 fluoresce green (Figure 7). The proportional CYP1A1 expression within Bax area was calculated with the aid of morphometric analysis as described in the Materials and Methods. The proportional CYP1A1 expression within area of Bax expression was gradually reduced by increasing CD exposure (Figure 6A) suggesting that the probability that cells concomitantly expressed Bax and CYP1A1 decreased with CD exposure. In contrast, the proportional expression of Bax colocalized with cytokeratins 8/18 (AT-II cell markers) gradually increased by increasing the CD exposure (Figure 6B) suggesting that CD exposure increases Bax expression in AT-II cells. In addition, the percentage of AT-II cells that concomitantly expressed both Bax and CYP1A1 gradually decreased with increasing the CD exposure (Figure 6C) suggesting an inverse relationship between CYP1A1 induction and Bax expression in AT-II cells. In contrast, the percentage of AT-II cells expressing Bax only gradually increased with the CD exposure (Figure 6D)

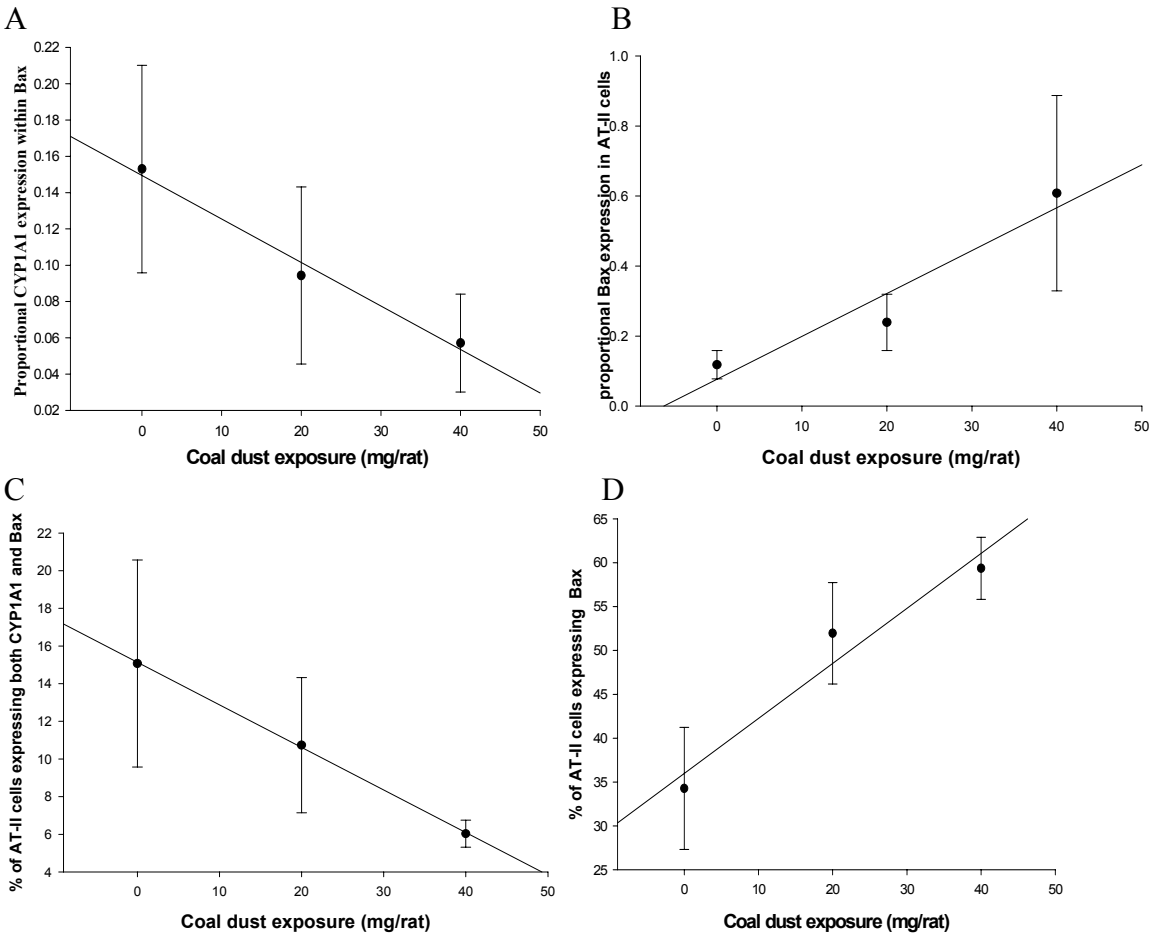

Figure 6. Graphical representation of morphometric analysis of tissue sections stained for CYP1A1, Bax, and cytokeratins 8/18 showing the relationship between CYP1A1 induction and Bax expression in AT-II cells. In A, the area of CYP1A1 colocalized with Bax in AT-II cells is reduced with CD exposure. In B, the area of Bax expression in AT-II cells is increased by the CD exposure. In C, the percentage of AT-II cells expressing both CYP1A1 and Bax is gradually decreased by CD exposure. In D, the percentage of AT-II cells expressing Bax alone is gradually increased by CD exposure.

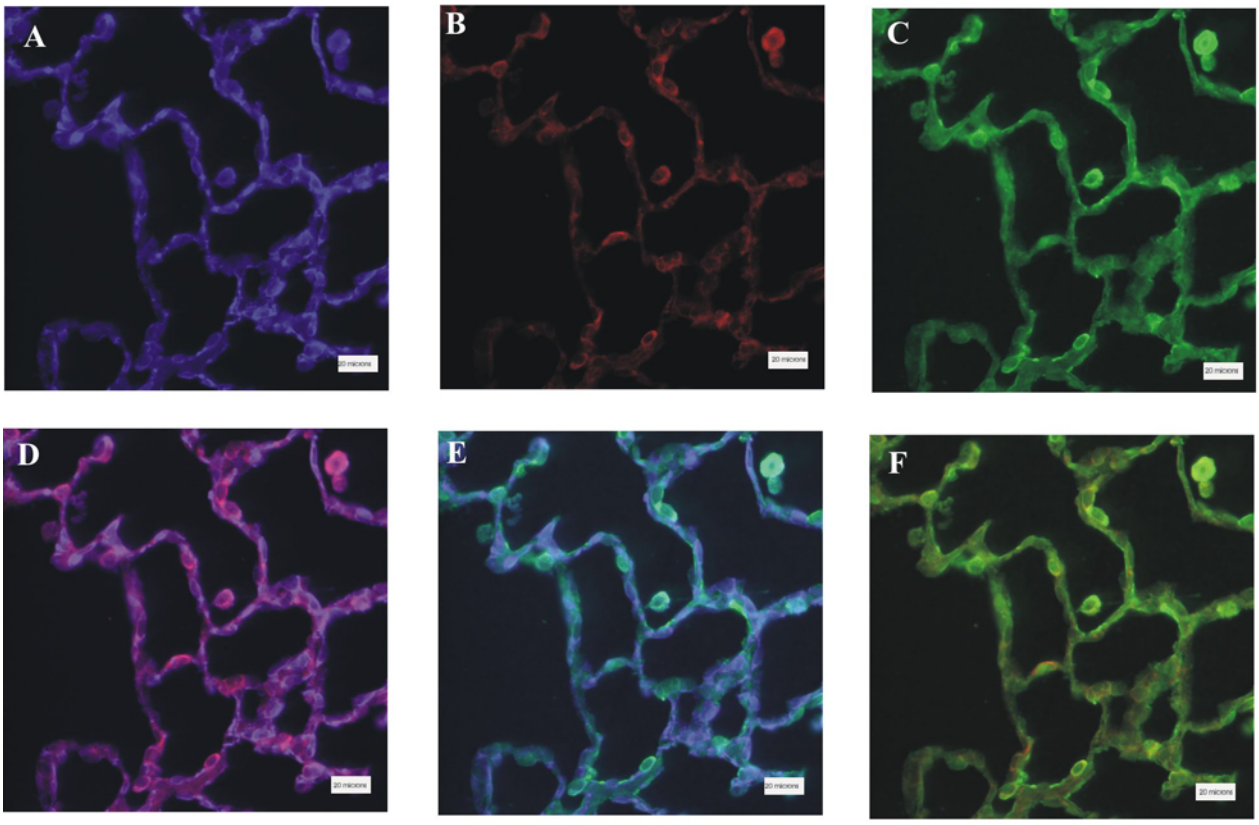

Figure 7. Immunofluorescence triple label for CYP1A1, Bax, and cytokeratins 8/18 of rats receiving BNF alone. CYP1A1 is blue (A), Bax is red (B), and cytokeratins 8/18 is green (C). D. Dual immunofluorescence for CYP1A1 (blue) and Bax (red) of the same section showing that Bax is localized to sites that do not express CYP1A1. In E, the CYP1A1 (blue) superimposes cytokeratins 8/18 (green) to help study expression of CYP1A1 in AT-II cells. In F, the Bax (red) superimposes cytokeratins 8/18 (green) to help study expression of Bax in AT-II cells. The three colors (blue, red, and green) are combined in one image (G) to investigate the relationship between CYP1A1 induction and Bax expression in AT-II cells. Reference bar is 20 micrometers.

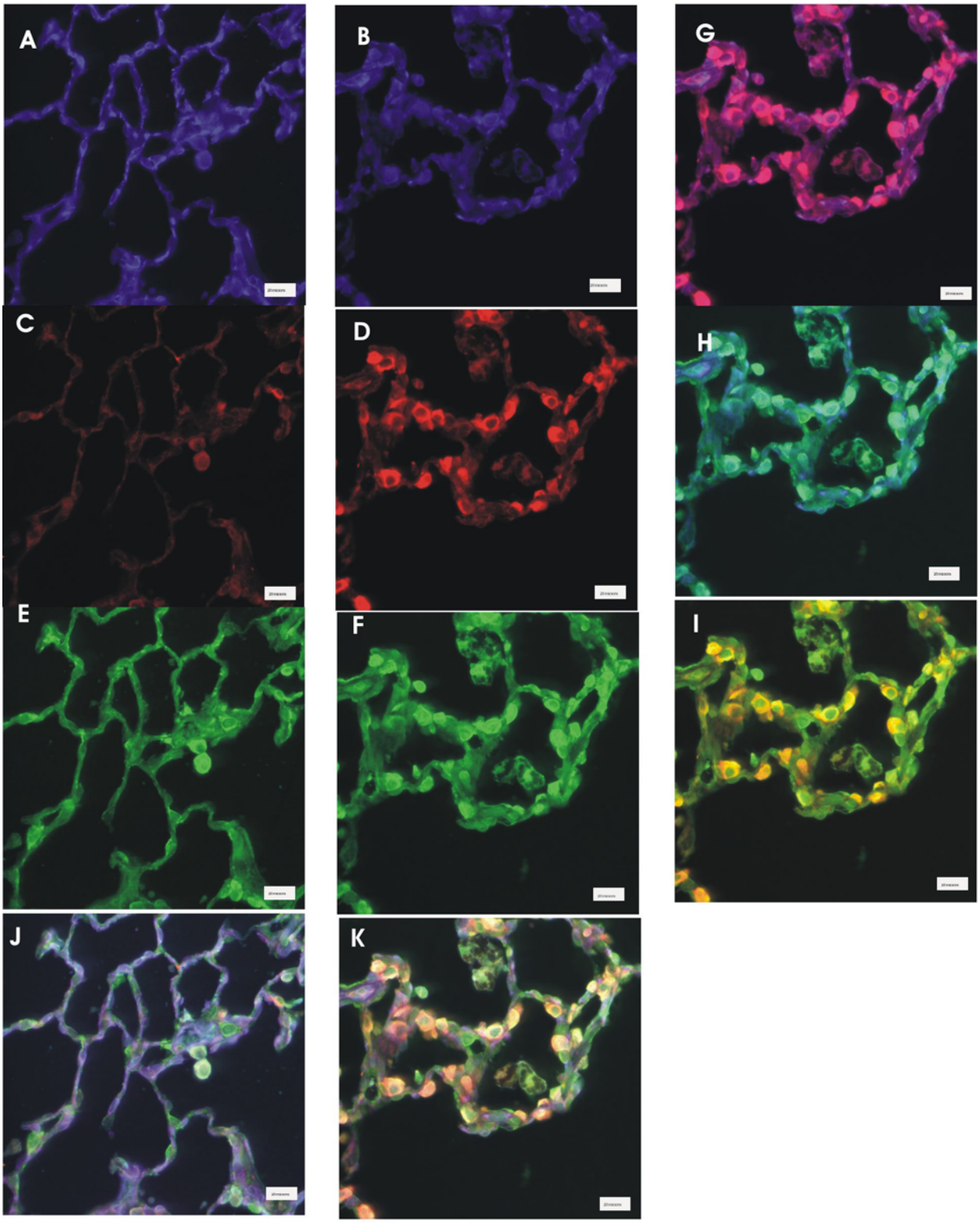

Figure 8. Triple label immunofluorescence (IF) showing the effect of CD on CYP1A1 and Bax expression in AT-II cells. A (blue CYP1A1), C (red Bax), E (green cytokeratins 8/18), and G (triple label) are images from control (BNF alone), while B, D, F, and H, I, J, and K are images from rat lungs exposed to 40 mg/kg CD with BNF. Cells expressing CYP1A1 are reduced in CD (B) relative to the control (A). Cells expressing Bax in CD-exposed rats (D) are increased relative to the control (C). Cells expressing cytokeratins 8/18 (AT-II cells) are increased in CD (F) relative to the control (E). G. dual IF for Bax (red) and CYP1A1 (blue) of the same section. Bax is expressed in sites that do not express CYP1A1. H. Dual IF for CYP1A1 and cytokeratins 8/18 of the same section showing that CYP1A1 is expressed in septal area that are not AT-II cells. I. Dual IF for Bax and cytokeratins 8/18 of the same section. Bax expression is frequently localized to AT-II cells, but not all AT-II cells express Bax. J and K are triple label IF.

Effect of Caspase Inhibitor, Q-VD-OPH on EROD

BNF-induced EROD activity was significantly reduced in CD-exposed rats but not affected by the caspase inhibitor, Q-VD-OPH (Figure 9).

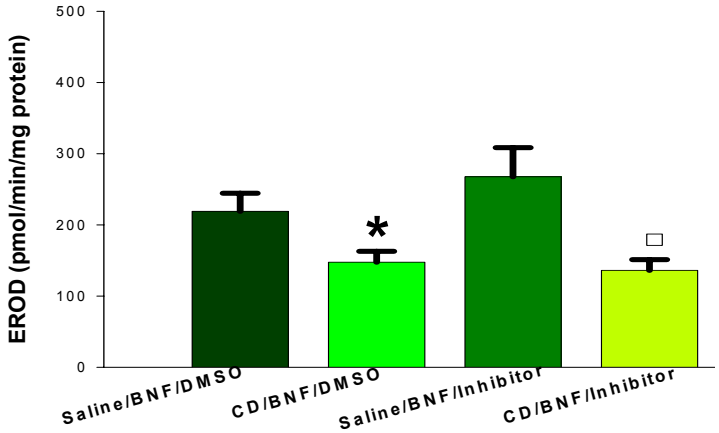

Figure 9. The pan-caspase inhibitor, Q-VD-OPH, did not alter the inhibition of EROD activity by CD exposure. No significant change is observed between rats receiving the inhibitor and those receiving the vehicle (DMSO). CD-exposed rats with DMSO have a significant reduction (P=0.03) of EROD activity compared to saline-exposed rats with DMSO. Also, CD-exposed rats with the Q-VD-OPH caspase inhibitor have a significant reduction (p=0.001) of EROD activity compared to saline-exposed rats with the inhibitor. * and □ mean significant difference at $p<0.05$ from rats unexposed to CD.

Effect of Caspase Inhibitor, Q-VD-OPH on PROD

CD significantly reduced PROD activity in BNF-treated rats and this effect persisted when caspases were inhibited by Q-VD-OPH. PROD activity in CD-instilled rats injected with Q-VD-OPH was not significantly different from CD-exposed rats injected with the vehicle (DMSO) (Figure 10).

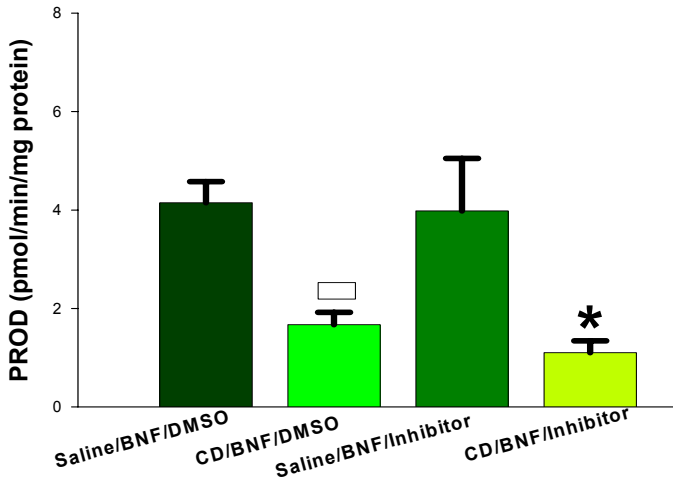

Figure 10. Effect of the caspase inhibitor, Q-VD-OPH on PROD activity. CD-exposed rats injected with the inhibitor are not significantly different from CD-exposed rats injected with vehicle (DMSO). PROD activity in rats exposed to CD and injected with DMSO is significantly ($p=0.003$) reduced compared to saline-exposed rats and injected with DMSO. PROD activity in rats exposed to CD and injected with the caspase inhibitor is significantly lower ($p=0.001$) than that in saline-exposed rats and injected with the inhibitor. ▭ and * significantly different from saline/BNF/DMSO and saline/BNF/Inhibitor at $p<0.05$, respectively.

Effect of Caspase inhibitor on CYP1A1 Induction by Western Blot

The CYP1A1 apoprotein measured by western blot analysis was not significantly changed in Q-VD-OPH-exposed rats. As observed in previous studies, CYP1A1 protein was significantly reduced in CD-exposed rats compared to BNF controls (Saline/BNF/DMSO). In rats injected with Q-VD-OPH, CD exposure reduced induction by BNF, albeit not significantly (Figure 11).

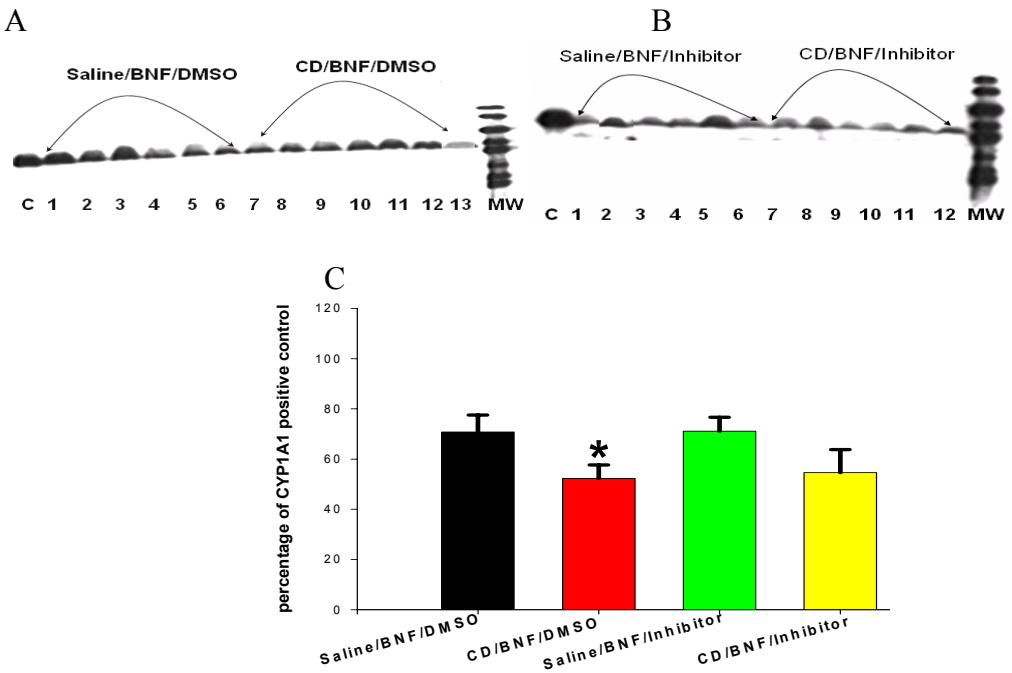

Figure 11. Western blot showing the effect of the Q-VD-OPH on CYP1A1 protein. The CYP1A1 protein is significantly reduced in CD-exposed rats with DMSO compared to saline-exposed rats with DMSO. The CYP1A1 protein is reduced (not significantly) in CD-exposed rats with Q-VD-OPH compared to saline-exposed rats with Q-VD-OPH. No significant change in CYP1A1 protein in CD-exposed rats with Q-VD-OPH vs. CD-exposed rats with DMSO. The designation of lanes is described above the blot. C is the positive control. MW is the molecular weight marker. * significantly different from saline/BNF/DMSO at $p<0.05$.

Effect of Caspase Inhibitor on CYP2B1 by Western Blot

The amount of CYP2B1 was not significantly affected by caspase inhibition with Q-VD-OPH. (Figure 12).

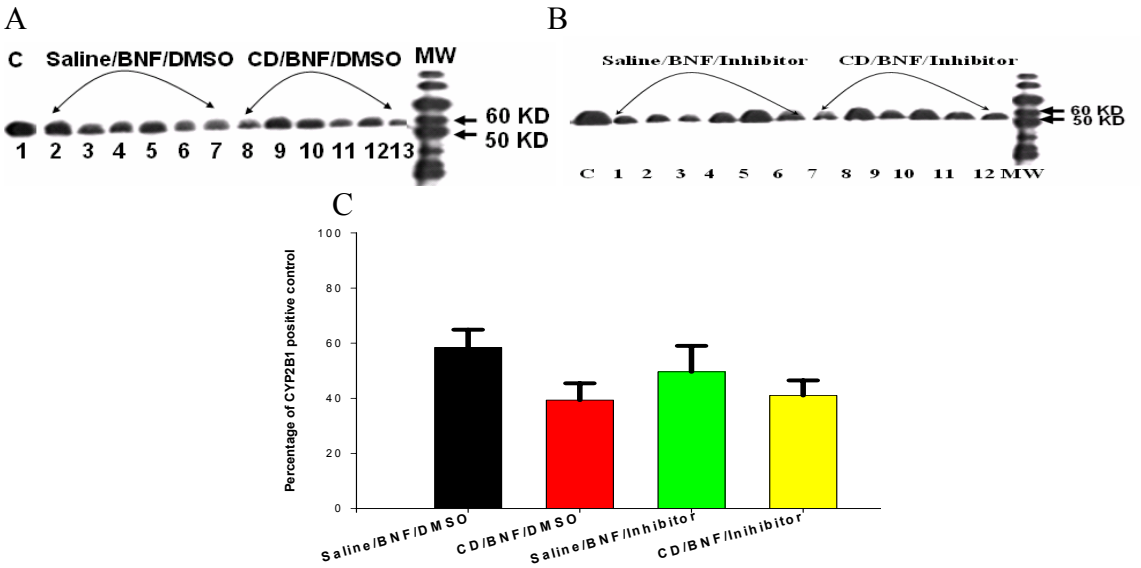

Figure 12. Western blot analysis of CYP2B1. In A, CD-exposed rats injected with DMSO have non significant reduction of CYP2B1 protein compared to saline-exposed rats injected with DMSO. In B, CD-exposed rats injected with caspase inhibitor have non significant reduction of CYP2B1 protein compared to saline-exposed rats injected with caspase inhibitor. No significant change is observed between CD-exposed rats injected with caspase inhibitor and CD-exposed rats injected with DMSO. C. Quantification graph of CYP2B1 protein in different treatment groups. The designation of lanes is described above the blot. C is the positive control. MW is the molecular weight marker.

Effect of Caspase Inhibitor on CYP1A1 Induction in PA regions by Immunofluorescence Double Labeling

By using the morphometric analysis of immunofluorescent double stained tissue sections for CYP1A1 and cytokeratins 8/18 (Figure 14), the areas of induced CYP1A1 expression were highly significantly reduced in NT-II cells ($p<0.001$), the entire alveolar septum ($p<0.001$), but not significantly reduced in AT-II cells by CD in BNF-exposed rats with DMSO compared with BNF exposed rats (Figure 13B, C, A). The proportional CYP1A1 expression in AT-II cells was significantly reduced (0.0028) by CD in BNF-exposed rats with DMSO relative to BNF-exposed rats (Figure 13D). Similar results were obtained when caspases were inhibited. In rats treated with both Q-VD-OPH and BNF, CD exposure reduced the area of CYP1A1 expression in NT-II cells, the entire alveolar septum as well as the proportional CYP1A1 expression in AT-II cells ($p<0.001$, $p<0.001$, $p<0.001$, respectively) (Figure 13B, C, and D, respectively), but not significantly reduced the area of CYP1A1 expression in AT-II cells (Figure 13A). However, the areas of CYP1A1 expression in AT-II cells, NT-II cells, and the entire

alveolar septum as well as the proportional CYP1A1 expression were not significantly changed in CD-exposed rats with inhibitor compared with CD-exposed rats with DMSO (Figure 13A, B, and C, respectively).

The injection of caspase inhibitor did not produce significant changes in AT-II cell hyperplasia and hypertrophy in CD-exposed rats (data not shown).

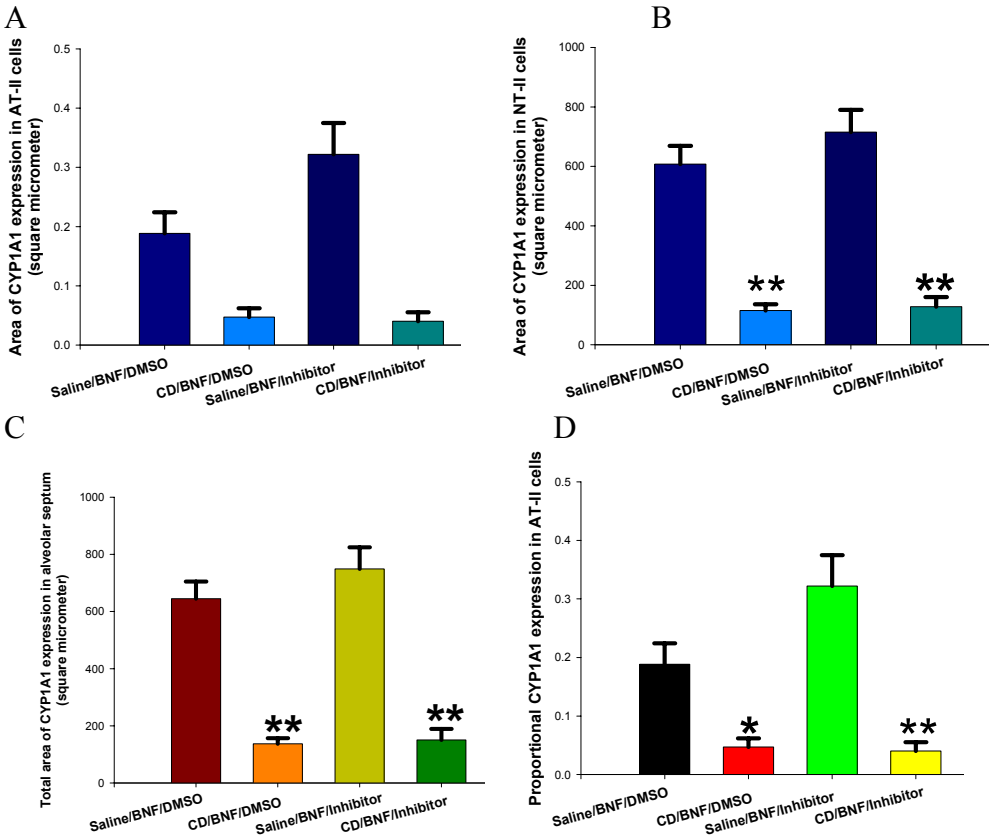

Figure 13. Morphometric analysis of dual immunofluorescence for BNF-induced CYP1A1, and cytokeratins 8/18 in the PA regions of rats receiving either the caspase inhibitor, Q-VD-OPH or the vehicle (DMSO) and IT CD or vehicle (saline). In **A**, the area of CYP1A1 expression in AT-II cells is not significantly decreased in rats receiving CD (CD/BNF/DMSO or CD/BNF/Inhibitor) and not significantly affected by caspase inhibition (Saline/BNF/Inhibitor or CD/BNF/Inhibitor). In **B**, the area of CYP1A1 expression in NT-II cells is highly significantly decreased in rats receiving CD (CD/BNF/DMSO or CD/BNF/Inhibitor) and not significantly affected by caspase inhibition (Saline/BNF/Inhibitor or CD/BNF/Inhibitor). In **C**, the area of CYP1A1 expression in the entire alveolar septum is highly significantly decreased in rats receiving CD (CD/BNF/DMSO or CD/BNF/Inhibitor) and not significantly affected by caspase inhibition (Saline/BNF/Inhibitor or CD/BNF/Inhibitor). In **D**, the proportional CYP1A1 expression in *AT-II* cells is highly significantly or significantly decreased in rats receiving CD (CD/BNF/DMSO or CD/BNF/Inhibitor, respectively) and not significantly affected by caspase inhibition (Saline/BNF/Inhibitor or CD/BNF/Inhibitor). ** indicate highly significant change at $p<0.001$. * indicates significant difference at $p<0.001$.

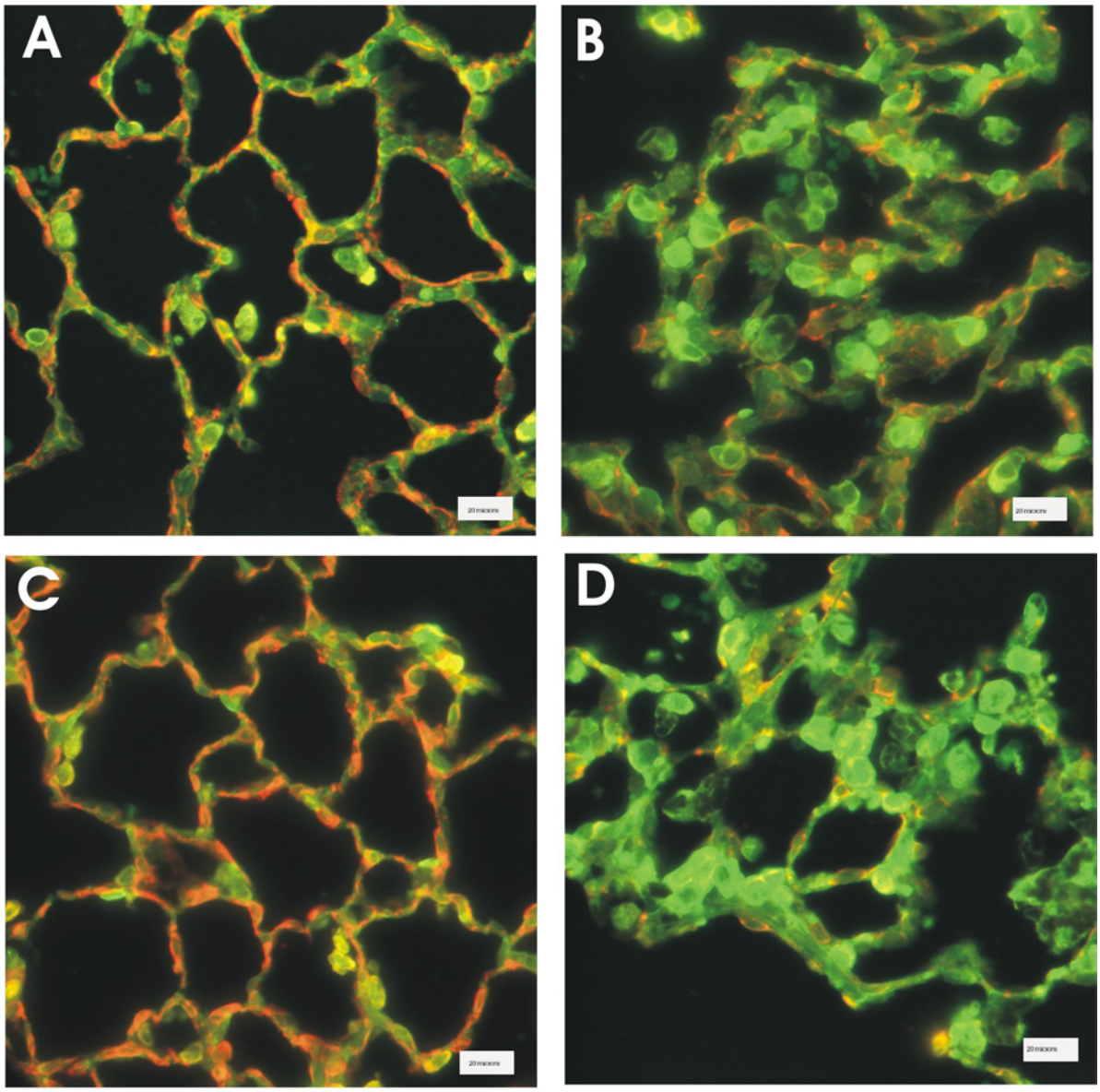

Figure 14. Double label Immunofluorescence images for CYP1A1 and cytokeratins 8/18 of rat lung. The CYP1A1 protein, indicated by red fluorescence, was reduced in NT-II cells, and in the entire alveolar septum and was proportionally reduced in AT-II cells of the CD/BNF/DMSO group (B) compared to control (saline/DNF/DMSO) group (A). Also, the CYP1A1 protein decreased in NT-II cells, and in the entire alveolar septum and was proportionally reduced in AT-II cells of CD/BNF/inhibitor group (D) compared to control (saline/BNF/inhibitor) group (C). No change in the CYP1A1 expression was detected between CD/BNF/DMSO group (B) and CD/BNF/inhibitor group (D). AT-II hyperplasia and hypertrophy (indicated by the green color of cytokeratins8/18 marker) is present in both CD/BNF/DMSO group (B) and CD/BNF/inhibitor group (D) and absent in saline/DNF/DMSO and saline/BNF/inhibitor. Reference bar is 20 micrometers.

Effect of the Caspase Inhibitor on Bax Expression in PA regions

Single label immunofluorescence for Bax (Figure 16) showed that the injection of the caspase inhibitor, Q-VD-OPH in CD-exposed rats highly significantly reduced the area of Bax expression ($p<0.001$) (Figure 15 A) and significantly decreased the number of cells expressing Bax ($p=0.001$) (Figure 15B) compared to CD-exposed rats injected with the vehicle (DMSO). However, the CD exposed rats injected with caspase inhibitor had a significant increase in the Bax area and highly significant increase in number of cells expressing Bax ($p=0.005$, $p< 0.001$, respectively) compared to saline-exposed rats injected with the inhibitor, suggesting that caspase inhibitor reduced Bax expression but not to the level of control values. These results were also confirmed by immunofluorescence-triple labeling for Bax, CYP1A1, and cytokeratins 8/18 (data not shown).

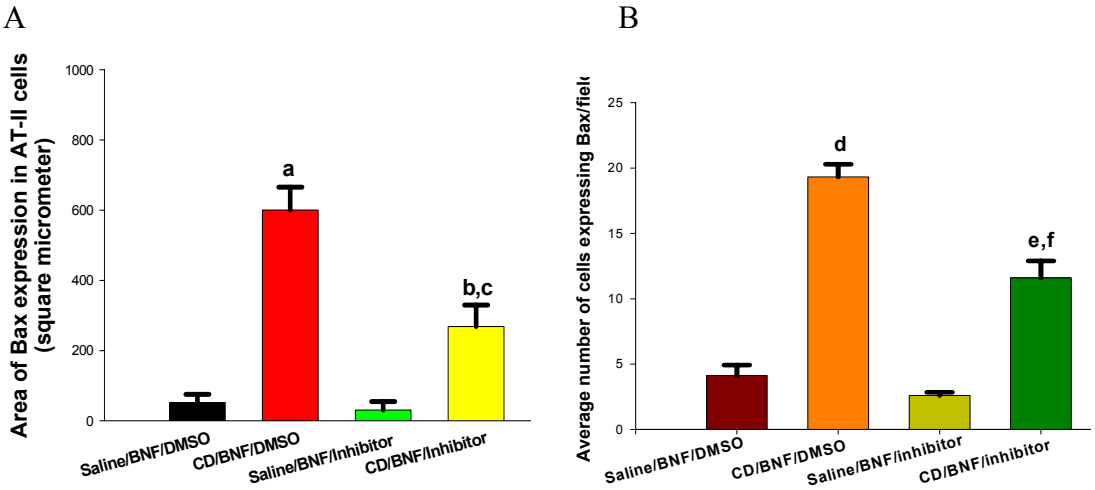

Figure 15. Morphometric analysis of single-labeled immunofluorescence for Bax in the PA region of BNF-treated rats after IT exposure to CD or saline with and without caspase inhibition with Q-VD-OPH. In **A**, the letter a above the bar indicates highly significant increase in the area of Bax expression in CD/BNF/DMSO group relative to saline/BNF/DMSO group. Bax expressed as area (μm^2) is highly significantly reduced by the caspase inhibitor (letter b above the bar), but still significantly increased relative to Saline/BNF/inhibitor group (letter c above the bar). In **B**, the letter d above the bar indicates highly significant increase in the number of cells expressing Bax CD/BNF/DMSO group compared to saline/BNF/DMSO group. The number of cells expressing Bax is significantly lower in CD/BNF/inhibitor group relative to CD/BNF/DMSO group (letter e above the bar), but highly significantly higher than Saline/BNF/inhibitor group (letter f above the bar). Letters a, b, d, and f indicate highly significant difference at $P<0.001$. Letters c and e indicate significant difference at $P<0.05$.

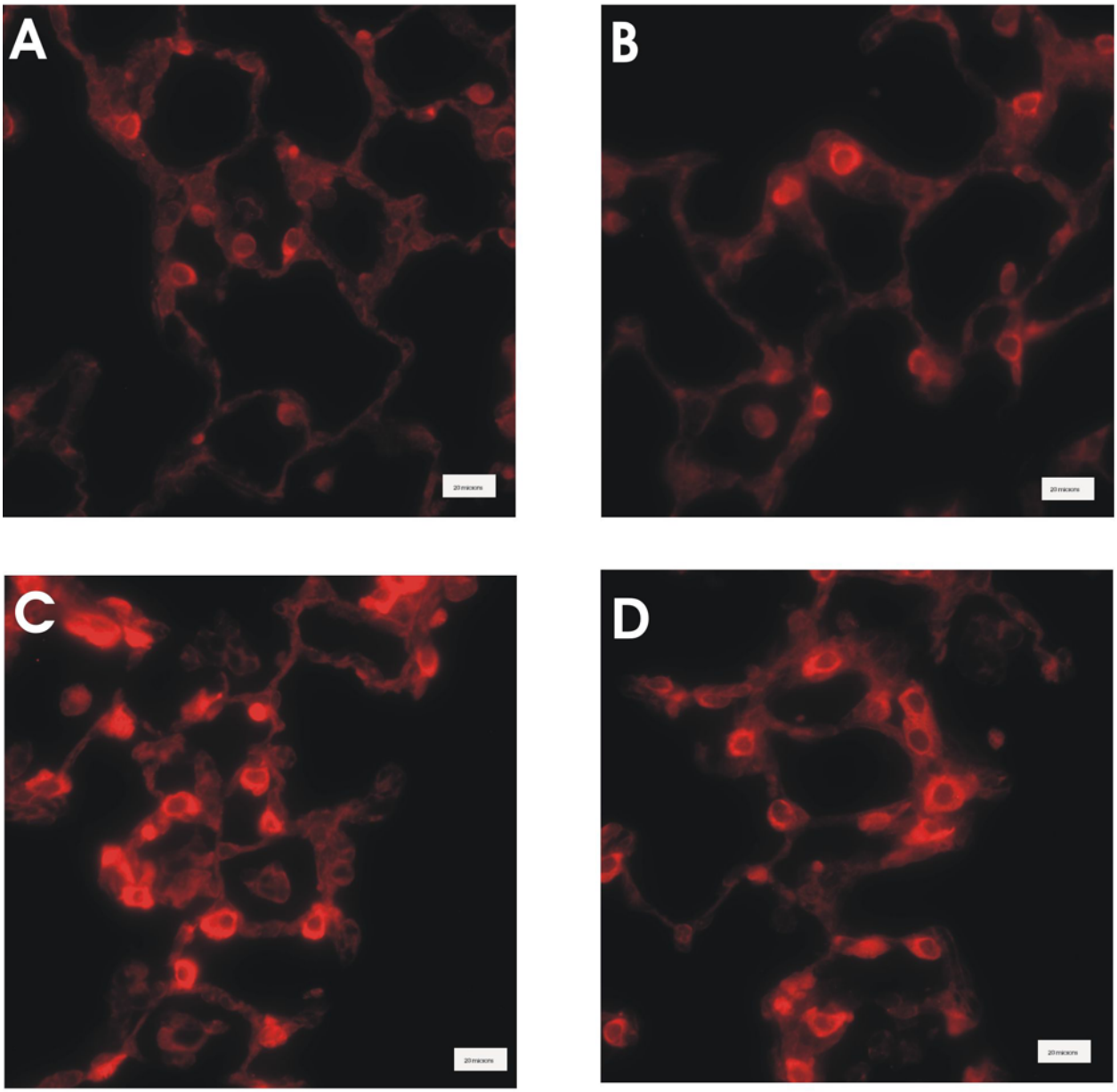

Figure 16. Images of immunofluorescent staining for Bax showing suppression of Bax expression in lung cells of the PA region by the caspase inhibitor, Q-VD-OPH. A) Alveolar region of a rat receiving saline/BNF/DMSO. B) Alveolar region of a rat receiving saline/BNF/caspase inhibitor. C) Alveolar region of a rat receiving CD/BNF/DMSO. D) Alveolar region of a rat receiving CD/BNF/caspase inhibitor. The number of positive cells and the intensity of Bax staining (red color) was reduced in CD-exposed rats injected with the caspase inhibitor (D) compared to the CD-exposed rats injected with the vehicle (DMSO) (C) but still significantly higher than the saline-exposed rats with caspase inhibitor (B) or DMSO (A). Reference bar is 20 micrometers.

Effect of the Caspase Inhibitor on CD-Induced Apoptosis.

In the TUNEL assay, the apoptotic cells were identified by their green fluorescence, while the non-apoptotic nuclei were identified by their red color (Figure 18). The percentage of apoptotic cells was highly significantly increased ($P<0.001$) in CD-exposed rats in the absence of caspase inhibition with Q-VD-OPH. In addition, the percentage of apoptotic cells was significantly increased ($P<0.048$) in CD-exposed rats injected with caspase inhibitor compared to saline-exposed rats injected with caspase inhibitor. In the CD-exposed rats, injection of caspase inhibitor significantly decreased the percentage of apoptotic cells ($p=0.013$) (Figure 17).

Comparison of the percentage of apoptotic cells in PA regions vs. RA regions revealed a significant increase in the PA regions compared to the RA regions in all groups including Saline/BNF/DMSO, CD/BNF/DMSO, Saline/BNF/inhibitor, and CD/BNF/Inhibitor with $p<0.013$, <0.001, 0.025, and <0.001, respectively (Figure 17).

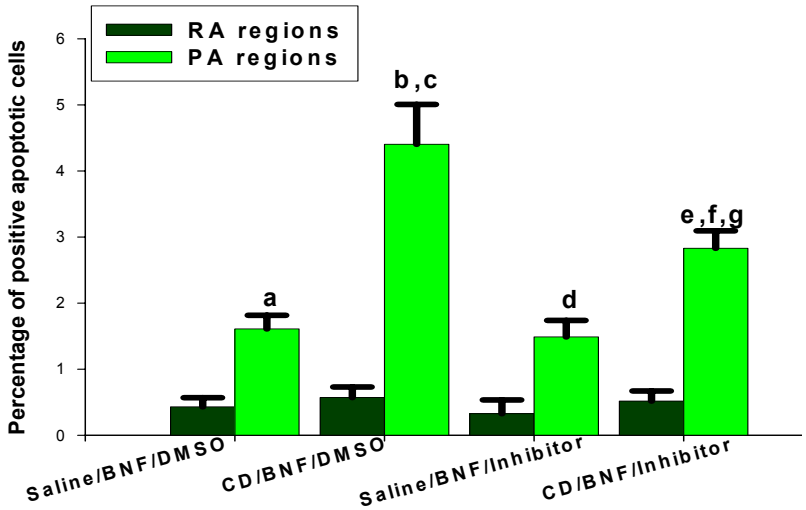

Figure 17. TUNEL assay results showing the percentage of apoptotic cells in BNF-treated rats after IT exposure to CD or saline with and without Q-VD-OPH caspase inhibitor. The percentage of apoptotic cells is highly significantly increased in rats with CD/BNF/DMSO compared rats with saline/BNF/DMSO (letter b above the bar). Rats with CD/BNF/inhibitor have a significant lower percentage of apoptotic cells than rats with CD/BNF/DMSO (letter f above the bar). Caspase inhibition does not entirely abrogate the CD-induced apoptosis and the apoptotic cell percentage in rats with CD/BNF/inhibitor is significantly higher that in rats with saline/BNF/inhibitor (letter e above the bar). The percentage of apoptotic cells in the PA region is significantly higher than that in the RA regions of all groups (letters a, c, d, and g above the bars). Letters a, d and e, and f indicate significant difference at $p<0.05$. Letters b, c, and g indicate highly significant difference at $p<0.001$.

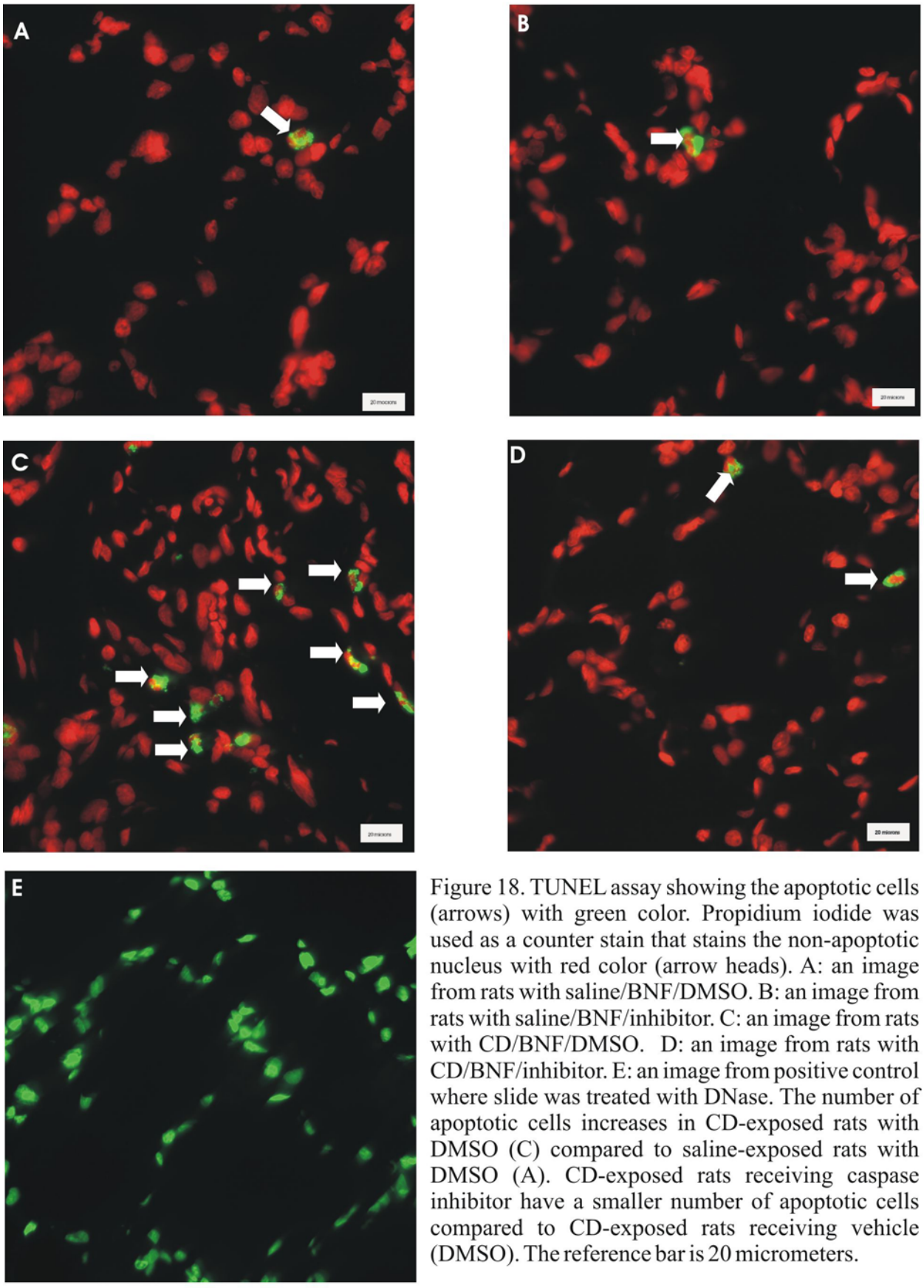

Figure 18. TUNEL assay showing the apoptotic cells (arrows) with green color. Propidium iodide was used as a counter stain that stains the non-apoptotic nucleus with red color (arrow heads). A: an image from rats with saline/BNF/DMSO. B: an image from rats with saline/BNF/inhibitor. C: an image from rats with CD/BNF/DMSO. D: an image from rats with CD/BNF/inhibitor. E: an image from positive control where slide was treated with DNase. The number of apoptotic cells increases in CD-exposed rats with DMSO (C) compared to saline-exposed rats with DMSO (A). CD-exposed rats receiving caspase inhibitor have a smaller number of apoptotic cells compared to CD-exposed rats receiving vehicle (DMSO). The reference bar is 20 micrometers.

Histopathological Changes

Histopathological alteration associated with CD exposure included histiocytic and suppurative alveolitis with accumulation of dark brown particles within the cytoplasm of many alveolar macrophages. No significant difference was observed in CD-exposed rats injected with the caspase inhibitor compared to those injected with vehicle (Figure 19) by scoring the severity and distribution of these changes. AT-II hyperplasia and hypertrophy was demonstrated in CD-exposed rats (Figure 20). No histopathological changes were observed in rats exposed to BNF or BNF and the caspase inhibitor, Q-VD-OPH

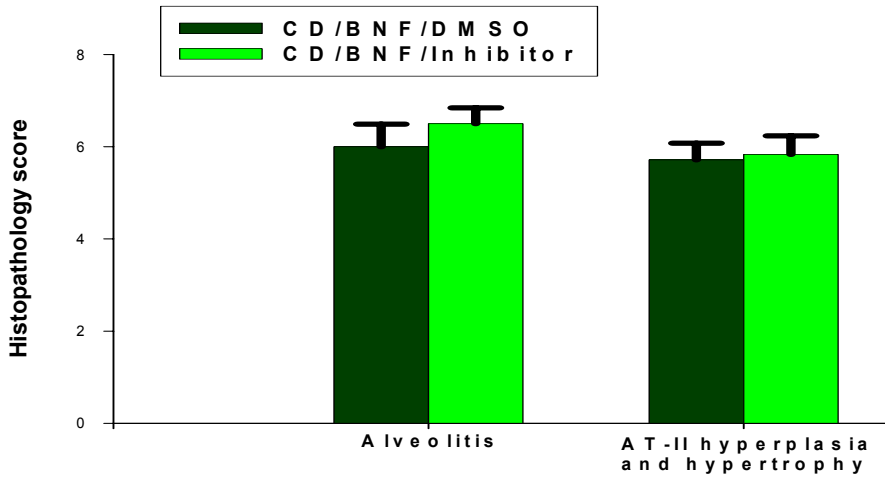

Figure 19. Histopathological score of the severity and distribution of alveolitis and AT-II hyperplasia in CD-exposed rats injected with caspase inhibitor or DMSO. No significant change is noted between rats with CD/BNF/DMSO and rats with CD/BNF/Inhibitor.

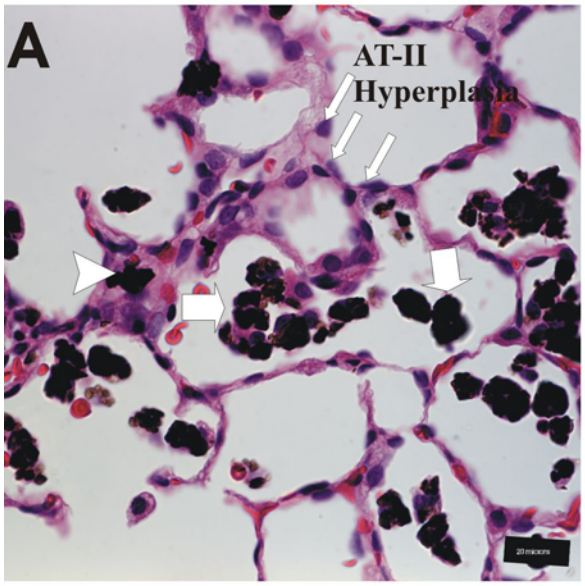

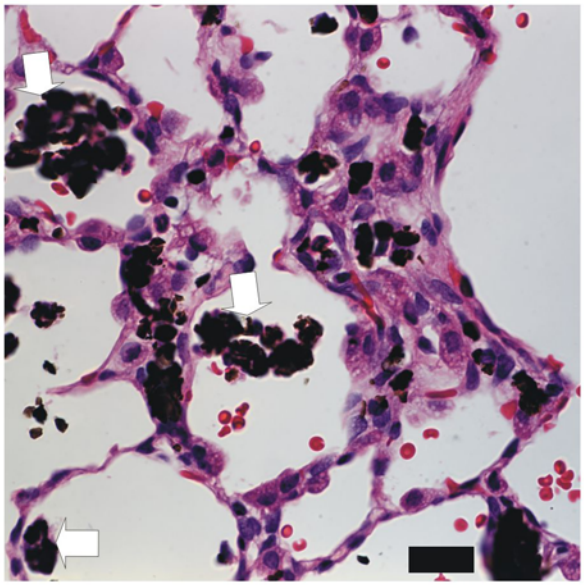

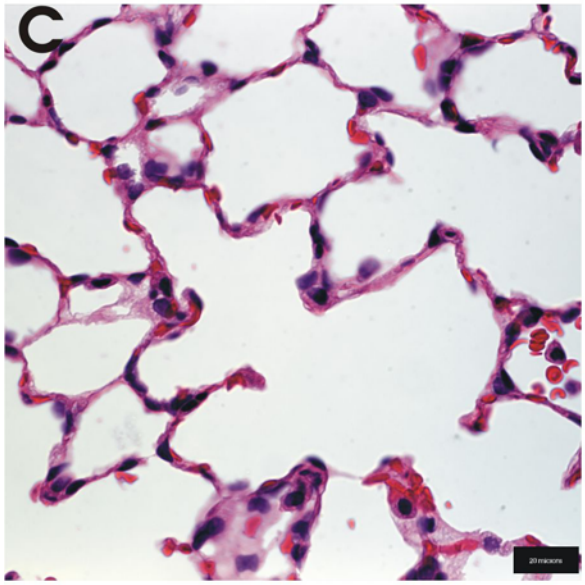

Figure 20. Photomicrographs showing the histopathological alterations of CD exposure and their persistence after caspase inhibition. The alveolitis is principally histiocytic and characterized by accumulation of dust-laden macrophages in the alveolar lumen (arrows) and interstitial tissue (arrow heads). AT-II hyperplasia and hypertrophy are also demonstrated. These changes are present in CD-exposed rats without (A) and with (B) caspase inhibitor. C. photomicrograph from saline-instilled rats showing no histopathological changes. Reference bar is 20 micrometers.

DISCUSSION

In this study, the pathogenesis of suppression of CYP1A1 induction in rat lung by coal dust exposure was investigated. Because alteration of pulmonary xenobiotic metabolism is an interplay with the inflammation (Ma and Ma, 2002), the inflammatory reaction to CD exposure was assessed by examining the BALF. We demonstrated that CD exposure enhanced the pulmonary inflammatory reaction in a dose-responsive fashion. This inflammatory reaction was illustrated by a significant increase of the AM and a dose-dependent recruitment of PMN in the BALF (Figure 1). The inflammatory reaction to CD instillation was previously investigated by Blackford and coworkers (Blackford *et al*, 1997) who demonstrated that CD had a less inflammatory effect than silica but a more potent effect than carbonyl iron and titanium oxide in inducing pulmonary inflammation. Activation of AM by CD exposure was also statistically significant in the highest dose (40mg/rat) as shown by measuring the AM CL (Figure 2A).

BAL Fluid Analysis: AM

Alveolar macrophages are free lung cells located on the surface of the small airways and the alveoli (Weibel, 1973). These cells act as the lung's first line of defense against the toxic effects of inhaled particles, as they play a major role in the protection of lung against these particles. The reaction of alveolar macrophages to the inhaled particles is complex. Upon contact with the particles, AM release superoxide anion (Sweeney *et al*, 1981), which can be monitored by the measurement of chemiluminescence (Miles *et al*, 1978; Castranova *et al*, 1980). Eventually, AM engulf these foreign particles and attempt to digest them by releasing lysosomal enzymes into phagocytic vacuoles (Myrvik and Evan, 1967). By histopathological examination of CD-exposed rats, dust-laden AM were localized in the alveolar spaces and interstitial tissue as a dark brown pigment (Figure 20).

BAL Fluid Analysis: LDH

LDH is an intracellular enzyme; therefore, its presence in the acellular BALF indicates cytotoxicity (Porter *et al*, 2002). The elevation of LDH, in a dose-dependent fashion, with CD exposure (Figure 3A) suggests that the reduction of CYP1A1

expression in alveolar septa could partly be attributed to cellular injury and cytotoxicity caused by CD exposure. Dinsdale and co-workers (Dinsdale and Verschoyle, 2001) showed a reduction of CYP2B1 expression and protein activity in rat lung following selective destruction of alveolar type I cells by pneumotoxic and nonpneumotoxic trialkylphosphrothiolate. In addition, the significant release of albumin in CD-exposed rats (Figure 3B) indicates damage of the blood-pulmonary barrier. Damage of the endothelial cells of alveolar septum by CD exposure could contribute to the total reduction of the CYP1A1 induction, since these cells are considered as NT-II cells that express CYP1A1 (Pairon *et al*, 1994).

BAL Fluid Analysis: Nitric Oxide

Nitric oxide is a short lived inter- and intracellular messenger produced by a family of enzymes known as nitric oxide synthases (NOSs) and brings about a number of bioregulatory functions (Kim and Sheen, 2002). The inducible nitric oxide synthase (iNOS) gene expression and NO production by BAL cells can be measured indirectly as NO-dependent chemiluminescence (John *et al*., 1997). The NO-dependent AM CL was significantly increased in rats exposed to 40 mg/rat CD with BNF compared to control, which suggests that CD induces nitric oxide synthesis by alveolar macrophages. This result is consistent with those reported by Blackford *et al* (1997) who concluded that coal mine dust is among the various dusts that induce iNOS by the recruited PMN into the alveolar spaces. In addition, Bingham *et al*, 1977, reported that *in vivo* exposure of rats to coal dust results in an increase in mRNA for the inducible form of nitric oxide synthase and elevated nitric oxide production by pulmonary phagocytes. The significant reduction of EROD activity and CYP1A1 protein (as shown by western blot) in rats exposed to 40mg/kg CD with BNF with enhancement of the NO-dependent AM CL of the same group suggests a possible relationship between nitric oxide and CYP1A1 expression and activity. Since NO reacts with hemeproteins, CYP1A1, being a heme-containing protein may represent a target of NO within the cells (Wink *et al*., 1993). Therefore, a number of studies have investigated the effect of NO on CYP450s. Nitric oxide binds to the heme moiety of the P450s forming an iron-nitrosyl complex in rat hepatic cells in a reversible phase, subsequently preventing the binding of oxygen which normally occurs in the course of catalytic sites and suppresses CYP1A1 functional activity (Wink *et al*, 1993).

The same study also showed irreversible inhibition of CYP1A1 and CYP2B1 activity due to destruction of the integrity of the primary structure of hemeprotein, resulting from the action of nitrogen oxides produced from the oxidation of nitric oxide by oxygen. Not only does nitric oxide inhibit CYP1A1 activity, but *in vitro* studies on Hepa I cells (Kim and Sheen, 2002) suggest that nitric oxide also down-regulates the CYP1A1 expression by inhibition of CYP1A1 promoter activity.

Bax Expression and CD exposure: Effect of the Caspase Inhibitor

Our results showed that Bax expression was increased in a dose dependent manner by CD exposure (Figures 4 and 5). In single label immunofluorescence, the Bax staining was mainly localized in the cytoplasm of cuboidal cells, suggestive to be AT-II cells. In triple label immunofluorescence, the proportional Bax expression in AT-II cells as well as the percentage of AT-II cells expressing Bax were gradually increased by increasing the exposure to CD particles (Figure 6B and 6D, respectively), suggesting that Bax was upregulated in the hyperplastic AT-II cells. These findings were consistent with those of Guinee *et al* (1997) who demonstrated that Bax expression was increased in diffused alveolar damage and was confined to hyperplastic AT-II cells. The proportional CYP1A1 expression localized in the area of Bax as well as the percentage of cells expressing both Bax and CYP1A1 were decreased by CD exposure (Figures 6A and 6C, respectively). Thus, by increasing the dose of CD exposure, the Bax expression was increased, but the CYP1A1 expression was reduced, suggesting an inverse relationship between the expression of both proteins.

Bax is a pre-apoptotic protein related to BCL-2 family (Oltvai *et al*, 1993) that predisposes cells to apoptosis (Narasimhan *et al*, 1998). We initially hypothesized that the overexpression of Bax in lung cells increased the apoptosis of these cells and was etiologically associated with the depression of CYP1A1 induction observed in CD. To investigate this relationship, we used the newly developed pan caspase inhibitor, Q-VD-OPD, which is known to inhibit caspases 1, 3, 8, and 9 to block the apoptotic pathway. Apoptosis of lung cells, assessed by TUNEL assay, showed that CD significantly increased the percentage of apoptotic cells (Figures 17 and 18) and rats injected with the caspase inhibitor had a significantly lower percentage of apoptotic cells. This finding indicated that Q-VD-OPH suppressed caspase-dependent apoptosis in pulmonary cells.

This result coincided with that obtained by Caserta *et al*, (2003) who demonstrated the effectiveness of the Q-VD-OPH in blocking three different pathways of apoptosis; caspase 9/3, caspase 8/10, and caspase 12. Although the caspase inhibitor significantly reduced the apoptosis, the percentage of apoptotic cells remained significantly elevated by IT CD exposure, suggesting that the caspase inhibitor did not completely inhibit the apoptotic pathway. In addition, the caspase inhibitor significantly suppressed the Bax expression in lung cells, but the area of Bax expression was significantly higher than the control saline, suggesting that the caspase inhibitor down-regulated but did not prevent all Bax expression in alveolar cells.

Although Bax expression and apoptosis in pulmonary cells were significantly suppressed by Q-VD-OPH, the BNF-induced CYP1A1-dependent EROD activity, CYP2B1-dependent PROD activity, the CYP1A1 and 2B1 proteins measured by Western blot, and the CYP1A1 measured by immunofluorescence, were not significantly affected. These findings suggested that the CD-associated suppression of CYP1A1 was not caused by cellular apoptosis and Bax expression. Moreover, it seemed that Bax expression was a feature of hyperplastic alveolar cells and the association of Bax with CYP1A1 expression was a simple association.

Effect of Caspase inhibitor, Q-VD-OPH on Pulmonary Inflammation

Histopathological alterations, such as alveolitis and AT-II hyperplasia and hypertrophy were not significantly different between CD-exposed rats injected with the caspase inhibitor and the CD-exposed rats injected with DMSO. This result suggested that the caspase inhibitor did not suppress the inflammatory process associated with CD exposure. Other pan caspase inhibitors, such as N-benzyloxy-carbonyl-Val-Ala-Asp- (*O*-methyl)-fluoromethyl ketone (zVAD-fmk) and BO*C*-Asp-(*O*-methyl)-fluoromethyl ketone (BOC-Asp-fmk) were reported to reduce the neutrophil accumulation in the lungs of silicotic mice by 50 % (Borges *et al*, 2002). However in our study, the principally histiocytic inflammatory reaction in the lungs of CD-exposed rats was not significantly suppressed by the injection of Q-VD-OPH. While previous studies have used Q-VD-OPH mostly in mice (Borges *et al*, 2002; Melnikov *et al*, 2002), our study clearly demonstrated inhibition of both Bax and apoptosis, but not pulmonary morphologic changes induced by CD. In addition, inhibition of Bax expression and apoptosis by caspase inhibition did not

significantly affect downregulation of CYP1A1 induction associated with CD. This suggested that neither caspase pathways, Bax, nor apoptosis was the cause of inhibition of CYP1A1 induction in alveolar cells.

Studies from a number of laboratories, principally investigating the liver or using *in vitro* systems, have noted an association between inflammation or inflammatory mediators and decreased activity of CYP isoforms including CYP1A, CYP2A, CYP2B, CYP2D9, CYP3A, CYP2E1 and CYP4A (Warren *et al*, 1999; Siewert *et al*, 2000; Jover *et al*, 2002; Carcillo *et al*, 2003). Recent studies suggest that diesel exhaust particles and carbon black downregulate CYP2B1 in the rat lung (Rengasamy *et al*, 2003). Consistent with these findings, we have found that respirable coal dust exposure also downregulated CYP2B1 in the rat lung. In addition, the induction of CYP1A1 was downregulated by respirable coal dust exposure in the rat lung. In our studies, the downregulation of CYP2B1 and induced CYP1A1 was positively associated with the severity of inflammation.

Previous studies suggest that during inflammation, some mediators and transcription factors, such as tumor necrosis factor alpha (TNF-α), interleukin 6, nitric oxide and the nuclear factor kappa B (NF-κB) are upregulated and turned on (Ke *et al*, 2001; Baldwin, 1996; Hubbard *et al*, 2002; Jover *et al*, 2002) and suppress CYP1A1. A physical association between the RelA subunit of the NF-κB and the AhR has been demonstrated *in vitro* by immunoprecipitation (Tian *et al*, 1999) producing an inactive complex that prevents the AhR from binding to the enhancer sequences of CYP1A1 (Ke *et al*, 2001). Moreover, NF-κB has been demonstrated to inhibit the ligand-induced acetylation of histone H4 at the *CYP1A*1 promoter area, especially around the TATA box region, thus preventing the AhR/Arnt heterodimer from binding to the XRE at the DNA resulting in downregulation of the *CYP1A1* expression (Tian *et al*, 2002). TNF-α suppresses the activity of RNA polymerase II, resulting in interference with the *CYP1A1* elongation in Hepa1c1c7 cells (Tian *et al*, 2003). TNF-α also enhances the FasL-mediated apoptosis in T lymphocytes (Bonetti *et al*, 2003), which occurs upstream of Bax activation. Another inflammatory mediator released during pulmonary inflammation is nitric oxide (Fubini and Hubbard, 2003). Nitric oxide demonstrated a high binding

affinity to the heme moiety of the P450s forming an iron-nitrosyl complex in rat hepatic cells suppressing the CYP1A1 metabolic activity (Wink *et al*, 1993). Nitric oxide is also associated with induction of apoptosis in IC-21 macrophage cell line, which was inhibited by the nitric oxide synthase inhibitor (Siewert *et al*, 2000). However, Sutherland *et al* (2001) concluded that the macrophage-derived nitric oxide provides an antiapoptotic mechanism that protects AT-II cells from undergoing apoptosis and enhancing the lung injury. NF-κB seems to play an important role in protection against apoptosis (Ravi *et al*, 2001) because the $RelA^{-/-}$ mouse fibroblasts are highly sensitive to TRAIL [(Tumor necrosis factor (TNF)-related apoptosis-inducing ligand)]-induced apoptosis. In addition, TRAIL-induced apoptosis of human hepatoma cells by interferon alpha is associated with NF-κB inactivation (Shigeno *et al*, 2003). However, other studies showed that, activation of NF-κB is correlated with the ability of p53 to induce apoptosis in tumor cells (Ryan *et al*, 2000). Based upon these studies, Chen *et al* (2003) concluded that opposite functions of NF-κB are dependent upon the expression of its subunits, where c-Rel and RelA function as proapoptotic and antiapoptotic proteins, respectively. Consequently, the NF-κB may contribute to or inhibit the apoptotic response in different conditions (Ryan *et al*, 2000). However, inflammation-associated suppression of hepatic CYP1A activity *in vivo* appears to be TNF-α independent but IL-6 dependent. CYP1A downregulation occurs in p55/p75 knockout mice that lack TNF-α receptors (Warren *et al*, 1999) but does not occur in interleukin-6 knockout mice (Siewert *et al*, 2000).

Our studies extend these findings to associate the *in vivo* downregulation of pulmonary CYP2B1 and induced CYP1A1 with inflammation that results from respirable coal dust exposure. In addition, we have found that the downregulation of pulmonary CYP2B1 and induced CYP1A1 appear inversely related to, but not caused by, Bax expression in the cytosol. Because we found that caspase inhibition had no effect on downregulation of CYP2B1 or induced CYP1A1 by respirable particle exposure, a possible explanation for these findings would be an event or signaling cascade producing both Bax activation and the CYP downregulation. These would include nitric oxide, NF-κB and/or initiators of alveolar epithelial proliferation. It is also possible that Bax expression and CYP downregulation are independent events which are both observed in response to respirable particle exposures. Additional studies will be needed to fully

elucidate how CYP2B1 activity and CYP1A1 induction are inhibited in the particle-exposed lung.

In conclusion, CD exposure enhanced the inflammatory processes of rat lung in a dose-dependent manner by increasing the recruitment of AM and PMN. In addition, CD caused significant cytotoxicity of lung cells and damage of the blood-pulmonary barrier as demonstrated by elevation of LDH and albumin levels, respectively. CD also enhanced the Bax expression and induced apoptosis in lung cells, changes that were inversely associated with suppression of CYP1A1 induction by CD exposure.

CHAPTER 7
GENERAL DISCUSSION

Cytochrome P450s (CYPs) generate continued interest because these enzymes play critical roles in the metabolism of drugs, carcinogens, dietary xenobiotics and steroid hormones (James and Whitlock 1999). The CYP proteins are heme-containing proteins, which are members of a gene super-family involving almost 1000 members in species ranging from bacteria to plants and animals (Hasler *et al*, 1999). Cytochrome P4501A1 (CYP1A1) has garnered particular interest because of its association with cancer. CYP1A1 is involved in the conversion of organic compounds, like polycyclic aromatic hydrocarbons (PAH) in cigarette smoke, into carcinogenic intermediates (Crepsi *et al*, 1989; Shimada *et al*, 1989; Eaton *et al*, 1995) that can bind to DNA producing adducts and initiate lung cancer. Moreover, the expression of CYP1A1 can be induced at the transcriptional level by its substrates. The transcriptional regulation of the *CYP1A1* gene by PAH is mediated through ligand-dependent activation of the aryl hydrocarbon receptor (AhR). Upon activation by binding of specific substrates, AhR translocates to the nucleus and dimerizes to the aryl hydrocarbon receptor nuclear translocator (Arnt) protein. This heterodimer binds to the xenobiotic responsive element (XRE) in the regulatory region of the *CYP1A1* gene inducing expression (Ma and Whitlock 1997; Tian *et al*, 1999). It has been demonstrated that high inducibility of CYP1A1 is considered to be a risk factor for lung cancer in tobacco smokers (Anttila *et al*, 2001; Ishibe *et al*, 2001). Since smokers are exposed to carcinogenic PAH, their CYP1A1 expression is induced (Willey *et al*, 1997). Therefore, modification of the induced CYP1A1 is of great importance in smoking populations.

Coal is a fossil fuel mined all over the world. Coal mine dust generated during underground coal mining results in significant respiratory exposure to coal miners. In addition to the carbon, which is the main component of coal, it also contains oxygen, nitrogen, hydrogen, and trace elements, including non-coal minerals. The trace element may include copper, nickel, cadmium, boron, antimony iron, lead, and zinc (Sorenson *et al* 1974). Some of these trace elements can be cytotoxic and carcinogenic in experimental models (Castranova, 2000). Mineral contaminants include quartz, kaolin, mica, pyrite and calcite (Parkes, 1994). Coal dust inhalation is associated with

development of a respiratory disease in coal miners called coal workers' pneumoconiosis (CWP). CWP is categorized according to severity into simple and complicated CWP. In the simple form, black dust macules appear and consist of dust-laden macrophages concentrated near respiratory bronchioles. In complicated CWP, also described as progressive massive fibrosis (PMF), the nodules are larger (> 1 cm diameter) and more numerous. These nodules contain increased amounts of collagen, coal dust, and inflammatory cells (Castranova, 2000). Silicosis is another occupational lung disease resulting from exposure to the crystalline form of the mineral silicon dioxide or silica (Driscoll and Guthrie, 1997). Silicosis is characterized by inflammation and fibrosis in the lower respiratory tract.

Recently, crystalline silica, but not coal dust, has been classified as a class I carcinogen by the International agency for Research on Cancer (IARC, 1997). However, epidemiological data demonstrate that lung cancer in coal miners occurs less frequently than in the general population after adjustment for age and smoking (Meijers *et al*, 1991 and Kuempel, 1995). In addition, lung cancer risk in coal miners exposed to silica and PAH was absent or even less than those exposed to silica alone (Cocco *et al*, 2001). Evaluating the lung cancer risk in coal miners is complex because these people are usually exposed to a mixture of environmental contaminants, including the particulate matter and the PAH in cigarette smoke. In this study, we investigated the hypothesis that pulmonary CYP1A1 induction is inhibited by exposure to respirable particles. We also investigated whether or not alterations in lung cell populations are associated with suppression of CYP1A1 induction.

Using the rat model alone to investigate these hypotheses was not satisfactory because of the existing debate concerning the species differences between rats and humans regarding their response to inhaled particles (Mauderly, 1997). Moreover, the pattern of particle retention as well as the lung tissue response to respirable particles in rats may not be predictive of those of primates who are exposed to poorly soluble particles, particularly at high occupational exposures (Nikula *et al*, 1997). For these reasons, we used rabbit and sheep, in addition to rats, to investigate our hypotheses. Generally, in any model, the respirable particulate suspension was intratracheally instilled by the aid of feeding needle in rats, endotracheal tube and laryngoscope in rabbits, and

flexible fiberoptic bronchoscope in sheep. In sheep, the right apical lobes were instilled while the left apical lobes were collected as internal controls. Then the CYP1A1 was induced in these animals by IP injection of the model PAH, beta-nephthoflavone.

In general, our results consistently showed that the CYP1A1-dependent EROD activity, measured by spectrophotometric assay was significantly lower in BNF-induced animals instilled with particles than control animals (receiving BNF alone). The suppression of activity was associated with reduction of CYP1A1 protein measured by Western blot. At the cellular level, the amount of CYP1A1 expression quantified by immunofluorescence was reduced in AT-II cells, NT-II cells, and the entire alveolar septum upon CD and silica exposure. Because particles tend to accumulate in different areas of the lung (Nikula *et al*, 1997), the CYP1A1 expression was compared in areas with maximal deposition to areas with minimal deposition. The area with maximum deposition was localized in the proximal alveolar regions, near microscopically visible alveolar ducts. For comparison, we also selected areas without visible alveolar ducts that were designated as random alveolar (RA) regions as internal controls. We found significant reduction of CYP1A1 expression in AT-II cells, NT-II cells and whole alveolar septum in the PA regions relative to RA region. This result suggests that the cell-type specific suppression is localized to areas where the particles aggregate. In addition, PROD activity, an indicator of the major constitutive pulmonary CYP which is not inducible in lung (CYP2B1, CYB2B4, and CYP2B in rats, rabbits, and sheep, respectively) was consistently lower in BNF-exposed animals instilled with particles than the controls.

In our study, the exposure to particles, either CD or silica, produced AT-II hyperplasia and hypertrophy. However, the expression of CYPA1 in the hyperplastic and hypertrophied AT-II cells was markedly reduced. A number of studies showed that P450 activities and the level of P450 apoproteins decreased after partial hepatectomy and regeneration of hepatic cells (Hino *et al*, 1974, Presta *et al*, 1980, Klinger and Karge, 1987, and Ronis *et al*, 1992). It was suggested that replication, but not transcription is the prioritized activity of DNA to regenerate the cells (Liddle *et al*, 1989, Waxman, 1989, Morgan *et al*, 1985, and Steer, 1995). In our studies, AT-II cells may behave similarly in regenerating other damaged epithelial cells instead of transcripting genes. Consistent with

that are the higher levels of CYP2B1 protein expression and mRNA in freshly isolated alveolar type II cells, but this level is diminished in cell culture (Lag *et al*, 1996). Moreover, the inducibility of CYP1A decreases slightly in the rat liver bearing hyperplastic nodules (Degawa *et al*, 1995). Consistent with that, the inducibility of CYP1A1 by BNF was markedly reduced in early lung hyperplastic foci associated with urethane exposure and the lung carcinomas were devoid of CYP1A1 protein expression (Forkert *et al*, 1998). All of these previous studies suggest that CYP protein is downregulated in proliferating cells - - a finding which is consistent with the downregulation of CYP1A1 induction and CYP2B in our study of CD-exposed rats and lambs.

In rats, CD exposure enhanced the inflammatory reaction in a dose dependent fashion by recruiting AM and PMN to the alveolar spaces as demonstrated by BAL fluid examination. Cytotoxicity and damage of the pulmonary blood barrier were also associated with CD exposure. Alveolitis and accumulation of dust-laden AM in the alveolar spaces and interstitial tissue were major findings in histopathological examination of CD-exposed sections. These findings were consistent with those described by Nikula *et al* (1997). Kuempel *et al* (2003) also demonstrated dose-response relationships between respirable crystalline silica in BAL collected from coal miners and pulmonary inflammation. AMs become activated after phagocytosis of CD particles and release a wide range of mediators including oxidants, cytokines, growth factors, and proteases that result in cellular damage or hyperplasia of epithelial cells, such as AT-II cells (Schins and Borm, 1999). *In vitro* exposure of AMs to CD particles elicited a significant release of TNF-α and interleukin-6, compared to titanium dioxide that was used as a biologically inert control dust (Vanhee *et al*, 1995). In addition, many other mediators such as IL-1, IL-6, TGF-β_1, and TGF-β_2, and fibronectin are elevated in the BALF of miners with radiographically defined CWP (Vallyathan *et al*, 2000). Our results of BALF analysis of rat lung are consistent with the previous studies and support the hypothesis that CD triggers inflammatory reactions and changes in cell populations in the deep lung in rats.

In sheep, the histopathological changes were comparable to those of rats, although relatively modest. Changes were bronchointerstitial pneumonia with accumulation of dust-laden alveolar macrophages, mainly in the interstitial tissue with only occasional foci of alveolar histiocytosis- - a finding that is consistent with a lavaged lung.

In rabbit silicosis, pulmonary inflammation varied from histiocytic and suppurative to necrogranulomatous bronchointerstitial pneumonia with thickening of the alveolar walls. Alveolar lipoproteinosis was a common finding in silica-exposed rabbit alveoli. In some rabbit lungs with silicosis, silicotic nodules were demonstrated. Consistent with that, previous studies on rats showed that the pulmonary reaction to the inhalation of crystalline silica resulted in lung damage, inflammation, and hypertrophy and hyperplasia of AT-II cells (Miller *et al*, 1986; Miller *et al*, 1990; Castranova *et al*, 2002).

The association of inflammation with the suppression of cytochrome P450 has previously been demonstrated *in vitro* and *in vivo* in several model systems. The acute inflammatory reaction caused by subcutaneous injection of bacterial lipopolysaccharide (LPS) (Morgan, 1989), turpentine (Kobusch *et al*, 1986), and viral and bacterial infection (El-Kadi and Du Souich, 1998) depressed the constitutive hepatic P450 expression. In addition, exposure of cultured hepatocytes to inflammatory stimuli decreases total microsomal cytochrome P450, P450-catalyzed enzyme activities, and levels of P450 proteins and mRNAs (Morgan, 1997). A number of proinflammatory mediators may play a role in *CYP1A1* downregulation during inflammation. For example, TNF-α interferes with *CYP1A1* elongation during the transcription process by inactivating the RNA polymerase II (Tian *et al*, 2003). In addition, nuclear factor kappa B (NF-κB) interacts with AhR and thus interfered with AhR-mediated CYP1A1 induction (Ke *et al*, 2001). NF-κB also inhibited the ligand-induced acetylation of histone H4 at the promoter region of *CYP1A1* gene and consequently prevented CYP1A1 induction in Hepa1c1c7 cells (Ke *et al*, 2001). Interleukin-6 (IL-6) also depressed multiple hepatic P450 isoforms such as CYP1A1, 1A2, 3A4, and 4A1, and IL-1β downregulates 1A2, 2C11, 2D6, 2E1, and 3A (Fukuda *et al*, 1992; Trautwein *et al*, 1992, Donato *et al*, 1997, Parmentier *et al*, 1997). In our study, using an *in vivo* rat model, we demonstrated that CD exposure elicited

pulmonary inflammation in a dose-responsive manner and suppressed the CYP1A1-dependent EROD activity in a dose dependent manner, suggesting an inverse relationship between CYP1A1 induction and activity, and pulmonary inflammation.

Our data illustrated that CD exposure enhanced the expression of Bax in a dose dependent manner suggesting that CYP1A1 suppression of induction was associated with upregulation of Bax expression, particularly in hyperplastic AT-II cells. Since Bax is a pre-apoptotic protein related to BCL-2 family (Oltvai *et al*, 1993) that predisposes cells to apoptosis (Narasimhan *et al*, 1998), we investigated whether the suppression of Bax expression and cellular apoptosis could ameliorate the suppression of CYP1A1 induction by CD exposure. Therefore, the pan-caspase inhibitor, Q-VD-OPH was administered IP to inhibit the Bax expression and the caspase-dependent apoptotic cascade. Our data showed that although Bax expression and CD-induced apoptosis of pulmonary cells were suppressed by the caspase inhibitor, the CD-mediated suppression of CYP2B1 expression and CYP1A1 induction was not significantly affected. This suggested that the suppression of these CYP isoforms appears to be inversely related to, but not caused by, Bax upregulation and apoptosis induction. One possible explanation for this result is that an event or signaling pathway initiated by one or more of the inflammatory mediators, which such as nitric oxide or NF-κB, produced both Bax expression and CYP downregulation. Alternatively, the Bax upregulation and CYP downregulation were independent events observed in particle-exposed lung.

.

CONCLUSIONS

The present study investigated the suppression of CYP1A1 induction by exposure to particles and its association with morphological changes in cell populations in the particle-exposed lung. To overcome the limitation of using rats alone as a model for human, rabbits and sheep were also utilized to explore our hypothesis. Our results demonstrated that:

1- CYP1A1 induction was suppressed by pulmonary exposure to CD and silica.

2- CYP1A1-dependent EROD activity was inhibited in a dose dependent-manner by CD exposure in rats and was significantly suppressed by silica exposure in rabbits and CD exposure in sheep.

3- PROD activity was suppressed in rabbit silicosis and rat and sheep CWP models, respectively. PROD activity is dependent upon the major constitutive CYP isoform of the lung which are CYP2B1 and its analogs, CYP2B4 and CYP2B in rats, rabbits, and sheep, respectively.

4- CD or silica exposure reduced CYP1A1 expression at sites of alveolar damage with reduced expression in alveolar epithelial cells, including AT-II cells and NT-II cells.

5- Silica and CD increased the size (hypertrophy) and number (hyperplasia) of AT-II cells and reduced CYP1A1 expression in these cells.

6- CD particles induced dose-dependent pulmonary inflammation, manifested by recruitment of alveolar macrophages and polymorphonuclear leucocytes.

7- CD particles upregulated the preapoptotic Bax protein expression in alveolar epithelial cells and triggered apoptosis.

8- Inhibition of cellular apoptosis and Bax expression by the caspase inhibitor, Q-VD-OPH, did not affect CYP1A1 induction and its suppression by CD exposure

These findings support the hypothesis that CYP1A1 induction and its metabolic activity (EROD) are inhibited by particle exposure and associated with pulmonary inflammation.

FUTURE STUDIES

1-Investigating the effect of the nitric oxide produced during particle-associated inflammatory processes on CYP1A1 induction by using nitric oxide synthase knockout mice.

2-Investigating the effect of NF-κB and TNF-α on CYP1A1 induction by using antisense olignucleotides techniques.

3- Localization of CYP1A1 expression in different alveolar non-type II cells by using makers of alveolar type I cells, endothelial cells, and alveolar macrophages.

BIBLIOGRAPHY

- Abbot B. D., Held, G. A., Wood, C. R., Buckalew, A. R., Brown, J. G., and Schmid, J. (1999) AhR, Arnt, and CYP1A1 mRNA quantitation in cultured human embryonic palates exposed to TCDD and comparison with mouse palate in vivo and in culture. Toxicological sciences 47:62-75.
- Aiba-Masago, S., Liu, Xb. XB., Masago, R., Vela-Roch, N., Jimenez, F., Lau, C. M., Frohlich, V. C., Talal, N., and Dang, H. (2002). Bax gene expression alters Ca(2+) signal transduction without affecting apoptosis in an epithelial cell line. Oncogene 21(17):2762-7.
- Aida, S., Takahashi, Y., Suzuki, E., Kimula, Y., Ito, Y., and Miura, T. (1992). Electronmicroscopic evidence for cytochrome P-450 in Clara cells and type I pneumocytes of the rat lung. Respiration 59:201-210.
- Albrecht, C., Adolf, B., Weishaupt, C., Hohr, D., Zeittrager, I., Friemann, J., Borm, P. J. (2001). Clara-cell hyperplasia after quartz and coal-dust instillation in rat lung. Inhal. Toxicol. 13(3):191-205
- Albrecht, C., Borm, P. J., Adolf, B., Timblin, C. R., and Mossman, B. T. (2002). In vitro and in vivo activation of extracellular signal–regulated kinases by coal dusts and quartz silica. Toxicol. Appl. Pharmacol. 184(1):37-45.
- Alexandrov, K., Cascorbi, I., Rojas, M., Bouvier, G., Kriek, E., Bartsch, H. (2002). CYP1A1 and GSTM1 genotypes affect benzo[a]pyrene DNA adducts in smokers' lung: comparison with aromatic/hydrophobic adduct formation. Carcinogenesis 23(12):1969-77.
- Allen, R. C. (1977). Evaluation of serum opsonic capacity by quantitating the initial chemiluminescent response from phagocytizing polymorphonuclear leukocytes. Infection and Immunity 15:828-833.
- Amadis, Z. and Timilar, T (1978). Studies on the effect of quartz, bentonite, and coal dust mixture on macrophage in vitro. British Journal of Experimental Pathology 59:411-419.
- Anttila, S., Hietanen, E., Vainio, H., Camus, A-M., Gelboin, H. V., Park, S. S., Heikkila, L., Karjalainen, A., Bartsch, H. (1991). Smoking and peripheral type of cancer are related to high levels of pulmonary cytochrome P450IA in lung cancer patients. International Journal of Cancer 47:681-685.
- Anttila, S., Tuominen, P., Hirvonen, A., Nurminen, M., Karjalainen, A., Hankinson, O., and Elovaara, E. (2001). CYP1A1 levels in lung tissue of tobacco smokers and polymorphisms of CYP1A1 and aromatic hydrocarbon receptor. Pharmacogenetics. 11(6):501-9.
- Arif, J. M., Khan, S. G., Mahmood, N., Aslam, M., and Rahman, Q. (1994). Effect of coexposure to asbestos and kerosene soot on pulmonary drug-metabolizing enzyme system. Environ Health Perspect. 102 Suppl 5:181-3.

- Archakov, A. I., Zgoda, V. G., and Karuzina, II (1998). Oxidative modification of cytochrome P450 and other macromolecules during its turnover. Voprosy Meditsinskoi Khimii 44: 3-27.
- Axelrod, J. (1955). The enzymatic demethylation of ephidrine. Journal of Pharmacology 114:430-8.
- Baba, T., Mimura, J., Gradin, K., Asato Kuroiwa, A., Watanabe, T., Matsuda, Y., Inazawa, J., Sogawa, K., and Fujii•Kuriyama, Y. (2001). Structure and expression of the Ah receptor repressor gene. J. Biol. Chem., 276 (35): 33101-33110.
- Bae, Y. S., Kang, S. W., Seo, M. S., Baines, I. C., Tekle, E., Chock, P. B. and Rhee, S. G. (1997). Epidermal growth factor (EGF)-induced generation of hydrogen peroxide: Role in EGF receptor-mediated tyrosine phosphorylation. J Biol. Chem. 272: 217-221.
- Baer, A. N. and Green, F. A. (1989). Cytochrome P-450 mediated-metabolism in active murine systemic Lupus erythematous. Journal of Rheumatology 16:335-338.
- Baldwin, A. S. (1996). The NF B and I B proteins: new discoveries and insights. Annu. Rev. Immunol. 14:649–681.
- Banks, D. E., Morring, K. L., Boehlecke, B. A., et al. (1981). Silicosis in silica flour workers. Am. Rev. Respir. Dis. 124:445-45.
- Baron, J., and Kawabata, T. T. (1983). Intratissue distribution of activating and detoxicating enzymes. In biological basis of detoxication. (Caldmwell J. and Jakoby, W. B., Eds), pp. 105-135. Academic Press, New York.
- Bardales, R. H., Xie, S. S., Schaefer, R. F., Hsu, S. M. (1996). Apoptosis is a major pathway responsible for the resolution of type II pneumocytes in, acute lung injury. Am. J. Pathol. 149:845-852.
- Barker, C. W., Fagan, J. B., and Pasco, D. S. (1992). Interleukin-1β suppresses the induction of P4501A1 and P4501A2 mRNA in isolated hepatocytes. J. Biol. Chem. 267(12): 8050-8055.
- Baron, J., and Kawabata, T. T. (1983). Intratissue distribution of activating and detoxicating enzymes. In biological basis of detoxication. (Caldmwell J. and Jakoby, W. B., Eds), pp. 105-135. Academic Press, New York.
- Baron, J., and Voigt, J. M. (1990). Localization, distribution, and induction of xenobiotic-metabolizing enzymes and aryl hydrocarbon hydroxylase activity within lung. Pharmncol. Ther. 47:419-445.
- Baserga, R. (1085). The Biology of Cell reproduction. Harvard University Press, Cambridge, MA.
- Battelli, L. A., Hubbs, A. F. Ma, J. Y., Kashon, M. L., and Castranova, V. (2001) Quantifying cellular expression of cytochrome P-4501A1 (CYP1A1) in the pulmonary alveolus: A comparison of indirect enzymatic immunohistochemistry

(IH) and indirect immunofluorescence (IF). Toxicological sciences 60(1):403 (abstract).

- Battelli, L. A., Hubbs, A. F., Simoskevitz, R. D., Vallyathan, V., Bowman, L., and Miles, P.R. (1999). Cytochrome P450 1A1 and 2B1 in rat lung: exposure to silica and inducers of xenobiotic metabolism. Toxicological Sciences, 48: 97 (abstract).
- Beck, F. J., and Whitehouse, M. W. (1974). Impaired drug metabolism in rats associated with acute inflammation: a possible assay for anti-injury agents. Proceedings of the Society for Experimental Biology and Medicine 145:135-140.
- Begin, R., Dufresne, A., Cantin, A., Possmayer, F., Sebastien, P., Fabi, D., Bilodeau, G., Martel, M., Bisson, D., Pietrowsk, B., et al. (1989). Quartz exposure, retention, and early silicosis in sheep. Exp. Lung. Res. 15(3):409-28.
- Bingham, E., Burkely, W., Murthy, R., In 'Inhaled Particles V,' ed. W.H. Walton, Pergamon, Oxford, 1977, pp. 543-550.
- Bissel, D. M., and Hammaker, L. E. (1976). Cytochrome P-450 heme and the regulation of hepatic heme oxygenase activity. Arch. Biochem. Biophys. 176:91-102.
- Bitterman, P. B., Rennard, S. I., Adelberg, S., and Crystal, R. G. (1983). Role of fibronectin as a growth factor for fibroblasts. J. Cell Biol. 97(6):1925-32.
- Bjelogrlic, N., Peng, R., Park, S. S., Gelboin, H. V., Honkakoski, P., Pelkonen, O., and Vahakangas, K. (1993). Involvement of P450 1A1 in benzo(a)pyrene but not in benzo(a)pyrene-7,8-dihydrodiol activation by 3-methylcholanthrene-induced mouse liver microsomes. Pharmacol. Toxicol.73(6):319-24.
- Black, S. D, and Gerhart, J. C. (1986). High-frequency twinning of Xenopus laevis embryos from eggs centrifuged before first cleavage. Dev. Biol. 116(1):228-40.
- Blackford, G.A., Jones, W., Dey, R.D., and Castranova, V. (1997). Comparison of inducible nitric oxide synthase gene expression and lung inflammation following intrtracheal instillation of silica, coal, carbonyl iron or titanium dioxide in rats. J. Toxicol. Envirn. Health 51:203-218.
- Bleau AM, Fradette C, El-Kadi AO, Cote MC, du Souich P. (2001). Cytochrome P450 down-regulation by serum from humans with a viral infection and from rabbits with an inflammatory reaction. Drug Metab. Dispos. 29(7):1007-12.
- Bonetti, B. Valdo, P., Ossi, G., De, Toni. L., Masotto, B., Marconi, S., Rizzuto, N., Nardelli, E., and Moretto, G. (2003). T-cell cytotoxicity of human Schwann cells: TNFalpha promotes fasL-mediated apoptosis and IFNgamma perforin-mediated lysis. Glia. 43(2):141-8.
- Borges, V. M., Lopes, M. F., Falcao, H., Leite-Junior, J. H., Rocco, P. R., Davidson, W. F., Linden, R., Zin, W. A., and DosReis, G. A. (2002). Apoptosis

underlies immunopathogenic mechanisms in acute silicosis. Am. J. Respir. Cell Mol. Biol. 27(1):78-84.

- Bowden, D. H. and Adamson, I. Y. R. (1978). Adaptive responses of the pulmonary macrophagic system to carbon in kinetic studies. Lab. Invest. 38:422-429.
- Boyer, C. S., Bannenberg, G. L., Neve, E. P., Ryrfeldt, A. and Moldeus, P. (1995). Evidence for the activation of the signal-responsive phospholipase A2 by exogenous hydrogen peroxide. Biochem. Pharmacol. 50: 753-761.
- Boyd, M. R. (1977). Evidence for the Clara cell as a site of cytochrome P450-dependent mixed-function oxidase activity in lung. Nature 269(5630):713-5.
- Bonner, J. C., Osornio-Vargas, A. R., Badgett A., and Brody, A. R. (1991). Differential proliferation of rat lung fibroblasts induced by the platelet-derived growth factor-AA, -AB, and -BB isoforms secreted by rat alveolar macrophages. Am. J. Resp. Cell. Mol. Biol. 5: 539-547.
- Bogaards, J. J. P., Bertrand, M., Jackson, P., Oudshoorn, M. J., Weavers, R. J., Van Bladeren, P. J., and Walther, B. (2000). Determining the best animal model for human cytochrome P450 activities: a comparison of mouse, rat, rabbit, dog, micropig, monkey and man. Xenobiotica 30 (12): 1131-1152.
- Boyd, M. R. (1977). Evidence for the Clara cell as a site of cytochrome P-450 dependent mixed-function oxidase activity in lung. Nature 269:713-413.
- Boyd, M. R., Stathan, C. N., Franklin, R. B., and Mitchell, J. R. (1978). Pulmonary bronchiolar alkylation and necrosis by 3-methyfuran, a naturally occurring potential atmospheric contaminant. Nature 272:270-271.
- Boyd, M. R., Statham, C. N., and Longo, W. S. (1980). The Pulmonary Clara cell is a target for toxic chemicals requiring metabolic activation; studies with carbontetrachloride. Journal of Pharmacology and Experimental therapeutics 212:109-114.
- Brandes, M. E., and Finkelstein, J. N. (1989). Stimulated rabbit alveolar macrophages secrete a growth factor for type II pneumocytes. Am J Respir Cell Mol Biol 1(2):101-9.
- Brodie, B., Axelrod, J., Cooper, J. R., Gaudette, L., LaDu, B. N., Mitoma, C., and Udenfriend, S. (1955). Detoxication of drugs and other foreign compounds by liver microsomes. Science 121:603-4.
- Burke, M. D., Thompson, S., Elcombe, C. R., Halpert, J., Haaparanta. T., and Mayer, R.T. (1985). Ethoxy-, pentoxy-, and benzyloxyphenoxazones and homologues to distinguish between different induced cytochromes p-450. Journal of Biological Chemistry, 34 (18): 3337-3345.
- Calleja, C., Eeckhoutte, C., Larrieu, G., Dupuy, J., Pineau, T., and Galtier, P. (1997). Differential effects of imterleukin-1β, interleukin –2 and interferon-γ on

the inducible expression of CYP 1A1 and CYP1A2 in culturd rabbit hepatocytes. Bioch. Biophys. Res. Commun. 239: 273-278.

- Carcillo, J. A., Doughty, L., Kofos, D., Frye, R. F., Kaplan, S. S., Sasser, H., and Burckart, G. J. (2003). Cytochrome P450 mediated-drug metabolism is reduced in children with sepsis-induced multiple organ failure. Intensive Care Med. 29(6):980-4.
- Caserta, T. M., Smith, A. N., Gultice, A. D., Reedy, M. A., and Brown, T. L. (2003). Q-VD-OPh, a broad spectrum caspase inhibitor with potent antiapoptotic properties. Apoptosis. 8(4):345-52.
- Castranova, V. (2000). From coal mine dust to quartz: Mechanism of pulmonary Pathogenecity. Inhalation Toxicology 12(suppl 3):7-14.
- Castranova, V., Bowman, L., Reasor, M.J., and miles, P. R. (1980). Effect of metal ions on selected oxidative metabolic processes in rat alveolar macophages. Toxicol. Appl. Pharmacol. 53: 14-19.
- Castranova, V., Bowman, L., Reasor, m. J. Lewis, T., Tucker, J., and Miles, P. R. (1985). The response of rat alveolar macrophages to chronic inhalation of coal dust and/or diesel exhaust. Environmental Research 36:405-419.
- Castranova, V. and Ducatman, B. S. Coal dust. In: Comperhensive Toxicology-toxicology of the Respiratory System. Vol 8 (Roth RA, ed). New York:Elsevvier Press, 1997; 361-372.
- Castranova, V., Jones, T. A., Barger, M. W., Afshari, A., and Frazer, D. G. (1990). Pulmonary responses of guinea pigs to consecutive exposures to cotton dust. In: R. R. Jacobs, P. J. Wakelyn and L. N. Domelsmith (Eds), Proceedings of the 14th Cotton Dust Research Conference, National Cotton Council, Memphis, pp. 131-135.
- Castranova, V., Lee, P., Ma, J. Y. C., Weber, K. C., Pailes, W.H. and Miles, P. R. (1987). Chemiluminescence from macrophages and monocytes. In: K. VanDyke and V. Castranova (Eds), Cellular Chemiluminescence, CRC Press, Boca Raton pp. 4-19.
- Castranova, V., Pallas, W. H., Dalal, N. S., Miles, P. R., Bowman, L., Vallyathan, V., Pack, D., Weber, K. C., Hums, Schwegler-Berry D., *et al*. (1996). Enhanced pulmonary response to the inhalation of freshly fractured silica as compared to aged dust exposure. Appl. Occup. Environ. Hyg. 11:937-941.
- Castranova, V., Porter, D., Millecchia, L., Ma, J. Y. C., Hubbs, A. F., and Teass, A. (2002). Effect of inhaled crystalline silica in a rat model: Time course of pulmonary reactions. Molecular and Cellular biochemistry 234/235:177-184.
- Castranova, V., Rabovsky, J., Tucker, J. H., and Miles, P. R. (1988). The alveolar type II epithelial cell: a multifunctional pneumocyte. Toxicol. Appl. Pharmacol. 93(3):472-83.

- Castranova, V., and Vallyathan, V. (2000). Silicosis and coal workers' pneumoconiosis. Am. J. Respir. Cell Mol. Biol. 8(6):597-604.
- Castranova, V., Vallyathan, V., Ramsey, R. M., McLaurin, J. L., Pack, O., Leonard, S., Barger, M. W., Ma, J. Y. C., Dalal, N. S., and Teass, A. (1997). Augmentation of pulmonary reactions to quartz inhalation by trace amounts of iron-containing particles. Environ. Health Perspectives 104 (suppl 105).1319-1324.
- Castranova, V., Vallyathan, V., and Wallace, W.E., ads. Silica and Silica-induced Lung Diseases. Boca Raton, FL.CRC Press. 1996.
- Cawley, G. F., Zhang, S., Kelley, R. W., Backes, W. L. (2001). Evidence supporting the interaction of CYP2B4 and CYP1A2 in microsomal preparations. Drug Metab. Dispos. 29(12):1529-34.
- Chechoway, H. and Franzblau, A. (2000). Is silicosis required for silica-associated lung cancer?. American Journal of Industrial Medicine 37:252-259.
- Chen, X., Kandasamy, K., and Srivastava, R. K. (2003). Differential roles of RelA (p65) and c-Rel subunits of nuclear factor κB in tumor necrosis factor-related apoptosis-inducing ligand signaling. Cancer Research 63:1059-1066.
- Chichester, C. H., Philpot, R. M., Weir, A. J., Buckpitt, A. R., and Plopper, C. G. (1991). Characterization of the cytochrome P-450 monooxygenase system in nonciliated bronchiolar epithelial (Clara) cells isolated from mouse lung. Am. J. Respir. Cell Mol. Biol. 4:179-186.
- Ciolino, H. P., Dankwah, M., and Yeh, G. C. (2002). Resistance of MCF-7 cells to dimethylbenz(a)anthracene-induced apoptosis is due to reduced CYP1A1 expression. Int. J. Oncol. 21(2):385-91.
- Clements, J. A. (1959). Surface tension of lung extracts. Proceedings of the Society for Experimental Biology 95:170-172.
- Cocco, P., Rice, C. H., Chen, J. Q., McCawley, M. A., McLaughlin J. K., Dosemeci, M. (2001). Lung cancer risk, silica exposure, and silicosis in Chinese mines and pottery factories: the modifying role of other workplace lung carcinogens. American Journal of Industrial medicine 40(6):674-82.
- Collis, E. L. and Gilchrist, J. C. (1928). Effect of dust upon coal trimmers. J. Ind. Hug. Toxicol. 10:101-109.
- Collman, J. P., Sorrell, T. N., Dawson, J. H., Bunnenberg, E. and Djerassi, c. (1976). Magnetic circular dichroism of ferrous carbonyl adducts of cytochrome P-450 and P-420 and their syntheric models. Proc. Nat. Acad. Sci. USA 73:6-10.
- Compton, M. M. (1992). A biochemical hallmark of apoptosis: Internucleosomal degradation of the genome. Cancer Metastasis Rev. 11:105-119.
- Conney, A. H. (1982). Induction of microsomal enzymes by foreign chemicals and carcinogenesis by polycyclic aromatic hydrocarbons: G. H. A. Clowes Memorial Lecture. Cancer Res. 42(12):4875-917.

- Cooper, D. Y., Levin, S., Narasimhulu, S., Rosenthal, O., and Estabrook, R. W. (1965). Photochemical action spectrum of the terminal oxidase of the mixed function oxidase systems. Science 147:400-402.
- Costello, J., Ortmeyer, C. E., and Morgan, W .K .C. (1974). Mortality from lung cancer in U.S. coal miners. American Journal of Public Health 64(3): 222-224.
- Craighead, J. E., Kleinerman J., Abraham J. L. et al. (1988). Diseases associated with exposure to silica and nonfibrous silicate minerals. Arch. Pathol. Lab. Med. 112: 673-720.
- Craighead J. E., Kleinerman J., Abraham, J. L., Gibbs, A. R., Green, F. H. Y., Harley, R. A., Ruettner, J. R., Vallyathan, N. V., and Juliano, E. B. (1998). Diseases associated with exposure to silica and non-fibrous silicate minerals. Arch Pathol Lab Mad 112:673-720.
- Crapo, J. D., Barry, B. E., Gehr, P., Bachofen M., and Weibel, E. R. (1982). Cell number and cell characteristics of the normal human lung. American Review of Respiratory Diseases 126:332-337.
- Crapo, J. D., Peters-Golden, M., Marsh-Salin, J., and Shelburne, J. S. (1978). Pathologic changes in the lungs of oxygen-adapted rats. A morphometric analysis. Laboratory investigations 39:640-653.
- Crapo, J. D., Young, S. L., Fram, E. K., Pinkerton, K. E., Barry, B. E., and Crapo, R. O. (1983). Morphometric characteristics of cells in the alveolar region of mammalian lungs. Am. Rev. Respir. Dis. 8(2 Pt 2):S42-6.
- Crespi, C. L., Langenbach, R., Rudo, K., Chem, Y. T., and Davies, R. L. (1989). Transfection of human cytochrome p-450 into the human the human lymphobastiod cell line, AHH-1, and use of recombinant cell line in gene mutation assays. Carcinogenesis, 10 (20): 295-301.
- Crespi, C. L., Penman, B. W., Steimel, D. T., Gelboin, H.V., and Gonzalez, F. J. (1991). The development of human cell line stably expressing human CYP3A4: Role in metabolic activation of aflatoxin B1 and comparison to CYP1A2 and CYP2A3. Carcinogenesis, 12(2): 355-359.
- Crouch, E. (1990). Pathology of pulmonary fibrosis. Am. J. physiol. 259:L159-L184.
- Dalal, N. S., Jafan, B., Vallyathan, V., Green, F. E. Y. Cytotoxicity and spectroscopic investigations of organic free radicals in fresh and stale coal dust. In. Proceedings 7th International Pneumoconiosis Conference. Part 2, 23-Z6 August 1988, Pittsburgh. Pennsylvania. NIOSH Publ. 90-108. Cincinnati. OH National Institute for Occupational Safety and Health, 1990; 1470-1477.
- Dalal, N. W., Jafari, B., Petersen, M., Green, F. H. Y., and Vallyathan, V. (1991). Presence of stable coal radicals in autopsied coal miners' lungs and its possible correlation to coal workers' pneumoconiosis. Arch. Environ. Health 46366-3721.

- Dalal, N. S., Newman, J., Pack, D., Leonard, S., and Vallyathan, V. (1995) Hydroxyl radical generation by coal mine dust: possible implication to coal workers' pneumoconiosis ICWPI. Free Radic. Biol. Med. 18: 11-201.
- Dalal, N. S., Shi, X., and Vallyathan, V. (1990). Role of free radicals in the mechanisms of hemolysis and lipid peroxidation by silica: comparative ESR and cytotoxmity studies. J. Toxicol. Environ. Health. 29: 307-316.
- Dale, K. (1973a). Early effects of quartz and titanium dioxide dust on pulmonary function and tissue. An experimental study on rabbits. Scand. J. Respir. Dis. 54(3):168-84.
- Dale, K (1973b). A method for inducing unilateral silicosis in rabbits by an injection technique with some observations on lung clearance and quantitative evaluation of experimental silicosis. Scand. J. Respir. Dis. 54(3):157-67.
- Daniels, J. M., and Massey, T. E. (1992). Modulation of aflatoxin B_1 biotransformation in rabbit pulmonary and hepatic microsomes. Toxicology 74:19-32.
- Davies, R., and Erdogdu G. (1989). Secretion of fibronectin by mineral dust-derived alveolar macrophages and activated peritoneal macrophages. Exp. Lung Res. 15: 285-297.
- Davis, G. S. (1986). Pathogenesis of silicosis: current concepts and hypotheses. Lung 164: 139-154.
- Dawson, J. H. Anderson, L. A. and Sono, M. (1982). Spectroscopic investigation of ferric cytochrome P-450-CAM ligand complex. J. Biol. Chem. 257:3606-3617.
- Degawa, M., Miura, S., Yoshinari, K., and Hashimoto, Y. (1995). Altered expression of hepatic CYP1A enzymes in rat hepatocarcinogenesis. Jpn. J. Cancer Res. 86(6):535-9.
- Denison, M. S. and Whitlock, J. P., Jr. (1995). Xenobiotic-inducible transcription of cytochrome P450 genes. J. Biol. Chem. 270:18175-78.
- Denison, M. S., Seidel, S. D., Rogers, W. J., Ziccardi, M., Winter, G. M., and Health-Pagliuso S. (1998). Natural and synthetic ligands for the Ah receptors. In Molecular Biology of the Toxic Response, ed. A Puga K. Wallacw, pp. 393-410. New York: Taylor and Francis.
- Desagher, S., Osen-Sand, A., Nichols, A., Eskes, R., Montessuit, S., Lauper, S., Maundrell, K., Antonsson, B., and Martinou, J. C. (1999). Bid-induced conformational change of Bax is responsible for mitochondrial cytochrome c release during apoptosis. Cell Biol. 144(5):891-901.
- Devereux, T. R., Domin, B. A., and Philpot, R. M. (1989). Xenobiotic metabolism by isolated pulmonary cells. Pharmacology and Therapeutics 41:243-256.

- Devereux, T. R., Hook, J. E. R., and Fouts, J. R. (1979). Foreign compound metabolism by isolated cells from rabbit lung. Drug Metabolism and Disposition 7:70-75.
- Devereux, T. R., Jones, K. G. Bend, J. R. Fouts, J. R., Statham, C. N, and Boyd, M. R. (1981). In vitro metabolic activation of the pulmonary toxin, 4-ipomeanol, in nonciliated bronchiolar epithelial (Clam) and alveolar type II cells isolated from rabbit lung. J. Pharmacol. Exp. Ther. 220:223-227.
- Dey, A., Jones, J.E., and Nebert, D. W. (1999). Tissues and cell-type specific expression of cytochrome P45o 1A1 and cytochrome P450 1A2 mRNA in the mouse localized in situ hybridization. Biochemical pharmacology 58: 525-537.
- Dinsdale, D., and Verschoyle, R. D. (2001). Cell-specific loss of cytochrome P450 2B1 in rat lung following treatment with pneumotaxic and non-pneumotaxic trialkylphosphorothiolates. Biochemical pharmacology 61:493-501.
- Dobbs, L. G. (1990). Isolation and culture of alveolar type II cells. Am. J. Physiol. 258(4 Pt 1):L134-47.
- Dobbs, L. G., and Mason, R. J. (1979). Pulmonary alveolar type II cells isolated from rats: Release of phosphatidylcholine in response to β-adrenergic stimulation. Drug Metabolism and Disposition 63:378-387.
- Domin, B. A., Devereux, T. R., and Philpot, R. M. (1986). The cytochrome P-450 monooxygenase system of rabbit lung: enzyme components, activities, and induction in the nonciliated bronchiolar epithelial (Clam) cell, alveolar type II cell, and alveolar macrophage. *Mot. Pharmacol.* 30: 296-303.
- Donato, M. T., Guillen, M. I., Jover, R., Castell, J. V. and Gomez-Lechon, M. J. (1997) Nitric oxide-mediated inhibition of cytochrome P450 by interferon-γ in human hepatocytes. J. Pharmacol. Exp. Ther. 281: 484-490.
- Doumas, B., Watson, W., and Biggs, H. (1971). Albumin standards and the measurement of serum albumin with bromcresol green. Clinica Chimica ACTA 31: 87-96.
- Driscoll, K. E. (1996). the role of interleukin-1 and tumor necrosis factor in the lung's response to silica. In: Silica and Silica-induced lung diseases, Current concepts (Castranova, V., Vallyathan, V., and Wallace, W. eds). Boca Raton, FL: CRC Press 136-184.
- Driscoll, K. E. and Guthrie, G. O. Crystalline silica and silicosis. In: Comperhensive Toxicology-Toxicology of the Respiratory System. Vol 8 (Roth R. A. ed). New York: Elsevier Press. 1997; 373-391.
- Driscoll, K. E., Hassenbein, D. J., Carter, J. M., Kunkel, S. L., Quinlan, T. R., and Mossman, B. T. (1995). TNF-α and increase of chemokine expression in rat lung after particle exposure. Toxicological latters 82/83:483-489.
- Driscoll, K. E., Hassenbein, D. J., Carter, J. M.,Poynvter, J., asquith, T. N., Grant, R. A., Whitten, J., Purdon, M. P., Takigiku, R. (1993). Macrophage

inflammatory protein 1 and 2 expression in by rat alveolar macrophages, fibroblasts, and epithelial cells in rat lung after mineral dust exposure. Am. J. Respir. Cell Mol. Biol. 8:311-318.

- Eaton, D. L. Gallagher, E. P., Bammler, T. K., and Kunze, K. L. (1995). Role of cytochrome P4501A2 in chemical carcinogenesis: Implication for human variability in expression and enzyme activity. Pharmacogenetics, 5: 259-274.
- Elferink, C. J., Ge, N-L., and Levine A. (2001). Maximal Aryl Hydrocarbon Receptor Activity Depends on an Interaction with the Retinoblastoma Protein. Mol. Pharmacol., 59: 664-673.
- El-Kadi, A. O., Bleau, A. M., Dumont, I., Maurice, H., and du Souich, P. (2000). Role of reactive oxygen intermediates in the decrease of hepatic cytochrome P 450 activity by serum of humans and rabbits with acute inflammatory reaction. Drug Metabolism and Disposition 28:1112-1120.
- El-Kadi, A. O. S. and du Souich, P. (1998). Depression of the hepatic cytochrome P450 by an acute inflammatory reaction; Characterization of the nature of mediators in human and rabbit serum, and in the liver. Life Sciences 63(15):1361-1370.
- Endo, Y., Tsuria, S., and Fujihira, E. (1981). Hepatic drug-metabolizing activities and anti-inflammatory potency of hydrocortisone in rats with granulatomous inflammation. Research Communications in Chemical Pathology and Pharmacology 33:195-206.
- Enterline, P. E. (1964). Mortality rates among coal miners. Am. J. Pub. Health 54: 758-771.
- Estabrook, R. W., Cooper, D. Y. and Rosenthal, O. (1963). The light-reversible carbon monoxide inhibition of the steroid C-21 hydroxylation system of the adrenal cortex. Biochem. Zeit. 338, 741-755.
- Evans, M. J., Cabral, L. J., Stephens, R. J., and Freeman, G. (1973). Renewal of alveolar epithelium in the rat following exposure to NO_2 . American Journal of Pathology 70:175-198.
- Fahey, J. W., Zhang, Y., and Talaly, P. (1997). Broccoli sprouts: an exceptional rich source of inducers of enzymes that protect against chemical carcinogens. Proc. Natl. Acad. Sci. USA 94:10367-72.
- Flowers, N. L. and Miles, P. R. (1991). Alterations of pulmonary benzo[a]pyrene metabolism by reactive oxygen metabolites. Toxicology, 68: 259-274.
- Foster, J. R., Elcombe, C. R., Boobis, A. R., Davies, D. S., Sesardic, D., McQuade, J., Robson, R. T., Hayward, C., and Lock, E. A (1986). Immunocytochemical localization of cytochrome P-450 in hepatic and extra-hepatic tissues of the rat with a monoclonal antibody against cytochrome P-450c. Biochem. Pharmacol. 35:4543-4554.

- Forkert, P. G., Lord, J. A., and Parkinson, A. (1998). Alterations in expression of CYP1A1 and NADPH-cytochrome P450 reductase during lung tumor development in SWR/J mice. Carcinogenesis 17(1):127-32.
- Fraser, R. S. S., and Nurse, P. (1978). Novel cell cycle control of RNA synthesis in yeast. Nature 271:726-730.
- Friemann, J., Albrecht, C., Breuer, P., Grover, R., Weishaupt, C. (1999). Time-course analysis of type II cell hyperplasia and alveolar bronchiolization in rats treated with different particulates. Inhal. Toxicol.11(9):837-54.
- Fukuda, Y., Ishida, N., Noguchi, T., Kappas, A. and Sassa, S. (1992) Interleukin-6 down regulates the expression of transcripts encoding cytochrome P450 IA1, IA2 and IIIA3 in human hepatoma cells. Biochem. Biophys. Res. Commun. 184**:** 960-965.
- Fulda, S. and Debatin, K. M. (2002). IFNgamma sensitizes for apoptosis by upregulating caspase-8 expression through the Stat1 pathway. Oncogene 21(15):2295-308.
- Garfinkel, D. (1958). Studies on pig liver microsomes. I. enzymic and pigment composition of different microsomal fractions. Archives of Biochemsitry and Biophysics 77:493-509.
- Gay, R.J., McComb, R. B., and Bowers, G. N. (1968). Optimum reaction conditions for human lactate dehydrogenase isoenzymes as they affect total lactate dehydrogenase activity. Clin. Chem. 14:740-753.
- Gavrieli, Y., Sherman, Y., Ben-Sasson, S. A. (1992). Identification of programmed cell death in situ via specific labeling of nuclear DNA fragmentation. J. Cell Biol. 119:493-501.
- Ge, N-L., and Elferink, C. J. (1998) A direct interaction between the aryl hydrocarbon receptor and retinoblastoma protein. J. Biol. Chem. 273 (35): 22708-22713.
- Gelboin, H.V. (1980). Benzo(a)pyrene metabolism, activation and carcinogen-esis: role and regulation of mixed-function oxidases and related enzymes. *Physiol. Rev., 6:* 1107-1166.
- Getty, Robert 1975. Sisson and Grossman's The Anatomy of the Domestic Animals, volume 1, pp 934. W.B. Saunders Company, Philadelphia.
- Ghanem, M. Porter, D., Battelli, L., Kashon, M., Barger, M., Ma, J. Y., Vallyathan, V., Nath, J., and Hubbs, A. (2003). Rat pulmonary CYP1A1 induction is inhibited by respirable coal dust exposure. Toxicological Sciences 72 (S-1):320 (Abstract).
- Ghezzi, P., Saccardo, B., Villa P., Rossi, V., Bianchi, M., and Dinarello, C. A. (1986). Role of interleukin-1 the depression of liver drug metabolism by endotoxin. Infect. Immun. 54:837-840.

- Goldstone, S. D. and Hunt, N. H. (1997). Redox regulation of the mitogen-hybridization and TUNEL to identify cells undergoing apoptosis. Biochim. Biophys. Acta 1355: 353-360
- Gonzalez, R.F. and Dobbs, L. G. (1998) Purification and analysis of RTI140, a type I alveolar epithelial cell apical membrane protein. Biochemica et Biophysica Acta. 1429:208-16.
- Gonzalez, F. J., Femandez-Salguero, P., Ward, J. M., (1996). The role of the aryl hydrocarbon receptor in animal development, physiological homeostasis, and toxicity of TCDD. J. Toxicol. Sci. 21:273-77.
- Goodglick, L. A. and Kane, A. B. (1986). Role of reactive oxygen in crocidolite asbestos toxicity to mouse macrophages. Cancer research 56:5558-5566.
- Gottlicher, M., Widmark, E., Li, Q., and Gustafsson, J. A. (1992). Fatty acids activate a chimera of the clofibic acid-activated receptor and the glucocorticoid receptor, Proc. Natl. Acad. Sci. USA 89:4653-4657.
- Gough, J. (1940). Pneumoconiosis of coal trimmers. J. Pathology and Bacteriology 51:227-285.
- Green, F. H. Y., and Vallyathan, V. Coal workers' pneumoconiosis and pneumoconiosis due to other carbonaceous dusts. In: Pathology of Occupational Lung Disease. 2nd ed (Churg, A., Green, F. H. Y., eds). Philadelphia Williams and Wilkins, 1998, 129-708.
- Green, H. Y., and Vallyathan, V., in `Silica and Silica-Induced Lung Disease: Current Concepts,' eds. Castranova, V., Vallyathan, V., and Wallace, W. CRC press, Boca Raton, Fl. 1995, pp. 39-59.
- Gregory, P. D., Hort, W. (1998). Chromatin and transcription-how transcription factors battle with a repressive chromatin environment. Eur. J. Biochem. 251:9-18.
- Getty, Robert. (1975). Sisson and Grossman's The Anatomy of the Domestic Animals, volume 1, pp 934. W.B Saunders company, Philadelphia.
- Gonzalez, R.F. and Dobbs, L.G. (1998) Purification and analysis of RT140, a type I alveolar epithelial cell apical membrane protein. Biochemica et Biophysica Acta. 1429:10208-16.
- Groves, J. T. (1985). Key elements of the chemistry of cytochrome P-450. The oxygen rebound mechanism. J. Chem. Edu. 62:928-931.
- Grunstein, M. (1997). Histone acetylation in chromatin structure and transcription. Nature 389:349-52.
- Guengerich, F. P. (1997). Role of cytochrome P450 enzymes in drug-drug interactions. Adv. Pharmacol. 43:7-35.
- Guengerich, F. P., Wang, P., and Davidson, N. K (1982). Estimation of isozymes of microsomal cytochrome P-450 in rats, rabbits and humans using

immunochemical staining coupled with sodium dodecyl sulfate-polyacrylamide gel electrophoresis. Biochemistry 21:1698-1706.

- Guinee, D. Jr., Brambilla, E., Fleming, M., Hayashi, T., Rahn, M., Koss, M., Ferrans, V., and Travis, W. (1997). The potential role of BAX and BCL-2 expression in diffuse alveolar damage. Am. J. Pathol. 151(4):999-1007.
- Haies, D. M., Gil, J., and Weibel, E. R. (1981). Morphometric study of rat lung cells. I. Numerical and dimensional characteristics of parenchymal cell population. Amer. Rev. Respir. Dis. 123, 533-541.
- Hakkola, J., Pasanen, M., Pelkonen, O., Hukkanen, J., Evisalmi, S., Anttila, S., Rane, A., Mantyla, M., Purkunen, R., Saarikoski, S., Tooming, M., and Raunio, H. (1997). Expression of CYP1B1 in human adult and fetal tissues and differential inducibility of CYP1B1 and CYP1A1 by Ah receptor ligands in human placenta and cultured cells. Carcinogenesis. 18(2):391-7.
- Hankinson, O. (1995). The aryl hydrocarbon receptor complex. Annu. Rev. Pharmacol. Toxicol. 35:307-40.
- Heppleston, A. G. (1947). The essential lesion of pneumoconiosis in Welsh cal workers. J. Pathol. Bacteriol. 59:453-460.
- Hardwick, J. P., Song, B. J., Huberman, E., and Gonzalez, F. J., 1987, Isolation, complementary DNA sequence, and regulation of rat hepatic lauric acid ω-hydroxylase (cytochrome P-$450_{LA\ \omega}$). J. Biol. Chem.262:801-810.
- Harkema, J. R., Wagner, J. G., Simon, J. A., McBride, S., Elder, A. C., Driscoll, K., and Oberdorster, G. (2003). Rats, but not Hamsters, have persistent alveolitis and type II cell proliferation after chronic inhalation of carbon black particles. Toxicological Sciences 72 (S-1): 289 (Abstract).
- Harrington, J. S. (1972). Investigative techniques in the laboratory study of coal Workers,s pneumoconiosis: recent advances at the cellular level. Ann. NY Acad. Sci. 200:816-834.
- Hasler, J. A., Estabrook, R., Murray, m., Pikuleva, I., Waterman, M., Capdevila, J., Holla, Vijakumar, Helvig, C., Falck, J. R., Farrell, G., Kaminsky, L. S., Spivack, S. D., Boitier, and Beaunes, P. et al (1999). Human cytochrome P450. Molecular Aspect of Medicine 20: 1-137.
- Hayaishi, O. (1962). History ans scope. In: O. Hayaishi (ed.), oxygenase, Academic Press, New york, pp 1-29.
- Hayashi, S., Watanabe, J., and Kawajiri, K. (1992). High susceptibility to lung cancer analysed in terms of combined genotypes of P4501A1 and Mu-class glutathione S-transferase genes. Japanese. J. Cancer Res. 83:866-870.
- Hayashi, Si., Watanabe, J., Nakachi, K., Eguchi, H., Gothoh, O., and Kawajiri, K. (1994). Interindividual difference in expression of human Ah receptor and related P450 genes. Carcinogenesis. 15(5): 801-806.

- Hayashi, S., Watanabe, J., Nakachi, K., and Kawajiri, K. (1991). Genetic linage of lung cancer-associated MSP1 polymorphisms with amino acid replacement in the heme binding region in the human cytochrome P4501A1 gene. Journal of Biochemistry (Tokyo) 110:407-411.
- Hetland, R., Cassee, F., Refsnes, M., Schwarze, P., Lag, M., Boere, A., and Dybing, A. (2003). Ambient air particles of different fractions causes release of inflammatory cytokines, cell toxicity and apoptosis in epithelial lung cells. Toxicological Sciences 72 (S-1): 289 (Abstract).
- Hildebrand, C.E., Gonzalez, F.J., McBride, O.W., and Nebert, D.W., (1985) Assignment of the human 2,3,7,8-tetrachlorodibenzo-p-dioxin-inducible cytochrome P1-450 gene to chromosome 15. Nucleic Acids Res. 13:2009-2016.
- Hill, H. R., Hogan, N. A., Bale, J. F., and Hemming, V. G. (1977). Evaluation of nonspecific (alternative pathway) opsonic activity by neutrophil chemiluminescence. International Archives of Allergy and Applied Immunology 53, 490-4977.
- Hino, Y., Imai, Y., and Sato, R. (1974). Induction by Phenobarbital of hepatic microsomal drug-metabolizing enzyme system in partially hepatectomized rats. J. Bioch. 76: 735-744.
- Holland, L. M. (1990). Crystalline silica and lung cancer: a review of recent experimental evidence. Regul. Toxicol. Pharmacol., 12:224-237.
- Hubbard, A. K., Timblin, C. R., Shukla, A., Rincon, M., and Mossman, B. T. (2002). Activation of NF-kappaB-dependent gene expression by silica in lungs of luciferase reporter mice. Am. J. Physiol. Lung Cell Mol. Physiol. (5):L968-75.
- Hubbs, A. F., Castranova, V., Ma, J. Y. C., Frazer, D. G., Siegel, P. D., Ducatman, B. S., Grote, A., Schwegler-Berry, D., Robinson, V. A., Van Dyke, C., Barger, M., Xiang, J., and Parker, J., (1997). Acute lung injury induced by a commercial leather conditioner. Toxicol. Appl. Pharmacol. 134:37-46.
- Hubbs, A. F., Minhas, N. S., Jones, W., Greskevitck, M., Battelli, L. A., Porter, D. W., Goldsmith, W. T., Frazer, D., Landsittel, D. P., Ma, J. Y. C., Barger, M., Hill, K., Schwegler-Berry, D., Robinson, V. A., Castranova, V. (2001). Comparative pulmonary toxicity of 5 abrasive blasting agents. Toxicol. Sci. 61:135-143.
- Hukkanen, J., Pelkonen, O., Hakkola, J., and Raunio, H. (2002). Expression and regulation of xenobiotic-metabolizing cytochrome P450 (CYP) enzymes in human lung. Crit. Rev. Toxicol. 32(5):391-411.
- IARC (International Agency for Research on Cancer). IARC Monograph on the evaluation of Carcinogenic Risk of Chemicals to Humans. Silica, Some Silicates, Coal Dust and Para-aramid Fibrils. Vol 68. Lyon: International Agency for Research on Cancer, 1997.
- International Life Science Institute (ILSI) Risk Science Institute Workshop Participant (2000). The relevance of the rat lung response to particle overload for

human risk assessment: a workshop consensus report. Inhalation Toxicology 12(1-2): 1-17.

- Ishibe, N., Wiencke, J. K, Zuo, Z. F., McMillan, A., Spitz, M., and Kelsey, K. T. (1997). Susceptibility to lung cancer in light smokers associated with CYP1A1 polymorphisms in Mexican- and African-Americans. Cancer Epidemiol. Biomarkers Prev. 6(12):1075-80.
- Issemann, L., and Green, S. (1990) Activation of a member of the steroid hormone receptor superfamily by peroxisome proliferators, Nature 347:645-650.
- Iyer, R., Hamilton, R. F., Li, L., and Holian, A. (1996). Silica-induced apoptosis mediated via scavenger receptor in human alveolar macrophages. Toxicol. Appl. Pharmacol. 141(1):84-92.
- Jaiswal, A. K., Gonzalez, F. J., Nebert, t. W. (1985a). Human dioxin-inducible cytochrome P_1- 450: complementary DNA and amino acid sequence. Science 228:80-83.
- Jaiswal, A. K., Gonzalez, F. J., Nebert, t. W. (1985b). Human cytochrome P_1- 450 gene sequence and correlation of mRNA with genetic differences in benzo[a]pyrene metabolism. Nucleic Acids Research. 13:4503-4520.
- James, P. and Whitlock, Jr. (1999). Induction of cytochrome P4501A1. Annu. Rev. Pharmacol. Toxicol. 39:103-25.
- Janig, G. R, Makower, A., Rabe, H., Bernhardt R. and Ruchpaul, K. (1984). Chemical modification of cytochrome P450 LM2. Characterization of tyrosine as axial heme iron ligand trans to thiolate. Biochem. Biophus. Acta 787:8-18.
- John, A., blackford, Jr., Jones, W., Dey, R.D., and Castranova, V. (1997). Comparison of inducible nitric oxide synthase gene expression and lung inflammation following intratracheal instillation of silica, coal, carbonyl iron, and titanium dioxide in rats. J. Toxicol. Environ. Health 51: 03-218.
- Jones, K. G., Holland, J. F., Fourman, G. L., Bend, J. R., and Fouts, J. R. (1983). Xenobiotic metabolism in Clara cells and alveolar type II cells isolated from lungs of rats treated with beta-naphthoflavone. Journal of Pharmacology and Experimental Therapeutics 225:316-319.
- Jones, G. S., Miles, P. R., Lantz, R. C., Hin D. E., and Castranova, V. (1982). Ionic content and regulation of cellular volume in rat alveolar II cells. J Appl. Physiol. Respir. Environ. Exercise Physiol. *53,* 258-266.
- Jover, R., Bort, R., Gomez-Lechon, M. J., and Castell, J. V. (2002). Down-regulation of human CYP3A4 by the inflammatory signal interleukin-6: molecular mechanism and transcription factors involved. FASEB J. 16(13):1799-801.
- Juers, J. A., Rogers, R. M., McCardy, J. B., Cook, W. W. (1976). Enhancement of bactericidal capacity of alveolar macrophages by human alveolar lining material. J. Clin. Invest. 58*,* 271-275.

- Juskevich, J. C. (1987). Comparative metabolism in food-producing animals: programs sponsored by the Center for Veterinary Medicine. Drug Metab. Rev. 18(2-3):345-62.
- Kadonaga, J. T. (1998). Eukarcotic transcription: an interlaced network of transcription factors and chromatin-modifying machines. Cell 92:307-13.
- Karuzina, I. L. and Archakov, A. I. (1994). Hydrogen peroxide-mediated inactivation of microsomal cytochrome P450 during monooxygenase reactions. Free Radical Biology and Medicine 17: 557-567.
- Kasper, M., Rudolf, T., Verhofstad, A. A., Schuh, D., and Muller, M. (1993). Heterogeneity in the immunolocalization of cytokeratin-specific monoclonal antibodies in the rat lung: evaluation of three different alveolar epithelial types. Histochemistry 100(1): 65-71.
- Kaufmann, S. H., Earnshaw, W. C. (2000). Induction of apoptosis by cancer chemotherapy. Exp. Cell Res. 256: 42-49.
- Kawajiri, K., Watanabe, J., Gotoh, O., Tagashira, Y., Sogawa, K., Fujii-Kuriyama, Y. (1986). Structure and drug inducibility of the human cytochrome P-450c gene. Eur. J. Biochem. 159:219-225.
- Kawajiri, K. and Fujii-Kuriyama, Y (1991). P450 and human cancer. Jpn. J. Cancer Res. 82: 1325-1335.
- Ke, S., Rabson, A. B, Germinoll, J. F., Gallo, M. A., and Tian, Y. (2001). Mechanism of suppression of cytochrome P-450 lA1 expression by tumor necrosis factor-α and lipopolysaccharide. The Journal of Biological Chemistry, 267 (43), 39638-39644.
- Keith, I. M., Olson, E. B., Wilson, N. M., and. Jefcoate, C. R (1987). Immunological identification and effects of 3-methylcholanthrene and phenobarbital on rat pulmonary cytochrome P-450. Cancer Res. 47:1878-1882.
- Kellermann, G., Shaw, C.R., and Luyten-Kellermann, M. (1973) Aryl hydrocarbon hydroxylase inducibility and bronchogenic carcinoma. New Engl. J. Med. 289:934-937.
- Kelley, J. (1990). Cytokines of the lung. American Review of Respiratory diseases 141:765-788.
- Khatsenko, O. G., Boobis, A. R. and Gross, S. S. (1997). Evidence for nitric oxide participation in down-regulation of CYP2B1/2 gene expression at the pretranslational level. Toxicol. Lett. 90: 207-216.
- Killander, D., and Zetterberg, A. (1965). Quantitative cytochemical studies on interphase growth. Exp. Cell Res. 38: 272-284.
- Kim, D. M., Koo, S. Y., Jeon, K., Kim, M. H., Lee, J., Hong, C. Y., and Jeong, S. (2003). Rapid induction of apoptosis by combination of flavopiridol and tumor necrosis factor (TNF)-alpha or TNF-related apoptosis-inducing ligand in human cancer cell lines. Cancer Res. 63(3):621-6.

- Kim, J. E., and Sheen, Y.Y. (2002). Nitric oxide inhibits dioxin action for the stimulation of CYP1A1 promoter activity. Biol. Pharm. Bull. 23: 575-580.
- Kim, D. W., Gazourian, L., Quadri, S. A., Romieu-Mourez, R., Sherr, D. H., and Sonenshein, G. E. (2000). The RelA NF-kappaB subunit and the aryl hydrocarbon receptor (AhR) cooperate to transactivate the c-myc promoter in mammary cells. Oncogene 19(48):5498-506.
- Kim, J., and Kemper, B. (1997). Phenobarbital alters protein binding to the *CYP2B1/2* phenobarbital-responsive unit in native chromatin. J. Biol. Chem. 272:29423-29425.
- Kimura, S., Kozak, C. A., and Gonzale, F. J. (1989). Identification of a novel P450 expressed in rat lung: cDNA cloning and sequence, chromosome mapping, and induction by 3-methylcholanthrene. Biochemistry 28:3798-3803.
- Kitanaka, C., Namiki, T., Noguchi, K., Mochizuki, T., Kagaya, S., Chi, S., Hayashi, A., Asai, A., Tsujimoto, Y., and Kuchino, Y. (1997). Caspase-dependent apoptosis of COS-7 cells induced by Bax overexpression: differential effects of Bcl-2 and Bcl-xL on Bax-induced caspase activation and apoptosis. Oncogene 15(15):1763-72.
- Kleinerman, J., Green, F. H. Y., Harley, R., Lapp, N. L., Laqueur, W., Naeye, R. L., Pratt, P., Taylor, G., and Wyatt, J. (1979). Pathology Standards far Coal Workers' Pneumoconiosis: Report of the Pneumoconiosis Committee of the College of American Pathologists to the National Institute for Occupational Safety and Health Arch. Pathol. Lab. Med. 103:375-431.
- Kleinman, M. T., Sioutas, C., Chang, M. C., Boere, A. J., Cassee, F. R. (2003). Ambient fine and coarse particle suppression of alveolar macrophage functions. Toxicol. Lett. 37(3):151-8.
- Klinger, W., and Karge, E. (1987). Interaction of induction, ontogenic development and liver regeneration on the monooxygenase level. Exp. Path. 31: 117-124.
- Kobusch, A. B., Erill, S., and Du Souich, P. (1986). Relationship between changes in seromucoid concentrations and the rate of oxidation or acetylation of several substrates. Drug Metabolism and Disposition 14:663667.
- Kolluri, S. K., Weiss, C., Koff, A., and Gottlicher, M. (1999). $P27^{Kip1}$ induction and inhibition of proliferation by the intracellular Ah receptor in developing thymus and hepatoma cells. Genes and development, 13:1742-1753.
- Kroemer, G., Reed, J. C. (2000). Mitochondrial control of cell death. Nat. Med., 6: 513-519.
- Kuempel, E. D., Attfield, M. D., Vallyathan, V., Lapp, N. L., Hale, J. M., Smith, R. J., and Castranova, V. (2003). Pulmonary inflammation and crystalline silica in respirable coal mine dust: dose-response. J. Biosci. 28(1):61-9.

- Kuempel, E. D., Stayner, L. T., Attfield, M. D., and Buncher, C. R. (1995). Exposure response analysis of mortality among coal miners in United States. Am. J. Ind. Med. 28: 167-184.
- Kumaki, K. and nebert, D. W. (1978). Spectral evidence for weal ligand in six position of hepatic microsomal P-450 low spin ferric iron *in vivo*. Pharmacology 17:262-279.
- Kuwano, K., Hagimoto, N., Tanaka, T., Kawasaki, M., Kunitake, R., Miyazaki, H., Kaneko, Y., Matsuba, T., Maeyama, T., and Hara, N. (2000). Expression of apoptosis-regulatory genes in epithelial cells in pulmonary fibrosis in mice. J. Pathol. 190(2):221-9.
- Lacy, S. A., Mangum, J. B., and Everitt, J. I. (1992). Cytochrome P-450 and glutathione-associated enzyme activities in freshly isolated enriched lung cell fractions from beta-naphthoftavone-treated male F344 rats. Toxicology 73:147-160.
- Laforce, F. M., Kelley, W. J., and Huber, G. L. (1973). Inactivation of Staphylocci by alveolar macrophages with preliminary observations on the importance of alveolar lining material. Amer. Rev Respir. Dis. 108, 784-790.
- Lag, M., Becher, R., Samuelsen, J. T., Wiger, R., Refsnes, M., Huitfeldt. H. S., and Schwarze, P. E. (1996). Expression of CYP2B1 in freshly isolated and proliferating cultures of epithelial rat lung cells. Exp Lung Res. 1996 Nov-Dec;22(6):627-49.
- Larivee, P., Cantin, A., Dufresne, A., and Begin, R. (1990). Enzyme activities of lung lavage in silicosis. Lung 168(3):151-8.
- Lee, Y., Hogg, R., and Rannels, D. E. (1994). Extracellular matrix synthesis by coal dust –exposed type II epithelial cells.
- Lee, C., Watt, K. C., Chang, A-M., Plopper, C. G., Buckpitt, A. R., and Pinkerton, K. E. (1998). Site selective differences in cytochrome P450 isoform activities comparison of expression in rat and Rhesus monkey lung and induction in rats.
- Leslie, C. C., McCormick-Shannon, K., and Mason, R. J. (1989). Bronchoalveolar lavage fluid from normal rats stimulates DNA synthesis in rat alveolar type II cells. Am. Rev. Respir. Dis. 39(2):360-6.
- Lesur, O., Bouhadiba, T., Melloni, B., Cantin, A., Whitsett, J. A., and Begin, R. (1995). Alterations of surfactant lipid turnover in silicosis: evidence of a role for surfactant-associated protein A (SP-A). Int. J. Exp. Pathol. 76(4):287-98.
- Levy, R. D., Hubbs, A. F., Ducatman, B. S., Singh, G., Vallyathan, V., Bowman, L., and Miles, P. R. (1997). Metabolic functions of alveolar type II cells in acute silicosis. The toxicologist, 36: 74 (abstract).

- Liang, Z., Lippman, S. M., Kawabe, A., Shimada, Y., and Xu, X. C. (2003). Identification of benzo(a)pyrene diol epoxide-binding DNA fragments using DNA immunoprecipitation technique. Cancer Res. 63(7):1470-4.
- Liddle, C., Hollands, M., Farrell, G. C., and Little, J. M. (1989). Serum estrogen and testosterone concentrations following partial liver resection in man. Gastroenterology 96: A622
- Liddle, C., murray, m., and Farrell, G. C. (1989). Effect of liver regeneration on hepatic cytochrome P450 isozymes and serum sex steroids in the male rat. Gastroenterology 96: 864-872.
- Lim, Y., Kim, J. H., Kim, K. A., Chang, H. S., Park, Y. M., Ahn, B. Y., and Phee, Y. G. (1999) Silica-induced apoptosis *in vitro* and *in vivo*. Toxicol. Lett. 108(2-3):335-9.
- Long, W. P., Pray-Grant M., Tsai, J. C., Perdew, G. H., (1998). Protein kinase C activity is required for aryl hydrocarbon receptor pathway-mediated signal transduction. Mol. Pharmacol. 53:691-700.
- Lowe, G. M., Hulley, C. E., Rhodes, E. S., Young, A. J. and Bilton, R. F. (1998). Free radical stimulation of tyrosine kinase and phosphatase activity in human peripheral blood mononuclear cells. Biochem. Biophys. Res. Commun. 245: 17-22.
- Ma, J. Y, and Ma, J. K. (2000). The dual effect of the particulate and organic components of diesel exhaust particles on the alteration of pulmonary immune/inflammatory responses and metabolic enzymes. Environ. Sci. Health Part C Environ. Carcinog. Ecotoxicol. Rev. 20(2):117-47.
- Ma, Q. and Whitlock, Jr. J.P. (1997). A novel cytoplasmic protein that interacts with the Ah receptor contains tetratricopeptide repeat motifs, and augments the transcriptional response to 2,3,7,8-tetrachlorodibenzo p-dioxin. J. Bio. Chem. 272 (14): 8878-8884.
- Ma, J. Y. C., Yang, H. M., Barger, M. W., Siegel, P. D., Zhong, B. Z., Kriech, A. J., and Castranova, V. (2002). Alteration of pulmonary cytochrome P-450 system: effect of asphalt fume condensate exposure. Journal of Toxicology and Environmental Health, Part A 65:101-104.
- Madtes, D. K., Raines, E. W., Sakariassen, K. S., Assoian, R. K., Sporn, M. B., Bell, G. I., and Ross, R. (1988). Induction of transforming growth factor-a in activated human alveolar macrophages. Cell 53:285-293.
- Mahu, J. L. and Feldman, J. (1984). Study of biochemical behavior of some exported and nonexported hepatic protein during an acute inflammation reaction in the rat. Enzyme (basel) 31:234-240.
- Mayer, B. and Oberbauer, R. (2003). Mitochondrial regulation of apoptosis. News Physiol. Sci. 18:89-94.

- Mann, K. K., MAtulka, R. A., Hahn, M. E., Trombino, A. F., Lawrence, B. P., Kerkvliet, N. I. and Sherr, D. H. (1999). The role of polycyclic aromatic hydrocarbon metabolism in dimethylbenz(a)anthracence-induced pre-B lymphocyte apoptosis. Toxicology and Applied Pharmacology 161:10-22.
- Martin, J., Dinsdale, D., White, L. N., H. (1993). Characterization of Clara and type II cells isolated from rat lung by fluorescence-activated flow cytometry. Biochemical journal 259:73-80.
- Mason, H. S. (1957). Mechanisms of Oxygen Metabolism, In: F. F. Nord (Ed.), Advances in Enzomology, Academic Press, New York, pp. 79-34.
- Matikainen, T., I. Perez, G.I, Jurisicova, A., K. Pru, J.K., Schlezinger, J.J., Heui-Young Ryu, H-Y., Laine, J., Sakais, t., Korsmeyer, S.J., Casper, R.F., Sherr, D.H., and Tilly, J.L. (2001). Aromatic hydrocarbon receptor-driven Bax gene expression is required for premature ovarian failure caused by biohazardous environmental chemicals. Nature Genetics, 28: 355-360.
- Mattison, D.R. and Nightingale, M.R. (1980). The biochemical and genetic characteristics of murine ovarian aryl hydrocarbon (benzo[a]pyrene) hydroxylase activity and its relationship to primordial oocyte destruction by polycyclic aromatic hydrocarbons. Toxicol. Appl. Pharmacol., 56: 399-408.
- Mauderly, J. L. (1997). Relevance of particle-induced rat lung tumors for assessing lung carcinogenic hazard and human lung cancer risk. Environmental Health Perspective 105 Suppl. 5:1337-46.
- Meijers, J. M. M., Swaen, G.M.h., Slangen, J. J. M., Vliet, K. V., and Sturmans, F. (1991). Long term mortality in miners with coal wotkers' pneumoconiosis in Netherlands: a pilot study. Am. J. Ind. Med. 19: 43-50.
- Melloni, B., Lesur, O., Cantin, A., and Begin, R. (1995). Silica exposed macrophages release a growth-promoting activity for type II pneumocytes. Journal of Leukocyte Biology 53: 327-335.
- Melnikov, V. Y., Faubel, S., Siegmund, B., Lucia, M. S., Ljubanovic, D., and Edelstein, C. L. (2002). Neutrophil-independent mechanisms of caspase-1- and IL-18-mediated ischemic acute tubular necrosis in mice. J. Clin. Invest. 110(8):1083-91.
- McFadyen, M. C., Rooney, P. H., Melvin, W. T., and Murray, G. I. (2003). Quantitative analysis of the Ah receptor/cytochrome P450 CYP1B1/CYP1A1 signalling pathway. Biochem. Pharmacol. 65(10):1663-74.
- McKinnon, R. A. (2000). Cytochrome P 450 multiplicity and function. Australian Journal of Hospital Pharmacy 30:54-6.
- Miles, P. R., Bowman, L., and Miller, M. R. (1993). Alterations in the pulmonary microsomal cytochrome P-450 system after exposure of rats to silica. Am. J. Respir. Cell Mol. Biol. 8(6):597-604.

- Miles. P.R., Castranova, V., and Lee, P. (1978). Reactive form of oxygen and chemiluminescence in phagocytizing rabbit alveolar macrophages. Am. J. Physiol. 235: C103-C108.
- Miller, B. E., Dethloff, L. A., and Hook, G. E. (1986). Silica-induced hypertrophy of type II cells in the lungs of rats. Lab. Invest. 55(2):153-63.
- Miller, E. C., Miller, J. A. (1981). Mechanisms of chemical carcinogenesis. Cancer 47(Suppl. 5):1055-64.
- Miller, B. E. and Hook, G. E. R. (1990). Hypertrophy and hyperplasia of alveolar type II cells in response to silica and other toxicants. Experimental Health Perspectives 85:15-23.
- Mimura, J., Ema, M., Sogawa, K. and Fujii-Kuriyama, Y. (1999). Identification of a novel mechanism of regulation of Ah (dioxin) receptor function. Genes and Development 13:20-25.
- Mkrtchian, S. L. and Andersson, K. K. (1990). A possible role of cAMP dependent phosphorylation of hepatic microsomal cytochrome P450: A mechanism to increase lipid peroxidation in response to hormone. Biochem. Biophys. Res. Commun. 166: 787-793.
- Morita, Y., Perez, G. I., Paris, F., Miranda, S. R., Ehleiter, D., Haimovitz-Friedman, A., Fuks, Z., Xie, Z., Reed, J. C., Schuchman, E. H., Kolesnick, R. N., Tilly, J. L. (2000). Oocyte apoptosis is suppressed by disruption of the acid sphingomyelinase gene or by sphingosine-1-phosphate therapy. Nat Med. 6(10):1109-14.
- Morgan, E. T. (1989). Suppression of constitutive cytochrome P-450 gene expression in livers of rats undergoing an acute phase response to endotoxin. Mol. Pharmacol. 36: 699-707.
- Morgan, E. T. (1997). Regulation of cytochromes P450 during inflammation and infection. Drug Metab. Rev. 29: 1129-1188.
- Morgan, E. T. (2001). Regulation of cytochrome P450 by inflammatory mediators: why and how? Drug Metab. Dispos. 29(6):932
- Morgan, E.T., MacGeogh, C., and Gustafsson, J. A. (1985). Hormonal and developmental regulation of the expression of the hepatic microsomal steroid 16α-idroxylase cytochrome P450 apoprotein in the rat. J. Biol. Chem. 260:11895-11898.
- Morgan, J. E., and Whitlock, J. P. Jr. (1992). Transcription-dependent and transcription-independent nucleosome disruption induced by dioxin. Proc. Natl. Acad. Sci. USA 89:11622-26.
- Morgan, W. K. (1984). Coal Workers' pneumoconiosis. In W. K. C. and A. Seaton, editors Occupational Lung Disease, 2nd ed. W. B. Saunders, Philadelphia, 377-448.

- Morita, Y. and Tilly, J. L. (2000). Oocyte apoptosis: like sand through an hourglass. Dev. Biol. 213(1):1-17.
- Moses, H. L., Yang, E. Y., and Pietenpol, J. A. (1990). TGF-β stimulation and inhibition of cell proliferation: new mechanism insights. Cell 63:245-247.
- Mossman, B. T. and March, J. P. (1989). Evidence supporting the role of active oxygen species in asbestos-induced toxicity and lung disease. Environmental Health Perspectives 81:91-94.
- Mucci. L. A., Wedren, S., Tamimi, R. M., Trichopoulos, D., and Adami, H. O. (2001). The role of gene-environment interaction in the aetiology of human cancer: examples from cancers of the large bowel, lung and breast. Journal of Internal Medicine. 249: 477-493.
- Murray, G. I., Taylor, M. C., McFadyen, M. C., McKay, J. A., Greenlee, W. F., Burke, M. D., and Melvin, W. T. (1997). Tumor-specific expression of cytochrome P450 CYP1B1. Cancer Res. 57(14):3026-31.
- Myrvik, Q. N., and Evan, D. G. (1967). Metabolic and immunologic activities of alveolar macrophages. Arch. Environ. Health 14: 92-96.
- Narasimhan, S. R., Yang, L., Gerwin, B. I., Broaddus, V. C. (1998). Resistance of pleural mesothelioma cell lines to apoptosis: relation to expression of Bcl-2 and Bax. Am. J. Physiol. 275(1 Pt 1):L165-71.
- Nebert, D. W., Adesnik m., Coon M. J. Estabrook, R. W., Gonzalez, F. J., Guengerich, F. P., Gunsalus, I. C., Johnson, E. F., Kemper, B., Levin, W., et al (1987). The CYP450 gene superfamily: recommended nomenclature. DNA 6:1-11.
- Nelson, D. R., Koymans, L., Kamataki, T., Stegeman, J. J., Feyereisen, R., Waxman, D. J., Waterman, M. R., Gotoh, O., Coon, M. J., Estabrook, R. W., Gunsalus, I. C., Nebert, D. W. (1996). P450 superfamily: update on new sequences, gene mapping, accession numbers and nomenclature. Pharmacogenetics 6:1-42.
- Nikula, K. J., Avila, K. J., Griffith, W. C., and Mauderly, J. L. (1997). Sites of particle retention and lung tissue responses to chronically inhaled diesel exhaust and coal dust in rats and cynomolgus monkeys. Environ. Health Perspect.105 Suppl 5:1231-4.
- Nolan, R. P., Longer, AM., Harlington, J. S., Oster, G., and Selikoff, I. J., (1981). Quartz hemolysis as related to its surface functionalities. Environ. Res. 26 503-570.
- Okey, A. B., Riddick, D. S., Harper, P. A. (1994). The molecular biology of the aromatic hydrocarbon (dioxin) receptor. Trends Pharmacol. Sci. 15:226-32.
- Olenchock, S. A., Stephen, A. Endotoxins. Morey, PR Freeley, JC Otten, JA eds. Biological contaminants in indoor environments 1990,190-200 American Society for Testing and Materials Philadelphia, PA.

- Olive, M., Ferrer, I. (1999). Bcl-2 and Bax protein expression in human myopathies. J. Neurol. Sci. 164(1):76-81.
- Oltvai, Z. N., Milliman, C. L., Korsmeyer, S. J. (1993). Bcl-2 heterodimerizes in vivo with a conserved homolog, Bax, that accelerates programmed cell death. Cell. 74(4):609-19.
- Omura, T. and Sato, R., (1962). A new cytochrome in liver microsomes. J. Biol. Chem. 237, 1375-76
- Omura, T. and Sato, R., (1964). The carbon monoxide-binding pigment of liver microsomes. I. Evidence for its hemoprotein nature. J. Biol. Chem. 239, PC 2370-78.
- Ortiz de Montellano P. R. ed. 1995. Cytochrome P 450: structure, Mechanism, and Biochemistry. New york: Plenum. 625 pp. 2nd ed.
- Orren, D. K., Peterson, L. N., and Bohr, V. H. (1997). Persistent DNA damage inhibits S-phase and G2 progression, and results in apoptosis. Molecular Biology of the Cell 8:1129-1142.
- Ortmeyer, C. E., Baer, E. J., and Crawford, G. M., Jr. (1973). Life expectancy of Pennsylvania coal miners compensated far disability. Arch Environ Health 27:227-230.
- Orton, T. C. and Parker, G. L. (1982).The effect of hypolipidemic drugs on the hepatic microsomal drug metabolizing enzyme system of the rat: Induction of cytochrome(s) P-450 with specificity toward terminal hydroxylation of lauric acid. Drug Metab. Dispos. 10:110-115.
- Overby, L. H., Nishio, S., Weir, A., Carver, G. T., Plopper, C. G., and Philpot, R. M. (1992). Distribution of cytochrome P450 IAI and NADPH cytochrome P450 reductase in lungs of rabbits treated with 2,3,7,8 tetrachlorodibenzo-p-dioxin: ultrastructure) immunolocalization and *in situ* hybridization. Mol. Pharmacol. 41:1039-1046.
- Pairon, J. C., Trabelsi, N., Buard, A., Fleury-Feith, J., Bachelet, C. M., Poron, F., Beaune, P., Brochard, P., and Laurent, P. (1994). Cell localization and regulation of expression of cytochrome P450 1A1 and 2B1 in rat lung after induction with 3-methylcholanthrene using mRNA hybridization and immunohistochemistry. Am. J. Respir. Cell Mol. Biol. 11(4):386-96.
- Panos, R. J., Suwabe, A., Leslie, C. C., and Mason, R. J. (1990). Hypertrophic alveolar type II cells from silica-treated rats are committed to DNA synthesis in vitro. Am. J. Respir. Cell. Mol. Biol. 3(1):51-9.
- Parandoosh, Z., Fujita, V. S., Coon, M. J., and Philpot, R. M. (1987). Cytochrome P-450 isozymes 2 and 5 in rabbit lung and liver. Comparisons of structure and inducibility. Drug Metab. Dispos. 15(1):59-67.
- Parent, C., Belanger, F. M., Jutras, L. and Du Souich, P (2992). Effect of inflammation on the rabbit hepatic cytochrome P-450 isozymes: alterations in the

kinetics and dynamics of tolbudamides. The Journal of pharmacology and Experimental Therapeutics 261:780-787.

- Parkes, W. R. (1982). Pneumoconiosis due to coal dust and carbon. In Occupational Lung Disorders. Butterworths, London. 175-232.
- Parkes, W. R. in 'Occupational lung disorders,' ed. Parkes W.R., 3rd edn, Butterworth-Heinmann, Oxford, 1994, p. 340-410
- Parmentier, J. H., Schohn, H., Bronner, M., Ferrari, L., Batt, A. M., Dauca, M. and Kremers, P. (1997) Regulation of CYP4A1 and peroxisome proliferator-activated alpha expression by interleukine-1beta, interleukine-6, and dexamethasone in cultured fetal hepatocytes. Biochem. Pharmacol. 54**:** 889-898.
- Pattle, R. E. (1955). Properties, function, and origin of the alveolar lining layer. Nature (London) 175:1125-1126
- Pattle, R. E. and Thomas, L. C. (1961). Lipoprotein composition of the film lining the lung. Nature 189:844.
- Paton, T. E., and Renton, K. W. (1998). Cytokine-mediated down-regulation of CYP1A1 in Hepa1 cells. Biochem. Pharmacol. 55(11):1791-6.
- Penault-Llorca, F., Bouabdallah, R., Devilard, E., Charton-Bain, M. C., Hassoun, J., Birg, F., and Xerri, L. (1998). Analysis of BAX expression in human tissues using the anti-BAX, 4F11 monoclonal antibody on paraffin sections. Pathol. Res. Pract. 194(7):457-64.
- Peters, J. I. M. Silicosis In Occupational Respiratory Diseases. NIOSH Publ 86-107 (Merchant JA, Boehlecke BA, Taylor G, Pickett-Harner M, ads). Cincinnati, OH: National Institute for Occupational Health and Safety, 1986.219-237.
- Perez, G. I., Knudson, C. M., Leykin, L., Korsmeyer, S. J., and Tilly, J. L. (1997). Apoptosis-associated signaling pathways are required for chemotherapy-mediated female germ cell destruction. Nat Med. 1228-32.
- Peter, M. E. and Krammer, P. H. (1998). Mechanisms of CD95 (APO-1/Fas)-mediated apoptosis. Curr. Opin. Immunol., 10: 545-551.
- Petersen, D. D., McKinney, C. E., lkeya, K., Smith, H.H., Allen E. Bale, A. E., McBride, O. W., and Daniel W. and Nebert D. W. (1991). Human CYPIAI gene: Cosegregation of the enzyme inducibility phenotype and an RFLP. Am. J. Hum. Genet. 48: 720-725.
- Phelan, D. M., Brackney, W. R., and Denison, M. S. (1998) The AhR receptor can bind ligand in the absence of receptor-associated heat-shock protein 90. Arch. Biochem. Biophys. 353:47-54.
- Phillips, D. H. (1983). Fifty years of benzo(a)pyrene. Nature 303:468-72.
- Philpot, R.M., Domin, B.A., Devereux, T.R., Harris, C., Anderson, M. W., Fouts, J.R., and Bend, J.R.: Cytochrome P-450-dependent monooxygenase systems of the lung: Relationship to pulmonary toxicity. In Microsomes and Drug

Oxidations, ed., by A.R. Boobis, J. Caldwell, F. DeMatteis and C.R. Elcombe, pp 248-255, Taylor and Francis, London, 1985.

- Plopper, C. G. (1983). Comparative morphologic features of bronchiolar epithelial cells. American Review of Respiratory Diseases 128:S37-S41.
- Plopper, C. G., Mariassay, A. T. and Hill, L. H. (1980). Ultrastructure of the non-ciliated bronchiolar epithelial (Clara) cells of mammalian lung:I. A comparison of rabbit, Guinea pig, rat, hamster, and mouse. Experimental Lung Research 1: 139-154.
- Plopper, C. G.,. Cram, D. L, Kemp, L., Serabjit-Singh, C. J., and Philpot, R. M. (1987). Immunohistochemical demonstration of cytochrome P-450 monooxygenase in Clara cells throughout the tracheobronchial airways of the rabbit. Exp. Lung Res. 13:59-68.
- Poland, A., Glover, E., Ebetino, F. H., and Kende, A. S. (1986). Photoaffinity labeling of the Ah receptor. J. Biol. Chem. 261:6352-65.
- Poland, A. and Knutson, J. C. (1982). 2,3,7,8-Tetrachlorodibenzo-p-dioxin and related halogenated aromatic hydrocarbons: examination of the mechanism of toxicity. *Annu. Rev. Pharmacol. Toxicol.* 22:517-54.
- Porter, D. W., Castranova, V., Robinson, V. A., Hubbs, A. F., Mercer, R. R., Scabilloni, J., Goldsmith, T., Schwegler-Berry, D., Battelli, L., Washko, R., Burkhart, J., Piacitelli, C., Whitmer, M., and Jones, W. (1999). Acute inflammatory reaction in rats after intratracheal instillation of material collected from a nylon flocking plant. J Toxicol Environ Health A 57(1):25-45.
- Porter, D. W., Hubbs, A. F., Robinson, V. A., Battelli, L. A., Greskevitch, M., Barger, M., Landsittel, D., Jones, W., and Castranova, V. (2002a). Comparative pulmonary toxicity of blasting sand and five substitute abrasive blasting agents. J. Toxicol. Environ. Health A. 65(16):1121-40.
- Porter, D. W., Millecchia, L., Robinson, V. A., Hubbs, A., Willard, P., Pack, D., Ramsey, D., McLaurin, J., Khan, A., Landsittel, D., Teass, A., and Castranova, V. (2002b). Enhanced nitric oxide and reactive oxygen species production and damage after inhalation of silica. Am. J. Physiol. Lung Cell Mol Physiol. 283(2):L485-93.
- Polunovsky, V. A., Chen, B., Henke, C., Snover, D., Wendt, C., Ingbar, D. H., Bitterman, P. B. (1993). Role of mesenchymal cell death in lung remodeling after injury. J. Clin. Invest. 92: 388-397.
- Poulos, T. L. (1988). Cytochrome P-450: molecular architexture, mechanism and prospects for national inhibitor design. Pharm. Res. 5:67-75.
- Poulos, T. L. (1991). Modeling of mammalian P450s on the basis of P450cam X-ray structure. In cytochrome P450 (eds Waterman M. R. and Johnson E. F.). pp. 11-30. Academic Press, San Deigo.

- Poulos, T. L. Finzel, B. C., and Howard, A. J. (1986). Crystal structure of substrate free *Pseudomonas Putida* cytochrome P-450. Biochemistry 25:5314-5322.
- Poulus, T. L. and Raag, R. (1992). Cytochrome $P450_{cam}$: crystallography, oxygen activation, and electron transfer. FASEB J. 6:674-679.
- Presta, M., Aletti, M. G., and Ragnotti, G. (1980). Decrease of the activity of the mixed function oxidase system in regenerating rat liver: An alternative explanation. Bioch. Biophys. Res. Commun. 95: 829-834.
- Pru, J. K. and Tilly, J. L. (2001). Programmed cell death in the ovary: insights and future prospects using genetic technologies. Mol. Endocrinol. 15(6):845-53.
- Rabovsky, J., Sapola, N. A., Judy, D. J., Pales. W. H., and Castranova, V. (1986). 7-ethoxoresorufin deethylase activity in rat alveolar type II cells. Federation Proceedings 45, 637.
- Rachtan J. (2002). A case control study of lung cancer in Polish women. Neoplasma 49(2): 75-80.
- Ravi, R., Bedi, G. C., Engstrom, L. W., Zeng, Q., Mookerjee, B., Gelinas, C., Fuchs, E. J. and Bedi, A. (2001). Regulation of death receptor expression and TRAIL/Apo2L-induced apoptosis by NF-kappaB. Nat. Cell Biol. 3:409-416.
- Razzaboni, B. L. and Bolsaitis, P. (1990). Evidence of an oxidative mechanism for the hemolytic activity of silica particles. Environmental health perspectives 87:337-341.
- Rebbaa, A., Zheng, X., Chou, P. M., and Mirkin, B. L. (2003). Caspase inhibition switches doxorubicin-induced apoptosis to senescence. Oncogene. 22(18):2805-11.
- Reddy, J. K., Goel, S. K., Nemali, M. R., Carrino, J. J., Laffier, T. G., Reddy, M. K., Sperbeck, S. J., Osumi, T., Hashimoto, T., Lalwani, N. D., and Rao, M. S. (1986). Transcriptional regulation of Peroxisomal fatty acyl-CoA oxidase and enoyl-CoA hydratase/3-hydroxyacyl-CoA dehydrogenase in at liver by peroxisome proliferators. Proc. Natl. Acad. Sci. USA 83:1747-1751.
- Reiners, J. J., Jr, Pavone,A., Cantu, A. R., Auerbach, C., and Malkinson, A. M. (1992). Differential expression of cytochrome P-450 in proliferating and quiescent cultures of murine lung epithelial cells. Biochem. Biophys. Res. Commun. 183(1):193-8.
- Remmer, H. and Merker, H. J. (1965). Effect of drugs on the formation of smooth endoplasmic and drug metabolizing enzymes. Annals of the New York Academy Sciences. 123:355-73.
- Rengasamy, A., Barger, M. W., Kane, E., Ma, J. K., Castranova, V., and Ma, J. Y. (2003). Diesel exhaust particle-induced alterations of pulmonary phase I and phase II enzymes of rats. J. Toxicol. Environ. Health A. 66(2):153-67.

- Rennard, S. I., Hunninghake, G. W., Bitterman, P. B., and Crystal, R. G. (1981). Production of fibronectin by the human alveolar macrophage: mechanism for the recruitment of fibroblasts to sites of tissue injury in interstitial lung diseases. Proc. Natl. Acad. Sci. U S A. 78(11):7147-51.
- Rhee, S. G. (1999). Redox signaling: Hydrogen peroxide as intracellular messenger. Exp. Mol. Med. 31: 53-59.
- Renton, K. W. and Nicholson, T. E. (2000). Hepatic and central nervous system cytochrome P450 are down-regulated during lipopolysaccharide-evoked localized inflammation in brain. J. Pharmacol. Exp. Ther. 294: 524-530.
- Roberts, E. S., Lin, H. l., Crowley, J. R., Vuletich, J. L., Osawa, Y. and Hollenberg, P. F. (1998). Peroxynitrite-mediated nitration of tyrosine and inactivation of the catalytic activity of cytochrome P450 2B1. Chem. Res. Toxicol. 11: 1067-1074.
- Ronis, M. J. J., Lumpkin, C. K., Thomas, P. E., Ingelman-sundberg, M. and Badger, T. M. (1992). The microsomal monooxygenase system of regenerating liver. Bioch. Pharmacol. 43: 567-573.
- Rooke, G. B., Ward, F. G., Dempsey, A. N. Dowler, J. B., and Whitaker, C. J. (1979). Carcinoma of the lung in Lancashire coal miners. Thorax 34: 229-233.
- Rom, W. N., Basset, B., Fells, G. A., Nukiwa, T., Trapnell, B. C., Crysal, R. G. (1990). Alveolar macrophages release an insulin-like growth factor I-type molecule. J. Clin. Invest. 82(5):1685-93.
- Rossiter, C.E., Rivers, D., Bergman, I., Casswell, C., and Nagelschemidt, G. (1967). Dust content, radiology, and pathology in simple pneumoconiosis of coal workers. In Inhaled Particles and Vapors; Proc. 2nd Int. Symp. Cambridge, 1965, edited by C.N. Davis, pp 419-437. Pergamon, Oxford.
- Ruf, H. H., Wende, P., and Ullrich, V. (1979). Models for ferric cytochrome P-450. Characterization of hemi mercaptide complexes by electronic and ESR spectra. J. Inorg. Biochem. 11:189-204.
- Ryan, K. M., Ernst, M. K., Rice, N. R., and Vousden, K. H. (2000). Role of NF-kappaB in p53-mediated programmed cell death. Nature. 404(6780):892-7.
- Saffiotti, U., and Stinson, S. F. (1988). Lung cancer induction by crystalline silica: relationships to granulomatous reactions and host factors.' Environ. Carcinogen Rev. C6:197-222.
- Savill, J., Fadok, V., Henson, P., and Haslett, C. (1993). Phagocyte recognition of cells undergoing apoptosis. Immunol. Today. 14(3):131-6.
- Scarisbrick D (2002). Silicosis and coal workers' pneumoconiosis. Practitioner 246(1631):114, 117-9.
- Skalova, L., Szotakova, B., Machala, M., Neca, J., Soucek, P., Havlasova, J., Wsol, V., Kridova, L., Kvasnickova, E., and Lamka, J. (2001). Effect of

ivermectin on activities of cytochrome P450 isoenzymes in mouflon (Ovis musimon) and fallow deer (Dama dama). Chem. Biol. Interact. 137(2):155-67.

- Schins, R. P. and Borm, P. J. (1999). Mechanisms and mediators in coal dust induced toxicity: a review. Ann. Occup. Hyg. 43(1):7-33.
- Seaton, A. 'In Occupational lung diseases' eds. Morgan, W. K. and Seaton, A., W. B. Saunders & Co., Philadelphia, PA, 1984, pp. 250-294.
- Seaton, A., Seaton, D. and. Leitch, A. G. Crofton and Douglas's Respiratory Diseases, 4th eds., Blackwell Scientific, Oxford, 1989, pp. 808-815.
- Sesardic, D., Cole, K. J., Edwards, D. S., Davies, D. S., Thomas, P. E., Levin, W., and Boobis, A. R. (1990). The inducibility and catalytic activity of cytochromes P450c (P450IA1) and P450d (P450IA2) in rat tissues. Biochemical Pharmacology 39:499-506.
- Serabjit-Singh, C. J., Albro, P.W., Roberson, I. G. C., and Philpot, R., M. (1983) Interactions between xenobiotics that increase or decrease the levels of cytochrome P-450 isozymes in rabbit lung and liver. J. Biol. Chem. 258:12827-12834.
- Serabjit-Singh, C. J., Nishio, S. I., Philpot, R. M., and Plopper, C. G. (1988). The distribution of cytochrome P-450 monooxygenase in cells of the rabbit lung: an ultrastructural immunocytochemical characterization. Mol. Pharmacol. 33:279-289.
- Serabjit-Singh, C. J., Wolf, C. R., and Philpot, R., M. (1979). The rabbit pulmonary monooxygenase system; immunochemical and biochemical characterization of the enzyme components. Journal of Biological Chemistry 254:9901-9907.
- Serabjit-Singh, C. J., Wolf, C. R., Philpot, R. M., and Plopper, C. G. (1980). Cytochrome P-150: localization in rabbit lung. Science 207:1469-1470.
- Sesardic, D., Cole, K. J., Edwards, R. J., Davies, D. S., Thomas, P. E., Levin, W. and Boobis, A. R. (1999). The inducibility and catalytic activity of cytochromes P450c (P450IA1) and P450d (450IA2) in rat tissues. Biochem. Pharmacol. 39:499-506.
- Scheidereit, C. (1998). Signal transduction. Docking IkappaB kinases. Nature 359:225-226.
- Schneeberger, E. E. (1987). Structural basis of some permeability properties of the air-blood barrier. Federation Proceedings 37:2471-2478.
- Shigeno, M., Nakao, K., Ichikawa, T., Suzuki, K., Kawakami, A., Abiru, S., Miyazoe, S., Nakagawa, Y., Ishikawa, H., Hamasaki, K., Nakata, K., Ishii, N., and Eguchi, K. (2003). Interferon-alpha sensitizes human hepatoma cells to TRAIL-induced apoptosis through DR5 upregulation and NF-kappa B inactivation. Oncogene. 22(11):1653-62.

- Shimada, T., Iwasaki, M., Martin, M.V., and Guengerich, F.P. (1989). Human liver microsomal cytochrome P-450 enzymes involved in the bioactivation of procarcinogens detected by Umu gene response in Salmonella typhimurium TA 1535/pSK1002. Cancer Research, 12: 3218-3228
- Shiromizu, K., Mattison, D. R. (1985). Murine oocyte destruction following intraovarian treatment with 3-methylcholanthrene or 7,12-dimethylbenz[*a*]anthracene: protection by α-napthoflavone. Teratogen Carcinogen Mutagen 5: 463–472.
- Shukla, A., Timblin, C., BeruBe, K., Gordon, T., McKinney, W., Driscoll, K., Vacek, P., and Mossman, B. T. (2000). Inhaled particulate matter causes expression of nuclear factor (NF)-kappaB-related genes and oxidant-dependent NF-kappaB activation in vitro. Am. J. Respir. Cell Mol. Biol. 23(2):182-7.
- Shull, L. R., Olson, B. A., Hughes, B. J., McKenzie, R. M., and Kinzell, J. H. (1985). Effect of pentachlorophenol on microsomal mixed-function oxidases in cattle. Pesticide Biochemistry and Physiology 25: 31-39.
- Siewert, E., Bort, R., Kluge, R., Heinrich, P. C., Castell, J., and Jover, R. (2000). Hepatic cytochrome P450 down-regulation during aseptic inflammation in the mouse is interleukin 6 dependent. Hepatology 32(1):49-55.
- Silver, J. and Lukas, B. (1982). Mossbauer studies on protoporphyrin IX iron(II) solutions containing sulphur ligands and their carbonyl adducts. Models for the active site cytochrome P-450. Inorganic Chemistry Acta 91279-283.
- Skalova, L., Szotakova, B., Machala, M., Neca, J., Soucek, P., Havlasova, J., Wsol, V., Kridova, L., Kvasnickova, E., and Lamka, J. (2001). Effect of ivermectin on activities of cytochrome P450 isoenzymes in mouflon (Ovis musimon) and fallow deer (Dama dama). Chem. Biol. Interact. 2137(2):155-67.
- Smith, A. G., Clother, B., Robinson, S., Scullion, M. J., Carthew, P., Edwards, R., Luo, J., Lim, C. K., and Toledano, M. (1998). Interaction between iron metabolism and 2,3,7,8- tetrachlorodibenzo-*p*-dioxin in mice with variants of the Ahr gene: A hepatic oxidative mechanism. Molecular Pharmacology, 53: 52-61.
- Smith, P. K., Krohn, R. I., Hermanson, G. T., Mallia, A. K., Gartner, F. H., Provenzano, M.D., Fujimoto, E.K., Geoke, N.M., Olson, B.J., and Klenk, D.C. (1985). Measurement of protein using bicinchoninic acid. Analytical biochemistry 150: 76-85.
- Snider, D. E. Jr. (1978). The relationship between tuberculosis and silicosis. Am. Rev. Respir. Dis. 118: 455-460.
- Song, B. J., Gelboin, H. V., Park, S. S., Tsokos, G. C., and Friedman, F. K. (1985). Monoclonal antibody-directed radioimmunoassay detects cytochrome P-450 in human placenta and lymphocytes. Science. 228(4698):490-2.
- Sorenson, J. R. L., Kober, T. A. I., and Petering, H.G. (1974). The concentration of Cd, Cu, Fe, Ni, Pb, and Zn in bituminous coal from mines with differing incidences of coal workers' pneumoconiosis. Am. Ind. Hyg. Assoc. J. 25: 93-98.

- Sorokin, S. P. (1970). The cells of the lung. In: Morphology of Experimental Respiratory Carcinogenensis (P. Nattesheim, Ed.). AEC Symposium Series, Vol 21, pp. 3-44.
- Sprick, M. R., Weigand, M. A., Rieser, E., Rauch, C. T., Juo, P., Blenis, J., Krammer, P. H., and Walczak, H. (2000). FADD/MORT1 and caspase-8 are recruited to TRAIL receptors 1 and 2 and are essential for apoptosis mediated by TRAIL receptor 2. Immunity, 12: 599-609.
- Stanley, M. W., Henry-Stanley, M. J., GajlPeczalska, K., and Bitterman, P. B. (1992). Hyperplasia of type II pneumocytes in acute lung injury: Cytologic findings of sequential bronchoalveolar lavage. Am. J. Clin. Pathol. 97:669-677
- Stadler, J., Trochfeld, J., Schemalex, W. A., Brill, T., Siewert, J. R., Greim, H., and Doehmer, J. (1994). Inhibition of cytochromes P450I by nitric oxide. Proceeding National Academy Science 91:3559-3563.
- Steer, J. C. (1995). Liver regeneration. FASEB J. 9: 1396-1400.
- Storm, D. K., Postlind, H., Tukey, R. H. (1990). Characterization of rabbit CYP1A1 and CYP1A2 genes: developmental and dioxin inducible expression of rabbit liver P4501A1 and P4501A2. Archives of Biochemistry and Biophysics 294(2):707-716.
- Strahl, B. D. and Allis, C. D. (2002). The language of covalent histone modifications. Nature 403:41-45.
- Srivastava, K. D., Rom, W. N., Jagirdar, J., Yie, T. A., Gordon, T., and Tchou-Wong, K. M. (2002). Crucial role of interleukin-1beta and nitric oxide synthase in silica-induced inflammation and apoptosis in mice. Am. J. Respir. Crit. Care Med. 165(4):527-33.
- Struhl, K. (1998). Histone acetylation and transcriptional regulatory mechanisms. Genes Dev. 12: 599-606.
- Suratt, P. M., Winn, W. C. Jr., Brody, A. R, and Bolton, W. K., and Giles, R.D. (1977). Acute silicosis in tombstone sandblasters. Am. Rev. Respir. Dis., 115: 521-529.
- Sutherland, L.M., Edwards, Y. S., and Murray, A. W. (2001) Alveolar type II cell apoptosis. Comparative Biochemistry and Physiology. Part A, Molecular and integrative physiology. 129 (1): 267-85.
- Suzuki, Y. J., Forman, H. J. and Sevanian, A. (1997) Oxidants as stimulators of signal transduction. Free Radical Biology and Medicine 22: 269-285
- Sweeney, T.D., Castranova, V., Bowman, L., and Miles, P.R. (1981). Factors which affect superoxide anion release from rat alveolar macrophages. Exp. Lung Res. 2: 85-96.
- Szeliga, J., and Dipple, A. (1998). DNA adduct formation by polycyclic aromatic hydrocarbon dihydrodiol epoxides. Chem. Res. Toxicol. 11(1):1-11.

- Taioli, E., Bradlow, H. I., Garbers, S., Ganguly, S., and Garte, S. J. (1999). Role of estradiol metabolism in CYP1A1 polymorphisms in breast cancer risk. Cancer Detect. Prev. 23:232-7.
- Taioli, E., Trachman, J., Chen, X., Toniolo, P., and Garte, J. J. (1995). A CYP1A1 RFLP is associated with lung cancer in African-American women. Cancer Research 55:3757-8.
- Takahashi, Y., Nakayama, K., Shimojima, T., Itoh, S., and Kamataki, T. (1996) Expression of aryl hydrocarbon receptor (AhR) and aryl hydrocarbon receptor translocator (Arnt) in adult rabbits known to be non-responsive to cytochrome P-450 1A1 (CYP1A1) inducers. Eur. J. Biochem. 242: 512-518.
- Tamburini, P. P., Masson, H., Bains, S. K., Makowski, R. J., Morns, B., and Gibson, G. G. (1984). Multiple forms of hepatic cytochrome P450: Purification, characterization, and comparison of a novel clofibrate-induced isozyme with other forms of cytochrome P-450. Eur. J Biochem. 139:235-246.
- Testa. B. (1995). The nature and Functioning of Cytochromes P450 and Flavin-containing monooxygenases. In The Metabolism of Drugs and Other Xenobiotics: Biochemistry of Redox Reactions. pp. 70-121. Academic Press, San Deigo.
- Thet, L. A., Parra, S. C. and Shelburne, J. D. (1984). Repair of oxygeinduces lung injury in adult rats;the role of ornithine decarboxylase and polyamines. American Review of Respiratory Diseases 129:174-181.
- Thompson, C. B. (1995). Apoptosis in the pathogenesis and treatment of disease. Science 1995; 267: 1456-1462.
- Thomas, J. H. and Gillham, B. (1989). Wills' Biochemical Basis of Medicine, 2nd edition, P. 454. London: Wright.
- Tian, Y. Rabson, A. B., Gallo, M. A., and Ke, S. (2002). TNF-α treatment suppresses CYP1A1 transcription by inhibiting acetylation of histone H4 and phosphorylation of the C terminal domain of RNA polymerase II. Toxicological Sciences 66:218 (Abstract).
- Tian, Y., Ke, S., Chen, M., Rabson, A. B., and Gallo, M.A. (2003). Regulation of CYP1A1 transcriptional elongation by AH receptor through interaction with P-TEF B. Toxicological Sciences 72 (S-1): 65 (Abstract).
- Tian, Y., Ke, S., Denison, M. S., Rabson, A. B., and Gallo, M.A. (1999). Ah Receptor and NF-κB Interactions, a potential mechanism for dioxin toxicity. The Journal of Biological Chemistry, 274 (1): 510-515.
- Tindberg, N., Baldwin, H. A., Cross, A. J. and Ingelman-Sundberg, M. (1996). Induction of cytochrome P450 2E1 expression in rat and gerbil astrocytes by inflammatory factors and ischemic injury. Mol. Pharmacol. 50: 1065-1072.
- Tindberg, N. and Ingelman-Sundberg, M. (1989). Cytochrome P-450 and oxygen toxicity. Oxygen-dependent induction of ethanol-inducible cytochrome P-450 (IIEI) in rat liver and lung. Biochemistry 28:44994504.

- Trautwein, C., Ramadori, G., Gerken, G., Meyer Zum Buschenfelde, K. H. and Manns, M. (1992) Regulation of cytochrome P450 IID by acute phase mediators in C3H/HeJ mice. Biochem. Biophy. Res. Commun. 182: 617-623.
- Ulich, T. R., Yi, E. S., Longmuir, K., Yin, S., Biltz, R., Morris, C. F., Housley RM, and Pierce G. F. (1994). Keratinocyte growth factor is a growth factor for type II pneumocytes in vivo. J. Clin. Invest. 1994 Mar;93(3):1298-306.
- Vallyathan, V., Brower, P. S., Green, F. H., and Attfield, M. D. (1996). Radiographic and pathologic correlation of coal workers' pneumoconiosis. Am J Respir. Crit. Care Med. 154(3 Pt 1):741-8.
- Vallyathan, V., Castranova, V., Pack, O., Shumaker, L. S., Hubbs, A. F., shoemaker, D. A., Ramsey, D. M., Pretty, J. R., Mclauren, J. L. et al, (1995). Freshly fractured quartz inhalation leads to lung injury and inflammation. AM. J. Crit. Care Med. 152:1003-1009.
- Vallyathan, V., Goins, M., Lapp., L. N., Pack, D., Leonard, S., Shi, X., Castranova, V., Vanhee, D., Gosset, P., Boitelle, A., Wallaert, B., and Tonnel, A. B. (1995). Cytokines and cytokine network in silicosis and coal workers' pneumoconiosis. Eur. Respir. J. 8(5):834-42.
- Vallyathan, V., Green, F. H. Y., Rodman, N. F., Boyd, C. B., and Althouse, R. (1985). Lung carcinoma by histologic type in coal miners. Arch. Pathol. Lab. Med., 109: 419-423.
- Vallyathan, V., Shi, X., and Castranova, V. (1998). Reactive oxygen species: their relation to pneumoconiosis and carcinogenesis. Environ. Health Perspect. 106 Suppl 5:1151-5.
- Vallyathan, V., Shi, X., Dalal, N. S., and Castranova, V., (1988). Generation of free radicals from freshly fractures silica dust; potential role in acute silica-induced lung injury. Am. Rev. Resp. Dis. 138:1213-1219.
- Vanderslice. R. R., Domin, B. A., Carver, G. T., and Philpot, R. M. (1987). Species-dependent expression and induction of homologues of rabbit cytochrome P-450 isozyme 5 in liver and lung. Mot. Pharmacol. 31: 320-325.
- Vanhee, D., Gosset, P., Boitelle, A., Wallaert, B., Tonnel, A. B. (1995). Cytokines and cytokine network in silicosis and coal workers' pneumoconiosis. Eur. Respir. J. 8(5):834-42.
- van't Klooster G. A., Horbach G. J., Natsuhori, M., Blaauboer, B. J., Noordhoek, J., and van Miert A. S. (1993a). Cytochrome P450 induction and metabolism of alkoxyresorufins, ethylmorphine and testosterone in cultured hepatocytes from goat, sheep, and cattle. Biochemical Pharmacology 46(10): 1781-1790.
- van't Klooster G. A., Horbach G. J., Natsuhori, M., Blaauboer, B. J., Noordhoek, J., and van Miert A. S. (1993b). Hepatic cytochrome P450 induction in goats. Effects of model inducers on the metabolism of alkoxyresorufins, testosterone and ethylmorphine, and on apoprotein and mRNA levels. Biochem. Pharmacol. 45(1):113-22.

- Vaughan, D. J., Brogan, T. V., Kerr, M. E., Deem, S., Luchtel, D. L., and Swenson, E. R. (2003). Contributions of nitric oxide synthase isozymes to exhaled nitric oxide and hypoxic pulmonary vasoconstriction in rabbit lungs. Am. J. Physiology- Lung Cellular and Molecular Physiology. 284(5):L834-43.
- Vogelstein, B. and Kinzler, K. W. (1996). Carcinogens leave fingerprints. Nature. 355(6357):209-10.
- Voigt, J. M., Kawabata' T. T., Burke, J. P., Martin, M. V., Guengerich, F. P., and Baron, J. (1990). In situ localization and distribution of xenobiotic-activating enzymes and aryl hydrocarbon hydroxylase activity in lungs of untreated rats. Mol. Pharmacol. 37:182-191.
- Wallace, W. E., Gupta, N. C., Hubbs, A. F., Mazza, S. M., Bishop, H. A., Keane, M. J., Battelli, L. A., Ma, J., and Schleiff, P. (2002). Cis-4-[(18)F]fluoro-L-proline PET imaging of pulmonary fibrosis in a rabbit model. J. Nucl. Med. 43(3):413-20.
- Wallace, W. E. Harrison, J. C., Grayson, A. L., Keane, M. J., Bolsaitis, P., Kennedy, R. D., Wearden, A. D., and Attfield, M. D. (1994). Aluminosilicate surface contamination of respirable quartz particles from coal mine dusts and from clay works dusts. Ann. Occup. Hyg. 38 439-445.
- Wallace, W. E., Jr., Vallyathan, V., Keane, M. J., and Robinson, V. (1985). In vitro Biologic toxicity of native and surface-modified silica and kaolin. Journal of Toxicology and Environmental Health 16:415-424.
- Wang, L., Antonini, J. M., Rojanasakul, Y., Castranova, V., Scabilloni, J. F., and Mercer, R. R. (2002a). Potential role of apoptotic macrophages in pulmonary inflammation and fibrosis. J. Cell Physiol. 194(2):215-24.
- Wang, H. C., Shun, C. T., Hsu, S. M., Kuo, S. H., Luh, K. T., and Yang, P. C. (2002b). Fas/Fas ligand pathway is involved in the resolution of type II pneumocyte hyperplasia after acute lung injury: evidence from a rat model. Crit. Care Med. 30(7):1528-34.
- Wang, D., You, L., Sneddon, J., Cheng, S. J., Jamasbi, R., Stoner, and Frameshift, G. D. (1995). mutation in codon 176 of the *p53* gene in rat esophageal epithelial cells transformed by benzo[*a*]pyrene dihydrodiol. Mol. Carcinog. *14:* 84-93.
- Warburg, O. (1949). Heavy metal prosthetic groups and enzymatic action. Chapter XI, Oxford at the Clarendon Press.
- Warheit, D. B. (1989). Interspecies comparisons of lung responses to inhaled particles and gases. Crit. Rev. Toxicol. 20(1):1-29.
- Warren, G. W., Poloyac, S. M., Gary, D. S., Mattson, M. P., and Blouin, R. A. (1999). Hepatic cytochrome P-450 expression in tumor necrosis factor-alpha receptor (p55/p75) knockout mice after endotoxin administration. Pharmacol Exp. Ther. 288(3):945-50.

- Waxman, D. J. (1989). Hepatic enzymes of Steroid Metabolism. Metabolism. Regulation of Growth Hormone Secretory Patterns in Cytochrome P 450 Biochemistry and Biophysics (Schuster, I., Ed.), pp 464-471, Taylor and Francis, London.
- Weibel, E. R. (1973). Morphological basis of alveolar-capillary gas exchange. Physiological Review 53:419-495
- Weibel, E. R. (1974). A note on differentiation and divisibility of alveolar epithelial cells. Chest 65:19S-21S.
- Weiss, S. J. and Lo Buglio, A. F. (1982). Biology of disease phagocyte-generated-oxygen metabolites and cellular injury. Lab. Invest. 47:5-18.
- Weissman, D. N. and Wagner, G. R. Silicosis. In: Weinberger SE, ed. UpToDate in Pulmonary and Critical Care Medicine. Wellesley, MA: UpTpDate, Inc.; 2002 (on CD-ROM).
- White, R. E. and Coon, M. J. (1980). Oxygen activation by cytochrome P-450. Ann. Rev. Biochem. 49:315-356.
- Whitlock, J.P. Jr. (1986). The regulation of cytochrome P450 gene expression, Annu. Rev. pharmacol. Toxicol. 26:333-369.
- Whitlock, Jr. J.P. (1999) Induction of cytochrome P4501A1. Annu. Rev. Pharmacol. And Toxicol. 39: 103-25.
- Whitlock J. P. Jr., Okino, S. T., Dong, L., Ko, H. P., Clarke-Katzenberg R, Ma, Q., and Li, H. (1996). Cytochromes P450 5: induction of cytochrome P4501AI: a model for analyzing Mammalian gene transcription. FASEB J. 10:809-18.
- Widdicombe J. G. and Pack, R. J. (1982). The Clara cells. Eur. J. Respir. Dis. 63(3):202-20.
- Williams, A. O., Flanders, K. C., and Saffiotti, U. (1993). Immunohistochemical localization of transforming growth factor-beta 1 in rats with experimental silicosis, alveolar type II hyperplasia, and lung cancer. Am. J. Pathol. 142(6):1831-40.
- Williams, D. E., Dutchuk, M., and Lee, M. Y. (1991). Purification and characterization of microsomal cytochrome P-450 IIB enzyme from a sheep lung. Xenobiotica 21(7): 979-989.
- Willey, J. C., Coy, E. L., Frampton, M. W., Torres, A., Apostolakos, M. J., Hoehn, G., Schuermann, W. H., Thilly, W. G., Olson, D. E., Hammersley, J. R., Crespi, C. L., and Utell, M. J. (1997). Quantitative RT-PCR measurement of cytochromes p450 1A1, 1B1, and 2B7, microsomal epoxide hydrolase, and NADPH oxidoreductase expression in lung cells of smokers and nonsmokers. Am. J. Respir. Cell Mol. Biol. 17(1):114-24
- Wink, D. A., Osawa, Y., Darbyshire, J.F., and Jones, C.R. (1993). Inhibition of cytochrome P450 by nitric oxide and nitric oxide releasing agents. Archives of Biochemistry and Biophysics 300 (1): 115-123.

- Wu, C. (1997). Chromatin remodeling and the control of gene expression. J. Biol. Chem. 272:28171-74.
- Wu, Z. L., Chen, J. K., Ong, T. M., Matthews, E. J., and Whong, W. Z. (1990). Induction of morphological transformation by coal-dust extract in BALB/3T3 A31-1-13 cell line. Mutational research 245 (3): 225-230.
- Wu, I. and Whitlock, Jr. J.P. (1992) Mechanism of dioxin action: Ah receptor-mediated increase in promoter accessibility in vivo. Proc. Natl. Acad. Sci. 89:4811-15
- Wylie, A. H. (1980). Cell Death. The significant of apoptosis. Int. Rev. Cytol. 68:251-306.
- Xipell, J. M., Ham, K. N., Price, C. G. and Thomas, D. P. (1977). Acute silicolipoproteinosis. Thorax 32:104-111.
- Yeoh, C. I., and Yang, S. C. (2002). Pulmonary function impairment in pneumoconiotic patients with progressive massive fibrosis. Chang Gung Med J. 25(2):72-80.
- Yun C. H., Park, H. J., Kim S. J., Kim, H. K. (1993). Identification of cytochrome P450 1A1 in human brain. Biochem. Biophys. Res. Commun. 243(3):808-10.
- Zhong, H., SuYang, H., Erdjument-Bromage, H., Tempst, P., and Ghosh, S. (1997). The transcriptional activity of NF-κβ is regulated by the I-κβ-associated PKAc subunit through a cyclic AMP-independent mechanism. Cell 89:413–424.
- Ziskind, M. Jones, R. N. and Weill, H. (1986) Silicosis. Am. Rev. Respir. Dis.113: 643-665.